VU VRIJE UNIVERSITEIT AMSTERDAM

VU Research Portal

Explaining Fatigue and Post-Exertional Malaise in Long COVID and ME/CFS

Charlton, Braeden Trey

2026

DOI (link to publisher)
10.5463/thesis.1979

document version
Publisher's PDF, also known as Version of record

Link to publication in VU Research Portal

citation for published version (APA)
Charlton, B. T. (2026). *Explaining Fatigue and Post-Exertional Malaise in Long COVID and ME/CFS: From Skeletal Muscle To Exercise Immunology*. [PhD-Thesis - Research and graduation internal, Vrije Universiteit Amsterdam]. https://doi.org/10.5463/thesis.1979

General rights
Copyright and moral rights for the publications made accessible in the public portal are retained by the authors and/or other copyright owners and it is a condition of accessing publications that users recognise and abide by the legal requirements associated with these rights.

- Users may download and print one copy of any publication from the public portal for the purpose of private study or research.
- You may not further distribute the material or use it for any profit-making activity or commercial gain
- You may freely distribute the URL identifying the publication in the public portal

Take down policy
If you believe that this document breaches copyright please contact us providing details, and we will remove access to the work immediately and investigate your claim.

E-mail address:
vuresearchportal.ub@vu.nl

Download date: 26. Oct. 2026

Explaining Fatigue and Post-Exertional Malaise in Long COVID and ME/CFS: From Skeletal Muscle To Exercise Immunology

Braeden T. Charlton

The work in this thesis was carried out at the Department of Human Movement Sciences at the Vrije Universiteit Amsterdam, Netherlands. Research projects were supported financially by ZonMw (Project Number 10091012110025), the Patient-Led Research Collaborative, the We&Me Foundation, Solve M.E., ICanCME, Jaarcampagne VUfonds, and the Amsterdam UMC foundation.















Cover Design: DrawImpacts

Layout: Braeden T. Charlton

Printed by: VU Repro Services

DOI: https://doi.org/10.5463/thesis.1979

© 2026 Braeden T. Charlton
All rights reserved. No part of this thesis may be reproduced or transmitted in any form or by any means, electronically or mechanically, including photocopying, recording, or any information storage and retrieval system, without written permission from the author.

VRIJE UNIVERSITEIT

Explaining Fatigue and Post-Exertional Malaise in Long COVID and ME/CFS: From Skeletal Muscle To Exercise Immunology

ACADEMISCH PROEFSCHRIFT

ter verkrijging van de graad Doctor of Philosophy aan
de Vrije Universiteit Amsterdam,
op gezag van de rector magnificus
prof.dr. J.J.G. Geurts,
volgens besluit van de decaan
van de Faculteit der Gedrags- en Bewegingswetenschappen
in het openbaar te verdedigen
op donderdag 12 november 2026 om 9.45 uur
in de universiteit

door

Braeden Trey Charlton

geboren te Regina, Canada

promotoren:	prof.dr. R.T. Jaspers prof.dr. M. van Vugt
copromotor:	dr. R.C.I. Wust
promotiecommissie:	prof.dr. C.A.C. Ottenheijm dr. M.T. Hooijmans prof.dr. F. Le Grand prof.dr. S. Nijhof prof.dr. M.A. Faghy

Index

1. Introduction (**Pgs. 1-26**)
2. Muscle Abnormalities Worsen After Post-Exertional Malaise in Long COVID (**Pgs. 29-77**)
3. Matters Arising 1
    a. Muscle Abnormalities in Long COVID (**Pgs. 79-84**)
    b. Reply: Muscle Abnormalities in Long COVID (**Pgs. 87-93**)
4. Matters Arising 2
    a. Should We Be Careful with Exercise in Post-Exertional Malaise After Long COVID? (**Pgs. 95-99**)
    b. Reply: Should We Be Careful with Exercise in Post-Exertional Malaise After Long COVID? (**Pgs. 101-106**)
5. Skeletal Muscle Adaptations and Post-Exertional Malaise in Long COVID (**Pgs. 109-127**)
6. Post-Exertional Malaise and the Myth of Cardiac Deconditioning: Rethinking the Pathophysiology of Long Covid (**Pgs. 129-135**)
7. The Impact of Bed Rest on Human Skeletal Muscle Metabolism (**Pgs. 137-191**)
8. Skeletal Muscle Properties in Long COVID and ME/CFS Differ From Those Induced by Bed Rest (**Pgs. 193-251**)
9. An Inability to Recover: Unresolved Regeneration and Satellite Cell Depletion in Post-Acute Infectious Diseases Associated With Altered Metabolic Landscape (**Pgs. 253-291**)
10. General Discussion (**Pgs. 293-329**)
11. Academic Summary (**Pgs. 331-335**)
12. General Summary (**337-339**)
13. Appendices
    a. Acknowledgements (**344-345**)

b. List of Publications
(**346-348**)

c. About The Author (**350**)





Chapter 1

INTRODUCTION



Acute SARS-CoV-2 Disease (COVID-19)

During the winter of 2019 and 2020, the SARS-CoV-2 epidemic took the world by storm. In the first several waves of the epidemic, the acute SARS-CoV-2 infection (resulting in coronavirus disease 2019; COVID-19) was one of the worst global viral diseases to date, resulting in over 700 million cases and over 7 million deaths globally[1].

Similar to other coronaviruses, SARS-CoV-2 entry occurs via the epithelium, typically in the respiratory tract[2]. Specifically, the interaction between the spike protein of SARS-CoV-2 and the angiotensin converting enzyme 2 (ACE2) receptor allows for viral entry[3,4]. During the incubation period, typically lasting 2-7 days, a myriad of symptoms occur, including fever, fatigue, muscle aches or pain, and respiratory distress, among others[5–7]. While many respiratory viruses may also cause the aforementioned symptoms[8–11], it is the severity of COVID-19 that has resulted in a global record of hospitalizations and deaths. In instances where COVID-19 results in severe infections not resulting in death, patients often are admitted to intensive care units and placed on ventilation due to the severe respiratory distress experienced[6,12].

Not all SARS-CoV-2 infections result in severe COVID-19 sequelae, such as respiratory distress or the need for intensive care unit admission. Particularly after vaccinations began, the proportion of reported infections and severe COVID-19 was reduced[13–15]. However, even in mild cases of COVID-19, individuals frequently report atypical symptoms, such as loss of taste or smell, brain fog, confusion, and heart palpitations or myocarditis[5,7,16,17]. Although the typical resolution of mild COVID-19 occurs between 7-14 days[14], it is not uncommon for individuals to report at least one symptom lingering upwards of one month following[5], typically being anosmia, inability to taste, brain fog or fatigue.

Long COVID

Despite the reductions in hospitalizations and deaths due to acute COVID-19, 10-26% of individuals did not show improvements in symptoms beyond 3 months[18]. The non-resolution of symptoms 3-months following an acute COVID-19 infection was termed long COVID or post-acute sequelae of COVID (PASC)[19,20]. Commonly, patients with long COVID report a debilitating fatigue, which does not allow them to conduct daily tasks as they would have prior to infection[21–23]. Often, this is also associated with brain fog and post-exertional malaise (PEM), which is the worsening of symptoms or development of new symptoms with physical, cognitive, or emotional exertion[24,25]. While the persistence of symptoms between acute and

long COVID are similar, the underlying mechanism as to the development of long COVID is unclear.

Patients with long COVID report a variety of different symptoms (Figure 1), however the most commonly reported are brain fog, myalgia, fatigue, and post-exertional malaise (PEM)[26]. While the heterogeneity of reported symptoms suggest a systemic dysregulation, symptoms such as myalgia, fatigue and post-exertional malaise imply a skeletal muscle characteristic may be present. While little is known about the persistence of any of the symptoms, myalgia and fatigue may be closely linked. Myalgia, or muscle pain, occurs from the noxious stimulus in response to acid accumulation[27], which occurs during heavy intensity exercise[28,29]. Fatigue, similarly, also generally occurs in a response to increased skeletal muscle acidity[30]. Fatigue is further dependent on complex interactions of metabolites and ions, as outlined in section 2.3. Both myalgia and fatigue therefore have a skeletal muscle origin, which is subsequently sensed by the central nervous system, as acid triggers acid sensing receptors in sensory neurons[27]. Early studies in long COVID patients suggest a higher lactate accumulation[31], indicative of more acidosis, however it is unknown whether this is a result of altered skeletal muscle metabolism or due to central nervous signal integration.

PEM, which can be instigated by both physical, cognitive and emotional exertion, still remains largely unknown as to its physiological onset and its functional repercussions following exertion. It is understood that PEM episodes result in worsening of patient condition, however the exertional threshold resulting in PEM is patient dependent and often will vary daily or weekly or by type of exertion within a single individual[32]. Thus, PEM creates a scenario in which the patient is largely unknowing of whether a certain stimulus may result in a PEM episode or not. Overtime, this can result in patients experiencing PEM abstaining from physical activity, reducing social contact, or decreasing work severely in order to manage PEM and the associated symptoms following a PEM episode. This removes the patient from their regular routine, and creates an instability in their daily lives. Further, it is well known that the reduction in social[33,34] and physical activity[35,36] can have dramatic impacts on patient well-being and mental health. Moreso, as it is poorly understood the underlying physiology behind PEM, it is unknown whether PEM may be triggered by oxidative or structural skeletal muscle damage during exercise.

It has been suggested that the severity of infection is likely predictive of long COVID occurrence[37–40]. However, in that mild COVID cases also develop into long COVID suggests that severity alone cannot account for the development of long COVID[22]. Thus, other likely

explanations include recurring immune response (possibly from viral persistence), the development of autoimmunity, the development of sarcopenia, physical inactivity, and psychological alterations[21,41–45].

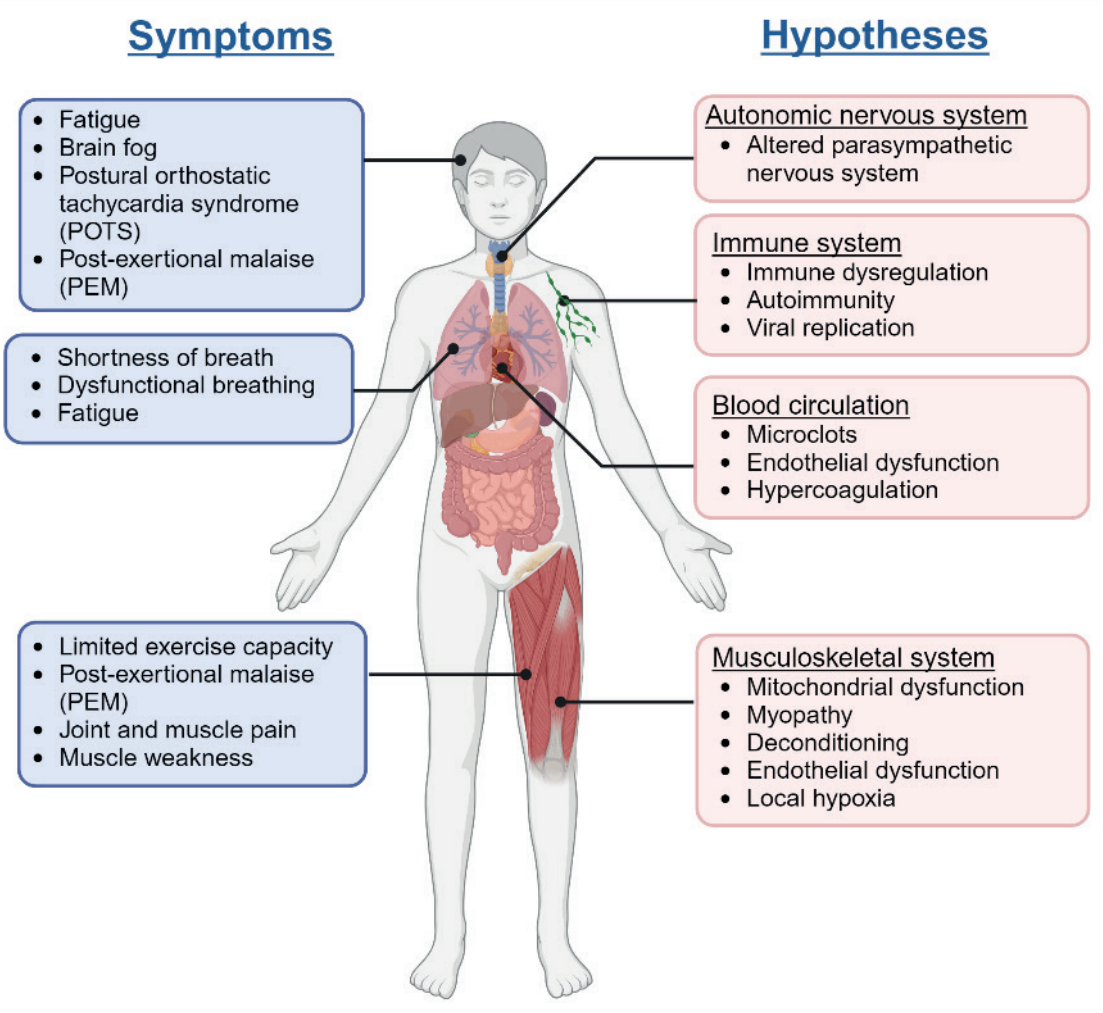


Figure 1: Symptoms (blue boxes) common to both patients with long COVID and ME/CFS, along with pathophysiological hypotheses (red boxes) with regards to each symptom. Common bodily systems of interest include the brain, lungs, skeletal muscle, autonomic nervous system, immune system, and circulatory system.

Although patient psychological state may be affected during acute infections, particularly in the case of hospitalizations[46] (i.e. similar to post-traumatic stress disorder), this has been largely discounted for being a sole contributor to long COVID development. Early studies have shown that SARS-CoV-2 could be detected via PCR testing upwards of 20 months following initial

infection[47], suggesting that persistent viral load may rather contribute. Additionally, imaging studies of individuals whom had recovered from an acute infection have been shown to have abnormal accumulations in the lungs[48], indicative of an ongoing inflammatory response. Thus, the evidence suggests an underlying physiological response in long COVID related to continuity of symptoms.

While there are some indications that there are persistent immune responses in patients, no studies have found alterations in blood immune cell activation, cytokine profiles, or markers such as c-reactive protein, which would normally be indicative of infection or inflammatory responses[21]. Some early research has indicated that long COVID indicated the development of sarcopenia[45]. However, due to the inconsistency with which long COVID is diagnosed, a large majority of these patients may have presented with pre-sarcopenia prior to infection, and patients recovering from an intensive care unit admission likely have a longer period of recovery[49–51]. This then called for a revision and definitive definition of long COVID for more accurate diagnosis[20,26]. Specifically, it is noted that symptoms experienced by patients cannot be accounted for by any other co-morbidity, hospitalization event, or sex- or age-related phenomena.

Due to the reduction in physical activity levels of patients with long COVID, it is surmised that deconditioning may be implicated in its progression[52,53]. It is well documented that mild to severe reductions in physical activity have reduced whole-body aerobic capacity, altered skeletal muscle oxidative function, and alterations to metabolism[54–63], all of which may negatively influence immune response and function[64]. Skeletal muscle itself has been implicated largely in endocrine function and can heavily influence immune function[65–67]. However, whether skeletal muscle alterations occur in long COVID patients is largely unknown.

Autoimmunity, which is the production of antibodies against one's own tissue such that one's self is recognized as a pathogen by immune cells, is not an uncommon development following some infections[68,69]. For example, it is well documented that cases of multiple sclerosis (MS) have developed after an initial Eppstein-Barr or measles viral infection[70–72]. While there are some indications of autoantibodies being present in patients with long COVID[73,74], it is unknown whether this impacts the skeletal muscle of patients.

Myalgic encephalomyelitis/chronic fatigue syndrome

Myalgic encephalomyelitis/chronic fatigue syndrome (ME/CFS) is another disease in which patients experience the poorly understood symptom of PEM[75]. Typically, following acute viral or bacterial infections, the majority of people are able to resolve symptoms within 1-2 weeks[76,77], and can return to normal routine. However, in some individuals, symptoms may never fully resolve, and in some cases symptoms may worsen or patients may develop new symptoms[78–80]. The prolonged continuation of symptoms longer than 6 months, which does not improve despite rest and the presence of PEM, results in ME/CFS diagnosis[75]. Patients with ME/CFS often observe reduced cognition (i.e. difficulties concentrating or remembering), orthostatic intolerance, disturbed sleep, and muscle pain[73]. Research of ME/CFS, which was initially recognized in the 1950's, has produced a myriad of theories as to the development of symptoms associated with ME/CFS. Some studies indicated that an exhausted or abnormal immune response in patients with ME/CFS, due to the frequent onset following an infection like stimulus. However, in many instances, patients could not recall a recent illness, but rather a trauma, high workload or other overstimulating life event[81,82]. Due to this association with high stress life events and epidemics, some historical accounts proposed that ME/CFS was largely a psychiatric disorder[81–83] and has been often compared to hysteria. However, whilst the disease remains poorly understood, there exists more evidence as an organic disease rather than psychiatric[84]. Early studies of patients with ME/CFS in indicated deranged mitochondrial formations[85,86], and as such was speculated that mitochondrial function may be impaired in patients with ME/CFS. While some studies have investigated metabolic alterations in ME/CFS, immune cells are reported to have lower respiration capacities[87–89], while skeletal muscle results are inconsistent[90,91], suggesting that perhaps the abnormal mitochondria do not result in significant alterations to patient skeletal muscle metabolism.

Skeletal Muscle Physiology: Implications in long COVID and ME/CFS Fatigue

Muscle contractile function

Everyday tasks involve movement of some kind, and while it may not be associated directly with voluntary exercise, skeletal muscle physiology dictates how we can perform these movements. For every movement we make, we perform skeletal muscle contractions, which is the result of multiple individual fibres contracting nearly simultaneously. For a muscle fibre to

contract, contractile elements must cycle between cross bridge formations, creating a ratcheting motion[92,93]. This involves myosin heads engaging with actin filaments, releasing, and sliding the myosin-titin structures past actin filaments. Therefore the ability for whole muscles to contract is dependent on several contractile and metabolic factors, but most predominantly myosin ATPase activity and oxidative function of the muscle fibre.

Muscle fibres can be classed by the myosin heavy chain, which can be classed generally as type I, type IIa, and type IIx in humans[94]. Type I fibres, known as "slow-twitch" myofibres, have myosin ATPases that have lower enzymatic rates, and are generally more oxidative in nature, typically possessing more mitochondria than type IIa and IIx fibres. Type IIx fibres then represent the other extreme, being "fast-twitch" and possessing myosin ATPases with high enzymatic rates, are heavily glycolytic in nature, whilst type IIa fibres are somewhat of an intermediate fast-twitch oxidative. The faster myofibres turn over ATP rapidly in order to accommodate rapid myosin-actin cross bridge cycling, whereas slower myofibres then turnover ATP and therefore the cross bridges at a slower rate. Early studies in ME/CFS show conflicting results with respect to fibre type dominance in patients[86,95,96].

Muscle Metabolic Demand

While all muscle fibre contractions have an energetic cost, not all muscle fibres have the same energetic needs. Muscle energetic needs are dictated largely by the contractile nature of myosin heads, due to their differing ATPase activities [90,93–95]. The generation of ATP is largely accounted for by four main biochemical processes: the phosphocreatine system, glycolysis, oxidative phosphorylation, and fatty acid oxidation (or β-oxidation)[97,98]. The phosphocreatine system plays a dual role in energy homeostasis, the first being rapid production of ATP by the transfer of phosphate from phosphocreatine to ADP, resulting in creatine and ATP[99]. The phosphocreatine system also supports the transfer of ADP and ATP in and out of the mitochondria too support oxidative phosphorylation[99]. Glycolysis, on the other hand, is primarily involved in ATP production[100,101], however metabolites can be shuttled through other metabolic pathways to support processes such as nucleotide production[101]. Glycolysis begins with glucose entry into the cell and through several biochemical reactions results in the production of lactate from pyruvate, and ultimately generating 2 ATP molecules per glucose molecule[101].

Oxidative phosphorylation (Figure 2) largely begins with the process of glycolysis, but rather than producing 2 lactate molecules from pyruvate, citric acid is produced, which subsequently

enters the tricarboxylic acid (TCA) cycle by conversion to acetyl CoA[102]. Within the TCA cycle, 2 ATP molecules are produced directly, with an additional 8 NADH and 2 $FADH_2$ reducing equivalents. These reducing equivalents then can be utilized by either complex I or complex II of the mitochondria to instigate transfer of electrons through to cytochrome c oxidase (or complex IV) of the respiratory chain. Cytochrome c oxidase then passes the donated electrons to the final electron acceptor: oxygen. The flow of electrons down the respiratory chain creates an electrochemical gradient, which can then be utilized by complex V (or ATP synthase) to generate ATP. Oxidative phosphorylation then results in 30-32 ATP per glucose molecule. Lastly, fatty acid oxidation is the process by which fatty acids are broken down into smaller chains, releasing a fatty-acyl CoA and acetyl-CoA, which can again enter the TCA cycle[103]. The total number of ATP generated then depends on the length of the fatty acid, but will generate 4-7 ATP per carbon length.

With the exceptions of the phosphocreatine system and glycolysis, the generation of ATP requires oxygen to generate the electrochemical gradient for ATP synthase to utilize. Therefore, for every contraction we perform, there is an associated oxygen cost to replenish ATP utilized, and as such oxygen utilization during exercise is an indirect reflection of ATP utilization and oxidative phosphorylation for a given workload. Thus, the use of cardiopulmonary exercise tests[104] (CPET), which measures oxygen consumption and carbon dioxide production at the mouth (or invasively using catheters), can be very informative of maximal oxidative function expected at the muscle. In instances where oxygen uptake at the lungs is restricted (in the case of chronic obstructive pulmonary disorder) or oxygen distribution to the muscles is impaired (in the case of chronic heart failure), there becomes a mismatch between oxygen consumption, carbon dioxide production, and oxygen utilization at the muscle[102–104].

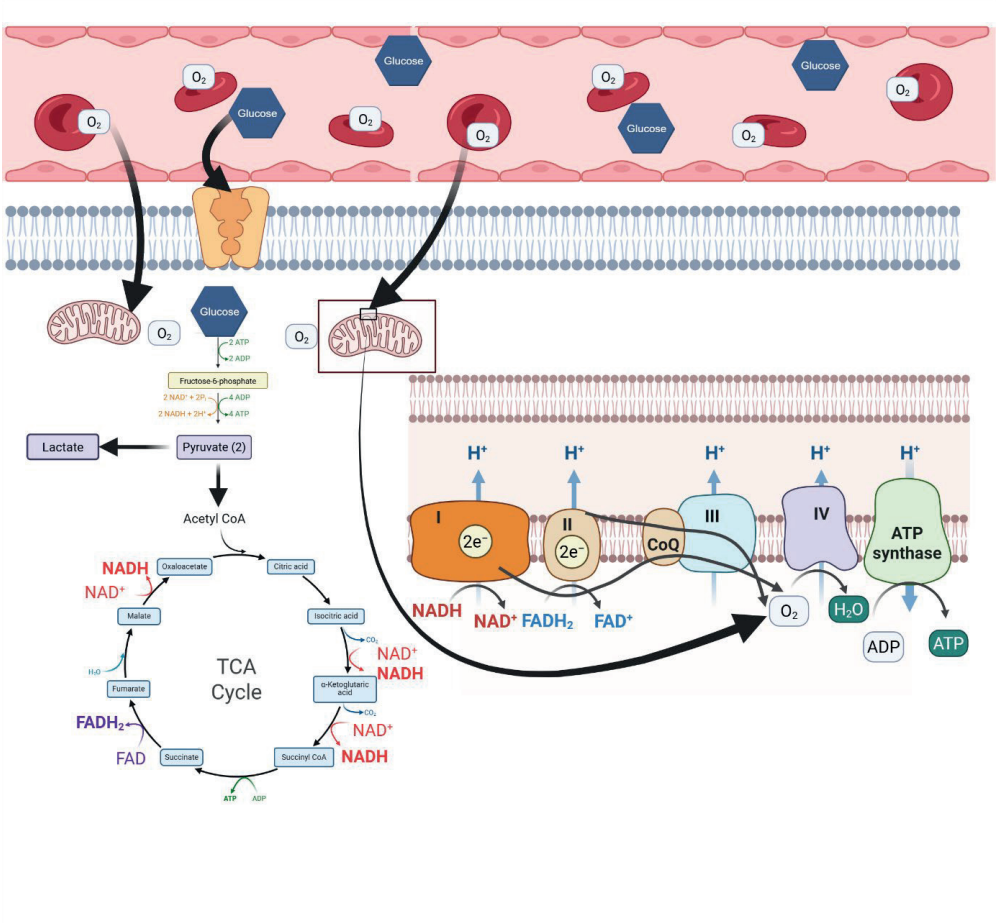


Figure 2: Graphical representation of oxygen and glucose utilization during exercise. Oxygen passively diffuses from the capillary into the myocyte, where it binds to myoglobin to be further distributed throughout the intracellular space. Oxygen is then utilized as the final electron acceptor of the electron transport chain at complex IV in the mitochondria. Complexes I-IV move protons into the intermembrane space to generate a proton gradient, which can be used by complex V to convert ADP to ATP. Glucose is taken up by the myocyte via either GLUT2 or GLUT4, and enters into glycolysis. Pyruvate, the final metabolite in glycolysis, will either be converted to lactate when oxygen is restricted or acetyl-CoA when oxygen is plentiful. Acetyl-CoA then enters the tricarboxylic acid cycle (TCA cycle), where the substrates NADH and $FADH_2$ are generated to initiate oxidative phosphorylation via complex I and II respectively.

Muscle Fatigue

Depending on duration and intensity of exercise, muscle fibres (and therefore whole muscles) will become fatigued. Muscle fatigue can be due to several factors, including low oxygen supply to the working muscle to support oxidative phosphorylation, insufficient substrates to

support, disbalance of intracellular sodium, potassium and calcium ions, and increased intracellular hydrogen ion concentration[30,105,106]. Due to oxygen being the final electron acceptor of oxidative phosphorylation, sufficient oxygen supply to the working muscle fibres is necessary to maintain efficient ATP production. When work rates exceed the rate of which oxygen can be extracted from the capillary into the muscle, muscle fibre metabolism shifts towards glycolysis to maintain ATP production despite oxygen restriction[100]. While this avoids the initial restriction of oxygen, glycolysis is then dependent on the amount of substrates available, namely glucose and glycogen. As the dependency on glycolysis increases, muscle fibres will take up glucose from the bloodstream or via breakdown of muscle glycogen. The final step of glycolysis is the conversion of pyruvate to lactate, which additionally produces a free hydrogen ion. Lactate can eventually enter the TCA cycle via monocarboxylate transporters, and can enter the bloodstream[107]. Thus, elevated blood lactate during exercise indicates the transition from oxidative phosphorylation to glycolysis.

While lactate can be used as fuel, the rise in intracellular hydrogen ions reduces cross bridge formation, reduces myosin calcium sensitivity, and decreases velocity of shortening[30]. Sodium-hydrogen exchangers become more active to move hydrogen extracellularly, resulting in increased intracellular sodium[108,109]. Subsequently, the sodium-potassium ATPase becomes increasingly more active, particularly the α_2-β heterodimer, which is instigated during exercise[110]. Whilst this aims to rebalance the sodium-potassium ion gradients (which is necessary for initiating contractions), this also consumes large amounts of ATP, driving energy production demand higher.

With each contraction, calcium is released from the sarcoplasmic reticulum, which then binds to troponin to initiate myosin head binding to actin[111]. As high intracellular calcium levels are cytotoxic, calcium must be quickly removed from the cytosol either via Sarcoplasmic reticulum calcium ATPases (SERCAs) back to the sarcoplasmic reticulum or via the sodium-calcium exchanger extracellularly[112,113]. As SERCA proteins utilize ATP hydrolysis to drive calcium back into the sarcoplasmic reticulum, increased contractions result in again higher ATP demands to support the removal of calcium via SERCA. Calcium is predominantly removed from the cytosol via the sodium-calcium exchangers, which are also known to be strongly inhibited by intracellular protons[114]. Intracellular calcium and sodium also can enhance and inhibit NCX activity respectively[113]. As exercise increases, the intracellular sodium concentration rises, thus reducing the efficiency of the sodium-calcium exchanger. Calcium

can also be sequestered in the mitochondria via mitochondrial calcium uptake 1, albeit to a much lesser extent than either SERCA or sodium-calcium exchangers.

Fatigue is then the result of the inability of working muscle to maintain sufficient ATP to maintain the various chemical gradients and perform cross bridge cycling. While very little is known about skeletal muscle alterations in either long COVID or ME/CFS, patients with long COVID or ME/CFS have been reported to have higher blood lactate levels either at rest or following exercise[95,115], which may indicate more glycolytic metabolic function. In patients with ME/CFS, where deranged mitochondria have been noted, it is plausible that their ability to generate sufficient ATP during exercise is impacted, resulting in earlier fatigue and lower exercise capacities. While it is generally known how alterations at the skeletal muscle level may relate to whole-body aerobic exercise capacity[55–57,116,117], this has not been assessed in either long COVID or ME/CFS. While studies have investigated whole-body aerobic capacity and cellular bioenergetics in ME/CFS, this typically involves the use of peripheral blood mononuclear cells. Therefore, it is largely unknown how skeletal muscle metabolic alterations in ME/CFS are subsequently reflected in whole-body aerobic capacity and earlier fatigue onset. Although patients with long COVID encounter similar symptoms, particularly debilitating fatigue, it is unknown whether skeletal muscle of long COVID patients also have evidence of altered metabolic function, and whether this contributes to lower exercise capacities. There is therefore a large gap in the field that may explain (at least in part) the debilitating fatigue experience by patients with long COVID and ME/CFS, and how these alterations may also relate to a differential response to exercise or other physical stressors.

Acute Exercise Responses: Possible Contributions to Post-Exertional Malaise

While the reduction in aerobic exercise capacity may be attributed to multiple factors, either in isolation or in concert, the adaptive response to acute exercise in ME/CFS and long COVID has not been investigated. Acute exercise bouts often lead to small amounts of microdamage, which instigates a brief pro-inflammatory period that is resolved rapidly by anti-inflammatory responses[118]. These signals often trigger transcriptional and translational changes, particularly involving mitochondrial biogenesis, oxidative phosphorylation, contractile protein maintenance, antioxidation, and capillarization[62,66,117,119–124]. For an appropriate response to exercise signalling, resident immune cells, satellite cells, fibroadipogenic progenitor cells, and

endothelial cells, amongst others must cooperate in concert[118,125–133]. Thus, any dysregulation in one or many of the signalling of these cells may have repercussions in muscle adaptation.

The initial inflammatory response (Figure 3) to acute exercise aids to dispose of damaged proteins and membranes and instigate cellular remodelling to adapt to the stress. Damage markers, such as mitochondrial-DNA[66], can be extruded by the organelles following exercise. These signals can subsequently activate the NLRP3 inflammasome[134], instigating type I interferon activation. Ultimately, this can result in the increase production of IL-6 and TNF-α, which then promotes a proinflammatory response in the local environment[118]. Cytokine release from the muscle then results in activation of resident macrophages, which phagocytose extracellular debris. While this is more widely seen with severe muscle damage, it does occur to a lesser extent with non-damaging exercise as well.

As debris is removed, $CD4^+$ T-helper cells secrete IL-4 and IL-13[135] to promote M2 macrophage polarization, instigating a transition from a pro-inflammatory to anti-inflammatory phenotype[136,137]. M2 macrophages then secrete anti-inflammatory IL-10 and TGF- β, the latter of which promotes fibroadipogenic progenitor cell activation[126,127].

In turn, fibroadipogenic progenitor cells also activate muscle stem cells[138], known as satellite cells. Satellite cells are quiescent, but once activated a proportion of the activated satellite cells will integrate as myonuclei. Only about 10% of the activated satellite cells will integrate as myonuclei, whilst the remainder will finish their cell cycle, replenishing the satellite cell pool, and return to quiescence. The integration of new myonuclei are necessary for proper muscle regeneration[139]. As with all stem cells, satellite cells can only undergo a finite number of cell cycles before senescence, complete arrest of the cell cycle. This is most often seen in aging, however has been associated with a number of other neuromuscular diseases that result in severe muscle damage.

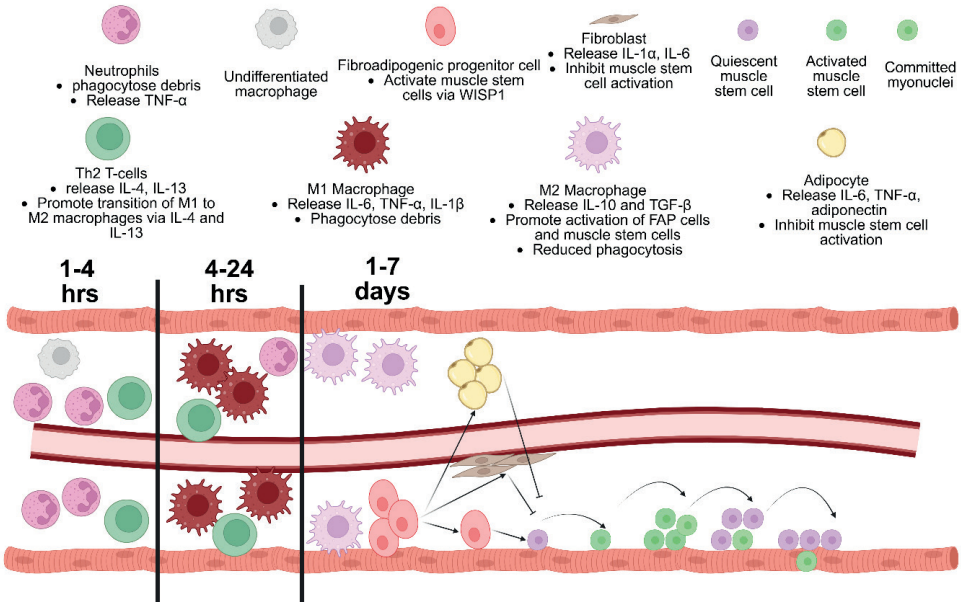


Figure 3: Graphical representation of typical resident mononuclear cell responses to damage. Neutrophils and macrophages are rapidly mobilized and remove debris from the damaged area (within 24hrs) producing an acute pro-inflammatory environment. Over several days, macrophages polarize to M2 macrophages, which promote an anti-inflammatory environment. Fibroadipogenic progenitor cells then may differentiate into an activated state, fibroblasts, or adipocytes. Activated fibroadipogenic progenitor cells activate satellite cells to proliferate and differentiate, of which ~10% of differentiated satellite cells integrate as myonuclei, while the remainder return to quiescence.

In both long COVID and ME/CFS, there are indications of continual immune responses. It has been shown in instances of acute infections that the immune response coincides with minor amounts of muscle damage[140,141], likely due to the pro-inflammatory cytokines IL-6 and TNF-alpha. Further, it is well known that intense exercise or exertion also results in initial pro-inflammatory responses to activate resident immune cells, which ultimately resolve with time. In both long COVID and ME/CFS, it may be that minor amounts of exertion coupled with possible persistent immune response results in an inappropriate pro-inflammatory response for the given stimulus, thus resulting in the worsening of symptoms. The time course of PEM has yet to been studied, and whether PEM itself results in muscle damage is unknown.

While little is known about PEM onset and the physiological underpinnings, it has been hypothesized that PEM induces a hyperinflammatory response, wherein resident cells are activated despite no occurrence of muscle damage. Thus, it may be that over time, repeated PEM exposure may reduce the viability of these resident cells to respond to acute stressors.

Thesis aims

This thesis therefore seeks to address several knowledge gaps related to long COVID and ME/CFS.

1. Do patients with long COVID that experience PEM exhibit skeletal muscle alterations that may contribute to symptoms, such as myalgia and PEM (Chapter 2)?
2. Can whole-body aerobic capacities and skeletal muscle alterations in patients with long COVID and ME/CFS be attributed to physical inactivity alone (Chapters 6 and 8)?
3. Do long COVID and ME/CFS share similar skeletal muscle adaptations (Chapters 8 and 9)?
4. How are resident mononuclear cell populations affected in long COVID and ME/CFS? Particularly, are distinct populations of resident mononuclear cells preferentially affected that may partially explain patient symptoms, such as myalgia and PEM (Chapter 9)?
5. With the onset of post-exertional malaise, how does the metabolic landscape of skeletal muscle change (Chapters 2 and 9)?
6. Is the ability for patients to respond to exercise affected by differences in either a) resident mononuclear cells or b) alterations to metabolic landscapes following exercise (Chapter 9)?

Chapters 2 and 8 aim to characterize the skeletal muscle alterations occurring in both patients with long COVID and ME/CFS. This chapter assesses the whole-body aerobic capacity of patients, which is compared to healthy age- and sex-matched controls whom recovered from an acute SARS CoV-2 infection. Here, skeletal muscle mitochondrial function, fibre type composition, capillarization and mitochondrial enzyme activity are also assessed to compare the underlying pathophysiology of the two diseases.

Chapters 3b, 4b, 5, 6, 7 and 8 all aim to address commonalities and differences in both whole-body and skeletal muscle alterations seen in a model of physical inactivity and in both long COVID and ME/CFS. Specifically, chapters 3b, 4b, 5, and 6 discuss the current state of literature of physical inactivity and how this compares to long COVID and ME/CFS. Chapter 7 specifically investigates the metabolic alterations over the course of 60 days of head-down tilt bed rest. Chapter 8 finally compares long COVID, ME/CFS and physical inactivity alongside one another, and assesses how these changes then relate to maximal aerobic capacity.

Chapter 9 aims to investigate the resident mononuclear cell populations and metabolic profile of long COVID and ME/CFS patients before and after post-exertional malaise onset. This chapter further addresses whether patients still maintain the potential to respond to exercise, or whether particular cell populations are impaired, which subsequently may explain the symptom of post-exertional malaise.

References

1. World Health Organization. WHO COVID-19 Dashboard. https://data.who.int/dashboards/covid19/cases?n=c (2024).
2. Cong, Y. & Ren, X. Coronavirus entry and release in polarized epithelial cells: a review. *Rev. Med. Virol.* **24**, 308–315 (2014).
3. Hikmet, F. *et al.* The protein expression profile of ACE2 in human tissues. *Mol. Syst. Biol.* **16**, MSB209610 (2020).
4. Jackson, C. B., Farzan, M., Chen, B. & Choe, H. Mechanisms of SARS-CoV-2 entry into cells. *Nat. Rev. Mol. Cell Biol.* **23**, 3–20 (2022).
5. Havervall, S. *et al.* Symptoms and Functional Impairment Assessed 8 Months After Mild COVID-19 Among Health Care Workers. *JAMA* **325**, 2015 (2021).
6. Jain, V. & Yuan, J.-M. Predictive symptoms and comorbidities for severe COVID-19 and intensive care unit admission: a systematic review and meta-analysis. *Int. J. Public Health* **65**, 533–546 (2020).
7. Bouwensch, C., Hahn, V. & Boulmé, F. Analysis of 160 nonhospitalized COVID-19 patients with mild to moderate symptoms from an Austrian general medical practice: from typical disease pattern to unexpected clinical features. *Wiener Medizinische Wochenschrift* **172**, 198–210 (2022).
8. Banholzer, N. *et al.* Absences, Symptoms and Respiratory Viruses in a Swiss School: Longitudinal Study With Serial Saliva Sampling. *Influenza Other Respir. Viruses* **19**, (2025).
9. Coverstone, A. M., Wang, L. & Sumino, K. Beyond Respiratory Syncytial Virus and Rhinovirus in the Pathogenesis and Exacerbation of Asthma. *Immunol. Allergy Clin. North Am.* **39**, 391–401 (2019).

10. McLean, H. Q., Peterson, S. H., King, J. P., Meece, J. K. & Belongia, E. A. School absenteeism among school-aged children with medically attended acute viral respiratory illness during three influenza seasons, 2012-2013 through 2014-2015. *Influenza Other Respir. Viruses* **11**, 220–229 (2017).

11. Diesner-Treiber, S. C. *et al.* Respiratory Infections in Children During a Covid-19 Pandemic Winter. *Front. Pediatr.* **9**, (2021).

12. van Diepen, S. *et al.* Association Between Vaccination Status and Outcomes in Patients Admitted to the ICU With COVID-19*. *Crit. Care Med.* **51**, 1201–1209 (2023).

13. Eyre, D. W. *et al.* Effect of Covid-19 Vaccination on Transmission of Alpha and Delta Variants. *New England Journal of Medicine* **386**, 744–756 (2022).

14. Laitin, S. M. D. *et al.* Impact of Vaccination Status on COVID-19 Severity and Pulmonary Involvement. *Medicina (B. Aires).* **60**, 1919 (2024).

15. Semenzato, L. *et al.* COVID-19 mRNA Vaccination and 4-Year All-Cause Mortality Among Adults Aged 18 to 59 Years in France. *JAMA Netw. Open* **8**, e2546822 (2025).

16. Wang, D. *et al.* Clinical Characteristics of 138 Hospitalized Patients With 2019 Novel Coronavirus–Infected Pneumonia in Wuhan, China. *JAMA* **323**, 1061 (2020).

17. Huang, C. *et al.* Clinical features of patients infected with 2019 novel coronavirus in Wuhan, China. *The Lancet* **395**, 497–506 (2020).

18. Mandel, H. *et al.* Long COVID Incidence Proportion in Adults and Children Between 2020 and 2024: An Electronic Health Record-Based Study From the RECOVER Initiative. *Clinical Infectious Diseases* **80**, 1247–1261 (2025).

19. World Health Organization. Clinical management of COVID-19: Living guideline, 18 August 2023. *https://www.who.int/publications/i/item/WHO-2019-nCoV-clinical-2023.2* (2023).

20. Kerkhoff, T. J., Charlton, B. T., Appelman, B., van Vugt, M. & Wüst, R. C. I. Post COVID-19 condition: critical need for a clear definition and detailed pathophysiology. *J. Cachexia Sarcopenia Muscle* **13**, 2754–2756 (2022).

21. Proal, A. D. & VanElzakker, M. B. Long COVID or Post-acute Sequelae of COVID-19 (PASC): An Overview of Biological Factors That May Contribute to Persistent

Symptoms. *Frontiers in Microbiology* vol. 12 Preprint at https://doi.org/10.3389/fmicb.2021.698169 (2021).

22. Subramanian, A. *et al.* Symptoms and risk factors for long COVID in non-hospitalized adults. *Nat. Med.* **28**, 1706–1714 (2022).

23. Davis, H. E. *et al.* Characterizing long COVID in an international cohort : 7 months of symptoms and their impact. *eClinical Medicine* **38**, 101019 (2021).

24. Jason, L. A., Holtzman, C. S., Sunnquist, M. & Cotler, J. The development of an instrument to assess post-exertional malaise in patients with myalgic encephalomyelitis and chronic fatigue syndrome. *J. Health Psychol.* **26**, 238–248 (2021).

25. Holtzman, C. S., Bhatia, S., Cotler, J. & Jason, L. A. Assessment of Post-Exertional Malaise (PEM) in Patients with Myalgic Encephalomyelitis (ME) and Chronic Fatigue Syndrome (CFS): A Patient-Driven Survey. *Diagnostics* **9**, 26 (2019).

26. Thaweethai, T. *et al.* Development of a Definition of Postacute Sequelae of SARS-CoV-2 Infection. *JAMA* **329**, 1934 (2023).

27. Ugawa, S. *et al.* Amiloride-blockable acid-sensing ion channels are leading acid sensors expressed in human nociceptors. *Journal of Clinical Investigation* **110**, 1185–1190 (2002).

28. Gaesser, G. & Poole, D. Blood Lactate During Exercise: Time Course of Training Adaptation in Humans. *Int. J. Sports Med.* **09**, 284–288 (1988).

29. Cairns, S. P. & Lindinger, M. I. Lactic acidosis: implications for human exercise performance. *Eur. J. Appl. Physiol.* **125**, 1761–1795 (2025).

30. Allen, D. G., Lamb, G. D. & Westerblad, H. Skeletal Muscle Fatigue: Cellular Mechanisms. *Physiol. Rev.* **88**, 287–332 (2008).

31. de Boer, E. *et al.* Decreased Fatty Acid Oxidation and Altered Lactate Production during Exercise in Patients with Post-acute COVID-19 Syndrome. *Am. J. Respir. Crit. Care Med.* **205**, 126–129 (2022).

32. Davenport, T. E., Stevens, S. R., Stevens, J., Snell, C. R. & Van Ness, J. M. Development and measurement properties of the PEM/PESE activity questionnaire (PAQ). *Work* **74**, 1187–1197 (2023).

33. Ma, X., Piao, X. & Oshio, T. Impact of social participation on health among middle-aged and elderly adults: evidence from longitudinal survey data in China. *BMC Public Health* **20**, 502 (2020).

34. Oshio, T., Sugiyama, K. & Ashida, T. Impact of residing in neighborhoods of high social participation on health of retired workers: A multilevel analysis using nationwide longitudinal data in Japan. *SSM Popul. Health* **20**, 101281 (2022).

35. Cunningham, C., O' Sullivan, R., Caserotti, P. & Tully, M. A. Consequences of physical inactivity in older adults: A systematic review of reviews and meta-analyses. *Scand. J. Med. Sci. Sports* **30**, 816–827 (2020).

36. Snedden, T. R. *et al.* Sport and Physical Activity Level Impacts Health-Related Quality of Life Among Collegiate Students. *American Journal of Health Promotion* **33**, 675–682 (2019).

37. Yong, S. J. Long COVID or post-COVID-19 syndrome: putative pathophysiology, risk factors, and treatments. *Infect. Dis.* **53**, 737–754 (2021).

38. Tenforde, M. W. *et al.* Symptom Duration and Risk Factors for Delayed Return to Usual Health Among[1] M. W. Tenforde et al., "Symptom Duration and Risk Factors for Delayed Return to Usual Health Among Outpatients with COVID-19 in a Multistate Health Care Systems Network — United. *MMWR Morb. Mortal. Wkly. Rep.* **69**, 993–998 (2020).

39. Kamal, M., Abo Omirah, M., Hussein, A. & Saeed, H. Assessment and characterisation of post-COVID-19 manifestations. *Int. J. Clin. Pract.* **75**, 0–2 (2021).

40. Sudre, C. H. *et al.* Attributes and predictors of long COVID. *Nat. Med.* **27**, 626–631 (2021).

41. Filho, M. S. *et al.* Skeletal muscle alterations in patients with acute Covid-19 and post-acute sequelae of Covid-19. *Journal of Sarcopenia and Cachexia* **31**, 1–24 (2021).

42. Patterson, B. K. *et al.* Persistence of SARS CoV-2 S1 Protein in CD16+ Monocytes in Post-Acute Sequelae of COVID-19 (PASC) up to 15 Months Post-Infection. *Front. Immunol.* **12**, (2022).

43. Su, Y. *et al.* Multiple early factors anticipate post-acute COVID-19 sequelae. *Cell* **185**, 881-895.e20 (2022).

44. Ramakrishnan, R. K., Kashour, T., Hamid, Q. & Halwani, R. Unraveling the Mystery Surrounding Post-Acute Sequelae of COVID-19. *Front. Immunol.* **12**, 1–16 (2021).

45. Martone, A. M. *et al.* Sarcopenia as potential biological substrate of long COVID-19 syndrome: prevalence, clinical features, and risk factors. *J. Cachexia Sarcopenia Muscle* **13**, 1974–1982 (2022).

46. Tarsitani, L. *et al.* Post-traumatic Stress Disorder Among COVID-19 Survivors at 3-Month Follow-up After Hospital Discharge. *J. Gen. Intern. Med.* **36**, 1702–1707 (2021).

47. Dobaño, C. *et al.* Sustained seropositivity up to 20.5 months after COVID-19. *BMC Med.* **20**, 379 (2022).

48. Fesu, D. *et al.* Post-COVID interstitial lung disease in symptomatic patients after COVID-19 disease. *Inflammopharmacology* **31**, 565–571 (2023).

49. Jolley, S. E., Bunnell, A. E. & Hough, C. L. ICU-Acquired Weakness. *Chest* **150**, 1129–1140 (2016).

50. Kress, J. P. & Hall, J. B. ICU-Acquired Weakness and Recovery from Critical Illness. *New England Journal of Medicine* **370**, 1626–1635 (2014).

51. Vanhorebeek, I., Latronico, N. & Van den Berghe, G. ICU-acquired weakness. *Intensive Care Med.* **46**, 637–653 (2020).

52. Edward, J. A. *et al.* Characteristics and Treatment of Exercise Intolerance in Patients With Long COVID. *J. Cardiopulm. Rehabil. Prev.* **43**, 400–406 (2023).

53. Naeije, R. & Caravita, S. Phenotyping long COVID. *European Respiratory Journal* **58**, 2101763 (2021).

54. Akins, J. D. *et al.* Inactivity induces resistance to the metabolic benefits following acute exercise. *J Appl Physiol* **126**, 1088–1094 (2019).

55. Coyle, E. F. *et al.* Time course of loss of adaptations after stopping prolonged intense endurance training. *J. Appl. Physiol.* **57**, 1857–1864 (1984).

56. Chi, M. M. *et al.* Effects of detraining on enzymes of energy metabolism in individual human muscle fibers. *American Journal of Physiology-Cell Physiology* **244**, C276–C287 (1983).

57. Coyle, E. F., Martin, W. H., Bloomfield, S. A., Lowry, O. H. & Holloszy, J. O. Effects of detraining on responses to submaximal exercise. *J. Appl. Physiol.* **59**, 853–859 (1985).

58. Bergouignan, A., Rudwill, F., Simon, C. & Blanc, S. Physical inactivity as the culprit of metabolic inflexibility: evidence from bed-rest studies. *J. Appl. Physiol.* **111**, 1201–1210 (2011).

59. Salvadego, D. *et al.* Functional impairment of skeletal muscle oxidative metabolism during knee extension exercise after bed rest. *J. Appl. Physiol.* **111**, 1719–1726 (2011).

60. Murgia, M. *et al.* Signatures of muscle disuse in spaceflight and bed rest revealed by single muscle fiber proteomics. *PNAS Nexus* **1**, (2022).

61. Zuccarelli, L. *et al.* Peripheral impairments of oxidative metabolism after a 10-day bed rest are upstream of mitochondrial respiration. *J. Physiol.* **599**, 4813–4829 (2021).

62. Buso, A. *et al.* Mitochondrial Adaptations in Elderly and Young Men Skeletal Muscle Following 2 Weeks of Bed Rest and Rehabilitation. *Front. Physiol.* **10**, (2019).

63. Salvadego, D. *et al.* PlanHab* : hypoxia does not worsen the impairment of skeletal muscle oxidative function induced by bed rest alone. *J. Physiol.* **596**, 3341–3355 (2018).

64. Pinto, A. J. *et al.* Physiology of sedentary behavior. *Physiol. Rev.* **103**, 2561–2622 (2023).

65. Pillon, N. J., Bilan, P. J., Fink, L. N. & Klip, A. Cross-talk between skeletal muscle and immune cells: muscle-derived mediators and metabolic implications. *Am J Physiol Endocrinol Metab* **304**, 453–465 (2013).

66. Ma, J., Son, A. Y., Son, Y., Wang, P. & Hwang, P. M. Mitochondrial innate immune signaling in skeletal muscle adaptation to exercise. *Trends in Endocrinology & Metabolism* **37**, 115–123 (2026).

67. Pedersen, B. K. & Febbraio, M. A. Muscle as an Endocrine Organ: Focus on Muscle-Derived Interleukin-6. *Physiol. Rev.* **88**, 1379–1406 (2008).

68. Herrath, M. G. von & Oldstone, M. B. Virus-induced autoimmune disease. *Curr. Opin. Immunol.* **8**, 878–885 (1996).

69. Panoutsakopoulou, V. & Cantor, H. On the Relationship Between Viral Infection and Autoimmunity. *J. Autoimmun.* **16**, 341–345 (2001).

70. Jason, L. A. *et al.* Differentiating Multiple Sclerosis from Myalgic Encephalomyelitis and Chronic Fatigue Syndrome. *Insights Biomed.* **02**, (2017).

71. Tucker, W. G. & Andrew Paskauskas, R. The MSMV hypothesis: Measles virus and multiple sclerosis, etiology and treatment. *Med. Hypotheses* **71**, 682–689 (2008).

72. Lünemann, J. D. Epstein-Barr virus in multiple sclerosis. *Neurology* **78**, 11–12 (2012).

73. Sotzny, F. *et al.* Dysregulated autoantibodies targeting vaso- and immunoregulatory receptors in Post COVID Syndrome correlate with symptom severity. *Front. Immunol.* **13**, (2022).

74. Wallukat, G. *et al.* Functional autoantibodies against G-protein coupled receptors in patients with persistent Long-COVID-19 symptoms. *J. Transl. Autoimmun.* **4**, 100100 (2021).

75. Carruthers, B. M. *et al.* Myalgic Encephalomyelitis/Chronic Fatigue Syndrome. *J. Chronic Fatigue Syndr.* **11**, 7–115 (2003).

76. Lessler, J. *et al.* Incubation periods of acute respiratory viral infections: a systematic review. *Lancet Infect. Dis.* **9**, 291–300 (2009).

77. Dunning, J., Thwaites, R. S. & Openshaw, P. J. M. Seasonal and pandemic influenza: 100 years of progress, still much to learn. *Mucosal Immunol.* **13**, 566–573 (2020).

78. Underhill, R. A. Myalgic encephalomyelitis, chronic fatigue syndrome: An infectious disease. *Med. Hypotheses* **85**, 765–773 (2015).

79. Shikova, E. *et al.* Cytomegalovirus, Epstein-Barr virus, and human herpesvirus-6 infections in patients with myalgic encephalomyelitis/chronic fatigue syndrome. *J. Med. Virol.* **92**, 3682–3688 (2020).

80. Grach, S. L., Seltzer, J., Chon, T. Y. & Ganesh, R. Diagnosis and Management of Myalgic Encephalomyelitis/Chronic Fatigue Syndrome. *Mayo Clin. Proc.* **98**, 1544–1551 (2023).

81. McEvedy, C. P. & Beard, A. W. Royal Free Epidemic of 1955: A Reconsideration. *BMJ* **1**, 7–11 (1970).

82. McEvedy, C. P. & Beard, A. W. Concept of Benign Myalgic Encephalomyelitis. *BMJ* **1**, 11–15 (1970).

83. White, P. *et al.* Comparison of adaptive pacing therapy, cognitive behaviour therapy, graded exercise therapy, and specialist medical care for chronic fatigue syndrome (PACE): a randomised trial. *The Lancet* **377**, 823–836 (2011).

84. Thoma, M. *et al.* Why the Psychosomatic View on Myalgic Encephalomyelitis/Chronic Fatigue Syndrome Is Inconsistent with Current Evidence and Harmful to Patients. *Medicina (B. Aires).* **60**, 83 (2023).

85. Plioplys, A. V. & Plioplys, S. Electron-Microscopic Investigation of Muscle Mitochondria in Chronic Fatigue Syndrome. *Neuropsychobiology* **32**, 175–181 (1995).

86. Behan, W. M. H., More, I. A. R. & Behan, P. O. Mitochondrial abnormalities in the postviral fatigue syndrome. *Acta Neuropathol.* **83**, 61–65 (1991).

87. Myhill, S., Booth, N. E. & Mclaren-howard, J. Chronic fatigue syndrome and mitochondrial dysfunction. *Int. J. Clin. Exp. Pathol.* **2**, 1–16 (2009).

88. Booth, N. E., Myhill, S. & McLaren-Howard, J. Mitochondrial dysfunction and the pathophysiology of Myalgic Encephalomyelitis/Chronic Fatigue Syndrome (ME/CFS). *Int. J. Clin. Exp. Med.* **5**, 208–20 (2012).

89. Tomas, C., Elson, J. L., Strassheim, V., Newton, J. L. & Walker, M. The effect of myalgic encephalomyelitis/chronic fatigue syndrome (ME/CFS) severity on cellular bioenergetic function. *PLoS One* **15**, e0231136 (2020).

90. Barnes, P. R., Taylor, D. J., Kemp, G. J. & Radda, G. K. Skeletal muscle bioenergetics in the chronic fatigue syndrome. *J. Neurol. Neurosurg. Psychiatry* **56**, 679–683 (1993).

91. Lane, R. J. M., Barrett, M. C., Taylor, D. J., Kemp, G. J. & Lodi, R. Heterogeneity in chronic fatigue syndrome: evidence from magnetic resonance spectroscopy of muscle. *Neuromuscular Disorders* **8**, 204–209 (1998).

92. Barclay, C. J. Energetics of Contraction. *Compr. Physiol.* **5**, 961–995 (2015).

93. Hendry, J. I. *et al.* A human skeletal muscle cross-bridge model to characterize the role of metabolite accumulation in muscle fatigue. *Exp. Physiol.* **110**, 1283–1301 (2025).

94. Schiaffino, S. & Reggiani, C. Fiber Types in Mammalian Skeletal Muscles. *Physiol. Rev.* **91**, 1447–1531 (2011).

95. Lane, R. J. M. *et al.* Muscle fibre characteristics and lactate responses to exercise in chronic fatigue syndrome. *J. Neurol. Neurosurg. Psychiatry* **64**, 362–367 (1998).

96. Edwards, R. H. T., Gibson, H., Clague, J. E. & Helliwell, T. Muscle Histopathology and Physiology in Chronic Fatigue Syndrome. 102–131 (2007) doi:10.1002/9780470514382.ch7.

97. Radda, G. K. Control of Energy Metabolism During Muscle Contraction. *Diabetes* **45**, S88–S92 (1996).

98. Yin, H. *et al.* Metabolic-sensing of the skeletal muscle clock coordinates fuel oxidation. *The FASEB Journal* **34**, 6613–6627 (2020).

99. Guimarães-Ferreira, L. Role of the phosphocreatine system on energetic homeostasis in skeletal and cardiac muscles. *Einstein (São Paulo)* **12**, 126–131 (2014).

100. Hargreaves, M. & Spriet, L. L. Skeletal muscle energy metabolism during exercise. *Nat. Metab.* **2**, 817–828 (2020).

101. Kierans, S. J. & Taylor, C. T. Glycolysis: A multifaceted metabolic pathway and signaling hub. *Journal of Biological Chemistry* **300**, 107906 (2024).

102. Martínez-Reyes, I. & Chandel, N. S. Mitochondrial TCA cycle metabolites control physiology and disease. *Nat. Commun.* **11**, 102 (2020).

103. Houten, S. M., Violante, S., Ventura, F. V. & Wanders, R. J. A. The Biochemistry and Physiology of Mitochondrial Fatty Acid β-Oxidation and Its Genetic Disorders. *Annu. Rev. Physiol.* **78**, 23–44 (2016).

104. Mattavelli, I. *et al.* Beyond VO2: the complex cardiopulmonary exercise test. *Eur. J. Prev. Cardiol.* **30**, ii34–ii39 (2023).

105. Wan, J., Qin, Z., Wang, P., Sun, Y. & Liu, X. Muscle fatigue: general understanding and treatment. *Exp. Mol. Med.* **49**, e384–e384 (2017).

106. Fitts, R. H. Cellular mechanisms of muscle fatigue. *Physiol. Rev.* **74**, 49–94 (1994).

107. Zhang, L. *et al.* Lactate transported by MCT1 plays an active role in promoting mitochondrial biogenesis and enhancing TCA flux in skeletal muscle. *Sci. Adv.* **10**, (2024).

108. Bangsbo, J., Johansen, L., Graham, T. & Saltin, B. Lactate and H+ effluxes from human skeletal muscles during intense, dynamic exercise. *J. Physiol.* **462**, 115–133 (1993).

109. Bangsbo, J., Juel, C., Hellsten, Y. & Saltin, B. Dissociation between lactate and proton exchange in muscle during intense exercise in man. *J. Physiol.* **504**, 489–499 (1997).

110. Pirkmajer, S. & Chibalin, A. V. Na,K-ATPase regulation in skeletal muscle. *American Journal of Physiology-Endocrinology and Metabolism* **311**, E1–E31 (2016).

111. WAKABAYASHI, T. Mechanism of the calcium-regulation of muscle contraction: In pursuit of its structural basis. *Proceedings of the Japan Academy, Series B* **91**, 321–350 (2015).

112. Bolaños, P. & Calderón, J. C. Excitation-contraction coupling in mammalian skeletal muscle: Blending old and last-decade research. *Front. Physiol.* **13**, (2022).

113. Valentim, M. A., Brahmbhatt, A. N. & Tupling, A. R. Skeletal and cardiac muscle calcium transport regulation in health and disease. *Biosci. Rep.* **42**, (2022).

114. Scranton, K., John, S., Escobar, A., Goldhaber, J. I. & Ottolia, M. Modulation of the cardiac Na+-Ca2+ exchanger by cytoplasmic protons: Molecular mechanisms and physiological implications. *Cell Calcium* **87**, 102140 (2020).

115. Lien, K. *et al.* Abnormal blood lactate accumulation during repeated exercise testing in myalgic encephalomyelitis/chronic fatigue syndrome. *Physiol. Rep.* **7**, (2019).

116. Coyle, E. F. Physiological determinants of endurance exercise performance. *J. Sci. Med. Sport* **2**, 181–189 (1999).

117. Holloszy, J. O. Biochemical adaptations in muscle. Effects of exercise on mitochondrial oxygen uptake and respiratory enzyme activity in skeletal muscle. *J. Biol. Chem.* **242**, 2278–82 (1967).

118. Peake, J. M., Neubauer, O., Della Gatta, P. A. & Nosaka, K. Muscle damage and inflammation during recovery from exercise. *J. Appl. Physiol.* **122**, 559–570 (2017).

119. Smith, J. A. B., Murach, K. A., Dyar, K. A. & Zierath, J. R. Exercise metabolism and adaptation in skeletal muscle. *Nat. Rev. Mol. Cell Biol.* **24**, 607–632 (2023).

120. White, A. T. & Schenk, S. NAD+/NADH and skeletal muscle mitochondrial adaptations to exercise. *American Journal of Physiology-Endocrinology and Metabolism* **303**, E308–E321 (2012).

121. Klausen, K., Andersen, L. B. & Pelle, I. Adaptive changes in work capacity, skeletal muscle capillarization and enzyme levels during training and detraining. *Acta Physiol. Scand.* **113**, 9–16 (1981).

122. Houston, M. E., Bentzen, H. & Larsen, H. Interrelationships between skeletal muscle adaptations and performance as studied by detraining and retraining. *Acta Physiol. Scand.* **105**, 163–170 (1979).

123. Wibom, R. *et al.* Adaptation of mitochondrial ATP production in human skeletal muscle to endurance training and detraining. *J. Appl. Physiol.* **73**, 2004–2010 (1992).

124. Egan, B. & Sharples, A. P. Molecular responses to acute exercise and their relevance for adaptations in skeletal muscle to exercise training. *Physiol. Rev.* **103**, 2057–2170 (2023).

125. Fry, C. S., Kirby, T. J., Kosmac, K., McCarthy, J. J. & Peterson, C. A. Myogenic Progenitor Cells Control Extracellular Matrix Production by Fibroblasts during Skeletal Muscle Hypertrophy. *Cell Stem Cell* **20**, 56–69 (2017).

126. Brorson, J. *et al.* Complementing muscle regeneration—fibro-adipogenic progenitor and macrophage-mediated repair of elderly human skeletal muscle. *Nat. Commun.* **16**, 5233 (2025).

127. Nawaz, A. *et al.* Depletion of CD206+ M2-like macrophages induces fibro-adipogenic progenitors activation and muscle regeneration. *Nat. Commun.* **13**, 7058 (2022).

128. Bensalah, M. *et al.* A negative feedback loop between fibroadipogenic progenitors and muscle fibres involving endothelin promotes human muscle fibrosis. *J. Cachexia Sarcopenia Muscle* **13**, 1771–1784 (2022).

129. Joe, A. W. B. *et al.* Muscle injury activates resident fibro/adipogenic progenitors that facilitate myogenesis. *Nat. Cell Biol.* **12**, 153–163 (2010).

130. Natarajan, A., Lemos, D. R. & Rossi, F. M. V. Fibro/adipogenic progenitors: A double-edged sword in skeletal muscle regeneration. *Cell Cycle* **9**, 2045–2046 (2010).

131. Heredia, J. E. *et al.* Type 2 Innate Signals Stimulate Fibro/Adipogenic Progenitors to Facilitate Muscle Regeneration. *Cell* **153**, 376–388 (2013).

132. Murphy, M. M., Lawson, J. A., Mathew, S. J., Hutcheson, D. A. & Kardon, G. Satellite cells, connective tissue fibroblasts and their interactions are crucial for muscle regeneration. *Development* **138**, 3625–3637 (2011).

133. Shang, M. *et al.* Macrophage-derived glutamine boosts satellite cells and muscle regeneration. *Nature* **587**, 626–631 (2020).

134. Li, H. *et al.* Acute Exercise-Induced Mitochondrial Stress Triggers an Inflammatory Response in the Myocardium via NLRP3 Inflammasome Activation with Mitophagy. *Oxid. Med. Cell. Longev.* **2016**, (2016).

135. Zhu, J. T helper 2 (Th2) cell differentiation, type 2 innate lymphoid cell (ILC2) development and regulation of interleukin-4 (IL-4) and IL-13 production. *Cytokine* **75**, 14–24 (2015).

136. Mantovani, A. *et al.* The chemokine system in diverse forms of macrophage activation and polarization. *Trends Immunol.* **25**, 677–686 (2004).

137. Tidball, J. G. & Villalta, S. A. Regulatory interactions between muscle and the immune system during muscle regeneration. *American Journal of Physiology-Regulatory, Integrative and Comparative Physiology* **298**, R1173–R1187 (2010).

138. Lukjanenko, L. *et al.* Aging Disrupts Muscle Stem Cell Function by Impairing Matricellular WISP1 Secretion from Fibro-Adipogenic Progenitors. *Cell Stem Cell* **24**, 433-446.e7 (2019).

139. Roman, W. *et al.* Muscle repair after physiological damage relies on nuclear migration for cellular reconstruction. *Science (1979).* **374**, 355–359 (2021).

140. Åström, E., Friman, G. & Pilström, L. EFFECTS OF VIRAL AND MYCOPLASMA INFECTIONS ON ULTRASTRUCTURE AND ENZYME ACTIVITIES IN HUMAN SKELETAL MUSCLE. *Acta Pathologica Microbiologica Scandinavica Section A Pathology* **84A**, 113–122 (1976).

141. Downey, J. *et al.* Influenza hijacks myeloid cells to inflict type-I interferon-fueled damage in the heart. *Immunity* **59**, 637-650.e12 (2026).



Chapter 2

Muscle Abnormalities Worsen After Post-Exertional Malaise in Long COVID

Brent Appelman, Braeden T. Charlton, Richie P. Goulding, Tom J. Kerkhoff, Ellen A. Breedveld, Wendy Noort, Carla Offringa, Frank W. Bloemers, Michel van Weeghel, Bauke V. Schomakers, Pedro Coelho, Jelle J. Posthuma, Eleonora Aronica, W. Joost Wiersinga, Michèle van Vugt, Rob C.I. Wüst

Published in Nature Communications, January 2024



Abstract

A subgroup of patients infected with SARS-CoV-2 remain symptomatic over three months after infection. A distinctive symptom of patients with long COVID is post-exertional malaise, which is associated with a worsening of fatigue- and pain-related symptoms after acute mental or physical exercise, but its underlying pathophysiology is unclear. With this longitudinal case-control study (NCT05225688), we provide new insights into the pathophysiology of post-exertional malaise in patients with long COVID. We show that skeletal muscle structure is associated with a lower exercise capacity in patients, and local and systemic metabolic disturbances, severe exercise-induced myopathy and tissue infiltration of amyloid-containing deposits in skeletal muscles of patients with long COVID worsen after induction of post-exertional malaise. This study highlights novel pathways that help to understand the pathophysiology of post-exertional malaise in patients suffering from long COVID and other post-infectious diseases.

Introduction

Chronic sequelae after acute infections contribute to debilitating conditions that affect millions worldwide[1–5]. After an acute SARS-CoV-2 infection, a subgroup of patients suffers from Post-Acute Sequelae of COVID-19 (PASC), also called long COVID[1,6–10]. The most reported symptoms of long COVID include a limited exercise tolerance and post-exertional malaise, representing the worsening of symptoms after mental or physical exertion[1,8,10]. Current, yet unproven hypotheses explaining exercise tolerance and post-exertional malaise in long COVID include mitochondrial dysfunction, amyloid-containing deposit accumulation in blood vessels causing local hypoxia, systemic and local inflammation, disturbed immunological responses, hormonal imbalance and viral persistence[11–18]. The extent to which the underlying physiology of impaired exercise capacity can be separated from factors related to the onset of post-exertional malaise remains unclear, largely due to indirect assessment of the underlying biomedical and psychological parameters, the cross-sectional nature of most studies, and patient heterogeneity.

In this study, we systematically induced post-exertional malaise in a cohort of 25 well-defined patients with long COVID and controls. We obtained blood and skeletal muscle biopsies before and after a maximal exercise test (Supplemental Fig.1) with the aim to study the biological factors contributing to the limited exercise capacity and post-exertional malaise in long COVID. Results were compared with those obtained from 21 age- and sex-matched controls who fully recovered from a mild SARS-CoV-2 infection (Table 1). We characterized Long COVID based on the criteria established by the World Health Organization, and an important inclusion criterion was the presence of post-exertional malaise[19]. Both groups were healthy and socially active prior to the initial PCR-proven SARS-CoV-2 infection. No participants were hospitalized due to SARS-CoV-2 infection. Fatigue questionnaires and accelerometer data confirmed the impact of long COVID on daily life (Supplemental Fig.2). We show that skeletal muscle structure is associated with a lower exercise capacity in patients, and that local and systemic metabolic disturbances, severe exercise-induced myopathy and tissue infiltration of amyloid-containing deposits in skeletal muscles of patients with long COVID worsen after induction of post-exertional malaise.

Table 1. Participant characteristics.

	Healthy controls	**Long COVID**	**p-value**
Number of participants	21	25	
Demographics			
Age, mean (SD), years	42 (10)	41 (11)	0.82
Sex, male (%)	10 (47.6)	12 (48.0)	>0.99
BMI, mean (SD), kg/m^2	24.14 (3.37)	25.60 (4.62)	0.24
Charlson Comorbidity Index, median [IQR]	0 [0, 0]	0 [0, 1]	0.76
Hospitalization for COVID-19	0 (0)	(0)	>0.99
SARS-CoV-2 vaccination before participation (%)	21 (100)	24 (96.0)	>0.99
Weekly working hours before initial SARS-CoV-2 infection, median [IQR]	36 [32, 40]	36 [32, 45]	0.520
Weekly working hours during the study, median [IQR]	36 [32, 40]	5 [0, 12]	<0.001
Time since initial SARS-CoV-2 infection, median [IQR], days	142 [105, 405]	545 [455, 686]	0.001
Time since latest SARS-CoV-2 infection, median [IQR], days	135 [93, 197]	504 [329, 665]	0.002

Continuous parametric data were analyzed using a two-sided t-test and are shown as mean with SD. Continuous non-parametric data were analyzed using a two-sided Wilcoxon-test and are shown as median with interquartile range. P-values were not corrected for multiple testing.

Results

Limited exercise capacity in long COVID

All participants performed a cardiopulmonary exercise test on a cycle ergometer. Maximal oxygen uptake ($\dot{V}O_{2max}$) and peak power output were substantially lower in long COVID patients (Fig. 1A+B), despite marked inter-patient heterogeneity. Patients with long COVID had lower maximal ventilation and lower maximal end-tidal partial pressure of CO_2 ($PETCO_2$) implying poorer ventilatory function during exercise (Supplemental Fig.3A-C)[20–22]. The cardiovascular system was not compromised in long COVID patients (Supplemental Fig.3D-E), suggesting that this system does not explain the limited exercise capacity in patients with long COVID. The lower maximal O_2 pulse (i.e. the product of stroke volume and arteriovenous O_2 difference; Supplemental Fig.3F), gas exchange threshold (Fig.1C) and peripheral O_2 extraction (determined via near-infrared spectroscopy; Fig.1D-E, Supplemental Fig.3I) during exercise all indicated peripheral skeletal muscle impairments in patients. The lower $\dot{V}O_{2max}$ in patients was not due to submaximal effort during the exercise test, as the proportion of participants attaining a plateau in $\dot{V}O_2$ did not differ between groups, the gas exchange threshold was at similar percentages of $\dot{V}O_{2max}$, and secondary criteria ([lactate], maximal RER and heart rate) were attained in both groups (Supplemental Fig.3E, G-H).

Next, we assessed skeletal muscle structure and function to explain the lower exercise capacity in patients. Capillary density and the capillary-to-fiber ratio were not different between groups (Fig.2A-B). However, patients exhibited a trend towards lower capillary-to-fiber ratios ($p=0.08$, degrees of freedom 46), and capillary-to-fiber ratio correlated to $\dot{V}O_{2max}$ in both groups with identical slope and intercept (Fig.2C). Compared to healthy controls, we observed a higher proportion of highly fatigable glycolytic fibers in the vastus lateralis muscle in long COVID patients (Fig.2D, Supplemental Fig.4A-G), along with a lower cross-sectional area of fatigue-resistant type I fibers in females only (Supplemental Fig.4D-F). Fiber cross-sectional area was positively associated with maximal power output in both groups (Fig.2E), albeit with a significantly lower intercept for patients. For a given skeletal muscle size, patients did not attain the same peak power output, suggesting that exercise performance in patients was at least partly explained by intrinsic alterations in skeletal muscle force and fatigue characteristics. Succinate dehydrogenase (SDH) activity (a marker for mitochondrial content) correlated with $\dot{V}O_{2max}$ in healthy controls, but not in patients (Fig.2F). While patients had a significantly lower oxidative phosphorylation capacity (Fig.3A, ED 5A-H), no differences were observed in SDH activity (Fig. 3B-C; Supplemental

Fig. 5I-J), suggestive of a qualitatively lower mitochondrial respiration rather than a lower mitochondrial enzyme activity. Collectively, our data indicate that the lower exercise capacity in long COVID patients is associated with a greater proportion of high-fatigable glycolytic fibers and lower mitochondrial function, with a possible additional limitation of a lower capillarization and the ventilatory system.

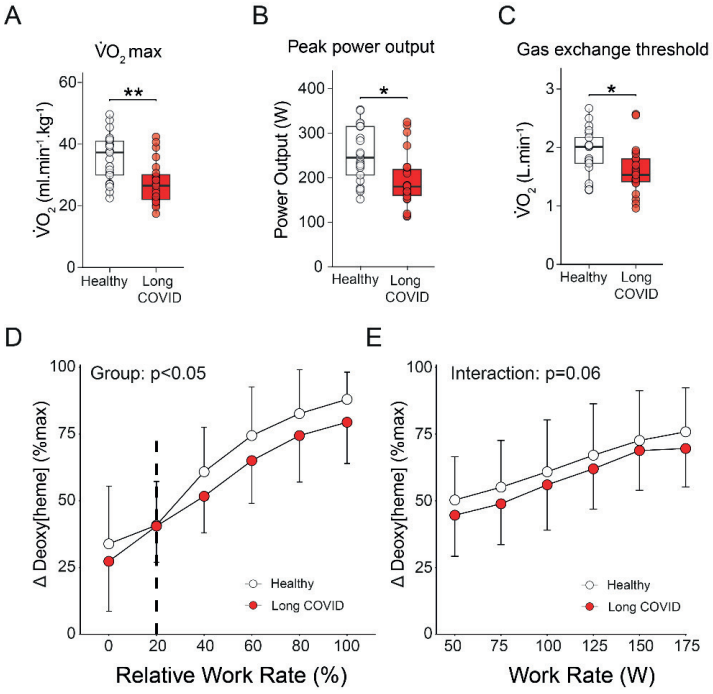


Figure 1. Lower exercise capacity in patients with long COVID. Maximal pulmonary oxygen uptake ($\dot{V}O_{2max}$, **A**, n=23 long COVID, n=21 healthy control), peak power output (**B**, n=25 long COVID, n=21 healthy control) and gas exchange threshold (**C**, n=23 long COVID, n=21 healthy control) were all lower ($p<0.0001$, $p=0.001$ and $p=0.014$, respectively)in patients with long COVID compared to healthy controls. **D-E**: Muscle deoxygenated [heme] responses (mean±SD) measured by near-infrared spectroscopy were lower ($p=0.023$) in long COVID (n=16), indicative of lower peripheral oxygen extraction during exercise compared to healthy controls (n=18; excessive adipose tissue precluded data analysis in remaining participants). Continuous parametric data were analyzed using a two-sided t-test (Panel **A-C**). Continuous parametric longitudinal data (mean+SD; Panel **D-E**) were analyzed with a generalized linear mixed model. P-values for panel **D-E** were determined with a two-sided ANOVA test. Dashed line (**D**) represents the average starting point of the exercise test. *$p<0.05$; **: $p<0.001$. Box plots show the median (centerline), the first and third quartiles (the lower and upper bound of the box) and the whiskers show the 1.5x interquartile range.

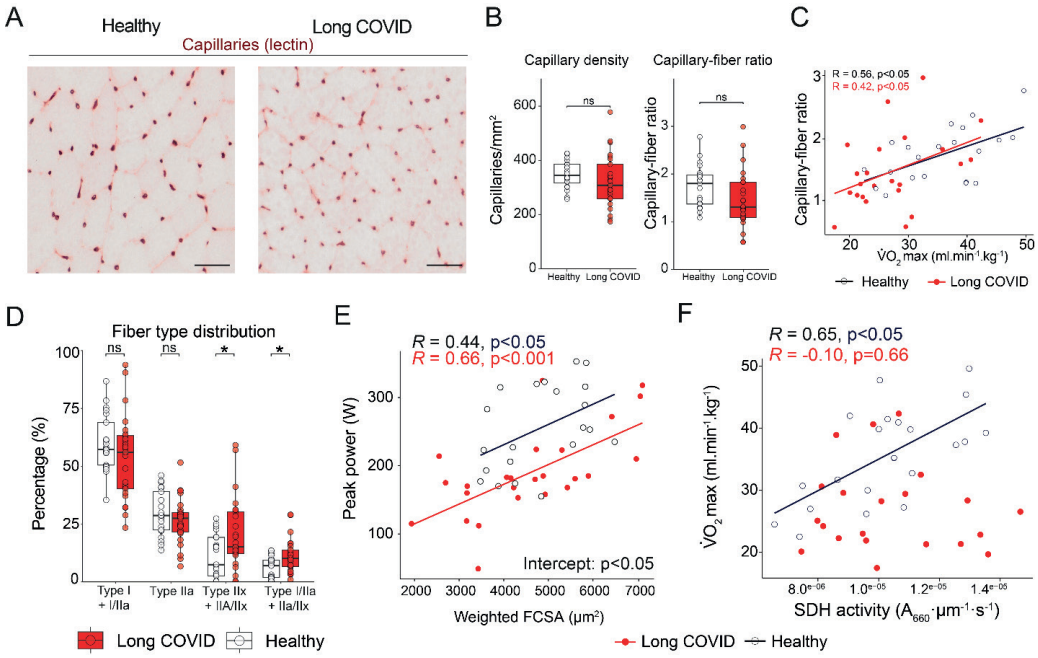


Figure 2. Skeletal muscle alterations are associated with exercise capacity in patients with long COVID. **A-B**: examples of skeletal muscle capillaries; no group-differences in capillary density (p=0.11) or capillary:fiber ratio (p=0.08) were observed (n=26 long COVID, n=21 healthy control). **C**: A significant association was found between capillary-to-fiber ratio and $\dot{V}O_{2max}$ for both groups (n=23 long COVID, p-value: 0.048, n=21 healthy control, p-value: 0.007). **D**: Patients with long COVID (n=25) had a higher percentage (p-value: 0.036) of glycolytic type IIx compared to healthy controls (n=21). **E**: For a given fiber cross-sectional area (FCSA), patients with long COVID (n=25) had a significantly lower peak power output (p-value: 0.045) as compared to healthy individuals (n=21). **F**: Succinate dehydrogenase (SDH) activity in sections (see also figure 3) was associated with maximal oxygen uptake consumption ($\dot{V}O_{2max}$) in healthy controls (n=21, p-value: 0.0014), but not in long COVID patients (n=23, p-value: 0.66), with significant different correlation coefficients. Continuous parametric data were analyzed using a two-sided t-test (**B, D**). Correlations were calculated using two-sided Pearson (**C, E-F**). The difference in intercept was calculated with a linear regression using a two-sided ANOVA (**E**). Correlation coefficients were compared using the R package *cocor*. *p<0.05; **: p<0.001. Bar: 100 µm. Box plots show the median (centerline), the first and third quartiles (the lower and upper bound of the box) and the whiskers show the 1.5x interquartile range.

Metabolic dysfunction and post-exertional malaise

To understand peripheral factors contributing to the development of post-exertional malaise, we obtained vastus lateralis muscle biopsies before and one day after the induction of post-exertional malaise. All long COVID patients experienced post-exertional malaise following maximal exercise, despite considerable heterogeneity in exercise capacity. Symptoms included

muscle pain, greater severity of fatigue and cognitive symptoms up to seven days after maximal exercise (Table 2, Supplemental Fig.2A-B). To systematically assess whether metabolic and mitochondrial dysfunction are associated to the pathophysiology of post-exertional malaise[23–26], we measured mitochondrial respiration and metabolomic signatures in skeletal muscle before and one day after the induction of post-exertional malaise. Mitochondrial respiration was assessed in hyperoxic conditions to avoid diffusion limitation for oxygen that could contribute to exercise intolerance in vivo. Oxidative phosphorylation capacity decreased one day following the maximal exercise in both controls and patients (Fig.3A). SDH activity was not reduced in healthy controls one day after exercise, but was reduced in the long COVID patients, suggesting that the combination of a reduced maximal mitochondrial respiration and decreased mitochondrial content are part of the pathophysiology of post-exertional malaise.

Table 2. Patient-reported symptoms before and during post-exertional malaise.

Symptoms	Baseline	1 day after induction of post-exertional malaise	1 week after induction of post-exertional malaise	p-value
	n=25	**n=25**	**n=25**	
Fatigue	25 (100.0)	25 (100.0)	24 (96.0)	0.36
Self-reported fatigue severity intensity (1-10), median [IQR]	6.00 [4.00, 7.00]	7.00 [7.00, 8.00]	7.00 [6.00, 7.25]	0.001
Cognitive problems	20 (80.0)	21 (84.0)	23 (92.0)	0.47
Self-reported cognitive severity intensity (1-10), median [IQR]	4.00 [3.00, 6.25]	6.00 [5.00, 8.00]	6.00 [4.00, 7.00]	0.06
Muscle or joint pain	16 (64.0)	20 (80.0)	15 (60.0)	0.276
Chest pain	8 (32.0)	11 (44.0)	8 (32.0)	0.59
Dyspnea	6 (24.0)	4 (16.0)	7 (28.0)	0.59
Anosmia	3 (12.0)	3 (12.0)	3 (12.0)	>0.99
Sore throat	2 (8.0)	5 (20.0)	3 (12.0)	0.45
Cold-like symptoms	1 (4.0)	0 (0.0)	2 (8.0)	0.35

Symptoms	Baseline	1 day after induction of post-exertional malaise	1 week after induction of post-exertional malaise	p-value
	n=25	**n=25**	**n=25**	
Cough	0 (0.0)	1 (4.0)	1 (4.0)	0.60

Continuous parametric data were analyzed using a two-sided t-test and are shown as mean with SD. Continuous non-parametric data were analyzed using a two-sided Wilcoxon-test and are shown as median with interquartile range. P-values were not corrected for multiple testing.

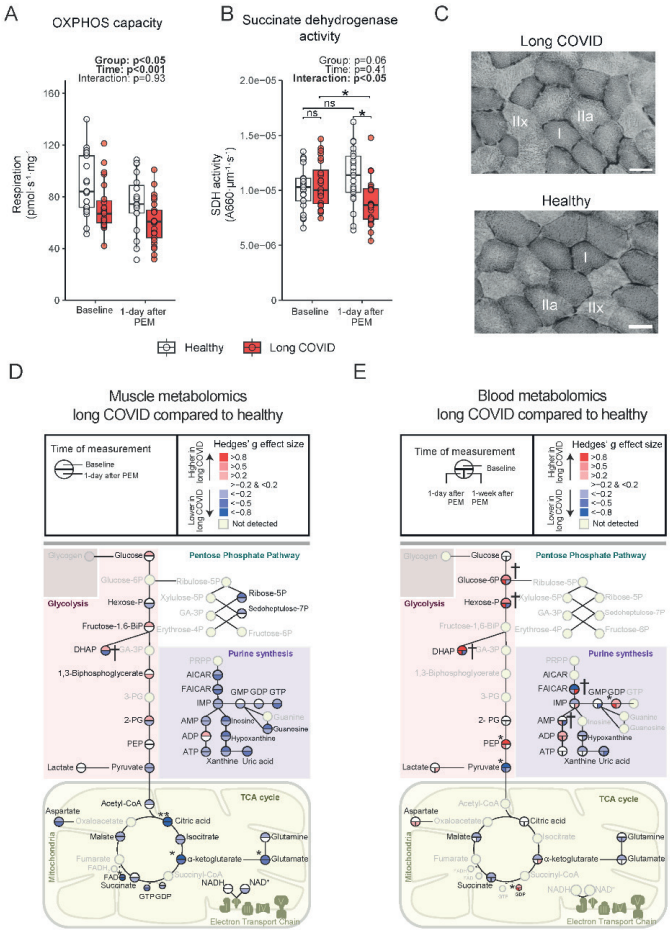


Figure 3. Metabolic and mitochondrial dysfunction in long COVID patients worsens with post-exertional malaise. **A:** Oxidative phosphorylation (OXPHOS) capacity was significantly lower in patients with long COVID (n=25) compared to healthy controls (n=21), and remained lower one day after induction of post-exertional malaise (PEM) in patients (Group: p=0.003, Time: p<0.001). **B:** Succinate dehydrogenase (SDH) activity, a marker for mitochondrial density, was not different between groups (p=0.06), and only reduced (p=0.0083) after induction of post-exertional malaise in long COVID patients (n=25) compared to healthy controls (n=21). A typical example of the SDH activity is shown in panel **C.** Skeletal muscle **(D)** and venous **(E)** metabolome pathways indicate slightly higher levels of metabolites related to glycolysis, and a lower abundance of metabolites related to purine synthesis and the tricarboxylic acid (TCA) cycle, indicative of a lower reliance on oxidative metabolism in patients with long COVID (n=25, both timepoints) as compared to healthy (n=19, both timepoints). Faded names were not measured and shown for clarity. A higher effect size in long COVID is shown in red, lower effect size in blue. Continuous parametric longitudinal data (Panel **A-B**, **D-E**) were analyzed with a generalized linear mixed model with a two-sided ANOVA. Post-hoc tests comparing each group were performed when the interaction term was significant and were performed using *emmeans* with BH adjustment (panel A-B). Effect sizes (**D-E**) were calculated with Hedges` g *p<0.05; **p<0.001; †p<0.05 indicates a significant interaction effect. Bar: 50 µm. Abbreviation: PEM; post-exertional malaise. Box plots show the median (centerline), the first and third quartiles (the lower and upper bound of the box) and the whiskers show the 1.5x interquartile range. Source data are provided in the Source Data File.

To better understand the resting skeletal muscle metabolism during post-exertional malaise, we annotated 116 metabolites in skeletal muscle and 83 metabolites in venous blood (Fig.3D-E, Supplemental Fig.6A-B). Skeletal muscle biopsies were obtained at rest, and while skeletal muscle glycolytic metabolites displayed few group differences, key metabolites of the tricarboxylic acid (TCA) cycle (including glutamate, FAD^+, alpha-ketoglutarate and citric acid) were lower in skeletal muscle of long COVID patients (Fig.3D). The ratio of citric acid to lactate in skeletal muscle was lower in long COVID patients, indicative of a shift away from oxidative metabolism in patients (Supplemental Fig.6C-D)[27]. Skeletal muscle creatine concentrations were lower in patients with long COVID (Supplemental Fig.6A), likely contributing to the lower oxidative phosphorylation capacity in patients. We also observed lower S-adenosylmethionine (SAM) in patients, possibly linking to a reduced methylation and SAM cycle activity in long COVID patients. Dihydroxyacetone phosphate, an important intermediate in lipid biosynthesis and glycolysis, was reduced in patient skeletal muscle following post-exertional malaise (Fig.3D). The lower hydroxyphenyllactic acid in patients is typically associated with increased mitochondrial production of reactive oxygen species (Supplemental Fig.6A-B)[28]. Metabolites related to pyrimidine and purine synthesis (such as ATP), which is a metabolically demanding process[29], tended to be lower between healthy controls and long COVID patients upon the induction of post-exertional malaise (Fig.3D,

Supplemental Fig.6A). Many amino acids were not different between groups at rest, but tended to be lower in patients upon the induction of post-exertional malaise (Supplemental Fig.6A). Glycolytic metabolites in the venous blood were significantly higher, but pyruvate and other TCA cycle metabolites were lower in patients compared to controls (Fig.3E). The induction of post-exertional malaise led to a reduction in blood glycolytic metabolites after one week, without changes in TCA cycle metabolites in long COVID patients. Various blood metabolites within the purine pathway were lower in patients compared to controls (Supplemental Fig.6B), but did not change with the induction of post-exertional malaise. From these analyses, we conclude that TCA cycle metabolites were lower in skeletal muscle and blood in long COVID patients, but did not change during post-exertional malaise. Venous blood glycolytic metabolites were higher at baseline and during post-exertional malaise, but decreased one week after the induction of post-exertional malaise.

Exercise-induced amyloid-containing deposit accumulation in skeletal muscle

It has been hypothesized that amyloid-containing deposits in the circulation can block local perfusion in long COVID, causing ischemia-reperfusion injury[30,31]. We studied whether amyloid-containing deposits were present in skeletal muscle of long COVID patients, and whether the indication of post-exertional malaise changed the concentration. We demonstrate that the concentration of amyloid-containing deposits was greater in the skeletal muscle of long COVID patients at baseline, and increased similarly in both groups after the induction of post-exertional malaise (Fig.4A-B). As an additional control group, skeletal muscle biopsies obtained before the outbreak of SARS-CoV-2 had similar amounts of amyloid-containing deposits as our healthy control group, confirming a basal, non-SARS-CoV-2-specific abundance of amyloid-containing deposits in healthy controls[13]. We next studied the location of these amyloid-containing deposits. Visualizing amyloid-containing deposits together with capillaries or lymph vessels revealed that the skeletal amyloid-containing deposits were not located in capillaries or lymphatic vessels, but rather next to capillaries and in the extracellular matrix between muscle fibers (Fig.4A+C-D). Amyloid-containing deposits did not overlap with cell nuclei suggesting that these deposits are located outside infiltrating (immune) cells. We conclude that amyloid-containing deposits are not present within capillaries. Neither did we observe any signs of skeletal muscle tissue hypoxia, as the skeletal muscle capillary-to-fiber ratio, capillary density (Fig.2B) and intracellular and circulating lactate concentrations (Supplemental Fig.3G+6A) were not different between long COVID patients and controls. Therefore, we conclude that post-exertional malaise cannot be explained by the hypothesis that

these deposits block vessel perfusion, causing local tissue hypoxia [30,32]. The underlying reason for the increased intramuscular accumulation of amyloid-containing deposits during post-exertional malaise remains elusive.

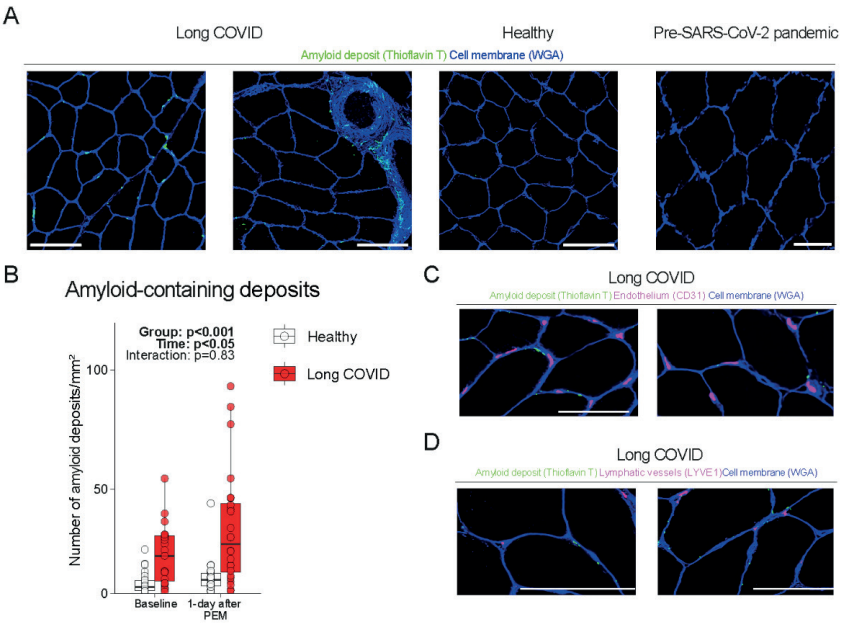


Figure 4. More amyloid-containing deposits in skeletal muscle, but not located inside capillaries or lymphatic vessels. **A**: Typical examples of amyloid-containing deposits in skeletal muscle. Pre-SARS-CoV-2 pandemic skeletal muscle sections stained with Thioflavin T showed similar levels of amyloid-containing deposits as healthy controls. **B**: The concentration of amyloid-containing deposits in skeletal muscle in long COVID patients (n=24) was higher (Group: $p<0.001$) than in healthy controls (n=21) and increases in long COVID patients and healthy controls upon exercise (Time: $p=0.008$). **C**: Amyloid-containing deposits were not found inside endothelial cells, but rather next to endothelial cells, or in the extracellular matrix between fibers. We performed the amyloid stainings on all patients and show a typical example in the figures. **D**: Amyloid-containing deposits were not located inside lymphatic vessels. Continuous parametric longitudinal data (Panel **B**) were analyzed with a generalized linear mixed model with a two-sided ANOVA. Bar: 100 µm. Abbreviation: PEM; post-exertional malaise. Box plots show the median (centerline), the first and third quartiles (the lower and upper bound of the box) and the whiskers show the 1.5x interquartile range.

Exercise-induced myopathy in long COVID

To further elucidate the pathophysiology of increased muscle weakness, fatigue and pain after exercise in long COVID patients, we determined whether specific pathological features were present in skeletal muscle before and after the induction of post-exertional malaise. As the

biopsy size was variable between participants and time-points, we scored biopsies negative/positive for pathological and immunological parameters. A larger percentage of long COVID patients displayed small atrophic fibers and focal necrosis (Fig.5A-B), which increased significantly after exercise, indicating an exacerbated tissue damage response in patients with long COVID. Since skeletal muscle is a plastic tissue, signs of skeletal muscle regeneration, such as centralized nuclei (Fig.5C), were more evident in long COVID patients, also before the induction of post-exertional malaise. Acutely regenerating fibers, evidenced by central nuclei and a basophilic cytoplasm, were seen in biopsies from both groups (Fig.5D), and exhaustive exercise increased the proportion of regenerating fibers in both healthy controls and long COVID patients without group differences. We conclude that severe exercise-induced muscle damage and subsequent regeneration are associated with the pathophysiology of post-exertional malaise, and can possibly explain muscle pain, fatigue and weakness in patients with long COVID experiencing post-exertional malaise.

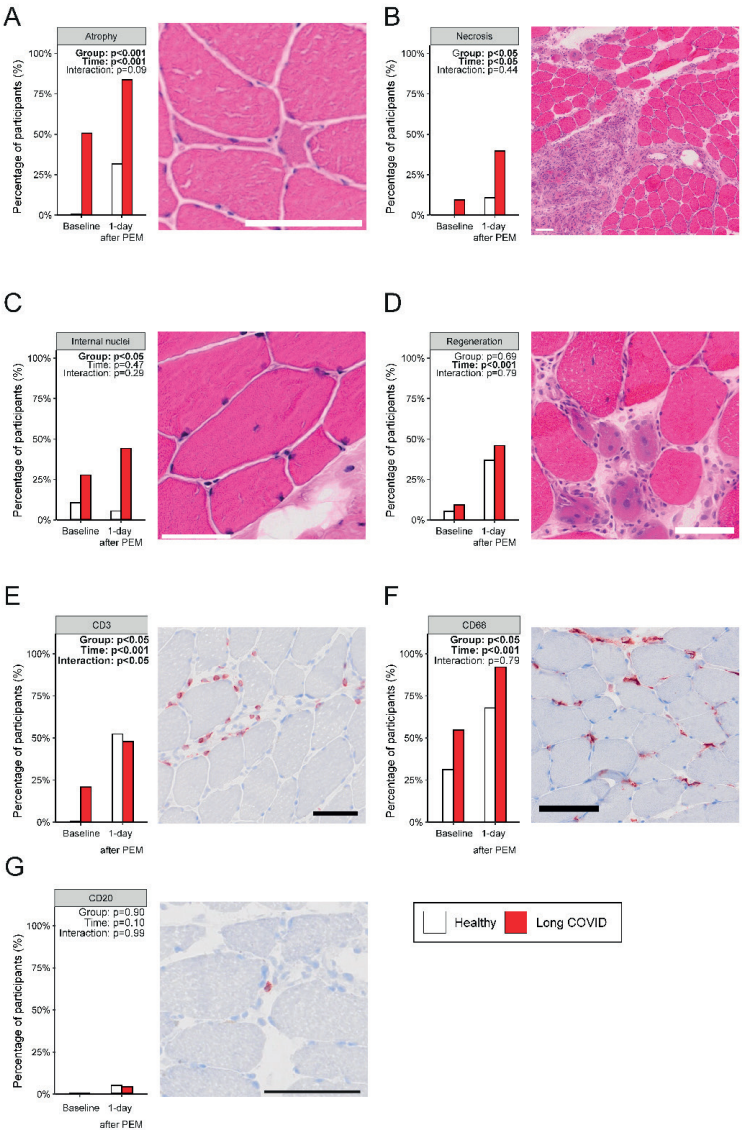


Figure 5. Pathological features in skeletal muscle in patients with long COVID. **A**: Very small and angulated atrophic fibers were more abundant in patients with long COVID and in the post-exercise biopsy in both groups (Group: p<0.001). **B**: Large areas of necrotic fibers were observed in 36% of patients with long COVID after exhaustive exercise (Group p-value: 0.09, as compared to healthy controls . **C**: Internal nuclei, indicative of fiber repair, were significantly more abundant (Group: p=0.002) in the skeletal muscle of patients with long COVID, but did not increase during post-exertional malaise (PEM). **D**: Regenerative fibers were not different between groups, but were more abundant in the post-exercise biopsy (Time: p<0.001). **E**: More patients with long COVID had CD3+ T-cell infiltration (Group: p=0.046). **F**: The presence of CD68+ macrophages was higher in long COVID patients (Group: p=0.03). **G**: CD20+ B-cells were not abundantly present in skeletal

muscle. All panels: n=25 long COVID, n=21 healthy controls. Categorical longitudinal data were analyzed using logistic regression with "time" as a covariate. Post-hoc comparisons (**E**) were using the Empirical Mean Differences using R package *emmeans* with BH adjustment. Bar: 100 μm. Abbreviation: PEM; post-exertional malaise.

Next, we explored infiltration of immune cells (macrophages, T- and B-cells) in skeletal muscle upon exhaustive exercise. More long COVID patients had $CD68^+$ macrophage infiltration in skeletal muscle compared to healthy controls (Fig.5E). Exercise caused a similar increase in infiltrating macrophages in both groups. $CD3^+$ T-cells were absent in healthy controls, but present in patients with long COVID before induction of post-exertional malaise (Fig.5F). Exercise resulted in an accumulation of $CD3^+$ T-cells inside skeletal muscle tissue, but this response was blunted in patients experiencing post-exertional malaise. $CD20^+$ B-cells were not different between groups and tended to be higher one day after exercise (Fig.5G).

We reasoned that the exercise-induced damage and infiltration of immune cells might be due to mitochondrial DNA (mtDNA) fragments circulating in the systemic circulation, that act as a damage-associated molecular pattern triggering a systemic inflammatory response[33–36]. However, we did not find any evidence of an exacerbated circulating mtDNA response in plasma from patients compared to controls (Supplemental Fig.7A-F). Neither did we observe an increase in muscle breakdown products, such as creatinine and creatine kinase, in plasma of both groups (Supplemental Fig.6B and 7G-H). Circulating cortisol concentrations, critical for mediating homeostatic stress responses, were not different between groups at the time of measurement, with and without adjustments for time since waking (Supplemental Fig.7I).

SARS-CoV-2 nucleocapsid presence in skeletal muscle

To determine whether viral remnants play a role in the differential immune response in skeletal muscle in long COVID upon induction of post-exertional malaise[1,37], we stained all muscle sections for SARS-CoV-2 nucleocapsid protein. We reasoned that if viral persistence plays a role, then the SARS-CoV-2 nucleocapsid protein, which is specific to SARS-CoV-2 and not influenced by vaccinations, should be at least present. While we did not observe any positive staining in samples obtained before the outbreak of SARS-CoV-2 (Fig.6A-B), we found SARS-CoV-2 nucleocapsid protein in almost all patients and healthy controls (Fig. 6A-B). Despite a greater duration since the latest infection in long COVID patients, the amount of SARS-CoV-2 nucleocapsid protein was not different between groups (Fig.6A), before and after adjusting for time since the latest infection. Participants with an infection >6 months prior to study enrolment showed no differences in abundance of SARS-CoV-2 nucleocapsid protein, but we

cannot exclude additional unknown asymptomatic infections. The SARS-CoV-2 nucleocapsid protein was not located inside muscle fibers, but rather in the extracellular matrix, however, its presence did not consistently overlap with cell nuclei. There was no correlation between the presence of SARS-CoV-2 nucleocapsid protein and amyloid-containing deposits (R^2=0.03). The concentration of SARS-CoV-2 nucleocapsid protein was not altered after the development of post-exertional malaise. Our results suggest that the presence of residual SARS-CoV-2 nucleocapsid protein is similar between patients and healthy controls, and therefore does not explain the limited exercise capacity or development of post-exertional malaise in patients with long COVID.

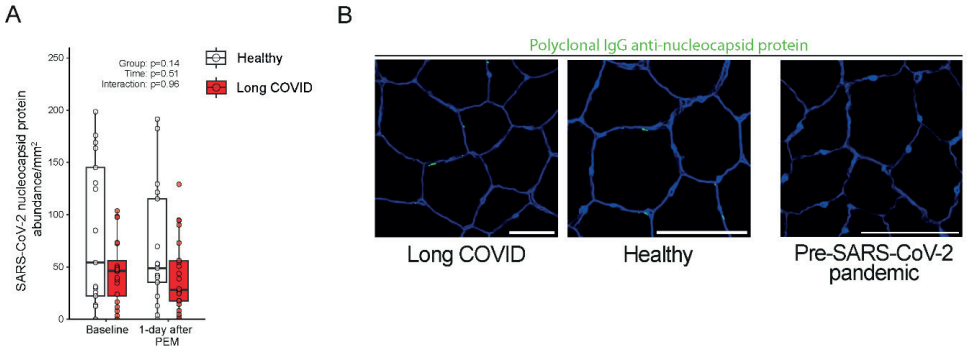


Figure 6. Similar concentrations of nucleocapsid protein in skeletal muscle in patients with long COVID as control. **A:** The SARS-CoV-2 nucleocapsid protein was present in almost all participants, but not more abundant in long COVID (n=23) compared to healthy controls (n=19). **B:** Typical examples of SARS-CoV-2 nucleocapsid protein, as a marker for viral persistence, in skeletal muscle. Skeletal muscle biopsies from before the SARS-CoV-2 pandemic showed no signal when stained with polyclonal IgG anti-SARS-CoV-2 nucleocapsid protein, indicating that SARS-CoV-2 nucleocapsid protein was not present in uninfected people which confirmed there was no aspecific binding. Continuous parametric longitudinal data (Panel **A**) were analyzed with a generalized linear mixed model with a two-sided ANOVA. Bar: 100 µm. Abbreviation: PEM; post-exertional malaise. Box plots show the median (centerline), the first and third quartiles (the lower and upper bound of the box) and the whiskers show the 1.5x interquartile range.

Discussion

We aimed to disentangle the pathophysiology of a lower exercise capacity and post-exertional malaise in patients with long COVID, and reveal distinct pathophysiological abnormalities in skeletal muscle and blood in long COVID patients using a longitudinal, case-controlled, cohort design. Patients with long COVID displayed a markedly lower exercise capacity, which related

to skeletal muscle metabolic alterations and a shift towards more fast-fatigable fibers. The pathophysiology of post-exertional malaise includes an acute exercise-induced reduction in skeletal muscle mitochondrial enzyme activity, an increased accumulation of amyloid-containing deposits in skeletal muscle, signs of severe muscle tissue damage, together with a blunted exercise-induced T-cell response in skeletal muscle. Collectively, these findings help to decipher the underlying physiology of fatigue and a limited exercise capacity from the development of post-exertional malaise in patients with long COVID.

A low exercise capacity is one of the hallmark signs of long COVID, associated with substantial burden for daily life[21]. The ventilatory and central cardiovascular system did not limit exercise capacity in long COVID patients, but our results confirm previous suggestions of a peripheral impairment in skeletal muscle metabolism in long COVID patients[21,23,38,39]. Consistent with previous hypotheses[21,38], we demonstrate that long COVID is associated with a lower skeletal muscle oxidative phosphorylation capacity. The occurrence of more IIA/X hybrid fibers and rare I/IIA hybrid fibers in patients with long COVID suggests that the pathophysiology of long COVID includes a fiber type shift towards a less oxidative, more glycolytic phenotype. Metabolic and structural alterations are supported by venous blood and skeletal muscle metabolomes of long COVID patients, in which glycolytic metabolites were higher and TCA cycle metabolites lower. We observed that a fiber-type shift and lower mitochondrial respiration are associated to the reduced exercise capacity in patients, but these do not necessarily contribute to the pathophysiology of post-exertional malaise, as fiber-type shifts occur at a very slow pace and could have been present before long COVID. Our participants showed a large variability in exercise tolerance ($\dot{V}O_{2max}$ and peak power), fiber type composition, and mitochondrial enzyme activity, but despite this large heterogeneity, all patients experienced post-exertional malaise one day after the exercise test. As such, we conclude that the pathophysiology of fatigue and a reduced exercise capacity is distinct from the rapid development of post-exertional malaise in long COVID patients. The development of post-exertional malaise could in turn, however, lead to a further reduction in exercise capacity in patients, as the acute reduction in mitochondrial SDH activity, occurrence of tissue necrosis and possibly intramuscular accumulation of amyloid-containing deposits could worsen skeletal muscle metabolism and force production over time, causing a vicious downward circle.

Tissue hypoxia, induced by amyloid-containing deposit accumulation in the smallest capillaries has been suggested to contribute to long COVID symptoms, such as fatigue[30,40]. We found an impaired peripheral oxygen extraction (and relatively lower deoxygenation) and a

higher concentration of amyloid-containing deposits in skeletal muscle, but we did not find evidence of blocked capillaries within the skeletal muscle. Our findings therefore do not support the hypothesis of chronic tissue hypoxia due to vessel blockage contributing to the development of skeletal muscle-related symptoms in long COVID or post-exertional malaise. We only evaluated the presence of amyloid, but not the function of the endothelium, or local blood flow. As such, the possible association of chronic endotheliitis or reduced blood flow to the development of post-exertional malaise and/or exercise intolerance in long COVID remains open[41,42]. Further studies into the composition of these amyloid-containing deposits and the possible role of entrapped (auto-)antibodies[45] in relation to post-exertional malaise and long COVID are warranted.

Both groups presented with more regenerating fibers following the second biopsy, indicating a possible effect of the first biopsy. Despite this, long COVID patients had more internal nuclei, atrophic fibers, and focal necrosis after induction of post-exertional malaise compared to healthy controls. Skeletal muscle atrophy and focal necrosis can occur during severe acute SARS-CoV-2 infection[43,44], but this is the first study providing evidence of severe tissue damage upon acute exercise in long COVID patients. The higher skeletal muscle infiltration of $CD68^+$ macrophages and $CD3^+$ T-cells suggests a locally disturbed immune response in patients with long COVID.

Viral infections can alter mitochondrial function, and multiple studies have shown that residual SARS-CoV-2 protein presence is associated with long COVID[45–47]. During acute SARS-CoV-2 infection the level of SARS-CoV-2 nucleocapsid protein rises sharply,[48] and although our patients suffered from exercise-induced myopathy, there were no signs of a higher presence of SARS-CoV-2 nucleocapsid protein in patients with long COVID before or after induction of post-exertional malaise. Furthermore, we did not observe more B-cell infiltration in skeletal muscle of patients before and during post-exertional malaise. The mere presence of SARS-CoV-2 nucleocapsid protein in skeletal muscle is unsurprising, as nucleocapsid protein can be present up to a year after infection in blood[49,50]. It is however unknown if the full virus is present, or only protein remnants. Because the spike protein is located on the exterior of the virus, this protein may have different proinflammatory/coagulatory effects compared with the nucleocapsid protein. The absence of clear distinctions in the quantity of nucleocapsid protein and the equal presence of B- and T-cells following exercise suggests that factors other than viral persistence are associated to the pathophysiology of post-exertional malaise in patients with long COVID.

This study is observational in nature, and therefore we cannot establish causality. We only included individuals with severe long COVID, but the observed abnormalities are not reflective of physical inactivity. Accelerometer data indicated that the long COVID patients were not bed-ridden, and had an average step-count of ~4000 steps/day (Supplemental Fig.2C). While our cohort might have displayed sedentary behavior, physical inactivity itself does not cause post-exertional malaise, and is linked with muscle atrophy and a lower mitochondrial SDH activity[51] , which we did not observe in our cross-sectional analysis. As the sample size of this study is relatively small, our results require replication in other cohorts. In support of our work, peripheral alterations in mitochondrial metabolism[39] and myopathy[12,52] have recently been observed in patients with long COVID, but how post-exertional malaise alters skeletal muscle alterations requires further confirmation. Post-exertional malaise is a symptom that is specific for certain patient populations, including long COVID and myalgic encephalomyelitis/chronic fatigue syndrome (ME/CFS). While it is unlikely that the pathophysiology of post-exertional malaise is completely different, future work should highlight if the underlying pathophysiology is similar in all patient populations, including children and adolescents.[53]

In conclusion, this study reveals that local and systemic metabolic disturbances, severe exercise-induced myopathy, infiltration of amyloid-containing deposits and immune cells in skeletal muscles of long COVID are key characteristics of post-exertional malaise. While these explain the symptomatology of post-exertional malaise in long COVID, the molecular pathways underlying these alterations in patients suffering from post-exertional malaise remains to be determined.

Methods

Study population

We performed a prospective case-control study in the post-COVID-19 clinic of the Amsterdam University Medical Centers (UMC) and the Faculty of Behavioral and Movement Sciences (Vrije Universiteit Amsterdam). The study protocol was approved by the medical ethics committee of the Amsterdam UMC (NL78394.018.21) and registered at www.clinicaltrials.gov (NCT05225688). All participants signed a written informed consent before participation. The study was conducted in accordance with the Declaration of Helsinki.

Long COVID patients were diagnosed by two experienced clinicians for long COVID symptomology and exclusion of potential differential diagnoses. All long COVID patients were diagnosed with post-exertional malaise (PEM) by the DSQ-PEM[54], had a minimum period of long COVID-related symptoms of six months, and were between 18 and 65 years old. No symptoms were present before confirmed diagnosis of SARS-CoV-2. Questionnaires regarding fatigue, fatigue severity score (FSS)[55], multidimensional fatigue inventory (MFI)[56] and DSQ-PEM were obtained throughout the study period. None of the included participants were admitted to the hospital during acute SARS-CoV-2 infection and were healthy prior to NAAT or serology-proven SARS-CoV-2 infection. Exclusion criteria were a medical history of cardiovascular/pulmonary disease, diabetes mellitus, concurrent treatment with metabolism or coagulant-altering drugs during the study period (statins, corticosteroids, SGLT2 inhibitors, GLP1 receptor agonists, platelet aggregation blockers and any anticoagulants), adiposity but not BMI (limiting the biopsy of the musculus vastus lateralis), pregnancy, active infection, severe renal dysfunction or any other prior chronic illness known to impact clinical performance or > 6 alcohol units per day or >14 alcohol units per week. Smoking was not an exclusion criteria.

None of the healthy controls had residual symptoms after the SARS-CoV-2 infection. One long COVID patient was excluded due to a recent SARS-CoV-2 re-infection (<7 days). Healthy controls withdrew because of the invasive nature of the protocol (n=2), symptoms related to a burn-out (n=1), and a novel diagnosis of uncontrolled hypertension (n=1).

Study design

All participants followed the same study protocol (Supplemental Fig. 1), with four visits over a two-week period. Participants arrived at the laboratory at least two hours postprandial and

were instructed to avoid caffeine on the day of the laboratory visit. Post-exertional malaise was induced by a maximal incremental ramp exercise test on day 7. Skeletal muscle biopsies were taken from the vastus lateralis on day 1 (before) and day 8 (1 day after exercise testing) using a suction-supported Bergström needle (Pelomi, Albertlund, Denmark). Both biopsies were taken from the same ~2 cm incision; the first biopsy was taken towards the proximal end of the muscle and the second biopsy was taken towards the distal part of the muscle. Samples were stored at -195ºC until subsequent analysis, or stored as otherwise stated. Venous blood was drawn on every visit. Ethylenediaminetetraacetic acid (EDTA) anticoagulated blood was obtained at each visit, and plasma was stored at -70 °C within 4 hours. The strobe checklist can be found in the supplementary data file.

Incremental ramp exercise test

To assess exercise tolerance and to induce post-exertional malaise in long COVID patients, we conducted an incremental ramp exercise test on a cycle ergometer with simultaneous ECG, pulmonary gas exchange/ventilation and muscle deoxygenation measurements. All exercise tests were conducted on an electronically braked cycle ergometer (Lode Excalibur Sport, Lode, Groningen, The Netherlands). The test was preceded by 2-min quiet rest on the ergometer and 4-min baseline cycling at low intensity (between 0-20 W depending on height, body mass and anticipated fitness). This was followed by a ramped, linear increase in work rate until task failure. The individual baseline work rates and ramp slopes were selected based on each participants anthropometric characteristics and physical activity levels and designed to elicit task failure within 8-12 minutes. Participants were instructed to maintain their cadence between 70-90 revolutions/minute, and task failure was defined as the point at which cadence dropped <60 revolutions/minute despite verbal encouragement. Capillary lactate concentrations were determined at rest prior to the onset of the test, during baseline cycling, and immediately following task failure (Lactate Pro 2 LT-1730, ARKRAY Ltd., United Kingdom). Pulmonary gas exchange and ventilation were measured on a breath-by-breath basis (Cosmed Quark CPET; Cosmed, Rome, Italy).

Near-infrared spectroscopy (NIRS)

Participants wore a spatially-resolved, continuous-wavelength portable NIRS device (Portamon, Artinis Medical Systems, Arnhem, The Netherlands) on the surface of the vastus lateralis muscle, halfway between head of the femur and lateral condyle. This was around the location of the muscle biopsy. Measurements for total (Δtotal[heme]), deoxygenated

(Δdeoxy[heme]) and oxygenated [heme] (Δoxy[heme]) [hemoglobin + myoglobin], as well as muscle saturation (SO_2, i.e., oxy[heme]/total[heme]·100) were normalized to a maximal and minimal value obtained during blood flow occlusion proximally to the NIRS device using an inflatable cuff. Briefly, a cuff was inflated between 300-500mmHg, and remained inflated until a plateau in Δtotal[heme], Δdeoxy[heme], and Δoxy[heme] signals were reached, and then subsequently released. The maximum and minimum yielded the physiological range for each individual, and all values were normalized to this physiological range. As the greatest source-detector separation distance of the NIRS device was 40 mm, participants with an adipose tissue thickness ≥20 mm (or skinfold thickness ≥ 40 mm) were excluded from this analysis. This resulted in the inclusion of 18 controls and 16 patients in the final analysis. Individual Δdeoxy[heme] data were averaged as a function of absolute and relative power output. All NIRS data was analyzed related to both absolute and relative work rates. Absolute work rates were analyzed at 25W increments from 50W until 175W, after which most participants could not continue the test. NIRS data was averaged for the 5W below and above each increment to reduce noise in the data set. Similarly for relative work rates, data was analyzed at 0%, 20%, 40%, 60%, 80%, and 100% of maximal work rate. Data was averaged for the 5% above and below each increment. All data was subsequently analyzed using a linear mixed model.

Daily life physical activity level

General daily activity was measured by an accelerometer (Actigraph wGT3X-BT, 60 Hz sampling time) worn on the right hip (anterior axillary line) during the entire study period, as described previously[57]. Participants were instructed to wear the accelerometer from early morning until bedtime. Daily physical activity level was determined by the number of steps per day. The time at which participants went to sleep and woke up was registered to allow adjustment of cortisol measurements.

Skeletal muscle measurements

Skeletal muscle respirometry

Mitochondrial function was assessed in permeabilized fibers as described previously[27]. Small bundles of freshly isolated fibers were permeabilized with 50 $\mu g \cdot mL^{-1}$ saponin for 20 min at 4ºC in a solution consisting of (in mM) CaEGTA (2.8), EGTA (7.2), ATP (5.8), $MgCl_2$ (6.6), taurine (20), phosphocreatine (15), imidazole (20), DTT (0.5) and MES (50) (pH 7.1). Tissue was washed in respiration solution containing EGTA (0.5), MgCl2 (3), K-lactobionate

(60), taurine (20), KH_2PO_4 (10), HEPES (20), sucrose (110) and 1 $g \cdot L^{-1}$ fatty acid-free BSA (pH 7.1), quickly blotted dry, weighed and transferred to a respirometer (Oxygraph-2k; Oroboros Instruments, Innsbruck, Austria) in respiration solution at 37 °C. Oxygen concentration was maintained above 300 µM throughout the experiment to avoid limitations in oxygen supply. Background respiration was assessed before adding substrates and was subtracted from all subsequent values. Leak respiration was assessed after the addition of sodium glutamate (10 mM), sodium malate (0.5 mM) and sodium pyruvate (5 mM). NADH (Complex I)-linked respiration was assessed after the addition of 5mM ADP, and 10 µM cytochrome c to confirm the absence of outer-mitochondrial membrane damage. Maximal oxidative capacity, with simultaneous input via NADH and succinate-linked respiration, was measured after the addition of 10 mM succinate. Maximum uncoupled respiration was determined via titration of carbonylcyanide-4-trifluoro- methoxyphenylhydrazone (FCCP) in 0.5 µM steps until no further increase in oxygen consumption was observed. Succinate-linked respiration was measured after blocking mitochondrial complex I with 0.5 µM rotenone. Two measurements per sample were performed simultaneously, and the results were averaged. Respiration values were normalized to wet weight and expressed in pmol $O_2 \cdot s^{-1} \cdot mg^{-1}$. Several ratios were subsequently calculated, namely the oxidative phosphorylation / electron transport system control ratio ($\frac{OxPhos}{ETS}$), the electron transport system/oxidative phosphorylation control efficiency ($\frac{ETS-OxPhos}{ETS}$), and the biochemical coupling efficiency ($\frac{ETS-Leak}{ETS}$)[58–60].

Immuno-histochemistry

To visualize muscle fiber morphology, signs of pathology, and the presence of amyloid-containing deposits and viral particles, (immuno-)histochemistry was carried out on 10 µm thick sections from the vastus lateralis muscle biopsies. Details about dilutions and vendors can be found in Table 3. Atrophy and necrosis in hematoxylin and eosin staining were evaluated by two pathologists blinded to the group allocation. Skeletal muscle infiltration of T-cells ($CD3^+$), B-cells ($CD20^+$) and macrophages ($CD68^+$) was scored positively or negatively.

Table 3. Details about antibodies, including dilutions and vendors. RRID: Research Resource Identifiers.

Parameter	***Antibody, dilution, vendor***	***Secondary antibody (dilution), vendor***	***RRID***
Muscle fiber type	BA-D5 (MHC-I), 1ug/ml, DSHB SC-71 (MHC-IIA), 1ug/ml, DSHB 6H1 (MHC-IIX) 5ug/ml, DSHB (60 min) WGA 350, 1:25, TMO W11263 (30 min MHCI (BA-D5), 1ug/ml, DSHB MHC IIA (SC-71), 1ug/ml, DSHB MHC IIX (6H1), 5ug/ml, DSHB (60 min) WGA 350, 1:25, TMO W11263 (30 min)	Goat-anti mouse IgG2b 555, 1:1000, Invitrogen A21147; Goat anti-mouse IgG1 647, 1:1000, Invitrogen A21240; Goat anti-mouse IgM 488, 1:1000, Invitrogen A21042 (60 min)	AB_2235587AB_2147165; AB_1157897; AB_2535783; AB_2535809; AB_2535711
Amyloid-containing deposits	Thioflavin T (50µM stock), 1:10, Sigma-Aldrich (30 minutes) WGA 555, 1:25, TMO W32464 (30 min)	N.A.	

Endothelial cells	CD31, IgG1 mouse, 1:50, Abcam ab9498 (overnight incubation) WGA 350, 1:25, TMO W11263 (30 min)	Goat anti-mouse IgG1 647, 1:200, Invitrogen A21240 (60 minutes)	AB_726362
Endothelial cells	Biotinylated UEA-1, 1:100, B-1065, Vector Laboratories (30 minutes)	Vectastain Elite ABC Kit PK-6100, Vector Laboratories (30 min); ImmPACT™ AMEC Red Peroxidase Substrate SK-4285, Vector Laboratories (10 min)	AB_2336766 AB_2336819 AB_2336519
Lymphatic vessel	LYVE1, IgG rabbit, 1:50 Abcam 10278 (overnight incubation) WGA 350, 1:25, TMO W11263 (30 min)	Goat anti-rabbit IgG 647, 1:200, Invitrogen A32733 (60 minutes)	AB_881387
SARS-CoV-2 nucleocapsid protein	SARS-CoV-2 Nucleocapsid Antibody, Rabbit PAb, Antigen Affinity Purified, 1:500; SinoBiological (60 min) WGA 555, 1:25, TMO W32464 (30 min)	Alexa fluor goat-anti rabbit IgG 488 1:500, Invitrogen A27034 (60 min)	AB_2892769
CD3	SP7 (rabbit moab), 1:200, Thermo Sc. Rm-9107-S		AB_149924

CD68	PG-M1 IgG 3, 1:200, DAKO M0876		AB_2074844
CD20	L26 IgG 2a, 1:1000,DAKO / M0755		AB_2282030

Fiber-type composition

Skeletal muscle fiber type quantification and size were assessed using immunofluorescence techniques using primary antibodies against myosin heavy chain (MHC) I (BA-D5), MHC II (SC-71), and MHC IIx (6H1)[61]. A negative control, without primary antibody, was included for background correction. Firstly, sections were air-dried for 10 minutes and then blocked with 10% Normal Goat Serum (NGS) for 60 minutes. Subsequently, slides were washed 3 times for 5 minutes each in 1x phosphate-buffered saline (PBS) and incubated with the primary antibodies for 60 minutes at room temperature. Again, slides were washed and subsequently incubated with the secondary antibodies for 60 minutes in the dark at room temperature. Once more, a washing step was performed and subsequently incubation of the slides with Wheat Germ Agglutinin (WGA) for 30 minutes in the dark at room temperature, followed by a final washing step and mounting the sections with coverslips using Vectashield Vibrance. Analysis was performed with ImageJ and Sandia Matlab AnalysiS Hierarchy (SMASH) Toolbox (version 1.0) in Matlab (version 2022a). Fiber type distribution was expressed using two methods: first, by calculating the percentage of fibers expressing each MHC compared to the total number of fibers present in the muscle section. This allowed for differentiation between fibers expressing both MHC-I and MHC-IIa, MHC-IIa only, and both MHC-IIx and MHC-IIa. Second, fiber distribution was expressed as the cross-sectional area occupied by each fiber type as a percentage of the cross-sectional area of all fibers. This allowed for quantification of hypertrophy/atrophy that may be occurring with particular MHC expression.

Succinate dehydrogenase activity

Sections were stained for succinate dehydrogenase (SDH) activity, which was used as a proxy for mitochondrial density, as described previously[62]. Immediately after cutting, sections were air-dried for 15 min and then immersed in a pre-heated (37°C) solution containing sodium phosphate buffer (0.1 M, pH 7.6), sodium succinate (0.2 M), sodium azide (14 mM) and tetranitro blue tetrazolium (TNBT, 0.55 mM, Sigma) for 20 min in the dark, and the reaction

was stopped by brief HCl (0.01 M) exposure before sections were washed and mounted with glycerin-gelatin. Sections were stored at 4°C and imaged within ten days. The averaged SDH activity was obtained by outlining individual skeletal muscle fibers and absorbance was assessed using ImageJ (NIH, Bethesda, USA). Values were expressed as ΔA_{660} per µm tissue thickness per second of staining time ($\Delta A_{660} \cdot \mu m^{-1} \cdot s^{-1}$).

Capillarization

Capillarization was assessed by staining for Ulex Europaeus Agglutinin 1 lectin (UEA-1)[63]. Sections were air-dried for 10 minutes and fixated in ice cold acetone (-20°C) for 15 minutes. Subsequently, slides were washed 3 times for 2 minutes in PBS and blocked with 1% bovine serum album for 30 minutes. Afterwards, slides were incubated with UEA-1 for 30 minutes at room temperature, followed by wash steps and an incubation with Vectastain Elite ABC kit for 30 minutes at room temperature. After washing, an incubation with Red Peroxidase substrate for 10 minutes at room temperature was performed, washed and sections mounted with glycerin-gelatin (heated in 37°C). Capillary-to-fiber ratio (C/F) and capillary density (CD) by capillaries per mm^2 muscle tissue were determined in ImageJ.

Amyloid-containing Deposits

To visualize amyloid-containing deposits, skeletal muscle sections were exposed to 5µM Thioflavin T (ThT). The muscle sections with the most amyloid-containing deposits were additionally stained with ThT in combination with a CD31-specific antibody to visualize endothelial cells and an LYVE-1-specific antibody to visualize lymph vessels. Firstly, sections were air dried for 10 minutes and then fixed in 4% paraformaldehyde (PFA) for 5 minutes only for the double staining. Subsequently, slides were washed 3 times for 5 minutes each in PBS Tween (PBST) and blocked with 10% NGS for 60 minutes. Then, again a washing step was completed, followed by incubation with the primary antibody (either CD31 or LYVE1) in 0.1% bovine serum albumin (BSA) in PBS overnight at 4°C. A negative control, without primary antibody, was included. Slides were washed in PBST and subsequently incubated with the secondary antibody for 60 minutes in the dark at room temperature. Subsequently, a washing step was performed and followed by incubation in ThT in 0.1% BSA in PBS for 30 minutes, followed by another washing step. Lastly, incubation of the slides with WGA for 30 minutes in the dark at room temperature, followed by a final washing step and mounting of the sections with coverslips using Vectashield Vibrance.

SARS-CoV-2

To determine viral presence in the muscle cells, the sections were stained for SARS-CoV-2[64]. Staining began with air drying the sections for 10 minutes, followed by a blocking step with 10% NGS for 60 minutes. A washing step consisting of 3 times 5-minute intervals in 1x PBS followed, after which the sections were incubated with the primary antibody anti-N for 60 minutes at room temperature. Another washing step followed, and then incubation with the secondary antibody for 60 minutes in the dark at room temperature. Afterwards, a washing step was again performed, followed by incubation with WGA for 30 minutes in the dark at room temperature. Sections were washed a final time and mounted with a coverslip using Vectashield hard set with DAPI.

Image acquisition

Slides were dried overnight at 4°C before imaging. Images for fiber type and capillarization analysis were taken at 20x magnification with VS200 Research Slide Scanner (Olympus) using Slideview 5.0. SDH images were taken with a DMRB microscope (Leica, Wetzlar) using a CCD camera, calibrated gray filters and an individual calibration curve at 660 nm. Images for the ThT combination staining were taken at 40x magnification using the fluorescence microscope (Axiovert 200M; Zeiss) and image processing software Slidebook 5.0. Approximately fifteen images were taken per sample, with 5 images per slide-section. All images were manually evaluated to exclude those containing out-of-focus areas, artifacts, and large areas of connective tissue. Background correction for CD31 and LYVE-1 was done based on the negative control. For the ThT, background correction was performed by thresholding the negative control for 99.0%. All typical examples were deconvolved with Huygens Professional version 22.40 (Scientific Volume Imaging, The Netherlands, http://svi.nl), using the CMLE algorithm, with Acuity: -90, 90 iterations, and default settings for SNR and background values. For the ThT staining, a manual background correction was applied.

Metabolomics

Metabolomics were performed on skeletal muscle biopsies and venous blood samples as previously described, with minor adjustments[27,65]. Our metabolomics method is specifically tailored to analyze key polar metabolites of the most fundamental metabolic pathways with high confidence, instead of a broader untargeted method where identifications are more uncertain. Positive and negative ionization measurements were performed separately. In a 2 mL tube, containing either 20 µL of plasma or an average of 3.2 mg of freeze dried muscle

tissue, the following amounts of internal standard dissolved in water were added to each sample: adenosine-$^{15}N_5$-monophosphate (5 nmol), adenosine-$^{15}N_5$-triphosphate (5 nmol), D_4-alanine (0.5 nmol), D_7-arginine (0.5 nmol), D_3-aspartic acid (0.5 nmol), D_3-carnitine (0.5 nmol), D_4-citric acid (0.5 nmol), $^{13}C_1$-citrulline (0.5 nmol), $^{13}C_6$-fructose-1,6-diphosphate (1 nmol), $^{13}C_2$-glycine (5 nmol), guanosine-$^{15}N_5$-monophosphate (5 nmol), guanosine-$^{15}N_5$-triphosphate (5 nmol), $^{13}C_6$-glucose (10 nmol), $^{13}C_6$-glucose-6-phosphate (1 nmol), D_3-glutamic acid (0.5 nmol), D_5-glutamine (0.5 nmol), D_5-glutathione (1 nmol), $^{13}C_6$-isoleucine (0.5 nmol), D_3-lactic acid (1 nmol), D_3-leucine (0.5 nmol), D_4-lysine (0.5 nmol), D_3-methionine (0.5 nmol), D_6-ornithine (0.5 nmol), D_5-phenylalanine (0.5 nmol), D_7-proline (0.5 nmol), $^{13}C_3$-pyruvate (0.5 nmol), D_3-serine (0.5 nmol), D_6-succinic acid (0.5 nmol), D_4-thymine (1 nmol), D_5-tryptophan (0.5 nmol), D_4-tyrosine (0.5 nmol), D_8-valine (0.5 nmol). Subsequently, solvents were added to achieve a total volume of 500 µL water, 500 µL methanol and 1 mL chloroform. Muscle tissues were homogenized before the addition of chloroform using a Qiagen TissueLyser II for 5 minutes at 30 times/s with a 5 mm Qiagen Stainless Steel Bead in each tube. All samples were thoroughly mixed, before centrifugation for 10 min at 14.000 rpm.

The top layer, containing the polar phase, was transferred to a clean 1.5 mL tube and dried using a vacuum concentrator at 60°C. Dried samples were reconstituted in 100 µL 6:4 (v/v) methanol:water. Metabolites were analyzed using a Waters Acquity ultra-high performance liquid chromatography system coupled to a Bruker Impact II™ Ultra-High Resolution Qq-Time-Of-Flight mass spectrometer. Samples were kept at 12°C during analysis, and 5 µL of each sample was injected. Chromatographic separation was achieved using a Merck Millipore SeQuant ZIC-cHILIC column (PEEK 100 x 2.1 mm, 3 µm particle size). The column temperature was held at 30°C. The mobile phase consisted of (A) 1:9 (v/v) acetonitrile:water and (B) 9:1 (v/v) acetonitrile:water, both containing 5 mmol/L ammonium acetate. Using a flow rate of 0.25 mL/min, the LC gradient consisted of: Dwell at 100% Solvent B, 0-2 min; Ramp to 54% Solvent B at 13.5 min; Ramp to 0% Solvent B at 13.51 min; Dwell at 0% Solvent B, 13.51-19 min; Ramp to 100% B at 19.01 min; Dwell at 100% Solvent B, 19.01-19.5 min. Column equilibration was done by increasing the flow rate to 0.4 mL/min at 100% B 19.5-21 min. MS data were acquired using negative and positive ionization in full scan mode over the range of m/z 50-1200. Data were analyzed using Bruker TASQ software version 2.1.22.3. All reported metabolite intensities were normalized to either freeze-dried tissue weight or plasma volume, as well as to internal standards with comparable retention times and response in the MS. Metabolite identification has been based on a combination of accurate mass, (relative)

retention times, ion mobility data and fragmentation spectra, compared to the analysis of a library of standards. Measurements below the lower limit of quantification were imputed as half the lowest value. Metabolites were excluded from analysis if they contained missing values for more than 5% of samples. Four samples from skeletal muscle metabolomics were excluded during quality control.

Venous blood measurements

Hormone concentrations

Venous concentrations of cortisol, creatine kinase and creatine kinase-MB were measured in the Amsterdam UMC clinical laboratory, and details are provided in Table 4.

Table 4. Details about methods for venous blood concentrations.

Parameter	***Equipment***	***Method***	***Reference limits***
Cortisol	Roche cobas C8000	Electro- chemiluminescence immunoassay "ECLIA" Roche Diagnostics	250-650 nmol/L
Creatine kinase	c702 Roche diagnostics	NAC-activated, 37°C Roche Diagnostics	Male <171 U/L Female <145 U/L
Creatine kinase-MB	e602 Roche Diagnostics	Enzyme-labeled sandwich immunoassay Roche Diagnostics	< 4 µg/L

Circulating mitochondrial DNA

Mitochondrial DNA (mtDNA) measurements were performed using plasma samples. DNA was isolated according to the BIOKE NucleoSpin® Tissue kit. Briefly, plasma was separated from blood collected in vials coated with ethylenediaminetetraacetic acid by centrifuging at 1500g for 10 minutes. Subsequently, 50uL of plasma was diluted in solution containing 150µL

PBS, 25µL proteinase K and 200µL Buffer B3. After incubation at 70°C for 15 minutes, 210µL of 96% ethanol was added to the solution and centrifuged for 1 minute at 11000g, where the solution passed through a silica membrane column. The column was then placed in a new collection tube, washed with 500µL Buffer BW and centrifuged for 1 min at 11000g. This was subsequently washed with 600µL of buffer B5 and centrifuged again for 1 minute at 11000g. Lastly, 100µL of buffer BE was added, incubated for 3 minutes and centrifuged a final time for 1 minute at 11000g to yield the final isolated DNA in solution. Both ND1 and ND6 mtDNA primers were used to quantify the mtDNA copy number, using the ΔΔCt-method. Each well contained 2µL of mtDNA, 3µL of primer mix, and 5µl of Power Up SYBR Green Master mix. Subsequently, qPCR in duplo was conducted using QuantStudio 3 real-time PCR to quantify concentrations of mtDNA relative to the nuclear reference 18S. Values were normalized to the first time point.

Statistical analysis

Distributions were assessed with histograms and Shapiro-Wilk tests. Categorical values are noted in the absolute numbers with percentages in brackets. Parametric quantitative variables are presented as means ± standard deviation (SD), and nonparametric quantitative variables are presented as median and interquartile ranges (IQR; 25th and 75th percentiles). Boxplots are shown with the median and IQR (25th and 75th percentiles), unless otherwise specified. All individual points represent a participant.

Non-normally distributed data were transformed using Box-Cox transformation in order to obtain a normal distribution for statistical analysis[66]. Categorical data were analyzed using a Fisher's exact test. Continuous parametric data were analyzed using a t-test or analysis of variance, with Tukey HSD post-hoc testing, where appropriate. Continuous nonparametric data were analyzed using the Mann–Whitney U test, Kruskal-Wallis H test, or pairwise Kruskal-Wallis test with Benjamini-Hochberg (BH) correction where appropriate. Correlations were analyzed using the Pearson correlation coefficient for linear relationships and the Spearman rank correlation coefficient for non-linear relationships. Correlation coefficients were compared using the R package *cocor*[67]. Categorical longitudinal data were analyzed using logistic regression with Time (baseline and 1-day after exercise) as a covariate. Continuous parametric longitudinal data and metabolomics were analyzed with a generalized linear mixed model with time (baseline, 1 day and 1 week after exercise), group and interaction effects. Metabolomics data were adjusted with BH correction within the pre-specified metabolome

pathway. Post-hoc comparisons of longitudinal data were, if the interaction term was significant, performed using the Empirical Mean Differences using R package *emmeans*[68] methods with BH adjustment. Continuous nonparametric longitudinal data analysis was conducted by comparing the delta (Δ) between the time points. Longitudinal metabolomic data were visualized with the effect size calculated using Hedges' g[69]. P-values less than 0.05 (two-tailed) were considered statistically significant. All data were analyzed using R studio built under R version 4.0.3 (R Core Team 2013, Vienna, Austria).

Data Availability

The source data file is available below. The raw metabolomics data generated in this study have been deposited in the data publication platform of the Vrije University Amsterdam, with DOI: https://doi.org/10.48338/VU01-KPABVO. Metabolomics is available on MetaboLights (with study identification code: MTBLS9103).

Code Availability

R codes are available at https://zenodo.org/doi/10.5281/zenodo.10171056.

References

1. Davis, H. E., Mccorkell, L., Vogel, J. M. & Topol, E. J. Long COVID: major findings, mechanisms and recommendations. *Nature Reviews Microbiology* | **21**, 133–146 (2023).
2. Hickie, I. *et al.* Post-infective and chronic fatigue syndromes precipitated by viral and non-viral pathogens: prospective cohort study. *BMJ* **333**, 575–578 (2006).
3. Ruiz-Pablos, M., Paiva, B., Montero-Mateo, R., Garcia, N. & Zabaleta, A. Epstein-Barr Virus and the Origin of Myalgic Encephalomyelitis or Chronic Fatigue Syndrome. *Front Immunol* **12**, 4637 (2021).
4. Ursinus, J. *et al.* Prevalence of persistent symptoms after treatment for lyme borreliosis: A prospective observational cohort study. *The Lancet Regional Health - Europe* **6**, 100142 (2021).
5. Herridge, M. S. & Azoulay, É. Outcomes after Critical Illness. *New England Journal of Medicine* **388**, 913–924 (2023).
6. Subramanian, A. *et al.* Symptoms and risk factors for long COVID in non-hospitalized adults. *Nature Medicine 2022 28:8* **28**, 1706–1714 (2022).

7. Kedor, C. *et al.* A prospective observational study of post-COVID-19 chronic fatigue syndrome following the first pandemic wave in Germany and biomarkers associated with symptom severity. *Nature Communications 2022 13:1* **13**, 1–13 (2022).

8. Kerkhoff, T. J., Charlton, B. T., Appelman, B., van Vugt, M. & Wüst, R. C. I. Post COVID-19 condition: critical need for a clear definition and detailed pathophysiology. *J Cachexia Sarcopenia Muscle* **13**, 2754–2756 (2022).

9. Chilunga, F. P. *et al.* Differences in incidence, nature of symptoms, and duration of long COVID among hospitalised migrant and non-migrant patients in the Netherlands: a retrospective cohort study. *The Lancet regional health. Europe* **29**, (2023).

10. Al-Aly, Z., Bowe, B. & Xie, Y. Long COVID after breakthrough SARS-CoV-2 infection. *Nature Medicine 2022 28:7* **28**, 1461–1467 (2022).

11. Klein, J. *et al.* Distinguishing features of Long COVID identified through immune profiling. *Nature 2023* 1–3 (2023) doi:10.1038/s41586-023-06651-y.

12. Hejbøl, E. K. *et al.* Myopathy as a cause of fatigue in long-term post-COVID-19 symptoms: Evidence of skeletal muscle histopathology. *Eur J Neurol* **29**, 2832–2841 (2022).

13. Pretorius, E. *et al.* Persistent clotting protein pathology in Long COVID/Post-Acute Sequelae of COVID-19 (PASC) is accompanied by increased levels of antiplasmin. *Cardiovasc Diabetol* **20**, 1–18 (2021).

14. Muri, J. *et al.* Autoantibodies against chemokines post-SARS-CoV-2 infection correlate with disease course. *Nature Immunology 2023* 1–8 (2023) doi:10.1038/s41590-023-01445-w.

15. Wang, E. Y. *et al.* Diverse functional autoantibodies in patients with COVID-19. *Nature* **595**, 283–288 (2021).

16. Kruger, A. *et al.* Proteomics of fibrin amyloid microclots in long COVID/post-acute sequelae of COVID-19 (PASC) shows many entrapped pro-inflammatory molecules that may also contribute to a failed fibrinolytic system. *Cardiovasc Diabetol* **21**, 1–23 (2022).

17. Guo, L. *et al.* Prolonged indoleamine 2,3-dioxygenase-2 activity and associated cellular stress in post-acute sequelae of SARS-CoV-2 infection. *EBioMedicine* **94**, (2023).

18. Soares, M. N. *et al.* Skeletal muscle alterations in patients with acute Covid-19 and post-acute sequelae of Covid-19. *J Cachexia Sarcopenia Muscle* **13**, 11–22 (2022).

19. Post COVID-19 condition (Long COVID). https://www.who.int/europe/news-room/fact-sheets/item/post-covid-19-condition.

20. Frésard, I. *et al.* Dysfunctional breathing diagnosed by cardiopulmonary exercise testing in 'long COVID' patients with persistent dyspnoea. *BMJ Open Respir Res* **9**, e001126 (2022).

21. Schwendinger, F., Knaier, R., Radtke, T. & Schmidt-Trucksäss, A. Low Cardiorespiratory Fitness Post-COVID-19: A Narrative Review. *Sports Med* **53**, 51–74 (2023).

22. Skjørten, I. *et al.* Cardiopulmonary exercise capacity and limitations 3 months after COVID-19 hospitalisation. *European Respiratory Journal* **58**, 2100996 (2021).

23. Singh, I. *et al.* Persistent Exertional Intolerance After COVID-19: Insights From Invasive Cardiopulmonary Exercise Testing. *Chest* **161**, 54–63 (2022).

24. Germain, A. *et al.* Plasma metabolomics reveals disrupted response and recovery following maximal exercise in myalgic encephalomyelitis/chronic fatigue syndrome. *JCI Insight* **7**, e157621 (2022).

25. McGregor, N. R., Armstrong, C. W., Lewis, D. P. & Gooley, P. R. Post-exertional malaise is associated with hypermetabolism, hypoacetylation and purine metabolism deregulation in ME/CFS cases. *Diagnostics* **9**, 1–11 (2019).

26. Missailidis, D. *et al.* An Isolated Complex V Inefficiency and Dysregulated Mitochondrial Function in Immortalized Lymphocytes from ME/CFS Patients. *International Journal of Molecular Sciences 2020, Vol. 21, Page 1074* **21**, 1074 (2020).

27. Wüst, R. C. I. *et al.* The Antibiotic Doxycycline Impairs Cardiac Mitochondrial and Contractile Function. *Int J Mol Sci* **22**, 4100 (2021).

28. Beloborodova, N. *et al.* Effect of phenolic acids of microbial origin on production of reactive oxygen species in mitochondria and neutrophils. *J Biomed Sci* **19**, 89 (2012).

29. Pedley, A. M., Pareek, V. & Benkovic, S. J. The Purinosome: A Case Study for a Mammalian Metabolon. *Annu Rev Biochem* **91**, 89–106 (2022).

30. Kell, D. B., Laubscher, G. J. & Pretorius, E. A central role for amyloid fibrin microclots in long COVID/PASC: origins and therapeutic implications. *Biochem J* **479**, 537–559 (2022).

31. Charnley, M. *et al.* Neurotoxic amyloidogenic peptides in the proteome of SARS-COV2: potential implications for neurological symptoms in COVID-19. *Nat Commun* **13**, 3387 (2022).

32. Aschman, T. *et al.* Post-COVID syndrome is associated with capillary alterations, macrophage infiltration and distinct transcriptomic signatures in skeletal muscles. *medRxiv* 2023.02.15.23285584 (2023) doi:10.1101/2023.02.15.23285584.

33. Nakahira, K., Hisata, S. & Choi, A. M. K. The Roles of Mitochondrial Damage-Associated Molecular Patterns in Diseases. *Antioxid Redox Signal* **23**, 1329 (2015).

34. Grazioli, S. & Pugin, J. Mitochondrial Damage-Associated Molecular Patterns: From Inflammatory Signaling to Human Diseases. *Front Immunol* **9**, 1 (2018).

35. Frere, J. J. *et al.* SARS-CoV-2 infection in hamsters and humans results in lasting and unique systemic perturbations after recovery. *Sci Transl Med* **14**, (2022).

36. Littlefield, K. M. *et al.* SARS-CoV-2-specific T cells associate with inflammation and reduced lung function in pulmonary post-acute sequalae of SARS-CoV-2. *PLoS Pathog* **18**, e1010359 (2022).

37. Iwasaki, A. & Putrino, D. Why we need a deeper understanding of the pathophysiology of long COVID. *Lancet Infect Dis* **23**, 393–395 (2023).

38. de Boer, E. *et al.* Decreased Fatty Acid Oxidation and Altered Lactate Production during Exercise in Patients with Post-acute COVID-19 Syndrome. *Am J Respir Crit Care Med* **205**, 126–129 (2022).

39. Colosio, M. *et al.* Structural and functional impairments of skeletal muscle in patients with postacute sequelae of SARS-CoV-2 infection. *J Appl Physiol (1985)* **135**, (2023).

40. Posthuma, J. J., van der Meijden, P. E. J., ten Cate, H. & Spronk, H. M. H. Short- and Long-term exercise induced alterations in haemostasis: a review of the literature. *Blood Rev* **29**, 171–178 (2015).

41. Charfeddine, S. *et al.* Long COVID 19 Syndrome: Is It Related to Microcirculation and Endothelial Dysfunction? Insights From TUN-EndCOV Study. *Front Cardiovasc Med* **8**, (2021).

42. Turner, S. *et al.* Long COVID: pathophysiological factors and abnormalities of coagulation. *Trends Endocrinol Metab* **34**, 321–344 (2023).

43. Aschman, T. *et al.* Association Between SARS-CoV-2 Infection and Immune-Mediated Myopathy in Patients Who Have Died. *JAMA Neurol* **78**, 948–960 (2021).

44. Mageriu, V., Zurac, S., Bastian, A., Staniceanu, F. & Manole, E. Histological findings in skeletal muscle of SARS-CoV2 infected patient. *J Immunoassay Immunochem* **41**, 1000–1009 (2020).

45. Swank, Z. *et al.* Persistent Circulating Severe Acute Respiratory Syndrome Coronavirus 2 Spike Is Associated With Post-acute Coronavirus Disease 2019 Sequelae. *Clin Infect Dis* **76**, (2023).

46. Patterson, B. K. *et al.* Persistence of SARS CoV-2 S1 Protein in CD16+ Monocytes in Post-Acute Sequelae of COVID-19 (PASC) up to 15 Months Post-Infection. *Front Immunol* **12**, 5526 (2022).

47. Buonsenso, D. *et al.* Viral persistence in children infected with SARS-CoV-2: current evidence and future research strategies. *Lancet Microbe* **4**, e745–e756 (2023).

48. Appelman, B. *et al.* Time since SARS-CoV-2 infection and humoral immune response following BNT162b2 mRNA vaccination. *EBioMedicine* **72**, (2021).

49. Wang, Z. *et al.* Naturally enhanced neutralizing breadth against SARS-CoV-2 one year after infection. *Nature* **595**, 426–431 (2021).

50. Gallais, F. *et al.* Evolution of antibody responses up to 13 months after SARS-CoV-2 infection and risk of reinfection. *EBioMedicine* **71**, (2021).

51. Hendrickse, P. W. *et al.* Capillary rarefaction during bed rest is proportionally less than fibre atrophy and loss of oxidative capacity. *J Cachexia Sarcopenia Muscle* **13**, 2712–2723 (2022).

52. Agergaard, J. *et al.* Myopathy as a cause of Long COVID fatigue: Evidence from quantitative and single fiber EMG and muscle histopathology. *Clin Neurophysiol* **148**, 65–75 (2023).

53. Pizzuto, D. A. *et al.* Lung perfusion assessment in children with long-COVID: A pilot study. *Pediatr Pulmonol* **58**, 2059–2067 (2023).

54. Cotler, J., Holtzman, C., Dudun, C. & Jason, L. A. A Brief Questionnaire to Assess Post-Exertional Malaise. *Diagnostics* **8**, (2018).

55. Krupp, L. B., Alvarez, L. A., Larocca, N. G. & Scheinberg, L. C. Fatigue in multiple sclerosis. *Arch Neurol* **45**, 435–437 (1988).

56. Smets, E. M. A., Garssen, B., Bonke, B. & De Haes, J. C. J. M. The multidimensional Fatigue Inventory (MFI) psychometric qualities of an instrument to assess fatigue. *J Psychosom Res* **39**, 315–325 (1995).

57. Clevenger, K. A. *et al.* Effect of sampling rate on acceleration and counts of hip- and wrist-worn ActiGraph accelerometers in children. *Physiol Meas* **40**, (2019).

58. View of Mitochondrial pathways and respiratory control. https://www.bioenergetics-communications.org/index.php/bec/article/view/gnaiger_2020_mitopathways/12.

59. Gnaiger, E. Capacity of oxidative phosphorylation in human skeletal muscle: new perspectives of mitochondrial physiology. *Int J Biochem Cell Biol* **41**, 1837–1845 (2009).

60. Gnaiger, E. *et al.* Mitochondrial coupling and capacity of oxidative phosphorylation in skeletal muscle of Inuit and Caucasians in the arctic winter. *Scand J Med Sci Sports* **25**, 126–134 (2015).

61. Horwath, O. *et al.* Variability in vastus lateralis fiber type distribution, fiber size, and myonuclear content along and between the legs. *J Appl Physiol (1985)* **131**, 158–173 (2021).

62. Wüst, R. C. I. *et al.* Region-specific adaptations in determinants of rat skeletal muscle oxygenation to chronic hypoxia. *Am J Physiol Heart Circ Physiol* **297**, (2009).

63. Van Der Zwaard, S. *et al.* Critical determinants of combined sprint and endurance performance: An integrative analysis from muscle fiber to the human body. *FASEB Journal* **32**, 2110–2123 (2018).

64. Grootemaat, A. E. *et al.* Lipid and Nucleocapsid N-Protein Accumulation in COVID-19 Patient Lung and Infected Cells. *Microbiol Spectr* **10**, (2022).

65. Schomakers, B. V. *et al.* Polar metabolomics in human muscle biopsies using a liquid-liquid extraction and full-scan LC-MS. *STAR Protoc* **3**, 101302 (2022).

66. Daimon, T. Box–Cox Transformation. *International Encyclopedia of Statistical Science* 176–178 (2011) doi:10.1007/978-3-642-04898-2_152.

67. Diedenhofen, B. & Musch, J. cocor: A Comprehensive Solution for the Statistical Comparison of Correlations. *PLoS One* **10**, e0121945 (2015).

68. Searle, S. R., Speed, F. M. & Milliken, G. A. Estimated Marginal Means, aka Least-Squares Means [R package emmeans version 1.8.5]. *American Statistician* **34**, 216–221 (2023).

69. Hedges, L. V. Distribution Theory for Glass ' s Estimator of Effect Size and Related Estimators. *Journal of Educational Statistics* **6**, 107–128 (1981).

Acknowledgments

We particularly thank all participants for their time and dedication in participating in this study. We also would like to thank all staff of the post-COVID outpatient clinic of the Amsterdam UMC, in particular Drs Mooij-Kalverda and Huismans, for their support during this study. We also acknowledge the help of Dr Eric Voorn in the data acquisition of the physical activity measurements, Onno van Driel in the analysis of the fiber type distribution and Jos de Koning in supporting exercise data collection.

This study was funded by own funding, the Patient-Led Research Collaborative for Long COVID (Grant ID: C1, [MvV]), the Talud Foundation for the Amsterdam UMC Corona Research Fund [WWJ], AMC Foundation [MvV], VU Foundation [RCIW], ZonMw Onderzoeksprogramma ME/CVS [RCIW] and the 2022 Ramsay Grant Program [RCIW].

Author contributions

BA, BC, MvV and RW have made substantial contributions to the conception, design, financial acquisition, analysis and interpretation of the data, drafting of the work and revised the manuscript. RG, TK, EB, WN and CO have made substantial contributions to the conception, design, analysis and interpretation of the data, drafting of the work and substantially revised the manuscript. FB, MvW, BS, PC, JP, EA, WJW have made substantial contributions to conception, design, analysis of the data, drafting and revision of the manuscript. All authors have approved the submitted version and agree to be personally accountable for the author's own contributions and to ensure that questions related to the accuracy or integrity of any part

of the work, even ones in which the author was not personally involved, are appropriately investigated, resolved, and the resolution documented in the literature.

Conflict of interest

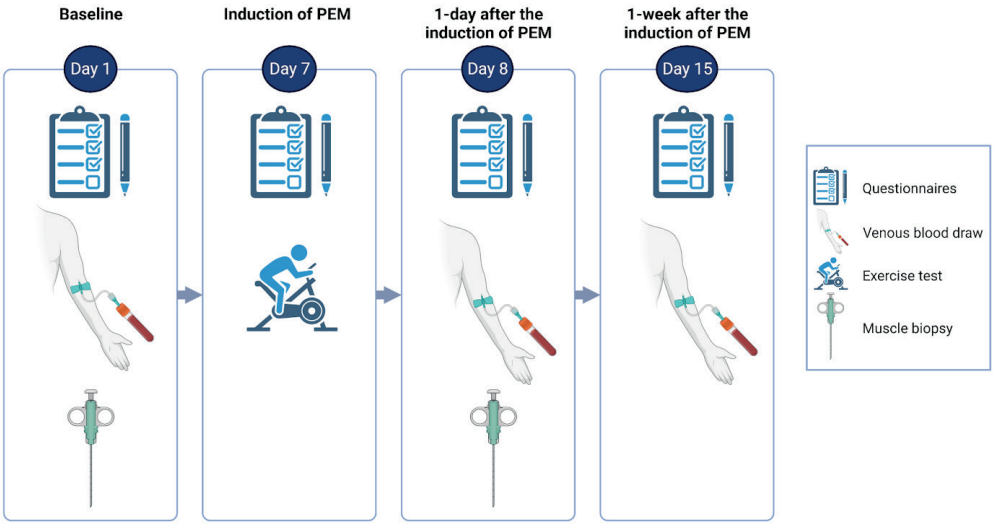
All authors have declared no conflict of interest.

Additional information

Source data is available for this paper.

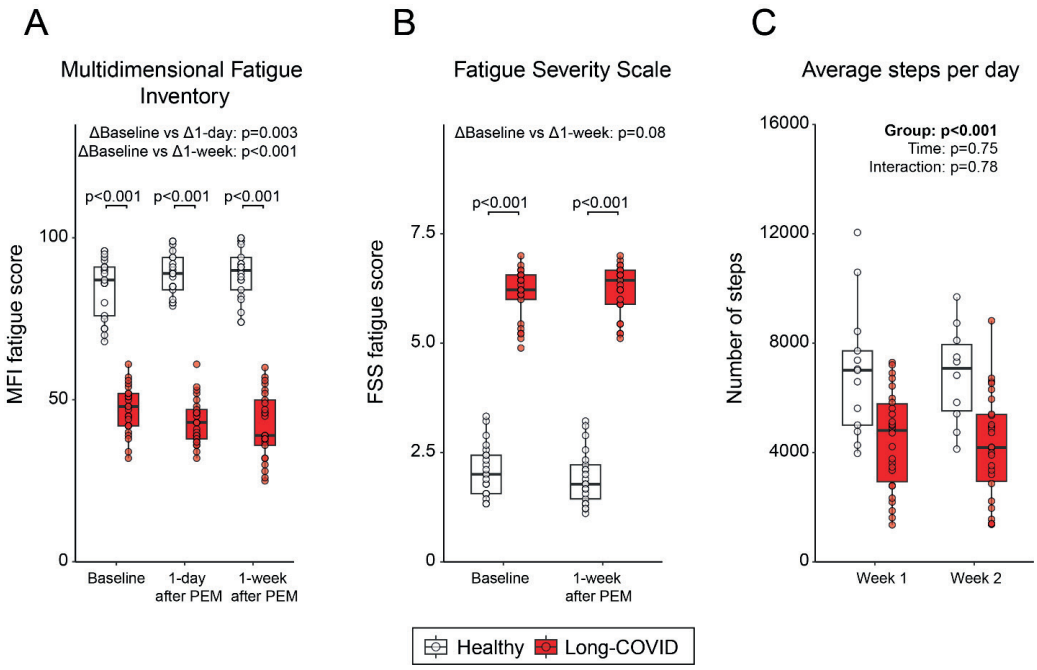
Supplementary Information is available for this paper.

Supplemental Figures

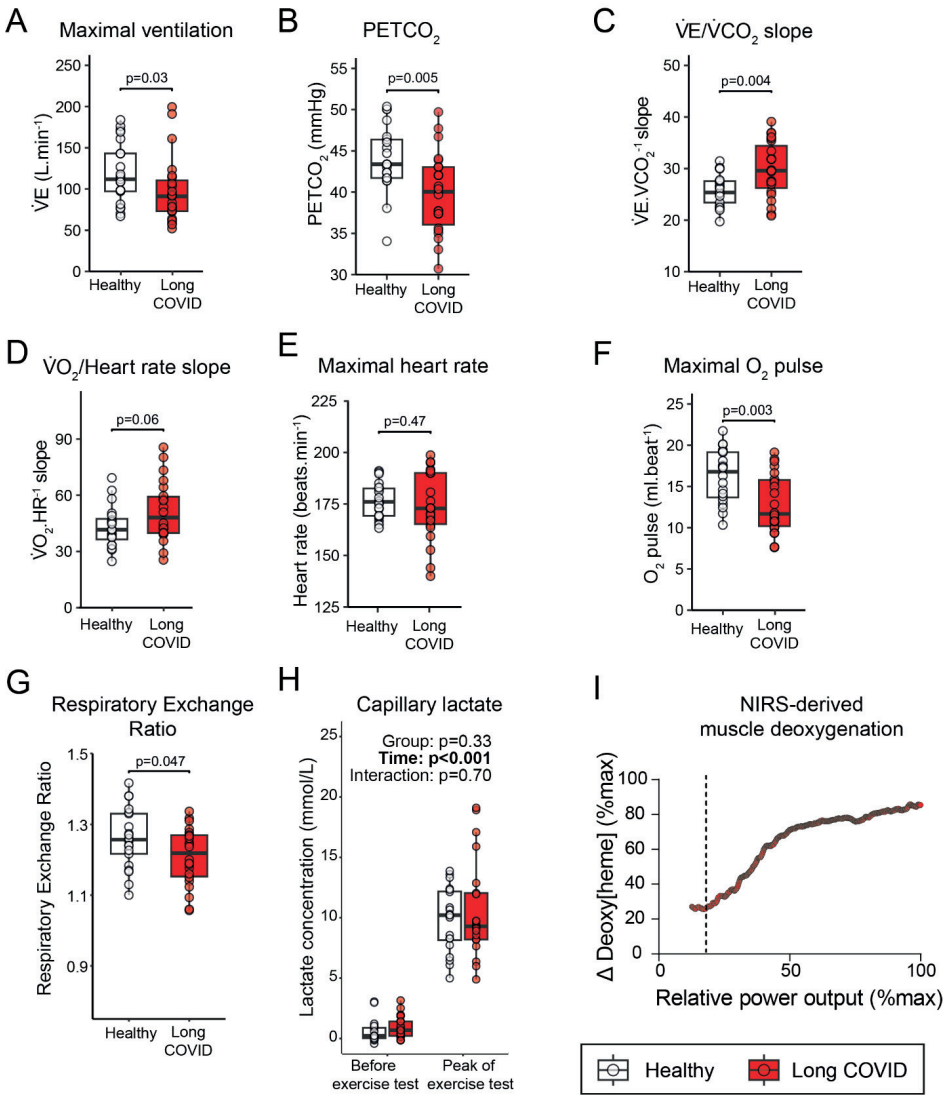


Supplemental Figure 1. Schematic overview of the study. In total, 25 patients with long COVID and 21 healthy controls were included. At baseline (day 1), venous blood in the fasted state, and a muscle biopsy of the vastus lateralis muscle was taken, alongside questionnaires (see text) about long COVID symptomatology. Six days later (day 7), a cardiopulmonary exercise test (CPET) was performed to evaluate exercise tolerance, and to induce post-exertional malaise in patients with long COVID. One day later, fasted venous blood and another skeletal muscle biopsy from the vastus lateralis muscle was taken, and questionnaires confirmed the worsening of long COVID symptoms, typical for post-exertional malaise. On day 15, 8 days after the CPET, another fasted venous blood sample was drawn, and questionnaires were filled in. During the entire study period, participants

wore an Actigraph to register the total steps taken. Abbreviations**:** PEM; post-exertional malaise.This image was created with BioRender (full license).

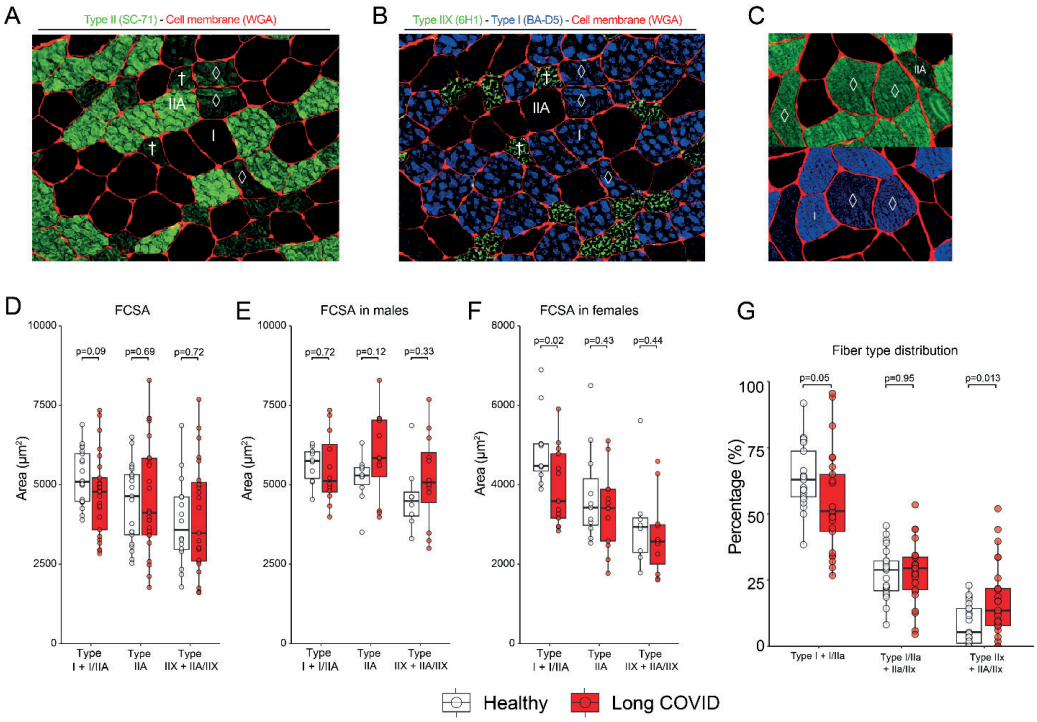


Supplemental Figure 2. Fatigue severity scores and physical activity in long COVID patients after induction of post-exertional malaise. Fatigue scores, measured with the Multidimensional Fatigue Inventory (**A**, n=25 long COVID, n=21 healthy) and the Fatigue Severity Scale (**B**) questionnaires were significantly worse in long COVID patients (n=25) compared to controls (n=21) and further worsened upon induction of post-exertional malaise for the Multidimensional Fatigue Inventory. **C**: Average step count per day at both the first week (baseline) and the second week (after the induction of PEM) was lower in patients (n=25) compared to healthy controls (n=15). Continuous nonparametric data were analyzed using a two-sided Mann–Whitney U test (panel A-B). Continuous nonparametric longitudinal data (panel A-B) were conducted by comparing the delta (Δ) between the time points using a two-sided Mann–Whitney U test and t-test. Continuous parametric longitudinal data (panel C) were analyzed with a generalized linear mixed model with a two-sided ANOVA. *p<0.05; **p<0.001. Abbreviations: PEM; post-exertional malaise. Box plots show the median (centerline), the first and third quartiles (the lower and upper bound of the box) and the whiskers show the 1.5x interquartile range.

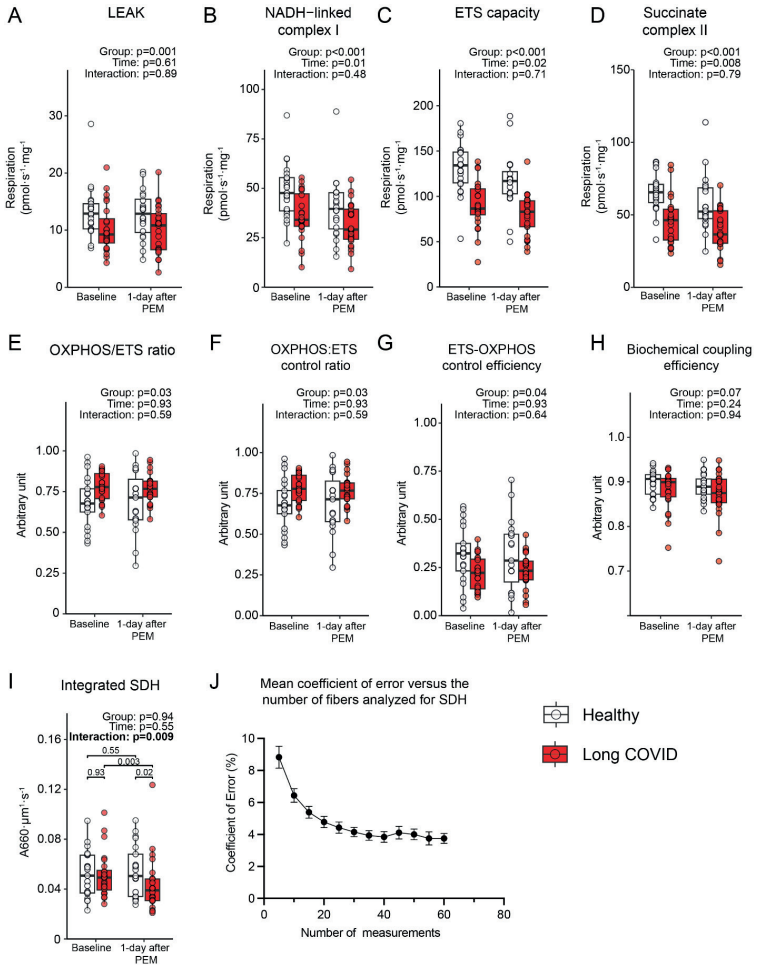


Supplemental Figure 3. Physiological measurements determined during exercise testing in healthy controls and long COVID. The maximal ventilation **(A)**, maximal end-tidal CO_2 tensions **(B)**, the slope of the relationship between ventilation and carbon dioxide output **(C)**, the slope of the relationship between oxygen uptake and heart rate **(D)**, maximal heart rate **(E)** and maximal O_2 pulse **(F)**. The respiratory exchange ratio was above 1.10 for almost all participants **(G)**. Panel **H** shows capillary lactate before and at the peak of the exercise test. Panel **I** shows the near-infrared spectroscopy-derived muscle deoxygenation responses to ramp incremental exercise in a representative participant. Panel A-C, G; Long COVID; n=23, Healthy; n=21, panel D-F; Long COVID; n=22, Healthy; n=20, panel G; Long COVID; n=21, Healthy; n=20. Continuous parametric data were analyzed using a two-sided t-test and two-sided non-parametric with a Mann–Whitney U test (panel A-G). Continuous parametric longitudinal data (panel H) were analyzed with a generalized linear mixed

model with a two-sided ANOVA. ns; non-significant, *p<0.05. Abbreviations: $PETCO_2$; end-tidal CO_2 tension, $\dot{V}E$; minute ventilation, $\dot{V}CO_2$; pulmonary carbon dioxide output, $\dot{V}O_2$; pulmonary oxygen uptake. Box plots show the median (centerline), the first and third quartiles (the lower and upper bound of the box) and the whiskers show the 1.5x interquartile range.

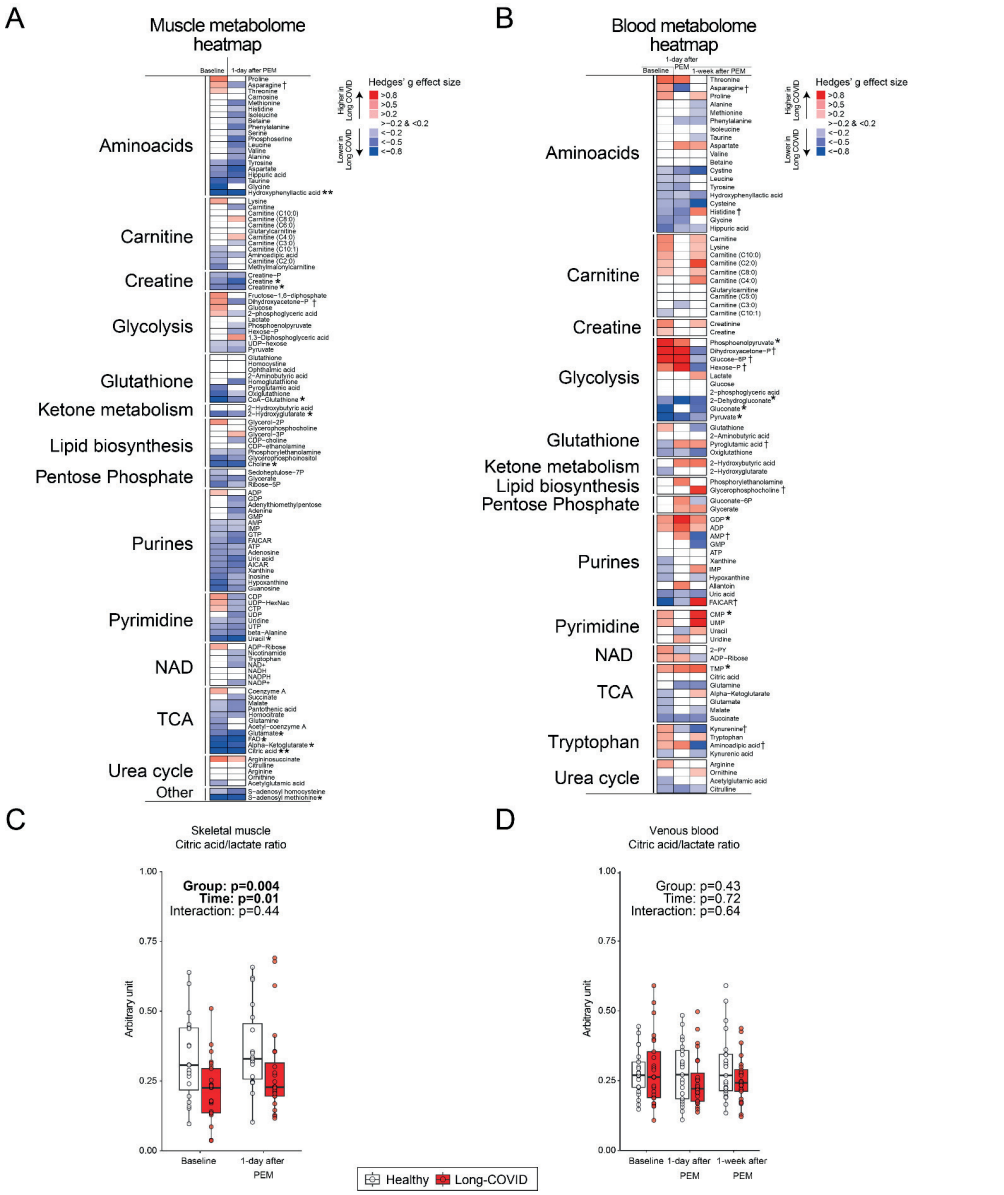


Supplemental Figure 4. Fiber types and cross-sectional area distribution in long COVID patients and healthy controls. Panels **A-C** show a typical example of immunofluorescence analysis of myosin heavy chain (MHC) expression in a 10-µm cross-section of the vastus lateralis of long COVID patients with a high proportion of hybrid fibers. In panels **D-F,** we show that there is no difference in the fiber cross-sectional area between healthy controls (n=21) and long COVID patients (n=25), although the type I fiber cross-sectional area is smaller in females with long COVID compared to healthy female controls **(F)**. **G:** Patients with long COVID (n=25) had a higher percentage of glycolytic type IIx skeletal muscle fibers compared to healthy controls (n=21). Continuous parametric data were analyzed using a two-sided t-test and non-parametric data with a two-sided Mann–Whitney U (panel D-F). Abbreviations: IIA; type IIA skeletal muscle fiber, IIX; type IIX skeletal muscle fiber, ◊; I/IIA hybrid skeletal muscle fibers, †; IIA/IIX hybrid skeletal muscle fiber, FCSA; fiber cross-sectional area. Box plots show the median (centerline), the first and third quartiles (the lower and upper bound of the box) and the whiskers show the 1.5x interquartile range. Source data are provided in the Source Data File.



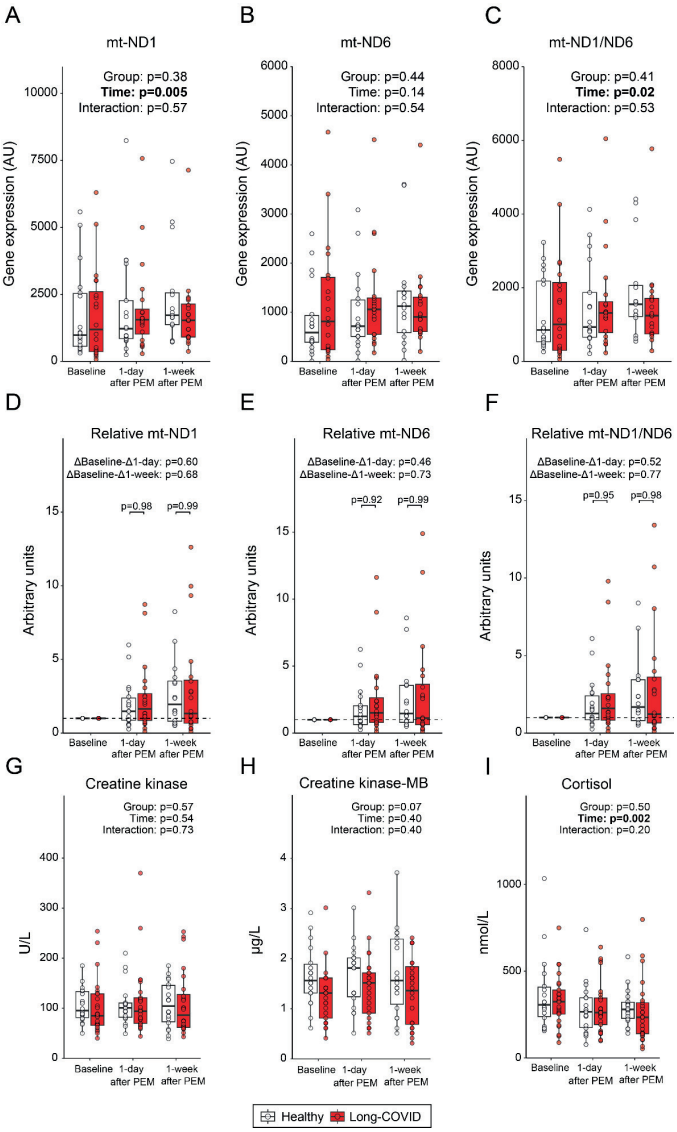
Supplemental Figure 5. Skeletal muscle mitochondrial respiration in patients with long COVID and healthy controls. Leak respiration (**A**), mitochondrial respiration with NADH-linked substrates (glutamate, pyruvate and malate, **B**), electron transport capacity (ETS, with succinate and FCCP, **C**) and uncoupled succinate-linked respiration (with rotenone, **D**) were lower in patients with long COVID compared to healthy controls, but no effect of PEM was observed. The ratio of oxidative phosphorylation (OXPHOS) capacity to ETS capacity **(E)**, the OXPHOS:ETS control ratio **(F)** and the ETS-OXPHOS control efficiency **(G)**

showed significant differences between long-COVID and healthy controls. The biochemical coupling **(H)** efficiency showed no difference between healthy control and long COVID. Integrated succinate dehydrogenase (SDH) activity (i.e. fiber cross-sectional area x SDH activity**, I**), indicative of the amount of oxidative enzyme per fiber, showed a significant interaction effect. Mean (± SD) coefficient of error versus the number of fibers analyzed for SDH activity **(J)**. This analysis indicated that a minimum of 40 fibers per participant was required to reduce the coefficient of error in the analysis of SDH activity. All panels consisted of 25 long COVID patients and 21 healthy controls. Continuous parametric longitudinal data (panel A-I) were analyzed with a generalized linear mixed model with a two-sided ANOVA. Abbreviations: PEM; post-exertional malaise. SDH; succinate dehydrogenase activity. Box plots show the median (centerline), the first and third quartiles (the lower and upper bound of the box) and the whiskers show the 1.5x interquartile range.



Supplemental Figure 6. Skeletal and venous metabolome before and after induction of post-exertional malaise in long COVID patients. **A:** Heatmap depicting Hedges' g effect size of muscle metabolites and the associated pathways comparing long COVID patients (n=25) with healthy controls (n=19) at both timepoints. **B:** Heatmap depicting Hedges' g effect size of venous blood metabolites and the associated pathways comparing long COVID (n=25) patients with healthy controls (n=21). Highlighted is the citric acid/lactate ratio in skeletal muscle **(C)** and in venous blood **(D)**. Continuous parametric longitudinal data (panel A-D) were analyzed with a generalized linear mixed model with a two-sided ANOVA. Effect sizes (panel

A-B) were calculated with Hedges `g. Abbreviations: NAD; Nicotinamide adenine dinucleotide. PEM; post-exertional malaise, TCA; tricarboxylic acid cycle. Significance of long COVID compared to healthy controls (Group) is shown with *p<0.05; **p<0.001. A significant interaction term is shown with: "†", depicting a p<0.05. Box plots show the median (centerline), the first and third quartiles (the lower and upper bound of the box) and the whiskers show the 1.5x interquartile range.



Supplemental Figure 7. Plasma mitochondrial DNA and circulating markers of tissue damage and stress. The gene expression of circulating mtDNA (ΔΔCt of ND1 and ND6) normalized to 18S **(A-C)** and the fold change as compared to the baseline measurement **(**ΔΔCt; **D-F)**. Panel A-F: Long COVID; n=21, Healthy; n=21. Creatine kinase **(G)**, creatine kinase-MB **(H)** as measured in venous blood were not significantly different. Cortisol **(I)** showed a significant difference over time with no difference between healthy controls and long COVID patients. Adjusting cortisol concentration for the minutes since waking up did not change results. Panel G-I; Long COVID; n=25, Healthy; n=18. The dotted lines in panels D-F represents the baseline value of 1. Continuous parametric longitudinal data (panel A-C, G-I) were analyzed with a generalized linear mixed model with a two-sided ANOVA. Continuous nonparametric longitudinal data (panel D-F) were

conducted by comparing the delta (Δ) between the time points using a two-sided Mann–Whitney U test and t-test. Abbreviations: mt-ND1; mitochondrially-encoded NADH-ubiquinone oxidoreductase chain 1, mt-ND6; mitochondrially-encoded NADH-ubiquinone oxidoreductase chain 6, PEM; post-exertional malaise. Box plots show the median (centerline), the first and third quartiles (the lower and upper bound of the box) and the whiskers show the 1.5x interquartile range.



Chapter 3a

Muscle Abnormalities in Long COVID

ARISING FROM B. Appelman et al. *Nature Communications*

https://doi.org/10.1038/s41467-023-44432-3 (2024)

B. Ranque, P. Garner, Y. Allenbach, D. Hupin, AS David, D. Wade, M. Sharpe, B. Garcin, P. Little, M. Tinazzi, P. Fink, W. Hamilton, T. Peto, C. Lemogne, V. B. B. Wyller, T. Chalder & J. Coebergh

Published in Nature Communications, February 2025



Dear Editor,

The biology of the "kickbacks" (post exertional malaise, PEM) after activity experienced by people with the post-COVID-19 condition (long COVID) is debated. Some specialists believe it is a result of a protective brain response, and others that it is the result of pathophysiology in the muscle itself. Appelman and colleagues report on muscle damage following a maximal effort physical exercise test in patients with PEM with the COVID-19 condition, and these results are interpreted as showing that exercise damages the tissues of people with PEM and should therefore be avoided. However, we believe the data reported do not support this interpretation, as the patients were substantially deconditioned; the physical activity was extreme and biological changes would be expected in anyone; and there were no control patients with a post-COVID-19 condition without PEM. The implications of erroneous interpretation of these data could result in patients fearing that PEM causes physical damage and consequently avoiding approaches to rehabilitation that could help them. Our criticisms are as follows: The patients studied with post-COVID-19 condition were substantially less active before the experiment than the controls were: average steps per day was 4000, compared to 8000 in the controls. Noteworthy, these data only concern the previous week, although deconditioning effects carry over from longer time periods. Moreover, no data are given about other physical activity, whereas patients experiencing PEM usually reduce significantly moderate to intense exercise[1]. It is already known that changes to muscle fibers are strongly related to training over several weeks[2]. Their baseline data showed deconditioning both from the maximal exercise test, and from skeletal muscle biopsy: higher proportion of highly fatigable glycolytic fibers, trend to lower capillary-to-fiber ratio, lower mitochondrial enzyme lower mitochondrial enzyme activity and lower ratio of citric acid to lactate (shift away from oxidative metabolism)[3–5]. As observed in ordinary life, there can be severe muscle pain when returning to intense exercise after periods of a few weeks of relative rest, which gradually disappears when the interval between exercises is shortened. Indeed, the observed morphological and metabolic muscle changes after maximal exercise test could all be consequences of unusually intense exercise, especially in patients who are physically deconditioned.

The study did not include muscle data from patients without PEM, so linking PEM to these muscle changes (which could be present also in people with post-COVID-19 condition without PEM) may be misleading, and furthermore this putative link lacks clinical

plausibility. No detailed clinical description of PEM symptoms is provided, but among symptoms reported by patients one and eight days after intense exercise, none indicative of muscle pathology changed. It is of note, that the usual PEM symptoms and their duration described in long COVID or myalgic encephalomyelitis/chronic fatigue syndrome (ME/ CFS, in which PEM is commonly reported[6]) do not correspond to the post-exercise symptoms of known inflammatory myopathies, metabolic, or mitochondrial disorders[7,8].

The authors note that all the patients experienced PEM, despite considerable variability in initial muscle characteristics, and conclude that "the pathophysiology of fatigue and a reduced exercise capacity is distinct from the rapid development of PEM in long COVID patients." An alternative interpretation is that a patient's experience of symptoms correlates poorly both to the physical effort and any pathological muscle changes seen in this population. A recent study on chronic fatigue conditions, including ME/CFS, shows an alteration of effort preference, rather than physical fatigue, due to dysfunction of integrative brain regions, with consequences on autonomic functioning and physical conditioning[9]. Therefore, an alternative explanation of post-exercise symptoms is that they result from the interaction between altered interoception (conscious and unconscious self-awareness of internal bodily state), allostatic load (failure of stress adaptation with perceived burden that influences how current and future energy needs are maintained) and peripheral influences (muscle fatigue).

The authors also note: "The development of post-exertional malaise could lead to a further reduction in exercise capacity in patients, as the acute reduction in mitochondrial SDH activity, occurrence of tissue necrosis, and possibly intramuscular accumulation of amyloid-containing deposits could worsen skeletal muscle metabolism and force production over time, causing a vicious downward circle." This suggestion is not supported by the observation that there were no significant differences in muscle pain, fatigue severity scale or daily step count before and after the PEM. In addition, many patients have reported complete recovery despite initially experiencing PEM[6]. Nevertheless, the fear of developing PEM has the potential to con-tribute to a vicious circle of an attentional focus on symptoms, leading to exercise avoidance which itself worsens the symptom experience and leads to further physical deconditioning and associated disability. Although the authors did not provide any recommendations about physical activity for patients with long COVID, their findings have been widely

interpreted in the media as indicating that exercise causes muscle damage in people with this condition, implying that exercise should be avoided.

We are of the view that this interpretation is both scientifically unfounded and harmful to patients. Indeed, although we agree that intense exercise, such as the type tested, is not to be recommended, several studies have reported benefit from more gradual increases exercise both in patients with ME/CFS[10] and patients with post-COVID-19 conditions[11]. It is particularly notable that no patient in these studies of the benefits of collaboratively graduated exercise had to stop because of worsening of symptoms[1,11–15]. An interpretation of the data that exercise is always harmful must therefore be robustly corrected.

Reporting summary

Further information on research design is available in the Nature Portfolio Reporting Summary linked to this article.

Author contributions

The authors confirm their contribution to the paper as follows: study conception, draft manuscript preparation: B.R., P.G., J.C.. All authors (B.R., P.G., Y.A., D.H., A.D., D.W., M.S., B.G., P.L., M.T., P.F., W.H., T.P., C.L.,

V.W., T.C., J.C.) contributed to the development and refining of the manuscript. All authors (B.R., P.G., Y.A., D.H., A.D., D.W., M.S., B.G., P.L.,

M.T., P.F., W.H., T.P., C.L., V.W., T.C., J.C.) reviewed the results and approved the final version.

Competing interests

This author declares the following competing interests. TC is part-funded by the National Institute for Health Research (NIHR) Biomedical Research Center at South London and Maudsley NHS Foundation Trust, King's College London. She has grants from Guy's St Thomas Charity Grants, NIHR, and UKRI for post COVID syndromes. She has received travel expenses, accommodation costs, and honorarium for several lectures in Europe and has received travel expenses and accommodation costs for attending the American Thoracic Society Conference. She was on the Expert Advisory Panel for Covid-19 Rapid Guidelines. All other authors declare no competing interests.

Additional information

Supplementary information The online version contains supplementary material available at https://doi.org/10.1038/s41467-025-56430-8.

References

1. Tryfonos, A. et al. Functional limitations and exercise intolerance in patients with Post-COVID condition: A randomized crossover clinical trial. *JAMA Netw. Open* 7, e244386 (2024).
2. Narici, M. et al. Impact of sedentarism due to the COVID-19 home confinement on neuromuscular, cardiovascular and metabolic health: Physiological and pathophysiological implications and recommendations for physical and nutritional countermeasures. *Eur. J. Sport Sci.* 21, 614–635 (2021).
3. Eggelbusch, M. et al. The impact of bed rest on human skeletal muscle metabolism. *Cell Rep. Med.* 5, 101372 (2024).
4. Oranger A., et al. Impact of 10-day bed rest on serum levels of irisin and markers of musculoskeletal metabolism. FASEB J. 2023 Jan [cited 2024 Mar 19];37. Available from: https://onlinelibrary.wiley. com/doi/10.1096/fj.202201005RR
5. Affourtit, C. & Carré, J. E. Mitochondrial involvement in sarcopenia.
6. *Acta Physiol.* 240, e14107 (2024).
7. The Oslo Chronic Fatigue Consortium. et al. Chronic fatigue syndromes: real illnesses that people can recover from. *Scand. J. Prim. Health Care* 41, 372–376 (2023).
8. Ricci, G., Fontanelli, L., Torri, F., Schirinzi, E. & Siciliano, G. Fatigue as a common signature of
9. inflammatory myopathies: clinical aspects and care. *Clin. Exp. Rheumatol.* 40, 425–432 (2022).
10. Finsterer, J. Update review about metabolic myopathies. *Life* 10, 43 (2020).
11. Walitt, B. et al. Deep phenotyping of post-infectious myalgic encephalomyelitis/chronic fatigue syndrome. *Nat. Commun.* 15, 907 (2024).
12. Larun L., Brurberg K. G., Odgaard-Jensen J., Price J. R. Exercise therapy for chronic fatigue syndrome. Cochrane Common Mental Disorders Group, editor. Cochrane Database of Systematic Reviews. 2017 Apr 25 [cited 2023 Nov 16]; Available from: https:// doi.wiley.com/10.1002/14651858.CD003200.pub7
13. Zeraatkar D., et al. Interventions for the management of post COVID-19 condition (long COVID): Protocol for a living systematic review & network meta-analysis. Infectious

Diseases (except HIV/ AIDS); 2024 [cited 2024 Nov 17]. Available from: http://medrxiv.org/lookup/doi/10.1101/2024.03.15.24304168

14. Sánchez-García, J. C. et al. Long COVID and physical therapy: a systematic review. *Diseases* 11, 163 (2023).
15. Espinoza-Bravo, C. et al. Effectiveness of functional or aerobic exercise combined with breathing techniques in telerehabilitation for patients with long COVID: A randomized controlled trial. *Phys. Ther.* 103, pzad118 (2023).
16. McGregor G., et al. Clinical effectiveness of an online supervised group physical and mental health rehabilitation programme for adults with post-covid-19 condition (REGAIN study): multicentre randomised controlled trial. *BMJ*, e076506. (2024).
17. Jimeno-Almazán, A. et al. Rehabilitation for POST-COVID -19 condition through a supervised exercise intervention: A randomized con-trolled trial. *Scand. Med Sci. Sports* 32, 1791–1801 (2022).



Chapter 3b

Reply to: Matters Arising: Muscle Abnormalities in Long COVID

Appelman, B., Charlton, B.T., Goulding, R.P., Kerkhoff T.J., Breedveld E.A., Noort W., Offringa C., Bloemers F.W., van Weeghel, M., Schomakers, B.V., Coelho, P, Posthuma J.J., Aronica E., Wiersinga, W.J., van Vugt M., Wüst, R.C.I.

Published in Nature Communications, February 2025



We thank Ranque et al. for their interest in our recent work and alternative interpretation of our data. We refute that our findings are due to deconditioning, as Long COVID-related skeletal muscle differ fundamentally from those caused by deconditioning. We demonstrated significant physiological differences in Long COVID patients with PEM compared to healthy controls, even at matched physical activity levels. PEM encompasses a variety of symptoms and not only muscle soreness. Our study did not address the efficacy of exercise training, and we reject misinterpretations that all forms of exercise cause PEM. We advocate further research to define safe exercise thresholds and improve the understanding of PEM.

Ranque et al. state that 'everyone can experience severe muscle pain when returning to intense exercise after periods of a few weeks of rest'. Every participant experienced maximal exercise, healthy participants with low fitness also participated, and a proportion of Long COVID patients still possessed fitness levels >50th percentile for their respective sex and age, despite all patients experiencing post-exertional malaise (PEM). Despite several controls having a $\dot{V}O_{2max}$ similar to patients, none reported PEM symptoms.

We acknowledge the general population experiences muscle soreness, particularly after eccentric contractions, but cycle exercise involves little or no eccentric work. PEM encompasses more than muscle pain, and as can be appreciated from our clinical evaluation in Table 2, we do not reduce PEM to muscle pain or fatigue alone. We also do not link PEM symptoms and duration described in Long COVID with post-exercise symptoms of known inflammatory myopathies, metabolic, or mitochondrial disorders, as PEM is a symptom specific to post-infectious diseases[1]. We utilized the DSQ-PEM questionnaire for the clinical definition of PEM, as is common practice[2]. Contrary to the assertion of Ranque et al., Long COVID patients reported more muscle or joint pain (64% before and 80% 1-day after PEM induction) and significantly greater fatigue intensity (self-reported and with the Multidimensional Fatigue Inventory; Table 2 and Figure S2A). Ranque et al. refer to pivotal work by Walitt and colleagues[3] to substantiate a psychological explanation of PEM, while the study rather provides multiple physiological explanations for ME/CFS pathophysiology, including autonomic dysfunction, differential cerebrospinal fluid catecholamines and metabolite profiles, and lower post-exercise cortisol responses. Ranque et al. claim that 'post-exercise symptoms could result from the interaction between altered [..] unconscious self-awareness of internal bodily state [… and] failure of stress adaptation with perceived burden that influences how current and future energy needs are maintained', however Wallit et al. state that 'peak measures did not correlate with effort preference in ME/CFS', refuting the

claim that effort preference dictates $\dot{V}O_{2max}$. Importantly, this paper also confirms our findings of lower $\dot{V}O_{2max}$ and impairments in skeletal muscle mitochondrial metabolism, albeit in ME/CFS patients[3]. That our Long COVID patients also exhibited significantly lower gas exchange thresholds and respiratory compensation points, which are effort-independent, indicates a reduction in aerobic function that is not effort-independent.

Ranque et al. state that we did not provide an adequate control group, and that the observed changes could be due to deconditioning. While we recognize that a full age-, sex- and activity-matched control group would have improved the quality of the study, we disagree that deconditioning alone explains these results. The skeletal muscle alterations observed in our Long COVID group display marked differences compared to healthy humans undergoing strict bed rest[4]. We found no differences in either capillarization or fibre cross-sectional area between Long COVID patients and healthy controls. Conversely, bed rest rapidly induces muscle atrophy, reduces capillary density, and alters mitochondrial structure and function within days[4,6,7]. Further, skeletal muscle intrinsic mitochondrial function was reduced in Long COVID patients compared to healthy controls (Figure S5), indicative of qualitative alterations in mitochondrial respiration, rather than loss of mitochondrial content typically observed with bed rest[4]. While step reduction alters muscle substantially[8,9], this is typically associated with reductions in fibre cross sectional area and reduced mitochondrial markers, which (at baseline) was not observed in Long COVID patients. We performed additional analyses on our publicly available data file, and matched participants by step count (5181 *vs.* 4727 steps/day for patients and controls, respectively). In this small, but matched cohort, we still observed a significant group difference for $\dot{V}O_{2max}$ (-24%, p=0.004) and peak power output (-31%, p=0.043). Althoff et al. indicated that the daily steps in the United States were 4774 steps/day[10]; therefore, our cohort, while likely less active than prior to infection, were not less active than expected in the general USA population. Yet, Long COVID patients presented with abnormal histopathology even prior to the exercise bout - also confirmed by others[11,12] - while our less aerobically fit, healthy controls exhibited little to no abnormal histopathology (see source data). These differences in skeletal muscle characteristics between Long COVID and human bed rest studies imply that the effect of Long COVID on skeletal muscle structure and function fundamentally differs from that of deconditioning alone. While we cannot neglect that deconditioning may impact Long COVID progression, the evidence provided suggests deconditioning itself does not fully explain symptoms experienced by Long COVID patients with PEM.

Long COVID is reported to be a heterogeneous disease, which is why we chose to focus on PEM, as ~90% of patients present with this symptom[13]. We recognize our results only pertain to those experiencing PEM. While we acknowledge that Long COVID patients without PEM were not included as a control group, the study was designed to use acute exercise to induce PEM and measure systemic changes before and after PEM induction. We therefore disagree that we cannot link the acute exercise mediated alterations of Long COVID patients to PEM[13]. Our findings demonstrated physiological alterations in Long COVID patients with PEM after maximal exercise that did not occur in healthy controls, whom do not experience PEM. PEM research is still in its infancy, and we will applaud studies with well-defined cohorts and experimental designs that can provide additional insights into PEM pathophysiology.

Ranque et al. suggest that many patients have reported full recovery in ME/CFS, despite experiencing PEM; however, the meta-analysis cited[14] concludes that while exercise provided a small positive effect, quality of life did not improve. Further, multiple studies included in the meta-analysis include participants with other comorbidities that would benefit from exercise (i.e. asthma, diabetes, chronic heart disease). Ranque et al. also refer to several other studies that have shown successful rehabilitation of patients, however these studies also include up to ~30% of patients exhibiting other comorbidities[15–17]. One strength of our current study is that patients did not exhibit other comorbidities that may conflate with Long COVID.

Ranque et al. state that our 'findings have been widely interpreted in the media as indicating that exercise in people with Long COVID causes muscle damage and implying that people with Long COVID should not exercise', but simultaneously agree 'that intense exercise, such as the one tested in the study, is not recommended', albeit without providing argumentation. While we speculate that PEM could result in fear of exercising at intensities above the PEM threshold, this was not the focus of our research, and feel this critique does not pertain to our publication. We appreciate that frequency, intensity, and duration are vital in improving aerobic fitness in healthy individuals[18], and positively modulate many chronic diseases. However, Long COVID and PEM are poorly understood, and our study did not address the efficacy or advisability of exercise training in Long COVID treatment. Further, we find there is a dearth of high-quality scientific information surrounding dedicated exercise training in Long COVID patients, and disagree with the standard of evidence surrounding graded exercise therapy. In the training studies cited, none involved interventions that systematically induced, monitored, or avoided PEM. Additionally, adherence and other comorbidities are often ill-described. While exercise below the PEM-inducing threshold may benefit Long COVID patients, this was

not the topic of our current publication, and therefore we refrained from conclusive scientific or clinical statements. Given our clinical experience and scientific evidence, we advocate caution regarding intense exercise in Long COVID patients with PEM. While pacing and moderate exercise below he PEM-inducing threshold may be performed, these thresholds are ill-defined and more research is needed to elucidate the physiological onset of PEM.

Author contributions

BA, BTC, RPG and RCIW drafted the response. BA, BTC, RPG, TJK, EAB, WN, CO, FWB, MvW, BS, PC, JJP, EA, WJW, MvV and RCIW critically reviewed and accepted the final version.

Conflict of interest

All authors have declared no conflict of interest.

References

1. Poenaru, S., Abdallah, S. J., Corrales-Medina, V. & Cowan, J. COVID-19 and post-infectious myalgic encephalomyelitis/chronic fatigue syndrome: a narrative review. *Ther Adv Infect Dis* **8**, 20499361211009384 (2021).
2. Cotler, J., Holtzman, C., Dudun, C. & Jason, L. A. A Brief Questionnaire to Assess Post-Exertional Malaise. *Diagnostics* **8**, (2018).
3. Walitt, B. *et al.* Deep phenotyping of post-infectious myalgic encephalomyelitis/chronic fatigue syndrome. *Nat Commun* **15**, 907 (2024).
4. Eggelbusch, M. *et al.* The impact of bed rest on human skeletal muscle metabolism. *Cell Rep Med* **5**, 101372 (2024).
5. Soares, M. N. *et al.* Skeletal muscle alterations in patients with acute Covid-19 and post-acute sequelae of Covid-19. *J Cachexia Sarcopenia Muscle* **13**, 11–22 (2022).
6. Hendrickse, P. W. *et al.* Capillary rarefaction during bed rest is proportionally less than fibre atrophy and loss of oxidative capacity. *J Cachexia Sarcopenia Muscle* **13**, 2712–2723 (2022).
7. Hyatt, H. W. & Powers, S. K. Mitochondrial Dysfunction Is a Common Denominator Linking Skeletal Muscle Wasting Due to Disease, Aging, and Prolonged Inactivity. *Antioxidants (Basel)* **10**, (2021).
8. Narici, M. *et al.* Impact of sedentarism due to the COVID-19 home confinement on neuromuscular, cardiovascular and metabolic health: Physiological and pathophysiological

implications and recommendations for physical and nutritional countermeasures. *Eur J Sport Sci* **21**, 614–635 (2021).

9. Edwards, S. J. *et al.* Short-term step reduction reduces citrate synthase activity without altering skeletal muscle markers of oxidative metabolism or insulin-mediated signaling in young males. *J Appl Physiol* **131**, 1653–1662 (2021).

10. Althoff, T. *et al.* Large-scale physical activity data reveal worldwide activity inequality. *Nature* **547**, 336 (2017).

11. Hejbøl, E. K. *et al.* Myopathy as a cause of fatigue in long-term post-COVID-19 symptoms: Evidence of skeletal muscle histopathology. *Eur J Neurol* **29**, 2832–2841 (2022).

12. Colosio, M. *et al.* Structural and functional impairments of skeletal muscle in patients with postacute sequelae of SARS-CoV-2 infection. *J Appl Physiol* **135**, (2023).

13. Thaweethai, T. *et al.* Development of a Definition of Postacute Sequelae of SARS-CoV-2 Infection. *JAMA* **329**, 1934–1946 (2023).

14. Larun, L., Brurberg, K. G., Odgaard-Jensen, J. & Price, J. R. Exercise therapy for chronic fatigue syndrome. *Cochrane Database of Systematic Reviews* (2017) doi:10.1002/14651858.CD003200.pub7.

15. McGregor, G. *et al.* Clinical effectiveness of an online supervised group physical and mental health rehabilitation programme for adults with post-covid-19 condition (REGAIN study): multicentre randomised controlled trial. *BMJ* e076506 (2024) doi:10.1136/bmj-2023-076506.

16. Espinoza-Bravo, C. *et al.* Effectiveness of Functional or Aerobic Exercise Combined With Breathing Techniques in Telerehabilitation for Patients With Long COVID: A Randomized Controlled Trial. *Phys Ther* **103**, (2023).

17. Jimeno-Almazán, A. *et al.* Rehabilitation for post-COVID-19 condition through a supervised exercise intervention: A randomized controlled trial. *Scand J Med Sci Sports* **32**, 1791–1801 (2022).

18. Holloszy, J. O. Biochemical adaptations in muscle. Effects of exercise on mitochondrial oxygen uptake and respiratory enzyme activity in skeletal muscle. *J Biol Chem* **242**, 2278–82 (1967).



Chapter 4a

Should We Be Careful with Exercise in Post-Exertional Malaise After Long COVID?

ARISING FROM B. Appelman et al. *Nature Communications* https://doi.org/10.1038/s41467-023-44432-3 (2024).

Christiaan G. J. Saris , Baziel G. M. van Engelen, Mirian C. H. Janssen, Benno Kusters, Richard J. T. Rodenburg, David E. Sluijs & Nicoline B. M. Voet

Published in Nature Communications, February 2025



Post-exertional malaise after COVID-19 infection is a debilitating postviral condition. We applaud the work of Appelman et al.[1] addressing the important questions on how long COVID develops and how to treat this condition. From our experience with mitochondrial diseases and training strategies in neuromuscular diseases, we would like to comment on the findings and conclusions drawn in this study. The suggestion that strenuous exercise increases symptoms of myalgia and exercise intolerance is, in our opinion, not specific for long COVID. In addition, it could now be interpreted that exercise should be avoided. However, the opposite is true as we will elaborate.

Establishing lower maximal (or peak) oxygen consumption in patients with long COVID is important and a confirmation of previous work in long COVID and other post-viral symptoms[2–5]. Besides a lower maximal oxygen consumption, Appelman et al. have found a higher proportion of glycolytic fibers, lower CSA of type I fibers, lower peak power output, lower OXPHOS capacity, lower citrate to lactate ratio, and lower concentration of creatine. The combination of these (latter) findings points in the direction of deconditioning in addition to a direct post viral effect. Decrease in mitochondrial content has also been found in patients with chronic fatigue syndrome compared to healthy controls[6], and mechanisms of post-viral loss of mitochondrial content could be similar.

Authors state that the examined long COVID patients were physically active with an average of 4000 steps a day, which equates to about 3.2 km or between 30 and 45 min of daily walking, depending on speed. However, the number of daily steps was significantly lower, around 30–40%, compared to the control group used in this study. This difference in daily exercise is on top of their low aerobic capacity. Favorable mitochondrial adaptations in muscle can only be achieved if training is performed at a sufficient frequency, intensity, and duration for an adequate length of time[7]. Appelman et al. state that severe exercise-induced myopathy and tissue infiltration of amyloid-containing deposits in skeletal muscles of patients with long COVID worsen one day after strenuous exercise. According to our experience such findings cannot arise in just one day. Muscle damage after strenuous exercise starts with sarcolemmal lysis and destruction of the basal lamina resulting in fiber necrosis with concomitant endomysial cell infiltrates to remove cell debris. Cytokines accelerate the inflammatory response and induce myoblast proliferation. Satellite cells become activated, proliferate, and differentiate into multinucleated myotubes and eventually into regenerated myofibers. Active muscle degeneration and inflammation occur in the first few days post-injury, whereas muscle regeneration usually occurs seven to ten days after

injury[8,9]. Muscle atrophy occurs as the rate of protein degradation exceeds that of protein synthesis[10]. The development of atrophied and regenerative cells in the muscle takes at least a few days since the half-life of contractile proteins is 3–4 days[11]. Therefore, it is unlikely that the incremental test itself cause post-exertional malaise in long-term COVID, based on these histological findings.

Mild histopathological abnormalities are often present in healthy control biopsies[12]. After training, muscle fiber turnover and regeneration are part of normal physiology[13]. There is no correlation between the abnormalities on histology and perceived myalgia and exercise intolerance. More importantly, normal muscle contains a considerable number of macrophages and T-lymphocytes[14]. The authors suggested a direct link between the found muscle abnormalities, perceived myalgia, and exercise intolerance. The current study lacks a control group with similar fitness levels, which limits the interpretations of findings.

In conclusion, the message that intensive exercise can damage the muscle in long COVID is, in our view, not demonstrated. Additionally, it can be interpreted by patients that exercise with concomitant muscle fatigue and myalgia might cause muscle damage, resulting in patients not exercising at all. Training at the correct intensity, where most time is spent at maximal aerobic metabolism, increases mitochondrial density and lactate membrane transporters and will improve oxidative capacity, also in long COVID patients[15–17]. Many patients have difficulty adjusting their intensity of physical activity and training to the new level of fitness.

We underline that research on the cause of decreased aerobic capacity in long-COVID and similar post-viral conditions is needed. Better therapies should become available. Improvements in muscle fitness can act as therapy in long COVID, and supervised training at different volumes and intensities should be tested at specialized centers according to established guidelines and compared to participants of equal fitness level.

Reporting summary

Further information on research design is available in the Nature Portfolio Reporting Summary linked to this article.

Author contributions

Writing - original draft: C.G.J.S. Writing - review & editing: C.G.J.S., B.G.M.v.E., M.C.H.J., B.K., R.J.T.R., D.E.S., and N.B.M.V.

Competing interests

The authors declare no competing interests.

Additional information

Supplementary information The online version contains supplementary material available at https://doi.org/10.1038/s41467-025-56427-3.

References

1. Appelman, B. et al. Muscle abnormalities worsen after post-exertional malaise in long COVID. *Nat. Commun.* 15, 17 (2024).
2. Norweg, A. et al. Exercise intolerance associated with impaired oxygen extraction in patients with long COVID. *Respir. Physiol. Neurobiol.* 313, 104062 (2023).
3. Schafer, H., Teschler, M., Mooren, F. C. & Schmitz, B. Altered tissue oxygenation in patients with post COVID-19 syndrome. *Microvasc. Res.* 148, 104551 (2023).
4. Durstenfeld, M. S. et al. Use of cardiopulmonary exercise testing to evaluate long COVID-19 symptoms in adults: a systematic review and meta-analysis. *JAMA Netw. Open* 5, e2236057 (2022).
5. Guarnieri, J. W. et al. Core mitochondrial genes are down-regulated during SARS-CoV-2 infection of rodent and human hosts. *Sci. Transl. Med.* 15, eabq1533 (2023).
6. Smits, B. et al. Mitochondrial enzymes discriminate between mitochondrial disorders and chronic fatigue syndrome. *Mitochondrion* 11, 735–738 (2011).
7. Holloszy, J. O. Biochemical adaptations in muscle. Effects of exercise on mitochondrial oxygen uptake and respiratory enzyme activity in skeletal muscle. *J. Biol. Chem.* 242, 2278–2282 (1967).
8. Huard, J., Li, Y. & Fu, F. H. Muscle injuries and repair: current trends in research. *J. Bone Joint Surg. Am.* 84, 822–832 (2002).
9. Wei, S. H. J. Tissue therapy implications of regenerative medicine for skeletal muscle. *Princ. Regener. Med*. https://doi.org/10.1016/ B978-012369410-2.50074-7 (2008).

10. Theilen, N. T., Kunkel, G. H. & Tyagi, S. C. The role of exercise and TFAM in preventing skeletal muscle atrophy. *J. Cell Physiol.* 232, 2348–2358 (2017).

11. Thomason, D. B., Herrick, R. E., Surdyka, D. & Baldwin, K. M. Time course of soleus muscle myosin expression during hindlimb sus-pension and recovery. *J. Appl. Physiol.* 63, 130–137 (1987).

12. Lassche, S. et al. Correlation between quantitative MRI and muscle histopathology in muscle biopsies from healthy controls and patients with IBM, FSHD and OPMD. *J. Neuromuscul. Dis.* 7, 495–504 (2020).

13. Hikida, R. S., Staron, R. S., Hagerman, F. C., Sherman, W. M. & Costill, D. L. Muscle fiber necrosis associated with human marathon runners. *J. Neurol. Sci.* 59, 185–203 (1983).

14. Johannssen, K. et al. Myalgia with the presence of pathologic EMG correlates with perimysial inflammatory infiltrates. *Neurol. Neu-roimmunol. Neuroinflamm.* 6, e549 (2019).

15. Voet, N. B., van der Kooi, E. L., van Engelen, B. G.& Geurts, A. C. Strength training and aerobic exercise training for muscle disease. *Cochrane Database Syst. Rev.* 12, CD003907 (2019).

16. Nopp, S. et al. Outpatient pulmonary rehabilitation in patients with long COVID improves exercise capacity, functional status, dyspnea, fatigue, and quality of life. *Respiration* 101, 593–601 (2022).

17. Daynes, E. et al. Pulmonary rehabilitation for individuals with persistent symptoms following COVID-19. *Chest* https://doi.org/10. 1016/j.chest.2024.01.029 (2024).

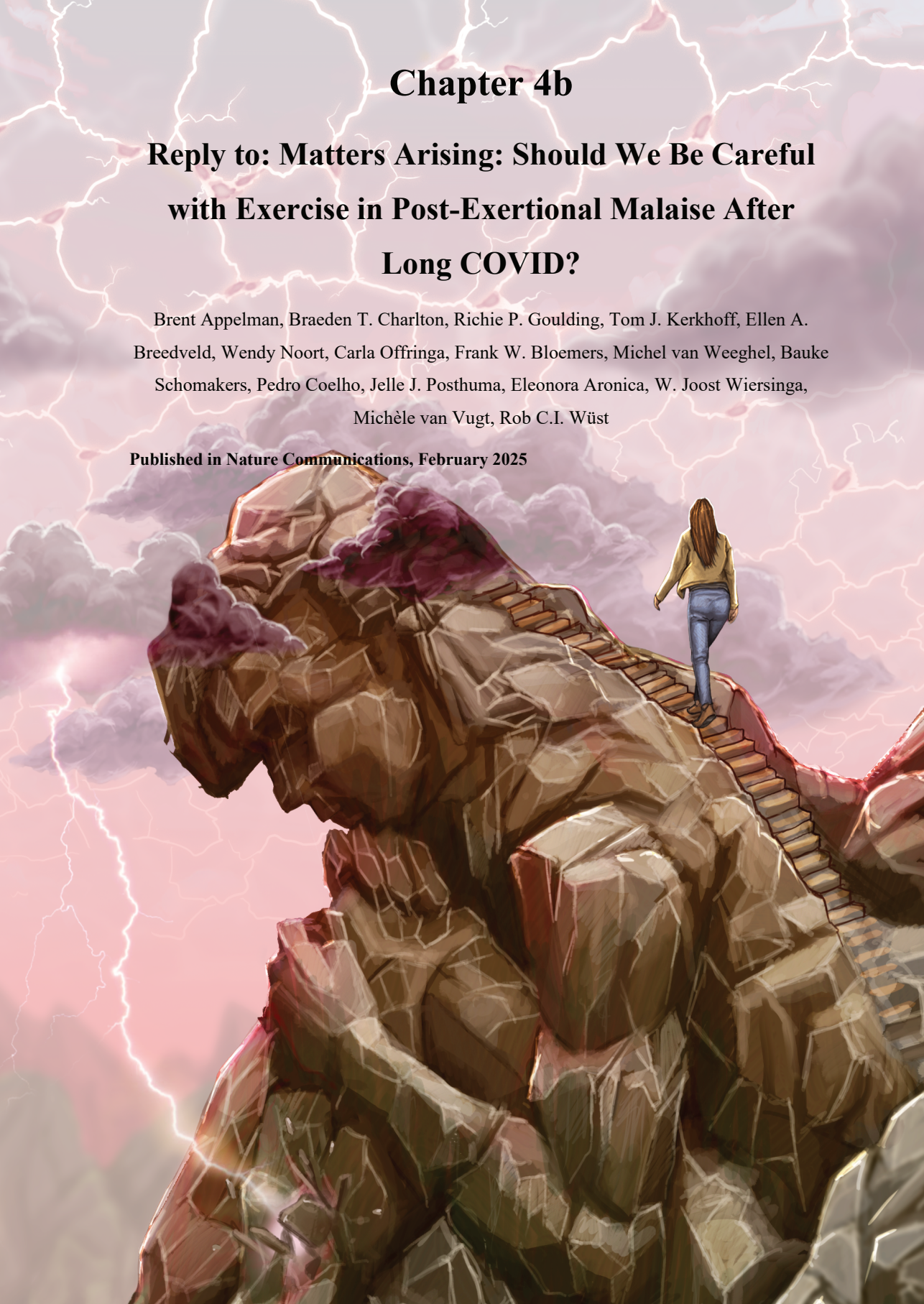


Chapter 4b

Reply to: Matters Arising: Should We Be Careful with Exercise in Post-Exertional Malaise After Long COVID?

Brent Appelman, Braeden T. Charlton, Richie P. Goulding, Tom J. Kerkhoff, Ellen A. Breedveld, Wendy Noort, Carla Offringa, Frank W. Bloemers, Michel van Weeghel, Bauke Schomakers, Pedro Coelho, Jelle J. Posthuma, Eleonora Aronica, W. Joost Wiersinga, Michèle van Vugt, Rob C.I. Wüst

Published in Nature Communications, February 2025



We thank Saris et al. for their interest in our recent paper[1], which focused on the skeletal muscle components of post-exertional malaise (PEM) in Long COVID patients. We did not address the efficacy of exercise as a treatment, but our findings do not support that deconditioning or bed rest explains the skeletal muscle abnormalities in Long COVID. PEM is a distinct symptom poorly understood and not analogous to other conditions. We caution against generalizing our results to all Long COVID patients or drawing causal conclusions beyond the study's design, and we advocate adherence to established guidelines that recommend avoiding activities triggering PEM.

Whilst we recognize the exercise therapy experience of Saris et al. in patients with mitochondrial and neuromuscular diseases, we firmly reject the notion that our findings regarding post-exertional malaise (PEM) are not specific to Long COVID, nor that we address 'how to treat this condition'. Saris et al. claim that "*improvements in muscle fitness can act as therapy in Long COVID*", based on assumptions and experiences with other diseases. PEM is a specific symptom of many post-viral infection diseases (including Long COVID and ME/CFS) which is poorly understood, and poorly recognized by clinicians. As such, intense exercise above an unknown time- and patient-dependent PEM-inducing threshold is often avoided by patients, because it worsens their Long COVID symptoms. Therefore, it was the explicit goal of our study to examine the systemic and skeletal muscle component of PEM in Long COVID.

Importantly, our publication did not provide any statement about the merit or avoidance of exercise in treating patients with Long COVID, and we are therefore surprised that Saris and colleagues concluded this. We clearly understand that frequency, intensity and duration are important parameters of exercise training in improving aerobic fitness in healthy people[2]. However, patients with Long COVID and PEM are unable to functionally recover completely after an exercise bout at a high intensity or duration, limiting their ability to frequently perform such exercise bouts. The interpretation of exercise-related results in Long COVID critically depends on which patients are included. Our patients could work ~5 hours/week, and all experienced PEM, which is a key symptom in 87% of all Long COVID patients[3]. Hence, our results should not be extrapolated to all Long COVID patients (i.e. those not suffering from PEM or with less debilitating symptoms, such as in a recent study[4]). Further, our results cannot be extrapolated to applicability of exercise training for treatment, simply because we did not study this.

Deconditioning has been proposed as causative of skeletal muscle changes in Long COVID patients. Our previous work on bed rest demonstrates that adaptations in skeletal muscle structure and function differ markedly between Long COVID patients and healthy persons exposed to severe deconditioning[5,6]. Bed rest induces rapid muscle atrophy and loss of capillarization[6], which was not observed in our Long COVID patients[1]. We did not observe alterations in fiber type composition after 60 days of strict bed rest[6], whereas our Long COVID patients exhibited a more glycolytic phenotype. Our Long COVID participants showed lower mitochondrial respiration, due to mitochondrial dysfunction (Figure S5)[1] rather than mitochondrial loss, the latter of which is more typically seen after long-term bed rest[5-7]. The absence of a correlation between $\dot{V}O_{2max}$ and succinate dehydrogenase activity also suggests that factors other than deconditioning contribute.

Saris et al. criticize us for not providing an adequate deconditioned control group. We acknowledge that deconditioning confounds the conclusions related to the underlying cause of a lower exercise capacity, and that an age-, sex- and activity-matched control group would be superior to age and sex alone. Althoff et al.[8] showed that the average daily steps in the United States is 4774 per day, roughly similar to our Long COVID group, but PEM is not experienced in the general US population. As can be appreciated from Figure 1A, there was considerable variability in exercise capacity, as some patients still possessed fitness levels >50th percentile for their sex and age (n=5), while some healthy controls had very low fitness levels (<25th percentile, n=7). Yet, all patients exhibited PEM and healthy controls did not, irrespective of fitness. Additional analysis matching participants for step count (5181 *vs.* 4727 steps/day for patients and controls, respectively) still resulted in a significant group difference for $\dot{V}O_{2max}$ (-24%, p=0.004), peak power (-31%, p=0.043) and gas exchange threshold (-20%, p=0.046; effort-independent). These data strongly suggest deconditioning alone does not cause the skeletal muscle abnormalities.

Our results of impaired mitochondrial function and skeletal muscle myopathy in Long COVID patients are in line with other recent publications[4,9-11]. The causal role of deconditioning in explaining skeletal muscle adaptations in Long COVID is impossible to ascertain from our study design, as we acknowledged in the paper. We do not know the underlying factors contributing to these changes, and as good scientific practice, we refrained from drawing causal relationships in our publication. We were therefore surprised to read that Saris et al. drew causal conclusions based on work which was not set up to be causal in nature. Recently, we and others described many possible factors contributing to Long COVID

symptomology, including viral persistence, immune cell and autonomous nervous system dysregulation and auto-immunity[11-13].

Saris et al. question the muscle damage following exercise. Biopsies were scored for pathological findings by a group-blinded pathologist, where the tissue needed to contain more than a "normal" number of atrophied fibers (2-4% in healthy people), regenerative fibers, or infiltrating macrophages and T-cells. As such, scoring negative did not mean that there was no staining at all. Also, the size of the biopsy could not be controlled for. We are aware of exercise-induced muscle damage, and the occurrence of exertional rhabdomyolysis in patients with mitochondrial diseases[14,15]. Saris et al. suggest that atrophied fibers cannot occur one day following exercise, but the reference they provide[16] proves the opposite. Hikida et al[16] show degeneration of myofibrils, and occurrence of atrophic fibers along with abnormal mitochondrial profiles one day following a marathon (which we would not refer to as '*training and normal physiology*'). Before PEM induction, patients show higher number of atrophied fibers, higher macrophage infiltration, higher T-cell infiltration and more cells with internalized nuclei compared to controls, similar to results by Hejbøl et al.[10]. Since some of these were already different in the pre-PEM biopsies, we agree that this cannot be associated with PEM, but we do not exclude remnants of previous PEM episodes, since the time-course of muscle regeneration can be slow.

In sum, we agree with the conclusion of Saris et al. that '*research on the cause of decreased aerobic capacity in long COVID and similar post-viral conditions is needed*', and feel our work makes a valuable contribution to this need. However, we strongly encourage Saris and colleagues not to draw causal conclusions that were not evidenced or supported by our work. It is essential to realize the infancy of PEM research and that previous findings in other diseases may not apply to PEM in Long COVID. We also agree that '*better therapies should become available*', as this is a clear wish for scientists, clinicians and patients. The established guidelines that Saris et al. refer to, in fact, include specific statements about avoiding "exercise and activities that cause PEM and aim to conserve your energy"[17]. While we value and promote exercise below the PEM-inducing threshold for patients with Long COVID with and without PEM[17], this was not the topic of our publication, and therefore we refrained from making conclusive statements. Because of the occurrence of PEM, intense exercise training above the PEM-threshold is unlikely to be a curative treatment for Long COVID patients with PEM.

Author contributions

BA, BTC, RPG and RCIW drafted the response. BA, BTC, RPG, TJK, EAB, WN, CO, FWB, MvW, BS, PC, JJP, EA, WJW, MvV and RCIW critically reviewed and accepted the final version.

Conflict of interest

All authors have declared no conflict of interest.

References

1. Appelman, B. et al. Muscle abnormalities worsen after post-exertional malaise in long COVID. *Nat Commun* 15, 17 (2024).
2. Holloszy, J. O. Biochemical adaptations in muscle. Effects of exercise on mitochondrial oxygen uptake and respiratory enzyme activity in skeletal muscle. *J Biol Chem* 242, 2278–2282 (1967).
3. Thaweethai, T. et al. Development of a Definition of Postacute Sequelae of SARS-CoV-2 Infection. *JAMA* 329, 1934–1946 (2023).
4. Tryfonos, A. et al. Functional Limitations and Exercise Intolerance in Patients With Post-COVID Condition: A Randomized Crossover Clinical Trial. *JAMA* Netw Open 7, E244386 (2024).
5. Eggelbusch, M. et al. The impact of bed rest on human skeletal muscle metabolism. *Cell Rep Med* 5, (2024).
6. Hendrickse, P. W. et al. Capillary rarefaction during bed rest is proportionally less than fibre atrophy and loss of oxidative capacity. *J Cachexia Sarcopenia Muscle* 13, 2712–2723 (2022).
7. Gollnick, P. D., Armstrong, R. B., Saubert, C. W., Piehl, K. & Saltin, B. Enzyme activity and fiber composition in skeletal muscle of untrained and trained men. *J Appl Physiol* 33, 312–319 (1972).
8. Althoff, T. et al. Large-scale physical activity data reveal worldwide activity inequality. *Nature* 547, 336 (2017).
9. Colosio, M. et al. Structural and functional impairments of skeletal muscle in patients with postacute sequelae of SARS-CoV-2 infection. *J Appl Physiol* (1985) 135, (2023).
10. Hejbøl, E. K. et al. Myopathy as a cause of fatigue in long-term post-COVID-19 symptoms: Evidence of skeletal muscle histopathology. *Eur J Neurol* 29, 2832–2841 (2022).

11. Soares, M. N. et al. Skeletal muscle alterations in patients with acute Covid-19 and post-acute sequelae of Covid-19. *J Cachexia Sarcopenia Muscle* 13, 11–22 (2022).
12. Castanares-Zapatero, D. et al. Pathophysiology and mechanism of long COVID: a comprehensive review. *Ann Med* 54, 1473–1487 (2022).
13. Davis, H. E., Mccorkell, L., Vogel, J. M. & Topol, E. J. Long COVID: major findings, mechanisms and recommendations. *Nature Reviews Microbiology* 21, 133–146 (2023).
14. Knottnerus, S. J. G. et al. Disorders of mitochondrial long-chain fatty acid oxidation and the carnitine shuttle. *Rev Endocr Metab Disord* 19, 93–106 (2018).
15. Acosta, I. J., Stenzel, W., Hofer, M. & Brady, S. Autophagy in non-immune-mediated rhabdomyolysis: Assessment of p62 immunohistochemistry. *Muscle Nerve* 67, 73–77 (2023).
16. Hikida, R. S., Staron, R. S., Hagerman, F. C., Sherman, W. M. & Costill, D. L. Muscle fiber necrosis associated with human marathon runners. *The Neurological Sciences* 59 (1983).
17. World Health Organisation. Support for rehabilitation: self-management after COVID-19-related illness, second edition. (Retrieved: 18th April 2024) https://www.who.int/europe/publications/i/item/WHO-EURO-2021-855-40590-59892

Chapter 4b: Reply to: Matters Arising: Should We Be Careful with Exercise in Post-Exertional Malaise After Long COVID?

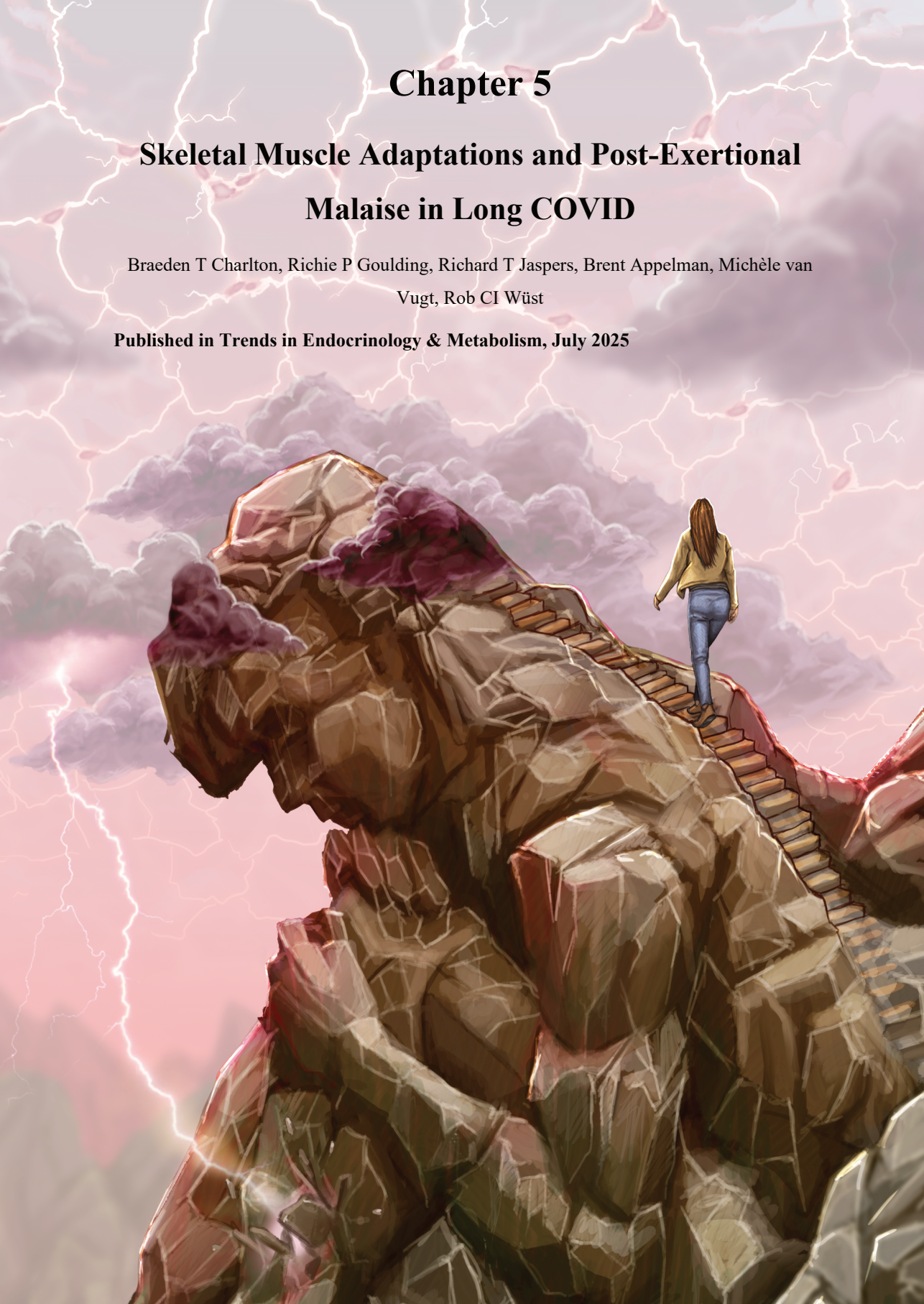


Chapter 5

Skeletal Muscle Adaptations and Post-Exertional Malaise in Long COVID

Braeden T Charlton, Richie P Goulding, Richard T Jaspers, Brent Appelman, Michèle van Vugt, Rob CI Wüst

Published in Trends in Endocrinology & Metabolism, July 2025



Abstract

When acute SARS-CoV-2 infections cause symptoms that persist longer than 3 months, this condition is termed long COVID. Symptoms experienced by patients often include myalgia, fatigue, brain fog, cognitive impairments, and post-exertional malaise (PEM), which is the worsening of symptoms following mental or physical exertion. There is little consensus on the pathophysiology of exercise-induced PEM and skeletal-muscle-related symptoms. Here, we highlight intrinsic mitochondrial dysfunction, endothelial abnormalities and a muscle fiber type shift towards a more glycolytic phenotype as main contributors to the reduced exercise capacity in long COVID. The mechanistic trigger for physical exercise to induce post-exertional malaise is unknown, but a rapid skeletal muscle tissue damage and intramuscular infiltration of immune cells contribute to post-exertional malaise related symptoms.

Long COVID: Persistent Symptoms After Acute Infection

Since 2020, acute SARS CoV-2 infections have affected 775 million people worldwide[1], of whom ~10% do not completely resolve their symptoms after 3 months[2]. The persistence of one or multiple symptoms beyond 3 months is known as post-acute sequelae of COVID-19 or long COVID, which cannot be explained by other diseases, comorbidities, hospitalization or aging[1,3]. The pathophysiology of long COVID is currently unknown, but deconditioning[4,5], viral persistence[6], dysregulated immune system[7], localized hypoxia and/or endothelial dysfunction[8], as well as autoimmunity[2] have been predominantly suggested as potential determinants (Figure 1).

The most prevalent long COVID symptoms are fatigue, brain fog, cognitive impairments, muscle pain (myalgia), and post-exertional malaise (PEM, Figure 1), the latter of which is the worsening of symptoms or onset of new symptoms up to 48 hours following physical or cognitive exertion above a patient- and time-specific threshold, and can last for days to weeks or even months[9–11] (Figure 2). Typically, exercise reduces mortality and improves treatment outcomes in almost all chronic diseases[12], but the occurrence of PEM prevents patients with long COVID from engaging in regular exercise.

PEM is also a hallmark diagnostic symptom for patients with myalgic encephalomyelitis/chronic fatigue syndrome (ME/CFS)[13], for which many cases are known to occur following either bacterial or viral infections, typically not requiring hospitalization[14,15]. Patients with ME/CFS exhibit similar symptoms as patients with long COVID, and many patients with long COVID tend to meet the Canadian Consensus Criteria for ME/CFS diagnosis[13]. Similar to long COVID[16], a large proportion of patients with ME/CFS are female and middle-aged[14,15]. While long COVID research is in its infancy, ME/CFS research can help further understand long COVID.

Given the increasing recognition of long COVID, understanding muscle-specific alterations is essential for developing targeted therapeutic strategies. Here we provide a comprehensive overview of current evidence and highlight knowledge gaps with respect to the current understanding of skeletal muscle adaptations occurring in long COVID, how this differs from or resembles other post-acute infectious diseases (e.g. ME/CFS), and we briefly outline potential therapies for patients with long COVID. Due to the high prevalence of patients exhibiting PEM and fatigue[11], the skeletal muscle abnormalities outlined here will reflect these

specific phenotypes, however it is unknown whether other phenotypes (i.e. those with smell/taste difficulties [11]) observe similar alterations.

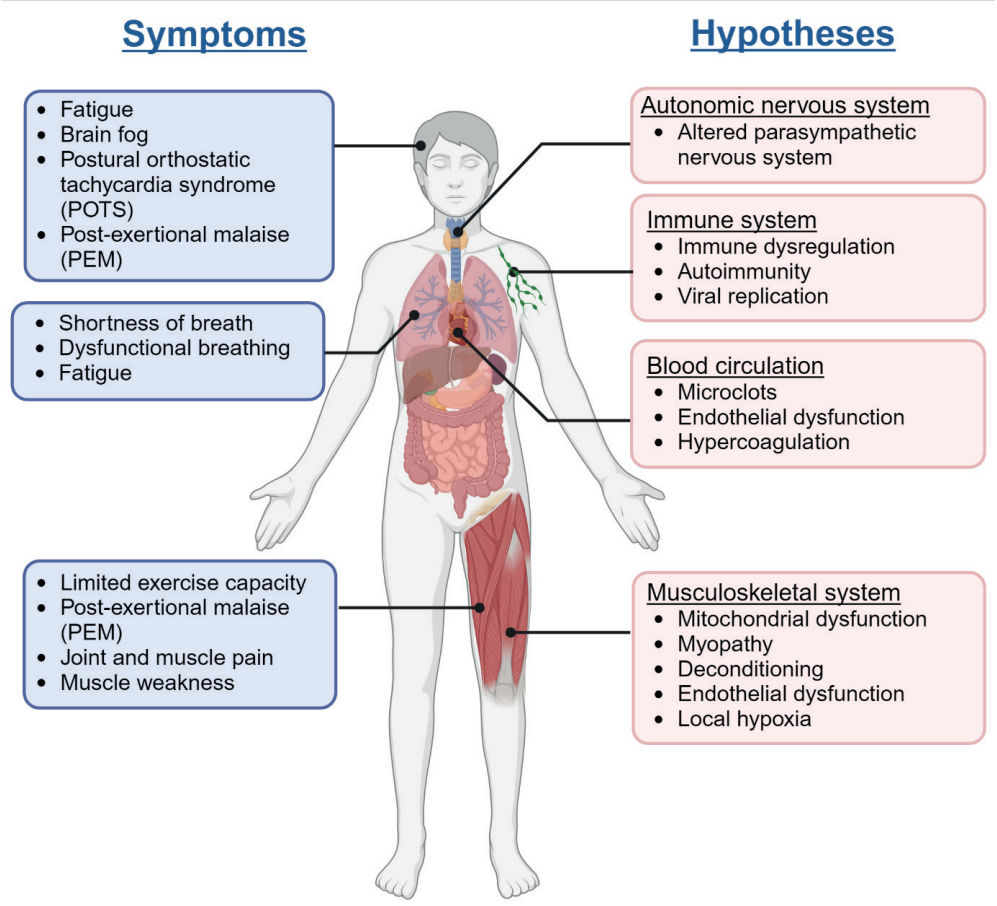


Figure 1. Common long COVID symptoms (blue) and pathophysiological hypotheses underlying tissue alterations (red) on the mechanisms. Figure was generated using BioRender.

Whole body exercise and skeletal muscle adaptations

Reduced aerobic capacity

The ability to perform aerobic exercise is a key determinant of quality of life[17]. Patients with long COVID exhibit a reduced aerobic capacity[18,19] and earlier onset of lactate accumulation during exercise[20,21]. The reduced exercise capacity in patients with long COVID has been most often attributed to alterations in skeletal muscle, with minor contributing impairments of pulmonary and cardiac alterations in long COVID[22]. Dysregulated breathing and improper

heart rate responses indicate that a dysfunctional autonomic nervous system might contribute. Alterations in skeletal muscle structure and function in long COVID, such as mitochondrial function and content, capillarization, and muscle fiber size and type, are likely to contribute to the reduced exercise capacity of patients[18,21]. Figure 3 outlines skeletal muscle alterations in patients with long COVID. While evidence for impaired aerobic capacities in long COVID continues to grow, the similarities to aerobic deficits observed in ME/CFS are becoming more apparent[23,24].

Skeletal muscle mitochondria and metabolism

Aerobic capacity is partly dictated by mitochondrial content and function[19-22], but fragmentation and spatial distribution of the mitochondrial reticulum also play important roles[25,26]. Markers for skeletal muscle mitochondrial content in patients with long COVID have yielded inconsistent results, with some studies reporting lower mitochondrial content[18], while others showed no differences compared to acute-COVID-recovered individuals[21]. Nonetheless, skeletal muscle mitochondrial respiration in long COVID is consistently impaired compared to healthy/recovered individuals[18,21], highlighting a contributing role for a lower intrinsic mitochondrial function to contribute to a lower exercise capacity. Recently, evidence of lower mitochondrial complex I activity in long COVID might indicate direct virus-induced alterations[19]. Some abnormalities in mitochondrial ultrastructure (i.e. size, density) in long COVID patients have been described, some of which are worsened in patients with ME/CFS[19,27]. An increased expression of mitochondrial fission proteins and decreased expression of mitochondrial fusion proteins[18] suggest altered mitochondrial fission/fusion regulation in patients with long COVID. It remains unknown whether mitochondrial distribution or mitophagy are also affected, and how this relates to disease severity and progression.

Capillary density and endothelial function

An optimal muscle capillary network and intact vascular function are needed to provide sufficient oxygen and substrates to skeletal muscle fibers. Skeletal muscle capillary-fiber ratios are either not altered[21] or lower[28] in patients with long COVID. Alterations in endothelial cells, such as vasodilatory dysfunction[29], endothelial basal laminae thickening[28,30], or endothelial barrier damage[31] have been described in these patients. This could cause capillary hypoperfusion, reduce oxygen and substrate diffusion or increase the resistance for diffusion of oxygen and oxidative metabolic substrates[22,32], but experimental data is lacking. Under

normal physiological conditions, skeletal muscle fatigue is related to the accumulation of fatigue-inducing metabolites[33], however it is unknown whether hypoperfusion, capillary thickening, or endothelial dysfunction may contribute to earlier fatigue in long COVID.

Muscle fiber type size and distribution

Muscle fiber type composition shapes the functional and metabolic alterations in skeletal muscle during exercise. Oxidative, type I, fibers typically have high mitochondrial densities, providing resistance to fatigue. Glycolytic, type IIa or IIa/x, fibers produce more power, but have lower mitochondrial densities[34]. Patients with long COVID have more glycolytic muscle fibers[18], similar to patients with other chronic diseases[35,36]. However, no longitudinal data exists to conclude whether those with higher glycolytic fiber proportions are more prone to develop long COVID, or whether the disease progression induces a shift in muscle fiber type composition.

Limited evidence suggests a sex-specific type I fiber atrophy in long COVID[21]. Whether muscle atrophy occurs in long COVID is currently unclear, as many studies also included patients that had been hospitalized or presented with other comorbidities, which may confound results[3]. Patients with long COVID exhibiting small fiber neuropathy[37,38] also present more frequently with very small, atrophic muscle fibers[21,30]. The relationship between small fiber neuropathy, prevalence of small, atrophic muscle fibers, and possible type I specific or general atrophy warrants further investigation.

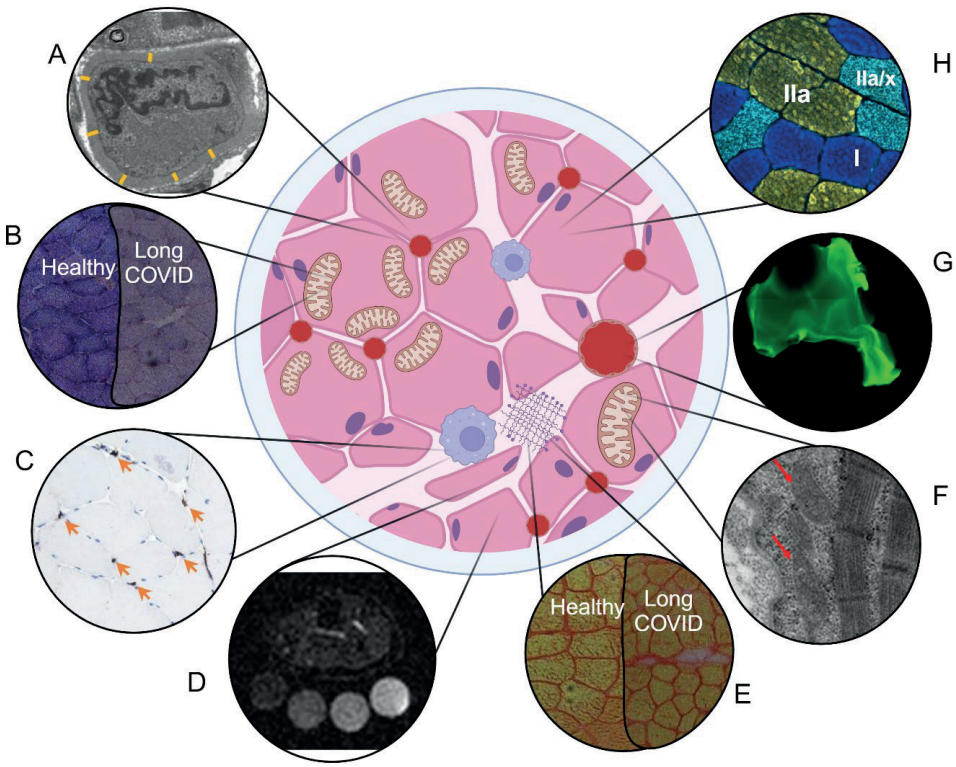


Figure 2. Contribution of skeletal muscle cell types in long COVID. (**A**) Capillary basal lamina thickening observed in patients with long COVID (from Aschman *et al*. 2023[28]). (**B**) Lower succinate dehydrogenase activity in patients with long COVID compared to healthy controls; (from Colosio *et al*. 2023[18]). (**C**) CD68+ macrophage infiltration between muscle fibers (from Aschman *et al*. 2023[28]). (**D**) High skeletal muscle sodium content, as viewed using 3T magnetic resonance imaging (from Petter *et al*. 2022[39]) (**E**) Connective tissue content was similar in long COVID as in healthy controls (from Colosio *et al.* 2023[18]) (**F**) Patients with long COVID have abnormal mitochondria imaged using electron microscopy (from Bizjak *et al* 2023[19]) (**G**) Amyloid-containing deposits can be found in skeletal muscle and blood of patients with long COVID (unpublished data). (**H**) Patients with long COVID have more glycolytic, type II muscle fibers. Dark blue represents type I fibers, yellow represents type IIa fibers, turquoise represents type IIa/IIx fibers (Appelman *et al*. 2024[21]). Figure was generated using BioRender.

Post-Exertional Malaise

Currently, diagnosis of PEM is strictly clinical, wherein patients must fulfill criteria for the DSQ-PEM questionnaire[40]. Two-day exercise tests and handgrip strength tests can help to confirm PEM diagnosis[41], but patient burden for a two-day exercise test is substantial. Future research should focus on biomedical biomarkers to compliment the DSQ-PEM. The underlying mechanism for PEM is currently unknown, however, PEM can also occur after cognitive

exertion, suggesting a neurological or circulating contributor to the onset of PEM. Skeletal muscle adaptations are poorly understood in the context of PEM, but a two-day muscle biopsy protocol after PEM induction suggested that skeletal muscle abnormalities worsen upon PEM onset[21]. Mitochondrial respiration and markers for mitochondrial density and metabolism decrease one day after maximal, PEM-inducing exercise in patients with long COVID[21]. Maximal exercise resulted in more severe skeletal muscle damage and enhanced immune cell infiltration[21]. Whether a similar process occurs in patients with ME/CFS or other post-acute infectious diseases is unknown. While long COVID and ME/CFS are the most prevalent diseases exhibiting PEM, subsets of patients with multiple sclerosis also experience PEM[42]. Future studies should include other populations to fully understand the underlying pathology of PEM.

Proposed pathological mechanisms

The underlying mechanisms for the skeletal muscle adaptations, and their time course of disease progression in patients with long COVID are unknown. Further, it is not understood how these structural alterations relate to rapid changes underlying PEM. Multiple hypotheses exist that may explain skeletal muscle abnormalities in long COVID patients (Figure 4). Here, we discuss the most likely candidates of these abnormalities, namely deconditioning, local hypoxia, autoimmunity, electrophysiological alterations, and central fatigue, according to the most recent literature.

Deconditioning

Due to the development of PEM, several research groups propose that the skeletal muscle alterations in long COVID are simply due to deconditioning or physical inactivity[4,5]. Although long COVID patients tend to be less active than healthy individuals[21], many still maintain physical activity levels that are similar to the average US citizen[43], who does not suffer from PEM. Physically inactive people do not suffer from PEM, and the skeletal muscle alterations in long COVID are distinct from those resulting from strict bed rest. Strict bed rest or limb immobilization induces muscle atrophy, capillary rarefaction (already present within 6 days of bed rest), insulin insensitivity and an altered mitochondrial substrate utilization[44–46], conditions that are not predominantly observed in patients with long COVID. It should be noted, as with any chronic disease, the increase in sedentary activity will have long-term impacts on health outcomes[47]. While the consequences of deconditioning could have long-term impacts on

severely affected patients with long COVID in particular, the observed skeletal muscle adaptations in long COVID are distinct from those occurring after deconditioning.

Local tissue hypoxia

Some of the skeletal muscle adaptations in patients with long COVID resemble those occurring following chronic hypoxia exposure, which have led to the suggestion that patients may experience hypoxia. In hypoxic conditions (i.e. high altitude), perceived exertion during exercise increases and exercise performance decreases[48]. Skeletal muscle metabolism shifts to nonoxidative, glucose oxidation[49], which increases blood lactate during submaximal exercise[50]. Chronic hypoxia results in higher hematocrit values[51], lower mitochondrial content and function, and increases in glycolytic enzymes[52]. While capillary-to-fiber ratio either increases or does not change in long COVID, hypoxia-induced atrophy results in higher capillary densities[51,53,54].

Patients with long COVID, however, do not exhibit reduced arterial oxygen pressures and saturation during exercise, but oxygen extraction[22] and muscle oxygen diffusing capacity[55] may be impaired. A lower mitochondrial function, independent of tissue oxygenation[18,19,21], also results in increased lactate production during exercise[56]. Such phenomena can be misinterpreted as simply caused by local hypoxia. However, the contribution of local hypoxia deserves further study. Local tissue hypoxia in patients with long COVID may be induced by capillary blockage and/or endothelial dysfunction, preventing oxygen and substrate delivery. Evidence of thickening of the capillary basal lamina has been observed in patients with long COVID[28], suggesting an impaired muscle oxygen diffusing capacity. Amyloid-containing clots (so-called microclots)[8] in venous blood from patients with long COVID may be big enough to block capillaries[57], causing a local hypoperfusion. However, these amyloid-containing clots were not found inside capillaries, but rather in the extracellular matrix, suggesting an alternative role[21]. Amyloid-containing clots may exert local cytotoxic effects resulting in endothelial dysfunction[8,57,58], similar to that observed in Alzheimer's disease[59]. The potential link between amyloid-containing clots, endothelial dysfunction, hypoperfusion and local hypoxia is currently unclear.

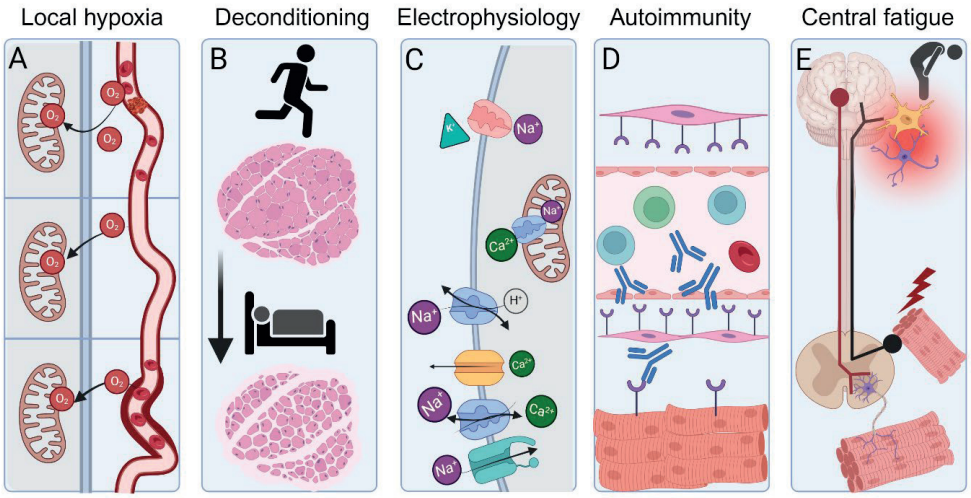


Figure 3: Schematic illustration of the five predominant mechanisms underlying long COVID skeletal muscle symptoms: local hypoxia, deconditioning, electrophysiological alterations, autoimmunity and central fatigue. (**A**): Local hypoxia may be due to amyloid-containing clots (top panel), endothelial dysfunction (middle panel), or capillary thickening increasing oxygen diffusion distances (bottom panel). (**B**): Deconditioning results in muscle fiber atrophy, a loss of mitochondria and capillary rarefaction, reducing aerobic capacity. (**C**): Electrophysiology may be altered by changes in ion distributions or effects on specific ion channels. (**D**): Generation of autoantibodies may target tissue receptors, including skeletal muscle. (**E**): Central fatigue may be caused by abnormal neurological processes, irregular responses to exercise and feelings of myalgia and pain. Figure was generated using BioRender.

Autoimmunity

There is substantial evidence indicating autoimmunity may be implicated in long COVID pathophysiology[2]. However, how autoimmune antibodies found in patients with long COVID may affect skeletal muscle, either acutely or chronically, is poorly understood. There is some evidence of autoantibodies for β-adrenergic receptors (β_2-AR) in patients with long COVID[60–62], which are implicated in a variety of exercise-related responses. Specifically, β_2-AR signalling is implicated in mitochondrial biogenesis, and oxidation and blood flow regulation[63,64]. Autoantibodies in myasthenia gravis and myositis, two well-studied autoimmune diseases which also exhibit muscle fatigue and worsening of symptoms with exercise[65,66], are known to be associated with muscle weakness and muscle fatigue[67,68]. However, the mechanistic role of autoantibodies in the development of skeletal muscle adaptations in long COVID and the development of PEM is unknown.

Electrophysiological alterations

Several recent studies indicate that some patients with long COVID exhibit signs of myopathies[69,70] with myopathic histopathology[30,69]. Small fiber neuropathy is common in patients with long COVID[37,38]. A recent study in ME/CFS patients indicated higher tissue sodium levels[39], although it is unclear whether this is an intra- or extracellular sodium accumulation. Sodium affects multiple channels including the mitochondrial sodium-calcium exchanger, which is critical in mitochondrial function. It has been hypothesized that disturbances in muscle sodium homeostasis make mitochondria and muscle fibers susceptible to damage[71], which is linked to an early fatigue development[72], and altered ion channel function. More studies are necessary to fully understand the electrophysiological changes apparent in long COVID.

Central fatigue

Various research groups have suggested that central fatigue and neurological alterations contribute to long COVID symptoms[73–75], including brain fog, sleep difficulties, anxiety, depression, headaches and somatic pain[76]. Neurophysiological alterations, such as neuro-inflammation and small fiber neuropathy likely modulate long COVID symptoms. Central fatigue, defined as a reduction in the central nervous system's capacity to drive skeletal muscle contractions, could play a role in limiting exercise tolerance, though the necessary studies involving voluntary activation assessment, transcranial magnetic stimulation, and peripheral nerve stimulation have not yet been performed. It is also possible that a heightened IL-6 induced perception of effort leads patients to terminate exercise earlier[77]. However, patients with long COVID often exhibit earlier lactate accumulation onset during moderate exercise[20,21,78], independent of physical effort and psychological state[23]. Future studies should include interpolated twitch techniques to fully investigate central fatigue in long COVID[79]. Non-invasive methods to assess neurological alterations, using (functional) MRI, are warranted to further understand the neurological consequences of PEM, as cognitive and mental exertion can also trigger PEM.

Therapeutic treatments in long COVID

To date, there are currently no therapies for long COVID, however ongoing clinical trials are promising. Recently, immunoadsorption therapy temporarily alleviated long COVID symptoms[62], however further investigations are required. Other recent trials found on ClinicalTrials.gov include dietary supplementation (mitoquinone, vitamin K2, vitamin D3 and

N-acetyl-cysteine), anti-inflammatory or immune regulatory drugs (i.e. lithium, naltrexone, and rintatolimod), and some antiviral drugs (i.e. Paxlovid)[80]. The majority of trials are ongoing, and we eagerly await new results.

Concluding Remarks and Future Directions

Most research on long COVID has focused on immune function, but skeletal muscle adaptations in these patients are gaining more attention. There is clear evidence of skeletal muscle alterations, including mitochondrial and endothelial abnormalities in patients with long COVID that may underly whole body exercise responses. The heterogeneity and the duration of the disease results in different skeletal muscle phenotypes, and these deserve further study. Future research should also investigate endothelial function, the possible implications of amyloid-containing deposits in skeletal muscle, and the underlying pathophysiology of PEM and how it contributes to long COVID disease progression. We applaud new studies that study the contributing factors towards skeletal muscle adaptations, including deconditioning, hyperbaric oxygen therapy, novel medications targeting autoimmunity, and the neurological component of PEM. As many new groups worldwide are now studying the fundamental pathophysiology of long COVID and testing potential new therapies to relieve patient symptoms and the disease burden, we await exciting times in this research field.

Acknowledgements

This study was supported the Patient-Led Research Collaborative for Long COVID, ZonMw Onderzoeksprogramma ME/CVS, the 2022 Ramsay Grant Program, ME Research UK, ME Stars of Tomorrow Scholarship award from the ICanCME Research Network (to BTC), and Stichting Long COVID Nederland. The authors want to thank our patient representatives for insightful discussions.

Conflict of interest

The authors declare no conflicts of interest.

References

1. World Health Organization (2024) WHO COVID-19 Dashboard[Online]. Available: https://data.who.int/dashboards/covid19/cases?n=c. [Accessed: 22-May-2024]

2. Altmann, D.M. *et al.* (2023) The immunology of long COVID. *Nat Rev Immunol* 23, 618–634

3. Kerkhoff, T.J. *et al.* (2022) Post COVID-19 condition: critical need for a clear definition and detailed pathophysiology. *J Cachexia Sarcopenia Muscle* 13, 2754–2756

4. Naeije, R. and Caravita, S. (2021) Phenotyping long COVID. *European Respiratory Journal* 58, 2101763

5. Edward, J.A. *et al.* (2023) Characteristics and Treatment of Exercise Intolerance in Patients With Long COVID. *J Cardiopulm Rehabil Prev* 43, 400–406

6. Proal, A.D. and VanElzakker, M.B. (2021) Long COVID or Post-acute Sequelae of COVID-19 (PASC): An Overview of Biological Factors That May Contribute to Persistent Symptoms*Frontiers in Microbiology*, 12Frontiers Media S.A.

7. Davis, H.E. *et al.* (2023) Long COVID: major findings, mechanisms and recommendations*Nature Reviews Microbiology*, 21Nature Research, 133–146

8. Kell, D.B. *et al.* (2022) A central role for amyloid fibrin microclots in long COVID/PASC: Origins and Therapeutic Implications. *Biochemical Journal* 479, 537–559

9. Vøllestad, N.K. and Mengshoel, A.M. (2023) Post-exertional malaise in daily life and experimental exercise models in patients with myalgic encephalomyelitis/chronic fatigue syndrome. *Front Physiol* 14

10. Jason, L.A. *et al.* (2015) Problems in defining post-exertional malaise. *J Prev Interv Community* 43, 20–31

11. Thaweethai, T. *et al.* (2023) Development of a Definition of Postacute Sequelae of SARS-CoV-2 Infection. *JAMA* 329, 1934–1946

12. Pedersen, B.K. and Saltin, B. (2015) Exercise as medicine – evidence for prescribing exercise as therapy in 26 different chronic diseases. *Scand J Med Sci Sports* 25, 1–72

13. Carruthers, B.M. *et al.* (2011) Myalgic encephalomyelitis: International Consensus Criteria. *J Intern Med* 270, 327–338

14. Chu, L. *et al.* (2019) Onset Patterns and Course of Myalgic Encephalomyelitis/Chronic Fatigue Syndrome. *Front Pediatr* 7

15. Evans, M. and Jason, L.A. (2018) Onset Patterns of Chronic Fatigue Syndrome and Myalgic Encephalomyelitis: A Mixed Method Approach. *Research on Chronic Diseases* 2, 001–0030

16. Lane, R.J.M. *et al.* (1998) Muscle fibre characteristics and lactate responses to exercise in chronic fatigue syndrome. *J Neurol Neurosurg Psychiatry*

17. Phyo, A.Z.Z. *et al.* (2020) Quality of life and mortality in the general population: a systematic review and meta-analysis. *BMC Public Health* 20, 1596

18. Colosio, M. *et al.* (2023) Structural and functional impairments of skeletal muscle in patients with postacute sequelae of SARS-CoV-2 infection. *J Appl Physiol* 135, 902–917

19. Bizjak, D.A. *et al.* (2024) Functional and Morphological Differences of Muscle Mitochondria in Chronic Fatigue Syndrome and Post-COVID Syndrome. *Int J Mol Sci* 25, 1675

20. de Boer, E. *et al.* (2022) Decreased Fatty Acid Oxidation and Altered Lactate Production during Exercise in Patients with Post-acute COVID-19 Syndrome. *Am J Respir Crit Care Med* 205, 126–129

21. Appelman, B. *et al.* (2024) Muscle abnormalities worsen after post-exertional malaise in long COVID. *Nat Commun* 15, 17

22. Singh, I. *et al.* (2022) Persistent Exertional Intolerance After COVID-19: Insights From Invasive Cardiopulmonary Exercise Testing. *Chest* 161, 54–63

23. Walitt, B. *et al.* (2024) Deep phenotyping of post-infectious myalgic encephalomyelitis/chronic fatigue syndrome. *Nat Commun* 15, 907

24. Joseph, P. *et al.* (2021) Insights From Invasive Cardiopulmonary Exercise Testing of Patients With Myalgic Encephalomyelitis/Chronic Fatigue Syndrome. *Chest* 160, 642–651

25. Parry, H.A. *et al.* (2024) Impact of capillary and sarcolemmal proximity on mitochondrial structure and energetic function in skeletal muscle. *J Physiol* 602, 1967–1986

26. Goulding, R.P. *et al.* (2024) Skeletal muscle mitochondrial fragmentation predicts age-associated decline in physical capacity [In Press]. *Aging Cell*

27. Behan, W.M.H. *et al.* (1991) Mitochondrial abnormalities in the postviral fatigue syndrome. *Acta Neuropathol* 83, 61–65

28. Aschman, T. *et al.* (2023) Post-COVID exercise intolerance is associated with capillary alterations and immune dysregulations in skeletal muscles. *Acta Neuropathol Commun* 11, 193

29. Kuchler, T. *et al.* (2023) Persistent endothelial dysfunction in post-COVID-19 syndrome and its associations with symptom severity and chronic inflammation. *Angiogenesis* 26, 547–563

30. Hejbøl, E.K. *et al.* (2022) Myopathy as a cause of fatigue in long-term post-COVID-19 symptoms: Evidence of skeletal muscle histopathology. *Eur J Neurol* 29, 2832–2841

31. Wu, X. *et al.* (2024) Damage to endothelial barriers and its contribution to long COVID. *Angiogenesis* 27, 5–22

32. Schäfer, H. *et al.* (2023) Altered tissue oxygenation in patients with post COVID-19 syndrome. *Microvasc Res* 148, 104551

33. Wan, J. *et al.* (2017) Muscle fatigue: general understanding and treatment. *Exp Mol Med* 49, e384–e384

34. Egginton, S. (2011) Physiological factors influencing capillary growth. *Acta Physiologica* 202, 225–239

35. Wüst, R.C.I. and Degens, H. (2007) Factors contributing to muscle wasting and dysfunction in COPD patients. *Int J Chron Obstruct Pulmon Dis* 2, 289–300

36. Niemeijer, V.M. *et al.* (2018) Skeletal muscle fiber characteristics in patients with chronic heart failure: impact of disease severity and relation with muscle oxygenation during exercise. *J Appl Physiol (1985)* 125, 1266–1276

37. Abrams, R.M.C. *et al.* (2022) Small fiber neuropathy associated with SARS-CoV-2 infection. *Muscle Nerve* 65, 440–443

38. Oaklander, A.L. *et al.* (2022) Peripheral Neuropathy Evaluations of Patients With Prolonged Long COVID. *Neurol Neuroimmunol Neuroinflamm* 9

39. Carruthers, B.M. *et al.* (2003) Myalgic Encephalomyelitis/Chronic Fatigue Syndrome. *J Chronic Fatigue Syndr* 11, 7–115

40. Thoma, M. *et al.* (2023) Why the Psychosomatic View on Myalgic Encephalomyelitis/Chronic Fatigue Syndrome Is Inconsistent with Current Evidence and Harmful to Patients. *Medicina (B Aires)* 60, 83

41. Jason, L.A. *et al.* (2017) Differentiating Multiple Sclerosis from Myalgic Encephalomyelitis and Chronic Fatigue Syndrome. *Insights Biomed* 02

42. Althoff, T. *et al.* (2017) Large-scale physical activity data reveal worldwide activity inequality. *Nature* 547, 336–339

43. Eggelbusch, M. *et al.* (2024) The impact of bed rest on human skeletal muscle metabolism. *Cell Rep Med* 5, 101372

44. Pinto, A.J. *et al.* (2023) Physiology of sedentary behavior. *Physiol Rev* 103, 2561–2622

45. Hendrickse, P.W. *et al.* (2022) Capillary rarefaction during bed rest is proportionally less than fibre atrophy and loss of oxidative capacity. *J Cachexia Sarcopenia Muscle* 13, 2712–2723

46. Schmid, D. *et al.* (2015) Associations of Objectively Assessed Physical Activity and Sedentary Time with All-Cause Mortality in US Adults: The NHANES Study. *PLoS One* 10, e0119591

47. Mujika, I. *et al.* (2019) Contemporary Periodization of Altitude Training for Elite Endurance Athletes: A Narrative Review. *Sports Medicine* 49, 1651–1669

48. Roberts, A.C. *et al.* (1996) Acclimatization to 4,300-m altitude decreases reliance on fat as a substrate. *J Appl Physiol* 81, 1762–1771

49. Grassi, B. *et al.* (1996) Peak blood lactate and blood lactate vs. workload during acclimatization to 5,050 m and in deacclimatization. *J Appl Physiol* 80, 685–692

50. Wüst, R.C.I. *et al.* (2009) Region-specific adaptations in determinants of rat skeletal muscle oxygenation to chronic hypoxia. *Am J Physiol Heart Circ Physiol* 297, H364-74

51. Favier, F.B. *et al.* (2015) HIF-1-driven skeletal muscle adaptations to chronic hypoxia: molecular insights into muscle physiology. *Cellular and Molecular Life Sciences* 72, 4681–4696

52. MacDougall, J.D. *et al.* (1991) Operation Everest II: structural adaptations in skeletal muscle in response to extreme simulated altitude. *Acta Physiol Scand* 142, 421–427

53. Hoppeler, H. *et al.* (1990) Morphological Adaptations of Human Skeletal Muscle to Chronic Hypoxia. *Int J Sports Med* 11, S3–S9

54. Roca, J. *et al.* (1992) Effects of training on muscle O2 transport at VO2max. *J Appl Physiol* 73, 1067–1076

55. Taivassalo, T. *et al.* (2003) The spectrum of exercise tolerance in mitochondrial myopathies: a study of 40 patients. *Brain* 126, 413–423

56. Pretorius, E. *et al.* (2021) Persistent clotting protein pathology in Long COVID/Post-Acute Sequelae of COVID-19 (PASC) is accompanied by increased levels of antiplasmin. *Cardiovasc Diabetol* 20, 172

57. Kruger, A. *et al.* (2022) Proteomics of fibrin amyloid microclots in long COVID/post-acute sequelae of COVID-19 (PASC) shows many entrapped pro-inflammatory molecules that may also contribute to a failed fibrinolytic system. *Cardiovasc Diabetol* 21

58. Fisher, R.A. *et al.* (2022) Pathological changes within the cerebral vasculature in Alzheimer's disease: New perspectives. *Brain Pathology* 32

59. Klein, J. *et al.* (2023) Distinguishing features of long COVID identified through immune profiling. *Nature* 623, 139–148

60. Wallukat, G. *et al.* (2021) Functional autoantibodies against G-protein coupled receptors in patients with persistent Long-COVID-19 symptoms. *J Transl Autoimmun* 4, 100100

61. Stein, E. *et al.* (2024) Efficacy of Repeat Immunoadsorption in Post-COVID ME/CFS Patients with Elevated B2-Adrenergic Receptor Autoantibodies: A Prospective Cohort Study. *SSRN [PREPRINT]*

62. Pearen, M.A. *et al.* (2009) Expression profiling of skeletal muscle following acute and chronic β2-adrenergic stimulation: implications for hypertrophy, metabolism and circadian rhythm. *BMC Genomics* 10, 448

63. Hagström-Toft, E. *et al.* (1998) β-Adrenergic regulation of lipolysis and blood flow in human skeletal muscle in vivo. *American Journal of Physiology-Endocrinology and Metabolism* 275, E909–E916

64. Dalakas, M.C. (2015) Inflammatory Muscle Diseases. *New England Journal of Medicine* 372, 1734–1747

65. Hehir, M.K. and Silvestri, N.J. (2018) Generalized Myasthenia Gravis. *Neurol Clin* 36, 253–260

66. Iorio, R. (2024) Myasthenia gravis: the changing treatment landscape in the era of molecular therapies. *Nat Rev Neurol* 20, 84–98

67. Gunawardena, H. (2017) The Clinical Features of Myositis-Associated Autoantibodies: a Review. *Clin Rev Allergy Immunol* 52, 45–57

68. Agergaard, J. *et al.* (2023) Myopathy as a cause of Long COVID fatigue: Evidence from quantitative and single fiber EMG and muscle histopathology. *Clinical Neurophysiology* 148, 65–75

69. Agergaard, J. *et al.* (2021) Myopathic changes in patients with long-term fatigue after COVID-19. *Clinical Neurophysiology* 132, 1974–1981

70. Petter, E. *et al.* (2022) Muscle sodium content in patients with Myalgic Encephalomyelitis/Chronic Fatigue Syndrome. *J Transl Med* 20, 580

71. Bravo-Sagua, R. *et al.* (2017) Calcium Transport and Signaling in Mitochondria. *Compr Physiol* DOI: 10.1002/cphy.c160013

72. Lunde, P.K. *et al.* (1998) Skeletal muscle fatigue in normal subjects and heart failure patients. Is there a common mechanism? *Acta Physiol Scand* 162, 215–228

73. Stefano, G.B. *et al.* (2021) Editorial: The Pathogenesis of Long-Term Neuropsychiatric COVID-19 and the Role of Microglia, Mitochondria, and Persistent Neuroinflammation: A Hypothesis. *Medical Science Monitor* 27

74. Koterba, C.H. *et al.* (2024) Neuropsychology practice guidance for the neuropsychiatric aspects of Long COVID. *Clin Neuropsychol*

75. Donnino, M. *et al.* (2023) Psychophysiologic Symptom Relief Therapy for Post-Acute Sequelae of Coronavirus Disease 2019. *Mayo Clin Proc Innov Qual Outcomes* 7, 337–348

76. Tang, S.W. *et al.* (2022) Long COVID, neuropsychiatric disorders, psychotropics, present and future. *Acta Neuropsychiatr* 34, 109–126

77. Robson-Ansley, P.J. *et al.* (2004) Acute Interleukin-6 Administration Impairs Athletic Performance in Healthy, Trained Male Runners. *Canadian Journal of Applied Physiology* 29, 411–418

78. Jamieson, A. *et al.* (2024) Mechanisms underlying exercise intolerance in long COVID: An accumulation of multisystem dysfunction. *Physiol Rep* 12

79. Dotan, R. *et al.* (2021) On the reliability and validity of central fatigue determination. *Eur J Appl Physiol* 121, 2393–2411

80. Sebők, S. and Gyires, K. (2023) Long COVID and possible preventive options. *Inflammopharmacology* 31, 2807–2817

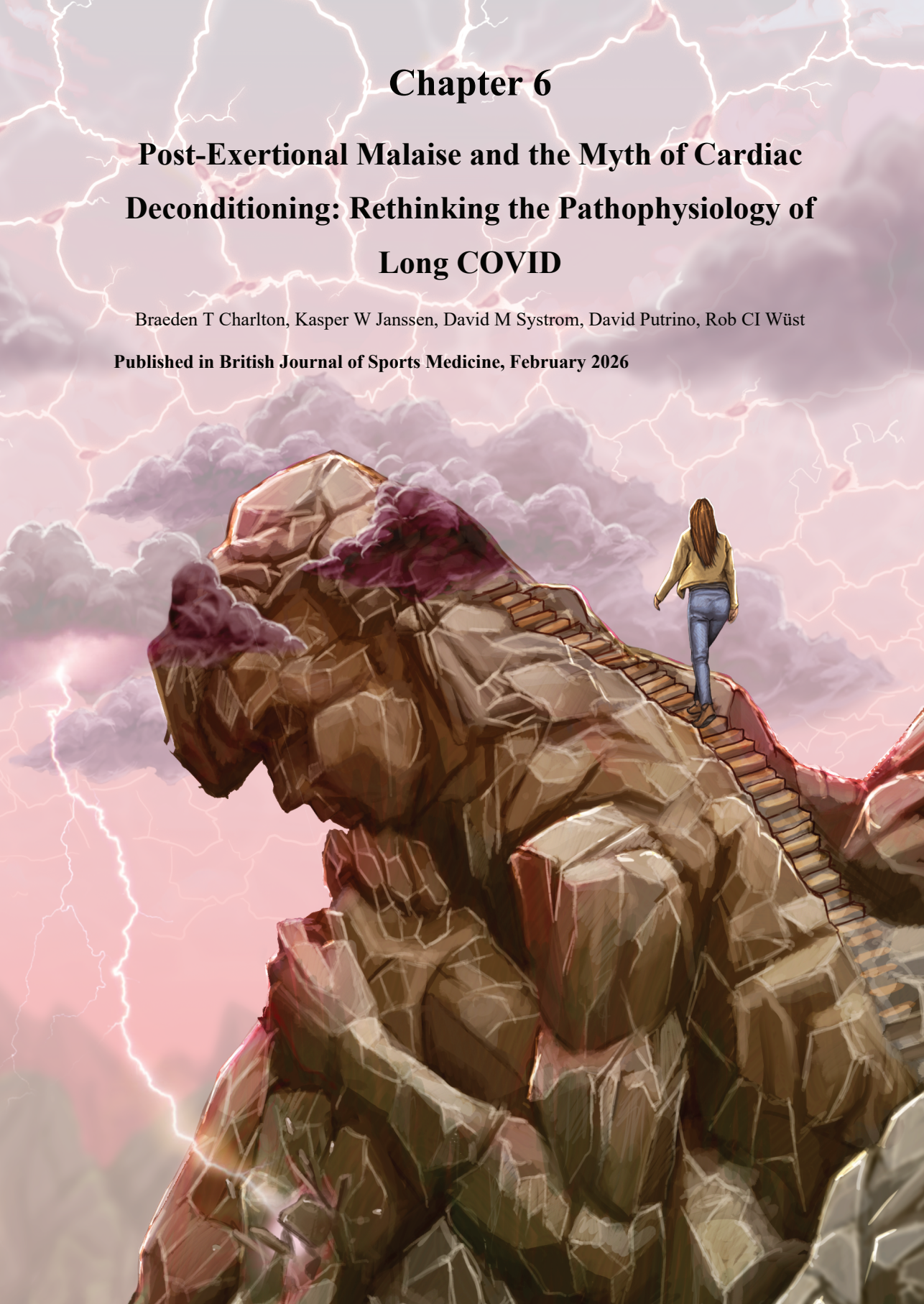


Chapter 6

Post-Exertional Malaise and the Myth of Cardiac Deconditioning: Rethinking the Pathophysiology of Long COVID

Braeden T Charlton, Kasper W Janssen, David M Systrom, David Putrino, Rob CI Wüst

Published in British Journal of Sports Medicine, February 2026



Post-exertional malaise: a defining feature of Long COVID

Whilst the number of fatal acute SARS-CoV2 infections has declined since 2020, the proportion of these infections that result in persisting symptoms has not reduced significantly[1]. The continuity or development of new symptoms longer than three months after an acute SARS-CoV-2 infection is clinically defined as Long COVID[2]. Post-exertional malaise (PEM), a hallmark and debilitating feature, is recognized as one of the most frequent manifestations of Long COVIDand present in ~80% of patients with the condition[3]. PEM is a delayed exacerbation (or new onset) of symptoms after physical or cognitive activity above a patient- and time-dependent threshold, which may persist for days, weeks, months or even result in a permanent change in a patient's baseline[2]. The need to screen for PEM in suspected Long COVID before initiating a rehabilitation strategy has already been recognized by major health authorities, inlcuding the World Health Organisation (WHO), who heavily cautioned against graded exercise therapies for patients experiencing PEM[2].

PEM in Long COVID - cardiac alterations and pathological mechanisms

Historically, and without physiological evidence, deconditioning has been proposed as a driver of physiological alterations in both Long COVID and myalgic encephalomyelitis / chronic fatigue syndrome (ME/CFS)[4]. MF/CFS is a related disease in which patients experience profound fatigue as well as PEM. The etiology of ME/CFS is unclear, but often starts with a viral infection, similar to SARS-CoV-2-induced Long COVID. Indeed, in a 2025 statement, the American Heart Association proposed that cardiac alterations in Long COVID may be attributed to deconditioning[5]. Perhaps this may apply in long-term ME/CFS, however, the peripheral adaptations seen in Long COVID patients cannot solely be explained by physical inactivity itself[6]. There is considerable heterogeneity of cardiac abnormalities in these patients. Studies on cardiopulmonary function and structure reveal significant cardiovascular alterations in patients with Long COVID including scarring, inflammatory changes and residual myocardial alterations in a subset of patients with Long COVID[7]. With invasive cardiopulmonary exercise test (CPET) measurements, patients commonly exhibit pre-load failure, such that there is insufficient cardiac filling[6]. While some Long COVID patients exhibit reductions in cardiac volumes that may be indicative of deconditioning, other notable alterations, such as the pre-load failure and inflammation-mediated scarring are not typical of deconditioning, and thus deconditioning alone is not sufficient to explain cardiac alterations in all Long COVID patients.

The pathophysiology of these cardiac alterations is currently unknown. Mitochondrial and endothelial dysfunction, autoimmunity, and electrophysiological alterations have been proposed to contribute to the pathophysiology of Long COVID and ME/CFS[3]. In multiple tissues of Long COVID patients, mitochondrial dysfunction including deranged mitochondria has been shown [3]. There is further evidence accumulating of endothelial damage and dysfunction in these patients[8], who may exhibit "leaky vessels" or impaired vasomechanical regulation. Both endothelial dysfunction and impaired mitochondrial function may also be implicated in the poor oxygen extraction in patients[6]. Whether these cellular and molecular alterations are also observed in cardiac muscle is currently unknown. The absence of validated animal models and the inability to obtain longitudinal cardiac biopsy data constrain the development of a clear pathophysiological theory for post-viral diseases. Cardiac deconditioning may indeed contribute to a subset of Long COVID patients, particularly in home- or bed-bound patients or as the disease progresses.

Incorporating PEM evaluation and monitoring in patient care

As no single factor has been elucidated as the main driver of Long COVID symptoms, it is of the utmost importance that patient-specific strategies are considered for clinical care. Rehabilitation that focuses solely on one symptom may not be beneficial for patient long-term care if other symptoms worsen at the same time. Health care providers should systematically screen for Long COVID etiology, exclude other pathologies, and quantify postural orthostatic tachycardia syndrome (POTS) and PEM severity (e.g. via functional capacity questionnaire (FUNCAP))[2]. PEM is also the core symptom and key diagnostic aspect of the Canadian Consensus Criteria for ME/CFS and can be diagnosed via the DePaul Symptom Questionnaire[9]. Stratification of patients by POTS or PEM status allows for tailored rehabilitation plans, prioritizing breathing exercises, low-intensity activities, and pacing strategies for those experiencing PEM.

While prolonged rest may initially seem beneficial for symptom management, extended periods of daytime lying or bed rest can induce cardiovascular and skeletal muscle deconditioning. Lying down during the day can be minimized by supported sitting or gentle upright postures, and compression garments – provided the patient's symptoms allow for such a strategy. Encouraging light, tolerance-based activity and postural variation is essential to prevent further functional decline while respecting post-exertional symptom thresholds[10].

The repetitive exposure to PEM events may perpetuate the worsening of patient health. Thus, monitoring patient response to various activities can aid in the reduction of PEM episodes, overall improving patient outcomes. Wearable heart rate monitors may be a practical method to monitor patient activity levels[11], however, we acknowledge that their use may not be feasble in less-resourced settings. Using first ventilatory threshold (VT_1)-guided heartrate pacing enables patients to remain within their individual energy envelope, minimising PEM exacerbations while supporting gradual, safe reconditioning. This personalised, data-driven method contrasts with traditional graded exercise therapy, which remains contraindicated for patients with PEM. Activity recommendations must be adjusted in real-time to prevent symptom exacerbations[2].

Incorporating PEM into a new conceptual model of Long COVID cardiac rehabilitation programs is essential to clinically distinguish it from cardiovascular deconditioning and to safeguard patients from unintended harm. New programs should deviate from historical guidelines for ME/CFS and include the latest insights into the pathophysiology of Long COVID. We emphasize the heterogeneous nature of the disease and the need for targeted pharmacotherapy for PEM and POTS (including low dose naltrexone, beta-blockers or pyridostigmine) to reduce symptom burden[10,12]. Such an interdisciplinary approach will assist in personalized exercise and recovery prescriptions to avoid relapses or worsening of symptoms.

In conclusion, PEM and cardiac alterations in Long COVID patients can occur, but these findings are largely independent of cardiac deconditioning. Thus, an individually tailored management strategy, guided by exercise physiology data, for patients with Long COVID and PEM is recommended.

Competing interests

The authors do not have competing interest related to this work.

Contributorship

BTC and RCIW conceived and initiated the project. BTC developed the manuscript's initial draft. All authors contributed to textual and structural revisions. RCIW serves as the guarantor. All authors approved the submission of the final version of the manuscript.

Funding

BTC was supported in part by The Interdisciplinary Canadian Collaborative Myalgic Encephalomyelitis (ICanCME) Research Network, and the research programme ME/CFS (project MuscleME, project number: 10091012110025) which is financed by the Netherlands Organization for Health Research and Development (ZonMW). MuscleME is member of the Netherlands ME/CFS Cohort and Biobank (NMCB) consortium funded by ZonMW.

Acknowledgements

We would like to extend our sincerest thanks to the following who contributed to the development of the present text: Brent Appelman, Yaneer Bar-Yam, Jonas Bergquist, Svetlana Blitshteyn, Danilo Buonsenso, Wolfam Doehner, Rae Duncan, Andrew Ewing, Mark A Faghy, Amine Ghram, Andréa Lúcia Gonçalves da Silva, Stephanie L Grach, Merel Hellemons, Jelle Y Huijts, Binita Kane, Amos Lal, Raina MacIntyre, Alexios-Fotios A Mentis, Javaid Nauman, Simone Porcelli, Ethresia Pretorius, Christian Puta, Alfonso J Rodríguez-Morales, Carmen Scheibenbogen, Anouk Slaghekke, Ioakim Spyridopoulos, Jürgen M Steinacker, Karl J Tronstad, Amber L Vermeesch, Azfar Zaman and Koen AE Zwetsloot.

Ethical approval information, institution and number(s)

Not applicable

Data sharing statement

Not applicable

References:

1. Mandel H, Yoo YJ, Allen AJ, et al. Long COVID Incidence Proportion in Adults and Children Between 2020 and 2024: An Electronic Health Record-Based Study From the RECOVER Initiative. *Clinical Infectious Diseases*. 2025;80(6):1247-1261. doi:10.1093/cid/ciaf046

2. World Health Organization. Clinical management of COVID-19: Living guideline, 18 August 2023. https://www.who.int/publications/i/item/WHO-2019-nCoV-clinical-2023.2.

3. Charlton BT, Goulding RP, Jaspers RT, Appelman B, van Vugt M, Wüst RCI. Skeletal muscle adaptations and post-exertional malaise in long COVID. *Trends in Endocrinology & Metabolism*. 2025;36(7):614-622. doi:10.1016/j.tem.2024.11.008

4. Edward JA, Peruri A, Rudofker E, et al. Characteristics and Treatment of Exercise Intolerance in Patients With Long COVID. *J Cardiopulm Rehabil Prev*. 2023;43(6):400-406. doi:10.1097/HCR.0000000000000821

5. Cornwell WK, Levine BD, Baptiste D, et al. Exercise Intolerance and Response to Training in Patients With Postacute Sequelae of SARS-CoV2 (Long COVID): A Scientific Statement From the American Heart Association. *Circulation*. Published online June 30, 2025. doi:10.1161/CIR.0000000000001348

6. Singh I, Joseph P, Heerdt PM, et al. Persistent Exertional Intolerance After COVID-19: Insights From Invasive Cardiopulmonary Exercise Testing. *Chest*. 2022;161(1):54-63. doi:10.1016/j.chest.2021.08.010

7. Trivieri MG, Devesa A, Robson PM, et al. Prevalence of Persistent Cardiovascular and Pulmonary Abnormalities on PET/MRI and DECT Imaging in Long COVID Patients. *Journal of Nuclear Medicine*. Published online April 30, 2025:jnumed.124.268980. doi:10.2967/jnumed.124.268980

8. Kruger A, Joffe D, Lloyd-Jones G, et al. Vascular Pathogenesis in Acute and Long COVID: Current Insights and Therapeutic Outlook. *Semin Thromb Hemost*. 2025;51(03):256-271. doi:10.1055/s-0044-1790603

9. Jason LA, Holtzman CS, Sunnquist M, Cotler J. The development of an instrument to assess post-exertional malaise in patients with myalgic encephalomyelitis and chronic fatigue syndrome. *J Health Psychol*. 2021;26(2):238-248. doi:10.1177/1359105318805819

10. Blitshteyn S, Whiteson JH, Abramoff B, et al. Multi-disciplinary collaborative consensus guidance statement on the assessment and treatment of autonomic dysfunction in patients with post-acute sequelae of SARS-CoV-2 infection (PASC). *PM&R*. 2022;14(10):1270-1291. doi:10.1002/pmrj.12894

11. Ruijgt T, Slaghekke A, Ellens A, Janssen KW, Wüst RCI. Wearable heart rate variability monitoring identifies autonomic dysfunction and thresholds for post-exertional malaise in Long COVID. Preprint posted online March 19, 2025. doi:10.1101/2025.03.18.25320115

12. Bonilla H, Tian L, Marconi VC, et al. Low-dose naltrexone use for the management of post-acute sequelae of COVID-19. *Int Immunopharmacol*. 2023;124:110966. doi:10.1016/j.intimp.2023.110966



Chapter 7

The Impact of Bed Rest on Human Skeletal Muscle Metabolism

Moritz Eggelbusch, Braeden T. Charlton, Alessandra Bosutti, Bergita Ganse, Ifigenia Giakoumaki, Anita E. Grootemaat, Paul W. Hendrickse, Yorrick Jaspers, Stephan Kemp, Tom J. Kerkhoff, Wendy Noort, Michel van Weeghel, Nicole van der Wel, Julia R. Wesseling, Petra Frings-Meuthen, Jörn Rittweger, Edwin R. Mulder, Richard T. Jaspers, Hans Degens, Rob C.I. Wüst

Published in Cell Reports Medicine, January 2024



Abstract

Insulin sensitivity and metabolic flexibility decrease in response to bed rest, but the temporal and causal adaptations in human skeletal muscle metabolism are not fully defined. Here, we use an integrative approach to assess human skeletal muscle metabolism during bed rest, and provide a multi-system analysis of how skeletal muscle and the circulatory system adapt to short- and long-term bed rest. We uncover that intracellular glycogen accumulation after short-term bed rest accompanies a rapid reduction in systemic insulin sensitivity and less GLUT4 localisation at the muscle cell membrane, preventing further intracellular glycogen deposition after long-term bed rest. We provide evidence of a temporal link between the accumulation of intracellular triglycerides, lipotoxic ceramides and sphingomyelins and an altered skeletal muscle mitochondrial structure and function after long-term bed rest. An intracellular nutrient overload therefore represents a crucial determinant for rapid skeletal muscle insulin insensitivity and mitochondrial alterations after prolonged bed rest.

Introduction

Physical inactivity or (forced) skeletal muscle disuse leads to deconditioning of multiple physiological systems and represents a major independent contributor to many metabolic diseases[1]. Alterations in skeletal muscle metabolism may interfere with insulin-stimulated glucose disposal, leading to insulin resistance[2-4]. Metabolic inflexibility is the failure to efficiently adapt substrate oxidation to energy demand and substrate supply[3], and precedes the development of type 2 diabetes mellitus[5-7], but the temporal contributions of altered insulin sensitivity, metabolic flexibility, and intracellular nutritional overload during physical inactivity[8] are not studied in detail. Similarly, the exact underlying molecular and metabolic signatures of physical inactivity-induced metabolic derangements are currently unknown.

Human bed rest studies represent a well-accepted model for prolonged muscle disuse in astronauts, acute injuries (e.g., limb immobilisation), acute and chronic diseases, or frailty and hospitalisation[2,9-10]. Here, we employed a comprehensive, well-controlled human bed rest intervention, combined with a multi-level mapping of body composition, insulin and glucose handling at the whole body and skeletal muscle level, and skeletal muscle mitochondrial metabolism to study the spatio-temporal alterations in skeletal muscle metabolism during short- and long-term bed rest.

Our study reveals that the low energy demand of muscle during physical inactivity is associated with an accumulation of intracellular glycogen and lipid droplets within 6 days of bed rest. Decreased whole body insulin sensitivity and GLUT4 localisation at the muscle cell membrane, triglyceride, ceramide and sphingomyelin synthesis, and a metabolic shift towards glucose oxidation provide a mechanistic basis of preventing further intracellular glycogen accumulation during long-term bed rest. Inactivity-induced accumulation of lipid droplets close to mitochondria, elongation of triglycerides, and lipotoxic species likely underly observed impairments in mitochondrial size, supercomplex formation, density, and ultimately a reduction in oxidative phosphorylation upon physical inactivity. We conclude that nutrient overload represents a major determinant for metabolic adaptations in human skeletal muscle, and propose that skeletal muscle insulin insensitivity is a positive adaptation to prevent excessive nutrient overload, which would otherwise negatively affect muscle mitochondrial metabolism.

Results

We obtained venous blood samples and vastus lateralis muscle biopsies from 24 healthy human participants (8 female, 16 male, 33±9 years, see Fig. S1 for Consort diagram), who volunteered to undergo a 60-day bed rest in collaboration with the European Space Agency (ESA) and the National Aeronautics and Space Administration (NASA) at the German Aerospace Centre in 2019-2020 (AGBRESA; Fig. 1a for experimental design). Nutritional intake was carefully monitored, and participants' total energy intake was reduced from 1.6 to 1.3 x their resting metabolic rate during bed rest[11]. Skeletal muscle biopsies were obtained before, after 6 days (short-term), and 55 days (long-term) of bed rest, exactly two hours after a controlled lunch meal. Blood samples were collected before, after 6 and 57-60 days of bed rest. All participants therefore served as internal controls. The objective of the AGBRESA study was to determine the efficacy of 30-min daily continuous or intermittent artificial gravity as a countermeasure to the adverse effects of inactivity[11], though we found this countermeasure not to mitigate skeletal muscle oxidative capacity and HOMA-IR scores (Table S1), nor other measurements related to cardiac and skeletal muscle[12-14]. Therefore, we pooled all groups, as has been done previously[12-13].

Body composition and resting substrate oxidation rates

Body composition and resting substrate oxidation during the fasted state before, after 15, 30-32 and 55-60 days of bed rest are depicted in Fig. S2-3. As body weight decreased, due to a progressive reduction in fat free mass (Fig. S2a-b), and height increased, body mass index (BMI) significantly decreased throughout the bed rest (Fig. S2d-e). Despite this reduced BMI, fat mass increased progressively during the bed rest period (Fig. S2c, i-k). While arm lean mass remained unchanged, leg and trunk lean mass decreased progressively throughout the bed rest (Fig. S2f-h), confirming earlier reports of disuse muscle atrophy[12]. With the use of the resting oxygen uptake and carbon dioxide release, measured during fasting conditions, we calculated resting whole-body carbohydrate and lipid oxidation rates. After 32 days of bed rest, resting whole-body carbohydrate oxidation was elevated and lipid oxidation was reduced, but both returned to pre-bed rest values after 55 days (Fig. S3a-d).

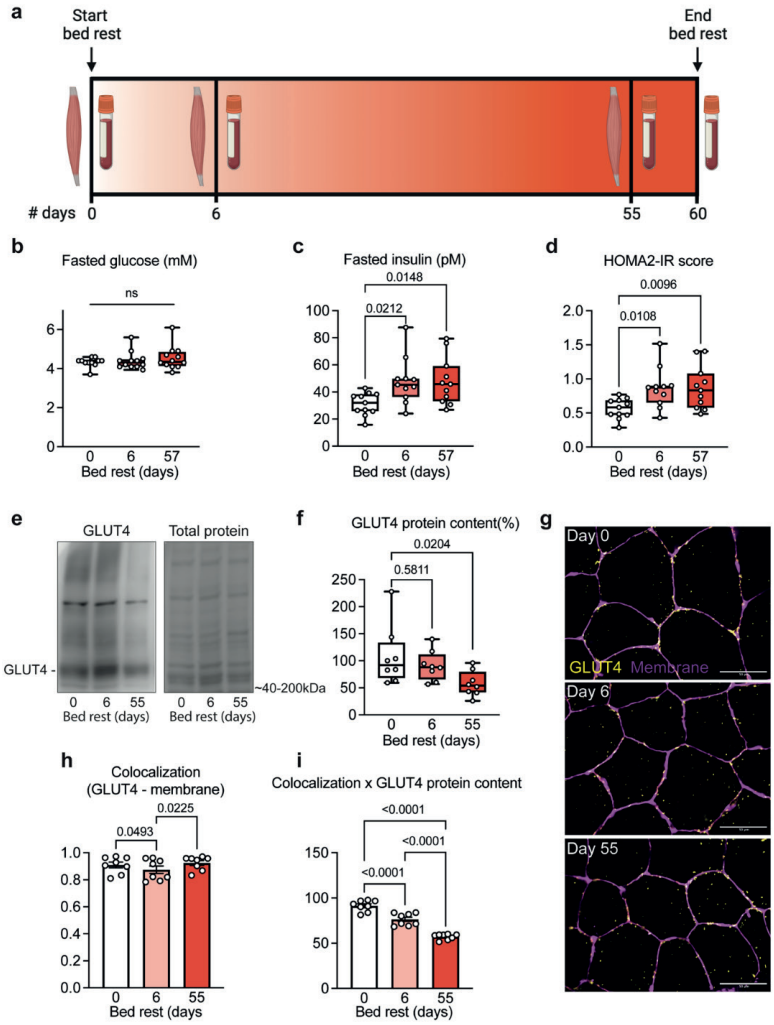


Figure 1. Short- and long-term bed rest induces whole body and skeletal muscle insulin insensitivity. a: Study design. Vastus lateralis muscle biopsies were taken one day before (pre), after 6 (short-) and 55 (long-term) days of bed rest (BR). Blood was drawn before, after 6 and 57 days of bed rest. **b-d:** Fasted blood glucose and insulin levels were used to calculate the HOMA2-IR score *(n*=12), which increased after bed rest. **e-f:** Western immunoblots of GLUT4 showed a lower GLUT4 protein concentration in skeletal muscle after long-term bed rest *(n*=6-7). **g:** Representative immunofluorescence microscopy images of skeletal muscle tissue stained for GLUT4 (yellow) and muscle cell membrane (magenta), before, after 6 and 55 days of bed rest (*n*=8). **h:** Mander's colocalization analyses showed a lower fraction of GLUT4 at the muscle cell membrane after short-, but not long-term bed rest. **i**: Estimates of absolute GLUT4 protein (panel **h** times **f**) at the cell membrane were significantly lower after short- and long-term bed rest. All data were analysed by repeated measures ANOVA,

mixed-effects model with Tukey's post hoc test. Scale bar=50μm. HOMA2-IR: homeostatic model assessment (HOMA) for insulin resistance, GLUT4: glucose transporter type 4.

Short-term bed rest decreases skeletal muscle insulin sensitivity

Fasted blood glucose concentrations (Fig. 1b) remained constant throughout the bed rest, but circulating insulin concentrations were elevated after 6 and 57 days (Fig. 1c). The higher values for the updated homeostatic model assessment for insulin resistance (HOMA2-IR; Fig. 1d)[15] suggest a reduced insulin sensitivity, albeit the critical cut-off for insulin resistance (1.8) was not reached. This decrease in systemic insulin sensitivity was confirmed by the higher HOMA2-%B and lower HOMA2-%S scores after short- and long-term bed rest (Fig. S4a-b). Similarly, the product of systemic insulin and plasma triglyceride levels, as an indirect marker for the adipose tissue insulin resistance index[16], progressively increased during bed rest (Fig. S4c). Circulating levels of the pro-inflammatory cytokines interleukin (IL)-6 and tumour necrosis factor (TNF)-α were higher after long-term bed rest (Fig. S4d-e), while C-reactive protein concentrations and cortisol levels did not change throughout the bed rest period (Fig. S4f-g).

To gain further insights into the putative underlying molecular mechanisms of a reduced insulin sensitivity, we studied the concentration and spatial localisation of the glucose transporter 4 (GLUT4) in biopsies taken two hours after a standardized meal[17-18]. GLUT4 protein concentration was not different after short-term, but tended to decrease after long-term bed rest (Fig. 1e-f). The spatio-temporal pattern of GLUT4 was visualised via fluorescence microscopy, and we quantified the relative amount of GLUT4 colocalized with the cell membrane. GLUT4 localisation at the cell membrane was transiently lower after short-term bed rest, but not different from pre-bed rest values after long-term bed rest (Fig. 1g-h). To account for the differences in overall GLUT4 protein, we multiplied the colocalization coefficient of GLUT4 at the muscle cell membrane (Fig. 1h) with GLUT4 protein concentration (Fig. 1f) to obtain an estimate of the absolute amount of GLUT4 at the cell membrane, and found that the total membrane-bound GLUT4 progressively decreased throughout the bed rest (Fig. 1i), indicating continuous alterations in the intracellular GLUT4 signalling pathway.

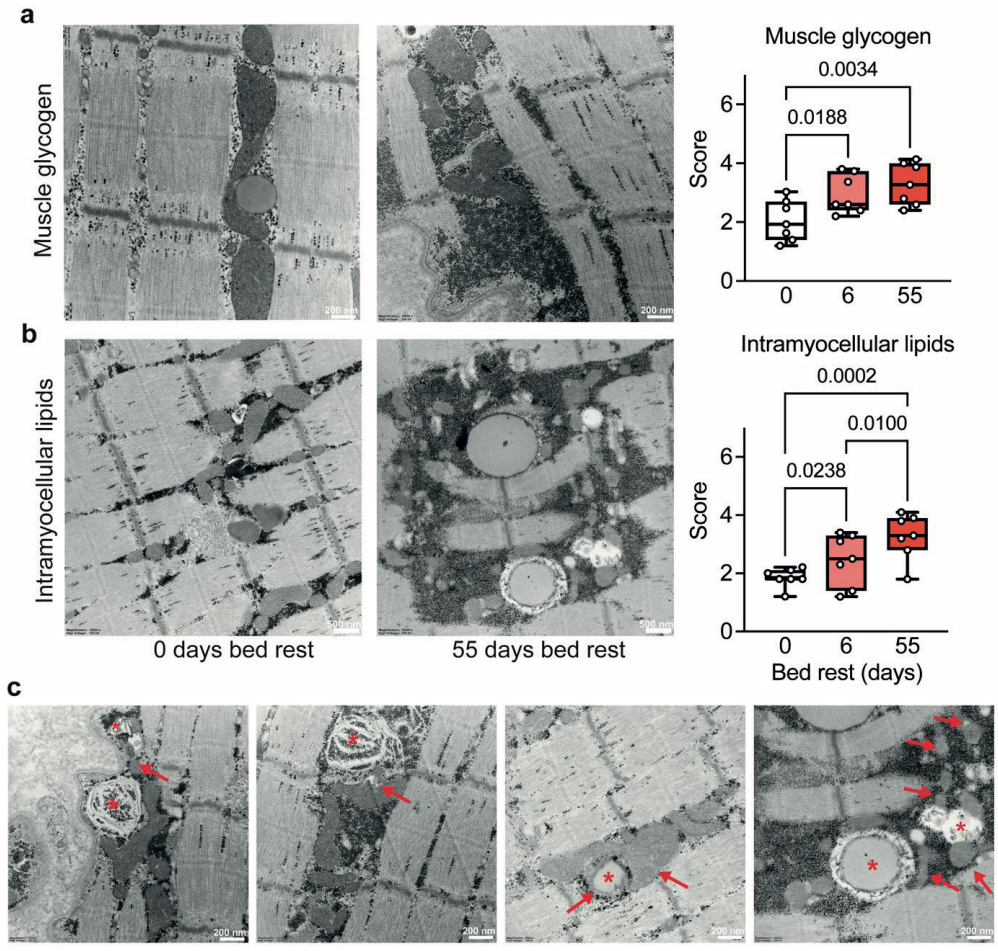


Figure 2. Bed rest-induced glycogen and lipid overload, particularly around mitochondria. Transmission electron microscopy (TEM) images of the vastus lateralis were used to quantify skeletal muscle glycogen (**a**) and intramyocellular lipid (**b**) accumulation before, and after 6 and 55 days of bed rest. Abnormal lipids and mitochondria are indicated by stars and arrows, respectively (**c**). All data were analysed by repeated measures ANOVA, with Tukey's post hoc test, *n*=7 participants for EM. Scale bar=200nm in **a+c** and 500nm in **b**.

Bed rest-induced nutrient overload

We hypothesised that a mismatch between nutrient uptake and substrate utilisation rates underlies the deleterious adaptations in intracellular glucose handling during bed rest. To analyse intracellular nutrient storage, we performed transmission electron microscopy to assess glycogen storage and intramyocellular lipid deposition (Fig. 2). Glycogen storage was significantly increased after short-term bed rest, but did not further increase after long-term

bed rest (Fig. 2a and S5a), possibly due to a saturated skeletal muscle glycogen storage, and/or as a result of the reduced insulin sensitivity that decreased glucose uptake and glycogen accumulation.

We did not observe extracellular lipid accumulation in our skeletal muscle biopsies, suggesting that the majority of the lipid accumulation occurred inside skeletal muscle fibres (Fig. S5b). Intramyocellular lipid deposition increased after short-term, and further accumulated after long-term bed rest (Fig. 2b and S5b). In many cases, we observed glycogen accumulation inside lipid droplets in the skeletal muscle during long-term bed rest (Fig. 2c). Near lipid droplets, the mitochondrial profiles appeared abnormal and fragmented, with many mitochondria surrounded by glycogen (Fig. 2c). As skeletal muscle lipid uptake is not regulated via a single mechanism[19], we reasoned that such continuing ectopic lipid accumulation may include lipotoxic species, explaining the altered GLUT4 signalling and circulating inflammation[20]. To explore which lipid species were present, we next performed in-depth lipidome analyses on blood plasma and skeletal muscle.

Bed rest increases lipid species associated with insulin resistance and inflammation

The lipotoxic effects of ectopic fat accumulation include the production of intramyocellular lipid species such as ceramides, sphingomyelins and diacylglycerols[21]. To study the lipid profile of secondary lipid derivatives, we performed mass-spectrometry-based lipidomics. Analysis of the vastus lateralis lipidome yielded 1362 different lipid species (Fig. 3a). In total, 44 lipid species were significantly altered (27 up- and 17 downregulated) after short-term bed rest, and 88 lipid species changed significantly (with 7 downregulated) following long-term bed rest (Fig. 3a).

A bed rest-induced lipid accumulation was confirmed by an increased skeletal muscle concentration of triglycerides of all carbon chain lengths after long-term bed rest (Fig. 3b). While short-term bed rest resulted in increased storage of triglycerides with a longer carbon length (~52-66 carbons), short carbon chain triglycerides (~30-50 carbons) were predominantly stored after long-term bed rest (middle and right panel Fig. 3b). The synthesis and storage of triglycerides containing longer carbon chains during short-term bed rest and those with relatively shorter chains during long-term bed rest indicates a dynamic response to different durations of inactivity. Lipidomics performed on fasted plasma samples similarly showed significantly elevated circulating triglyceride levels after long-term bed rest (Fig. S6a).

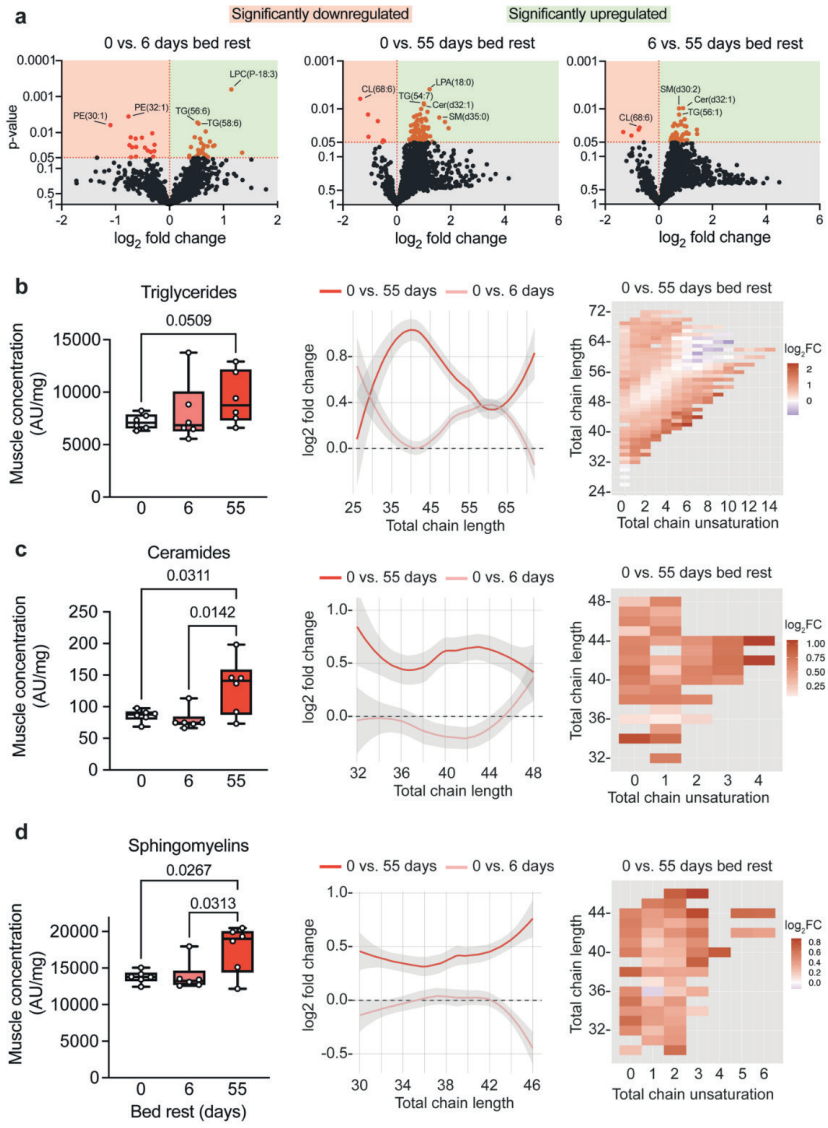


Figure 3. Bed rest induces skeletal muscle triglyceride accumulation, lipid elongation and accumulation of lipotoxic species. a: Volcano plots based on mass-spectrometry based lipidomics analysis performed in vastus lateralis biopsies comparing pre vs. 6, pre vs. 55, and 6 vs. 55 days of bed rest. Out of 1362 identified lipid species, 44 were significantly altered after short- (17 downregulated) and 88 lipids changed significantly (7 downregulated) after long-term bed rest. **b-d:** Tissue concentration of triglycerides (**b**), ceramides (**c**) and sphingomyelin (**d**) increased with long-term bed rest, but not short-term bed rest. Elongation of all chain lengths and saturation increased with long-term bed rest. All lipidomics data were normalized to dry tissue weight. Concentration changes of lipid species were analysed using repeated measures ANOVA, with Tukey's post hoc test, n=6.

Skeletal muscle ceramide (Fig. 3c) and sphingomyelin (Fig. 3d) concentrations were increased after long-term bed rest. The increase in ceramides and sphingomyelins was present across all fatty acid chain lengths, with a particular increase in concentration of saturated lipid species. Alterations in blood triglyceride concentrations, chain-lengths and saturation level (Fig. S6a) resembled those observed in skeletal muscle (Fig. 3b). Plasma ceramides and sphingomyelins, however, did not significantly change during bed rest, but increased in the skeletal muscle (Fig. S6b, c). This indicates that plasma lipid profiles cannot be used as qualitative and/or quantitative markers of lipotoxicity-associated lipid species in skeletal muscle. Skeletal muscle cardiolipin concentrations tended to decrease (on average 24%) after long-term bed rest (Fig. S6d).

Collectively, we demonstrate here a bed rest-induced synthesis of triglycerides, ceramides and sphingomyelins and other intricate changes in lipid composition and metabolism, providing mechanistic insight into the temporal development of lipotoxicity-associated mediators during physical inactivity.

Skeletal muscle metabolic alterations after bed rest

We next combined our lipodome and metabolome mapping of skeletal muscle and blood plasma to provide a metabolic signature of skeletal muscle and blood during bed rest. Partial least squares-discriminant analysis showed different metabolite clusters during bed rest in skeletal muscle, whereas classes showed more overlap for the blood metabolome (Fig. 4a and S7a). Some metabolic pathways in skeletal muscle and blood showed opposite changes during short- compared to long-term bed rest (Fig. 4b, c and S7b). Metabolites related to glycolysis, the pentose-phosphate pathway and tryptophane metabolism were reduced after short-term bed rest, but increased significantly after long-term bed rest. Metabolites in the tricarboxylic acid (TCA) cycle did not change significantly throughout the bed rest (Fig. 4b-d and S8a).

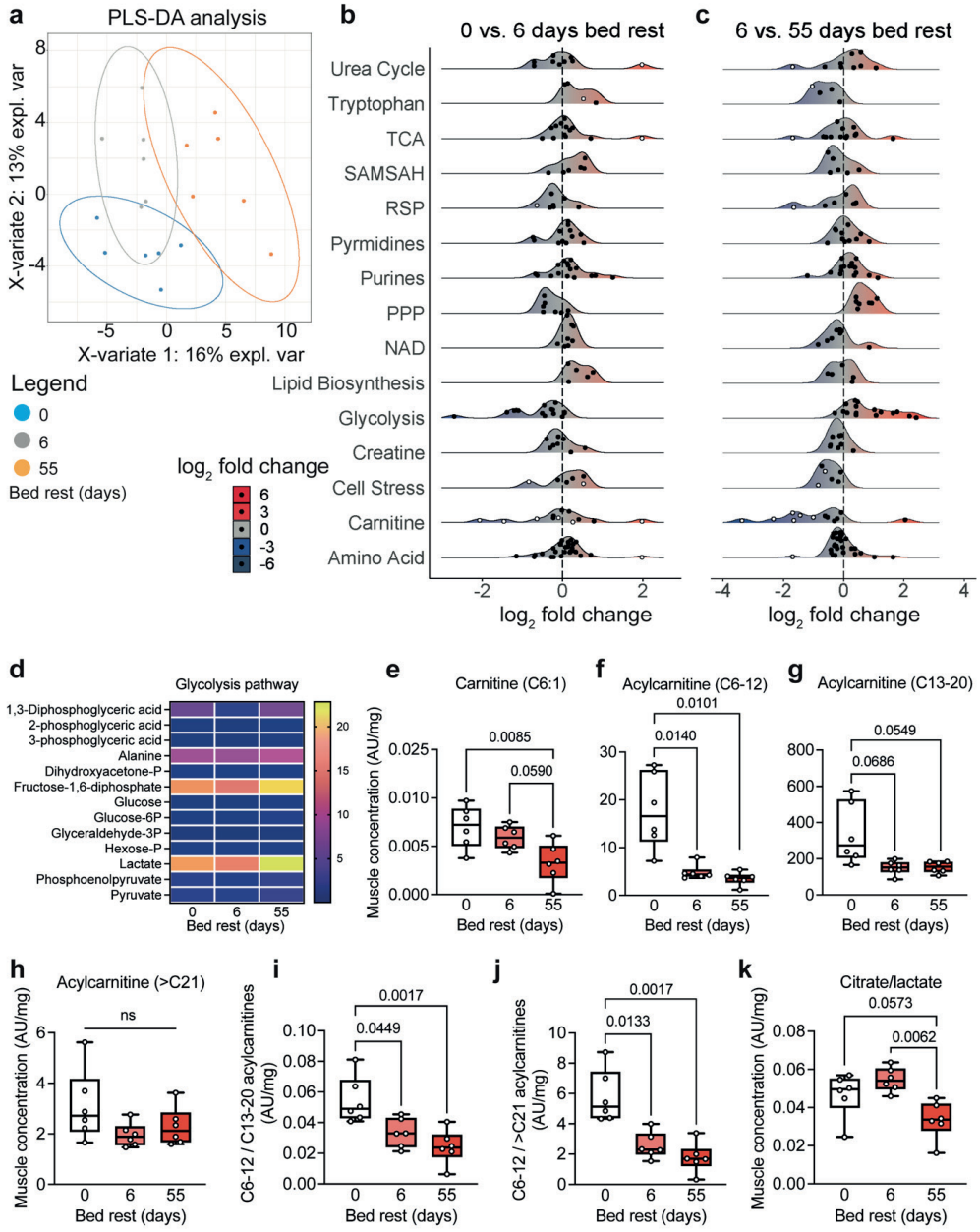


Figure 4. Altered skeletal muscle metabolism after bed rest. **a:** Primary component analysis of time-dependent metabolic changes. **b-c:** Landscape plots based on vastus lateralis metabolomics analysis, indicating the response of various metabolic pathways upon bed rest. White dots represent significantly altered (p<0.05) metabolites. Metabolite concentration shifts are presented as log2fold changes to indicate directionality of alterations. **d:** Heat map of changes in metabolites associated with the glycolysis. **e-h:** Carnitine (**e**) and acylcarnitine concentrations with medium- (**f**), long- (**g**), and very long (**h**) chain lengths decreased during bed

rest, indicative of a reduced fatty acid oxidation capacity. **i:** Ratio of medium- over long-chain length acylcarnitines. **k**: the altered citrate/lactate tissue concentration is indicative of a shift towards glucose oxidation. All metabolomics data were normalized to dry tissue weight. Concentration changes of individual metabolites were analysed using repeated measures ANOVA, with Tukey's post hoc test, n=6. TCA: tricarboxylic acid cycle; SAMSAH: S-adenosylmethionine / S-adenosylhomocysteine cycle; RSP: reductive stress panel; PPP: pentose phosphate pathway; NAD: Nicotinamide adenine dinucleotide pathway.

Metabolites related to carnitine, the rate-limiting substrate for mitochondrial long-chain fatty acids import, were decreased after long-term bed rest (Fig. 4e-j). We found that skeletal muscle acylcarnitine concentrations were significantly decreased after short- and long-term bed rest (Fig. 4f-j and S8b). Especially acylcarnitines with medium-chain length (C6-12) decreased after bed rest (Fig. 4f), relative to the reductions in long-chain (C13-20) or very long-chain (>C21) lengths (Fig. 4g-j). These results are suggestive of a lower maximal capacity for fatty acid β-oxidation during bed rest. From the alterations in the lipidome and metabolome, we infer a higher reliance on glycolysis away from fatty acid oxidation. Such higher reliance on glucose oxidation was corroborated by a decrease in the ratio of citrate over lactate after long-term bed rest (Fig. 4k), whilst a reduction in fatty acid oxidation is consistent with our observed triglyceride synthesis (Fig. 3b) and lipid droplet accumulation (Fig. 2b) after long-term bed rest. These observations are consistent with the development of metabolic inflexibility during bed rest[3].

We observed an increase in levels of circulating amino acids (Fig. S7c-f) and creatine (Fig. S7g), likely due to a breakdown of skeletal muscle proteins. Other metabolites that were significantly altered in the skeletal muscle upon physical inactivity included markers for cellular stress, including 2-aminoadipic acid, ophthalmic acid, and hydroxyphenyllactic acid. We observed a tendency of higher skeletal muscle levels of 2-aminoadipic acid, a biomarker for insulin resistance in humans[22] after short-term, but not long-term bed rest (Fig. S8c). Ophthalmic acid, indicative of glutathione depletion upon oxidative stress[23], decreased after short- and long-term bed rest (Fig. S8d). Metabolite levels of hydroxyphenyllactic acid, an antioxidant[24-25], were increased after short-term (Fig. S8g), but returned to baseline levels after long-term bed rest. Together these findings indicate short-term alterations in the intracellular response to cell stress (Fig. S8f). Although most metabolites in the NAD^+ pathway were reduced after long-term bed rest, no significant differences were observed (Fig. 4b and S8g).

Taken together, our metabolic and lipidomic signature of skeletal muscle reveal that the bed rest-induced increase in lipid accumulation and insulin insensitivity were accompanied by a

reduced ability of fatty acid oxidation following long-term bed rest with an increased reliance on glycolysis, indicating a shift from fatty acid oxidation to glycolysis and glucose oxidation.

Mitochondrial function

We observed that lipid droplets were located in the vicinity of mitochondria, and reasoned that intramyocellular lipid accumulation likely interferes with mitochondrial structure and respiration due to lipid peroxidation-induced mitochondrial damage[26]. We therefore next provide a multi-level assessment of morphological and functional alterations of mitochondria upon bed rest.

We first assessed mitochondrial ultrastructure in our electron microscopy images to provide structural information about mitochondrial morphology (Fig. 5a). We observed that long-term bed rest reduced muscle mitochondrial density (Fig. 5a, b). Mitochondrial size was reduced after bed rest (Fig. 5c, Fig. S9c), but aspect ratio and circularity remained unchanged (Fig. S9a, b). Mitochondrial fragmentation index (total number of mitochondria / total mitochondrial area) was significantly higher after bed rest (Fig. S9d). Protein concentrations of the mitochondrial complexes II, III, IV, and ATP synthase were decreased after long-term bed rest (Fig. S9e-i), as was the total protein concentration of mitochondrial subunits (Fig. 5d, e).

Individual mitochondrial complexes are structurally and functionally assembled into high-molecular mass supercomplexes or respirasomes[27-28]. Aerobic exercise is known to enhance supercomplex assembly in humans[29], but it is currently unknown whether mitochondrial supercomplex assembly is altered upon physical inactivity. We therefore assessed the supramolecular organisation of complexes I–IV and ATP synthase into supercomplexes, and normalized for total mitochondrial protein, after isolating and purifying the mitochondrial protein fraction from vastus lateralis biopsies. We found fewer mitochondrial supercomplexes after long-term bed rest (Fig. 5f, g), as was V_n, III_2+IV and the free form of complex IV, while free complex II and III tended to be lower (Fig. S9j-m). Our observed decrease in supercomplex abundance after long-term bed rest was not accompanied by significant changes regarding the incorporation of individual complexes into mitochondrial supercomplexes (Fig. 5h), overall suggesting that bed rest reduced mitochondrial supercomplex formation and individual

complexes, with no reorganization from the supercomplexes into free complexes.

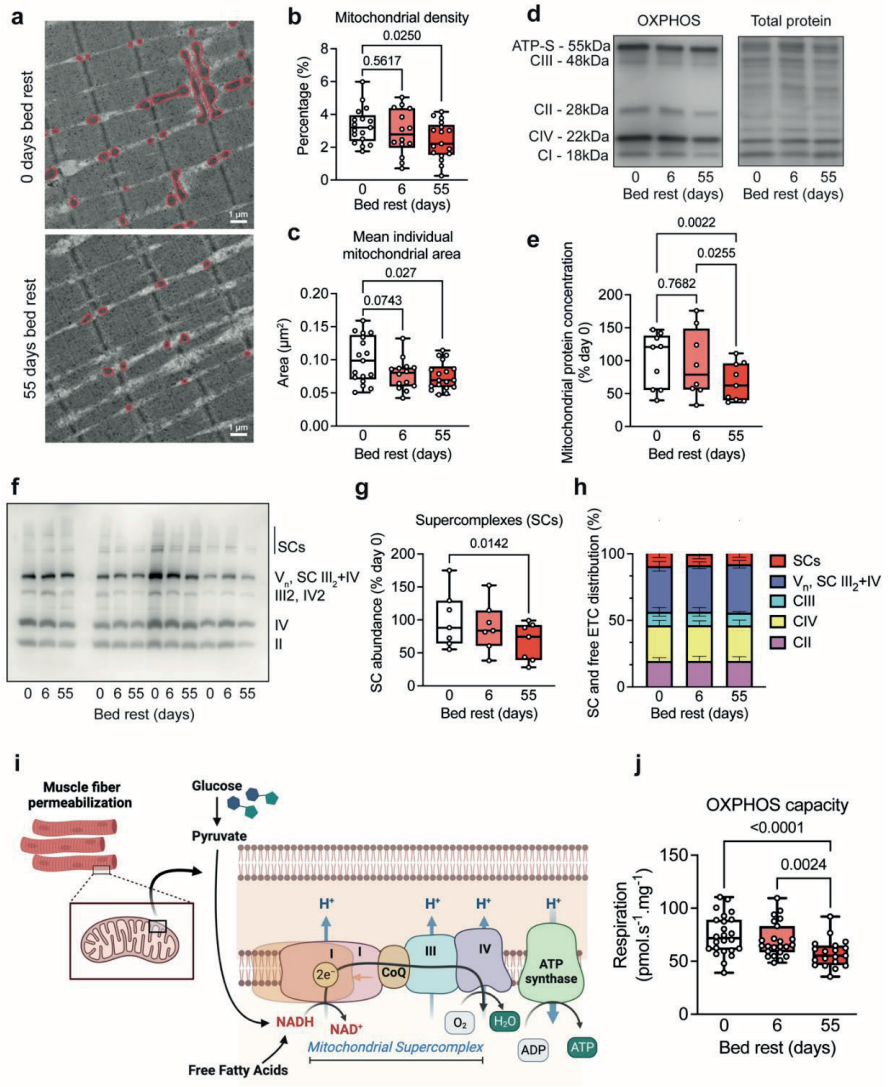


Figure 5. Mitochondrial structure and function reduce after long-term bed rest. a: Representative electron microscopy images were used to assess mitochondrial density (**b**) and size (**c**) which were both reduced after long-term bed rest. **d-e:** Typical Oxidative phosphorylation capacity (OXPHOS) western blot and normalization. Individual protein concentrations of mitochondrial complexes were only reduced after long-term bed rest. **f-h**: Representative BN-PAGE to assess mitochondrial supercomplexes (SC). Relatively less mitochondrial proteins were incorporated into SCs after long-term bed rest (**g**), but the make-up of these supercomplexes was the same (**h**). **i-j**: Saponin-permeabilized fibres were used to assess mitochondrial respiratory respiration. OXPHOS capacity was unaffected after short- but significantly decreased after long-term bed rest.

All data were analysed using repeated measures ANOVA, with Tukey's post hoc test, *n*=14-17 for mitochondrial density and area, *n*=9 for immunoblotting, *n*=7 for BN-PAGE, *n*=24 for respirometry. Scale bar=1µm in **a.**

To assess mitochondrial respiration, we performed high-resolution respirometry in permeabilised muscle fibres (Fig. 5i). Short-term bed rest did not cause significant changes in any parameter of mitochondrial respiration. Long-term bed rest resulted in a lower leak, NADH-linked respiration, oxidative phosphorylation capacity (Fig. 5j), electron transport capacity and succinate-linked respiration (Fig. S9n-q). We observed no significant alterations in respiratory control ratios as measures for qualitative differences in mitochondrial respiration (Fig. S9r-t). The 24% reduction in mitochondrial respiration upon long-term bed rest was paralleled by a ~30% reduction in mitochondrial density and protein concentration.

Our multi-level analysis of mitochondrial morphology and function collectively indicate that short-term bed rest does not alter mitochondrial size, density or respiration, but long-term bed rest results in a lower oxidative phosphorylation capacity that was mechanistically explained by fewer and smaller mitochondria, rather than preferential reductions in specific components of the electron transport system.

Discussion

Our longitudinal study provides information about the time course of the development of nutrient overload, insulin sensitivity, lipotoxicity and metabolic changes in skeletal muscle after physical inactivity. The reduced energy demand during physical inactivity was accompanied by the accumulation of intracellular glycogen and lipid droplets. Long-term bed rest did not further increase intracellular glycogen compared to short-term bed rest, due to decreased whole body insulin sensitivity, less GLUT4 at the skeletal muscle cell membrane, and a metabolic shift away from lipid towards glucose oxidation. Lipid accumulation, also in close vicinity to mitochondria, increased from short- to long-term bed rest, together with an accumulation of lipid species associated with inflammation and lipotoxicity. This intramuscular accumulation of lipotoxic lipid species coincided with a reduction in mitochondrial size, density, supercomplex formation and respiration.

A diminished energy demand results in nutritional oversupply

We anticipated a reduced ATP demand of skeletal muscle and lower resting whole-body energy utilization rates during bed rest[30], and therefore reduced the participants' total energy intake from 1.6 to 1.3 x their resting metabolic rate during the bed rest[11]. Still, we observed an intramuscular glycogen and lipid droplet accumulation after short-term, while only lipid

droplet accumulation further increased after long-term bed rest, likely due to this reduced energy demand, and relative nutritional oversupply[31].

Our findings of intramyocellular lipid accumulation in the vastus lateralis muscle are in line with intramuscular lipid accumulation in gluteal[32] and lumbar[14] muscles following bed rest. While intramuscular fat accumulation can normally be either inside or in between fibres, we did not observe abnormal extracellular lipid accumulation in skeletal muscle after bed rest. Insulin resistance and obesity are linked to the development of inter-muscular adipose tissue[33], but how nutritional overload and/or physical inactivity contribute to the development of inter-muscular adipose tissue, potentially via the activation of fibro-adipogenic progenitors[34], remains unknown.

Intramyocellular storage of lipid droplets provides an important energy source for skeletal muscle, also in well-trained athletes[35], but intramyocellular lipid accumulation is also associated with metabolic organ dysfunction[36]. Likely, the turnover rate of fatty acids contributes to a different signature of intracellular lipid species between highly-trained athletes and sedentary individuals. Future work is needed to determine the exact content and distribution of intracellular lipid droplets. We observed lower levels of acylcarnitines and a shift towards longer-chain acylcarnitines after short-term bed rest, as well as a decline in carnitine after long-term bed rest, suggesting that the reduced resting fatty acid oxidation after short-term bed rest was due to a lower capacity to import fatty acids into mitochondria. Indeed, a limited capacity of carnitine palmitoyl-transferase-1 (CPT-1) to transport cytosolic long-chain acyl-CoAs across the mitochondrial membrane contributes to metabolic inflexibility due to the accumulation of incompletely oxidized lipid intermediates[3,37]. The decrease in fatty acid oxidation and increased glucose oxidation after long-term bed rest likely contributed to our observed triglyceride accumulation and intramyocellular lipid droplets, and ultimately, the appearance of lipid species associated with lipotoxicity, such as ceramides and sphingomyelins.

Our lipidomics data show a higher abundance of longer triglycerides in blood (Fig. S6a) and skeletal muscle (Fig. 3b). The increased number in skeletal muscle is likely due to an increased intramuscular synthesis of triglycerides from fatty acyl-CoAs and glycerol-3-phosphate. We could not detect glycerol-3-phosphate abundance in our metabolomics dataset, but pentose phosphate pathway metabolites were elevated upon bed rest (Fig. 4b)[38]. We also observed glycogen molecules accumulating inside lipid droplets (Fig. 2c), but the biological link between glycogen and triglyceride synthesis remains unclear. The origin of the fatty acids is however unknown, since such longer fatty acids could have been imported from the circulation,

possibly via CD36[39], or produced locally via *de novo* lipogenesis. We were unable to provide clear evidence of the conversion of citrate into fatty acids, but it has been suggested that *de novo* lipogenesis can occur in skeletal muscle, particularly under hyperglycaemic conditions[38,40-42]. Gene expression or protein content of key enzymes in this pathway do not necessarily provide evidence of an increased flux through this pathway. Our study design cannot provide the relative contribution of *de novo* lipogenesis in the intramuscular triglyceride accumulation, as we did not perform experiments with labelled substrates. Despite this, our lipidome analysis indicates intramyocellular lipogenesis in the form of an increased synthesis of triglycerides, ceramides and sphingomyelins upon long-term bed rest. Clearly, the regulation of lipogenesis and the underlying metabolic regulation in the context of physical inactivity deserves further study.

Intracellular insulin insensitivity

We observed a reduced whole-body insulin sensitivity, altered GLUT4 signalling, and glycogen accumulation upon short-term bed rest. We reason that the glycogen accumulation preceded the decrease in insulin sensitivity. Firstly, if reduced insulin insensitivity -all else staying the same- had occurred before glycogen accumulation, then glucose uptake (and glycogen accumulation) would have been lower, not higher. Secondly, it has been reported that glycogen accumulation provides a negative feedback signal to insulin-mediated GLUT4 translocation[48] that may contribute to the absence of further significant glycogen accumulation between short- and long-term bed rest, facilitated by a metabolic shift towards more glucose oxidation and a transient rise in resting carbohydrate oxidation. We therefore suggest that glycogen accumulation occurred before the reduction in insulin sensitivity, but future work is required to confirm this.

Elevated levels of elongated triglycerides, ceramides and sphingomyelins in skeletal muscle are strongly associated with local and systemic impaired insulin action[43] and critical illness myopathy[44]. It remains unclear, however, whether intramyocellular lipid accumulation causes insulin resistance or whether skeletal muscle insulin resistance occurs due to an excess accumulation of intramyocellular lipids[6]. We observed that intracellular lipid accumulation accompanied the decreases in systemic insulin sensitivity and less GLUT4 located at the muscle cell membrane after short-term bed rest, but the reduction in insulin sensitivity preceded the accumulation of lipotoxic ceramides and sphingomyelins. The additional accumulation of intramyocellular lipids after long-term bed rest was accompanied by a worsening of intracellular GLUT4 signalling, but not by a progressive decline in whole-body insulin

sensitivity. The circulating levels of the pro-inflammatory cytokines IL-6 and TNF-α were only measured and increased after long-term bed rest. From the integration of our observed circulating and skeletal muscle lipids signatures, we therefore propose that skeletal muscle insulin insensitivity preceded, rather than followed, the accumulation of lipotoxic species and systemic inflammation.

While lipotoxicity and reduced oxidative phosphorylation capacity followed rather than preceded the decline in insulin sensitivity during bed rest, a decreased local insulin sensitivity may serve to minimise excessive intramyocellular glycogen accumulation. An impaired insulin-induced GLUT4 translocation towards the membrane reduces cellular glucose uptake, manifesting in a higher circulating insulin concentration to "push" glucose into peripheral tissue, ultimately resulting in a decreased whole-body insulin sensitivity[44]. It should be noted that GLUT4 localisation and expression not only depend on circulating insulin and its local insulin receptor, as also physical exercise represents a potent stimulus for insulin-independent GLUT4 translocation and glucose uptake, as well as increasing GLUT4 gene transcription levels[45-47]. The increase in muscle glucose uptake induced by acute exercise is partly independent of insulin, and the enhanced post-exercise skeletal muscle insulin sensitivity is characterised by more GLUT4 localisation at the skeletal muscle membrane that persists up to 16-24 hours[45,48-50]. As such, the acute reduction in insulin sensitivity and GLUT4 localisation at the muscle cell membrane during bed rest may be a direct consequence of a reduction in the long-lasting effect of exercise-evoked sensitisation of GLUT4 signalling. As such, glucose uptake via an intracellular "pull"-mechanism is reduced after physical inactivity.

Channelling away intracellular glycogen towards triglycerides and other lipid species might be the consequence of a ceiling effect in intracellular glycogen storage. Intracellularly stored glycogen is also known to modulate muscle GLUT4 translocation via posttranslational modifications[50], such as protein acetylation, glycosylation and O-GlcNAcylation[51-52], modulating protein and enzyme activities[53]. How physical inactivity alters the post-translational landscape in skeletal muscle requires future studies.

Bed rest alters skeletal muscle substrate oxidation

Metabolic inflexibility is often associated with physical inactivity, insulin resistance and type 2 diabetes mellitus[3,5,26]. We showed a reduction in body mass index upon bed rest, despite an increase in fat mass. Whole-body resting glucose and lipid oxidation, measured in the fasted state, were transiently altered, whereas fat mass progressively increased throughout the bed

rest. Whether the transient changes in whole-body carbohydrate and lipid oxidation are therefore due to a reduction in resting metabolic rate, increased fat mass, or daily variation in diet is currently unknown. Despite this, we observed markedly altered resting metabolite concentrations, indicative of a bed rest-induced shift in substrate oxidation, consistent with metabolic inflexibility.

Metabolites related to the glycolysis were higher, and those associated with fatty acid oxidation were lower after long-term bed rest, indicative of a shift away from fatty acid oxidation towards a higher reliance on glucose oxidation at rest[5]. We observed a short-term reduction, but long-term increase in metabolites of glycolysis and the pentose-phosphate pathway. The metabolic shift from fatty-acid to glucose metabolism caused a spill-over in the pentose phosphate pathway, likely associated with an increased triglyceride synthesis, but other molecular consequences for *in vivo* nucleotide synthesis are unknown.

Regular aerobic exercise training is widely accepted to shift mitochondrial metabolism towards a predominant free fatty acid metabolism[3], and detraining or physical inactivity is associated with a shift towards more glucose metabolism[5], which we confirmed via our whole-body substrate oxidation rates and skeletal muscle metabolome signatures. Maintaining intracellular nutrient homeostasis is dependent on substrate availability (push concept) and energy requirement (pull concept). Substrate oxidation in mitochondria plays an important role for understanding the pull concept of metabolic flexibility, while excess nutrient supply alters metabolic flexibility by a push-mechanism[3].

Bed rest-associated mitochondrial alterations in structure and respiration

Although physical inactivity is traditionally associated with a reduction in muscle mitochondrial density and function, there is considerable discrepancy in the literature. We previously showed a dissociation between skeletal muscle size and mitochondrial density in the same cohort of participants[12]. Daily reduction in muscle size was largest in the first six days of bed rest, while a marker for mitochondrial density (succinate dehydrogenase activity) was only reduced after long-term bed rest[12]. Our results show a decreased mitochondrial respiration (per mg of tissue) and density only after long-term bed rest, indicating that the loss of sarcomeric and mitochondrial protein are proportionally similar after short-term bed rest, but that mitochondrial proteins are predominantly lost after long-term bed rest. Our results are in line with studies reporting no alterations in mitochondrial respiratory function after a 6-10 days of bed rest[12,54-55], and studies reporting lower mitochondrial respiration after long-term bed

rest[12,56-59]. Other groups, however, report a significantly lower mitochondrial respiration after 7-10 days of bed rest[60-62], or even a higher mitochondrial respiration[63-64]. We reason that differences in age, pre-study fitness levels, and nutritional control (particularly overnutrition) contribute to these discrepancies.

Notably, no change in fibre type composition was observed at any time point of the bed rest[12], in accordance with other recent findings[65]. Independent of fibre type changes, a reduction in the succinate dehydrogenase activity in muscle fibres[12] and whole muscle metabolic alterations have been described before[5,60], because the molecular pathways underlying metabolic alterations and myosin heavy chain expression are different. Therefore, we conclude that the metabolic changes occur in the absence of significant changes in muscle fibre type composition.

The decrease in mitochondrial density (28%) and OXPHOS capacity (24%) was proportional to the reduction in cardiolipin concentration (24%) after long-term bed rest.

Our mitochondrial supercomplex measurements were normalized to mitochondrial protein content. The reduced mitochondrial respiration coincided with a decrease in supercomplex formation after long-term bed rest, at the time when also mitochondrial density and proteins were reduced. A lower mitochondrial supercomplex formation correlates with impairments in oxidative phosphorylation capacity[66], and is linked to a more fragmented mitochondrial network (Fig. S9d)[66-67]. Moderate-intensity aerobic exercise training on the other hand, increases supercomplex abundance and a redistribution towards larger supercomplexes in older participants[29]. High-intensity training in younger participants increased supercomplex abundance, but similarly to our results, did not induce stoichiometric changes to the mitochondrial supercomplexes[68]. Mitochondrial supercomplex abundance in skeletal muscle is therefore reduced during periods of physical inactivity, but future work should decipher which molecular signals are involved in the formation of mitochondrial supercomplexes.

Our electron microscopy results show a higher mitochondrial fragmentation index upon short-term bed rest, driven by smaller individual mitochondria. The aspect ratio and circularity, however, did not change. As mitochondrial density did not reduce upon short-term bed rest, we conclude that short-term bed rest results in more mitochondria, each with a smaller individual area. This more fragmented mitochondrial network does not reduce oxidative phosphorylation capacity upon short-term bed rest. However, smaller mitochondria may be more susceptible to damage upon bed rest-induced nutrient overload, as we observed in Figure

2c. How mitochondrial fission and fragmentation relate to changes in nutrient overload is currently unknown, but deserves further study.

Here, we highlight a role of intracellular lipotoxicity-associated lipid species in the preferential loss of mitochondrial protein after long-term bed rest. Lipotoxicity is known to contribute to skeletal muscle mitochondrial dysfunction in patients with type 2 diabetes[69]. We observed a greater proportion of smaller mitochondria in close vicinity of large lipid droplets after long-term bed rest. Lipotoxicity and overnutrition have also been suggested to be the primary initiating factor for mechanical-ventilation-induced diaphragm dysfunction, as induction of hyperlipidemia worsened diaphragmatic dysfunction after mechanical ventilation in mice[8]. Our findings therefore lead us to hypothesise that a nutrient oversupply precedes a reduction in insulin sensitivity, which in turn prevents further intramyocellular glycogen loading, but not lipid accumulation. The resultant triglyceride, ceramide and sphingomyolin synthesis can cause mitochondrial damage and dysfunction by lipid peroxidation, causing a positive feedback loop where a reduced oxidative capacity increases intracellular lipid accumulation in the vicinity of mitochondria[69].

Clinical implications and future perspectives

The negative health impacts of physical inactivity are often linked to other confounding lifestyle alterations, such as a western diet, alcohol use or sedentary behaviour[70-71]. The total amount of calories in the nutrition in this study consisted of 15% protein, 32% fat and 52% carbohydrates, representing a 'healthier' diet compared to a 'real-world' scenario where a sedentary lifestyle is commonly combined with a diet rich in saturated fat and sugar. Despite the fact that total nutritional intake of participants in this study was carefully controlled and adjusted to their individual resting metabolic rates and body weight[11], we still observed an increase in intramyocellular lipid and glycogen accumulation after six days of bed rest. The bed rest-induced muscle atrophy[12] was accompanied by a relative increase in cell membrane lipids per mg of tissue, because of a proportionally larger atrophy than loss of cell membrane lipids. We acknowledge the limitation that the ~20% reduction in energy intake was not enough to compensate for the larger reduction in whole-body energy utilization rates during bed rest[31]. Importantly, despite the hypercaloric diet, body mass still decreased over the bed rest period[11]. In healthy humans, disuse-associated reductions in fat-free mass might be regarded as beneficial in order to dampen whole-body metabolic consequences of physical inactivity. A hypocaloric diet-induced loss in fat-free mass in hospitalized older, malnourished people with the risk of developing sarcopenia might, however, become problematic with post-hospital

recovery[72]. Patients in the intensive care unit often have high circulating glucose and free fatty acids levels[73], and early delivery of a high caloric intake has been associated with a longer stay at the intensive care unit[74] and high mortality[72]. Clinical measures designed to reduce the risks of substrate overload or rescuing dysfunctional mitochondria via the AMPK-PGC1α pathway[75], i.e. via metformin[76], could be useful in preventing metabolic dysfunction, and ultimately mortality, upon physical inactivity in the hospital setting[77]. What the molecular interplay is between insulin sensitivity, intramyocellular lipotoxicity and mitochondrial metabolism in hospitalized patients, who also suffer from systemic inflammation, warrants further study.

Conclusion

Our findings reveal that the low energy demand of the skeletal muscle during physical inactivity is associated with a rapid accumulation of intracellular glycogen and reduced insulin sensitivity. The observation that lipid, but not glycogen accumulation or insulin insensitivity, kept increasing from short- to long-term bed rest, indicates that lipid accumulation is not linked to a decrease in insulin sensitivity. Rather, a metabolic shift away from fatty acid towards glucose oxidation, impaired GLUT4 localisation at the muscle cell membrane, and triglyceride synthesis minimised further glycogen accumulation during prolonged bed rest. The appearance of lipotoxic species, such as ceramides and sphingomyelins, occurred only after long-term bed rest, and coincided with the reduced mitochondrial density and respiration, but did not aggravate insulin sensitivity. We conclude that an elevated nutritional supply to substrate utilisation represents a major determinant for inactivity-associated skeletal muscle adaptations, providing a target for the alleviation of muscle-specific detrimental alterations upon physical inactivity.

Limitations of the study

Limitations of the current study include the lack of skeletal muscle metabolic flux analyses, and dynamic measures of metabolic flexibility and insulin sensitivity, such as insulin clamp, oral glucose tolerance test and pre-post-meal GLUT4 localisation in skeletal muscle. Further limitation pertains to the relatively small sample size of some of the experiments, due to scarcity of biopsy material, which also prevented us from measuring phosphorylation status, as well as gene and protein content of markers of the insulin signalling pathway and *de novo* lipogenesis. How intracellular lipid accumulation relates to the development of inter-muscular adipose tissue and the contribution to muscle insulin resistance deserves further study.

STAR Methods

Key Resources Table

REAGENT or RESOURCE	SOURCE	IDENTIFIER
Antibodies		
Rabbit polyclonal anti-GLUT4	Thermo Fisher Scientific	Cat#PA5-23052; RRID: AB_11153908
Mouse anti-Human OxPhos cocktail	Thermo Fisher Scientific	Cat#45-8199; RRID: AB_2533836
Mouse monoclonal anti-NDUFA9	Thermo Fisher Scientific	Cat#459100: RRID: AB_2532223
Rabbit polyclonal anti-Mouse IgG (H+L) secondary antibody, HRP	Thermo Fisher Scientific	Cat#61-6520; RRID: AB_2533933
F(ab')2-Goat anti-Rabbit IgG (H+L) cross-adsorbed secondary antibody, Alexa Fluor™ Plus 488	Thermo Fisher Scientific	Cat#A48282; RRID: AB_2896345
Bacterial and virus strains		
Biological samples		
Human muscle biopsies	This paper	N/A
Human blood plasma	This paper	N/A
Chemicals, peptides, and recombinant proteins		
Wheat Germ Agglutinin	Thermo Fisher Scientific	Cat#W32466
Normal Goat Serum (10%)	Life technologies	Cat#50062Z
Periodic acid	Sigma-Aldrich	Cat#P7875
Schiff's reagent	Sigma-Aldrich	Cat#3952016
Propylene glycol	Sigma-Aldrich	Cat#W294004

Sudan Black B	Sigma-Aldrich	Cat#199664
VECTASHIELD Mounting Medium with DAPI	Vector Laboratories	Cat#H-1500-10
RIPA lysis buffer	Sigma-Aldrich	Cat#R0278
Protease inhibitors	Roche	Cat#04693124001
Phosphate inhibitors	Roche	Cat#04906837001
NativePAGE sample buffer	Thermo Fisher Scientific	Cat#BN2003
Digitonin	Novex life technologies	Cat#BN2006
No-Stain Protein Labeling Reagent	Thermo Fisher Scientific	Cat#A44717
3 - 12% Bis-Tris gradient gel	ThermoFisher Scientific	Cat#BN2012BX10
NuPAGE transfer buffer	Life Technologies	Cat#NP0006-1
Critical commercial assays		
Pierce BCA Protein Assay Kit	ThermoFisher Scientific	Cat#23225
Deposited data		
Full metabolomics dataset	This paper	MetaboLights accession number: MTBLS9114
Lipidomics	This paper	MetaboLights accession number: MTBLS9114
Software and algorithms		
ImageJ	Schneider et al[78].	https://imagej.nih.gov/ij/
FIJI	Schindelin et al.[79]	https://fiji.sc/
Huygens Professional 22.4	Scientific Volume Imaging, The Netherlands	http://svi.nl
R studio 4.2.2	R Core Team 2022, Vienna, Austria	http://www.r-project.org/

GraphPad Prism 10.0.2	GraphPad Software, Boston, Massachusetts, USA	http://www.graphpad.com/
Other		
HOMA2 computer model	Levy et al. and Wallace et al.[15,80]	https://www2.dtu.ox.ac.uk/homacalculator/

Resource Availability

Lead contact

Further information and requests for resources and reagents should be directed to and will be fulfilled by the lead contact, Rob C.I. Wüst (r.wust@vu.nl).

Materials availability

This study did not generate new unique materials.

Data and code availability

- The full metabolomics and lipidomics datasets are available at MetaboLights accession number MTBLS9114.
- This paper does not report original code.
- Any additional information required to reanalyse the data reported in this paper is available from the lead contact upon request.

Acknowledgements

The authors acknowledge the support of the European Space Agency (ESA, 16-16ESA AGBR-0013, contract number 4000113871/15/NL/PG) and the National Aeronautics and Space Administration (NASA, contract number 80JSC018P0078). BG is supported by the German Research Foundation (grant number GA2420/1-1) and German Aerospace Center (grant number 50WB1928). AB is supported by the Italian Space Agency grant (MIAG project ASI n.2021-13-U.0). HD, IG and PH are supported by the UK Space Agency (ST/S0001735/1 & ST/T00066X/1). ME and RCIW are supported by an Amsterdam Movement Sciences PhD fellowship grant (2019). ESA and NASA were involved in the overall study design, but not in the collection, data analysis and interpretation, in the writing of the report, and in the decision to submit the article for publication. The authors would like to thank Dr Angelique van

Ombergen for her assistance with ESA bed rest data sharing. Illustrations were created with BioRender.com (full license).

Author contributions

Study design, M.E., A.B., B.G., E.R.M., H.D. and R.C.I.W.; data collection and analysis, M.E., B.T.C., B.G., I.G., A.E.G., P.W.H., Y.J., S.K., T.J.K., W.N., M.v.W., N.v.d.W., J.R.W., P.F.M., J.R., H.D. and R.C.I.W.; data interpretation, M.E., R.T.J., H.D. and R.C.I.W; first draft, M.E. and R.C.I.W.; all authors reviewed the manuscript and approved the final version.

Experimental Model And Study Participant Details

Participant recruitment

The CONSORT diagram for participant recruitment and screening is depicted in supplementary Figure S1[11]. In short, after ethical approval and advertisement, interested participants received detailed information and a screening questionnaire and had to attend a mandatory information session at the German Aerospace Centre Cologne or Hamburg (Visit 1). During the information session a preliminary psychological test, including a Freiburger Personality Questionnaire. If deemed eligible (i.e., willing to participate and likely to finish the intervention), potential participants were invited to successive, more rigorous screening procedures including a modified Air Force Class III physical and psychological evaluation (Visit 3), and a criminal background check. All participant selection and assessment were performed by physicians and psychologists of the German Aerospace Centre, with ample experience in selection of participants for bed rest studies.

Study design

Twenty-four healthy participants (16 men, 8 women, 33±9 years; 175±9 cm; 74±10 kg) participated in the AGBRESA study, in collaboration with the German Aerospace Centre, the European Space Agency and the National Aeronautics and Space Administration[11]. All participants gave written informed consent prior to the study. The study was conducted in accordance with the declaration of Helsinki and was registered at the German Clinical Trials Register under number DRKS00015677. The protocol was approved by the ethics commissions of the Medical Association North Rhine (number 2018143) and NASA (Johnson Space Center, Houston, United States). The primary objective of the study was to determine the efficacy of 30-min daily artificial gravity in the form of continuous or intermittent centrifugation as a countermeasure to the adverse effects of physical inactivity. Participants were pseudo-

randomly assigned to an experimental group, to match participants at baseline for age, gender and body mass index. Participants underwent physical and psychological testing to assess their suitability to be included in the study[11].

Participants were instructed to undergo a 60-day strict 6° head-down bed rest. No pillows were allowed except for a thin cushion when participants lay on their side; one shoulder always had to touch the mattress, and all daily activities including personal hygiene were done in the −6° position. In total, participants spent 87 days at the research facility, including pre- and post-bed rest measurements. All participants ingested a standardised diet with an energy intake of 1.6 times the resting metabolic rate before and 1.3 times resting metabolic rate during bed rest. Fluid intake was controlled and ingestion of caffein and alcohol was prohibited. Participants were subjected to regulated bed times[11].

Method Details

Body composition

Appendicular, trunk and total fat and lean mass distribution was assessed by DXA, using the whole-body scan feature of the Prodigy Full Pro system (GE Healthcare GmbH), before, after 15 or 30, and 60 days of bed rest, and analyzed using the manufacturer's enCORE software (version 16.10.151).

Indirect calorimetry

Substrate oxidation values were collected via indirect calorimetry using a canopy device (Quark RMR, COSMED Deutschland GmbH, Fridolfing, Germany) in the morning after an overnight fast. Before each test, the gas analyzers were calibrated using a reference gas mixture (17% O_2 and 5% CO_2 in nitrogen). The rate of oxygen consumption ($\dot{V}O_2$) and carbon dioxide production ($\dot{V}CO_2$), standardized for temperature, barometric pressure, and humidity, were recorded at 10-s intervals. After about 30 min of acclimatization, measurements were continuously performed for 30 min in thermo-neutral environment, while the participants were lying calm in the 6° head down tilt position. The last 20 min of acquired data were used for analyses. The rate of fat oxidation and carbohydrate oxidation expressed in g/h have been calculated using common stoichiometric equations.

Plasma substrate analyses of HOMA-IR parameters

Fasting blood samples were collected one day before the start of the bed rest, and after 6 and 57 days of bed rest, always at the same time before breakfast. The blood was centrifuged and

the aliquoted serum stored at -80 ˚C. Plasma concentration of insulin was measured by an automated immunoassay (Atellica IM, Siemens Healthcare Diagnostics) with an inter-assay variation of <5% over the whole concentration range[81]. Plasma glucose concentration was assessed with the use of the hexokinase reaction. Measurements were carried out on Cobas c502 and e801 automated clinical chemistry analysers respectively (Roche Diagnostics GmbH). The homeostatic model assessment (HOMA) for insulin resistance (HOMA2-IR), pancreatic beta cell function (HOMA2-%B) and insulin sensitivity (HOMA2-%S) were calculated using the correctly solved HOMA computer model with no linear solutions (https://www2.dtu.ox.ac.uk/homacalculator/;[15,80]). The product of systemic insulin and plasma triglyceride levels was used as an indirect marker for the adipose tissue insulin resistance index[16].

Plasma substrate analyses of inflammatory markers

Circulating inflammatory markers and cortisol were assessed in blood samples collected after 10 hours of overnight fasting. Plasma concentrations of interleukin (IL)-6, and serum concentrations of tumor necrosis factor (TNF)-α, C-reactive protein (CRP) and cortisol were determined in a local accredited laboratory, using standard methods. IL-6 was quantified with the Elecsys IL-6 immunoassay (IL-6 CalSet). C-reactive protein was measured on a Cobas 8000 analyser using the latex-enhanced immunoturbidimetry method (Cat#05172373 190, Roche Diagnostics).

Muscle biopsy

Skeletal muscle biopsies were taken from the vastus lateralis muscle using a rongeur (4-mm diameter) under sterile conditions and local anaesthesia with lidocaine, before bed rest, and after 6 and 55 days of bed rest. A subpart of the sample was mounted on cork with Tissue-Tek O.C.T. compound (Sakura, Torrance, CA, USA) oriented for transverse sectioning, quickly frozen in liquid nitrogen and stored at -80 °C until further use. Another part of the biopsy was stored in preservation solution for the assessment of mitochondrial respiration (see below), and one part in fixative (1.5 % potassium ferrocyanide) for electron microscopy (see below). Due to very low tissue availability, not all experiments could be performed on all participants.

Immunofluorescence microscopy

Ten µm sections were cut using a cryostat (Microm HM550; ThermoFisher Scientific) at -20 °C, collected on adhesive microscope slides, and stored at -80 °C until further processing.

Immunofluorescent staining

For 9 participants (6 men, 3 women, 36 ± 10 years; 172 ± 8 cm; 75 ± 7 kg) immunofluorescent staining for the glucose transporter type 4 (GLUT4) and the sarcolemma was performed for subsequent colocalization determination. Sections on slides were air-dried for 10 minutes. Sections were fixed in a solution of 75% acetone and 25% ethanol and washed in 1x phosphate-buffered saline (PBS) 3x5 min. GLUT4 Polyclonal Antibody (Thermo Fisher Scientific, Cat#PA5-23052) diluted 1:200 with 10% Normal Goat Serum (Life technologies, Cat#50062Z) was added to each slide except a negative control. The sections were incubated overnight at 4 °C in humid conditions. Sections were washed 3 x 5 min in PBS, and incubation of the secondary antibody (Thermo Fisher Scientific, Cat#A48282) diluted 1:200 in 10% NGS was performed in the dark for 60 min at room temperature. After washing in PBS, sections were incubated with Wheat Germ Agglutinin (Thermo Fisher Scientific, Cat#W32466; 1:25 in PBS) for 30 min at room temperature. After washing, VECTASHIELD Mounting Medium with DAPI (Vector Laboratories, Cat#H-1500-10) and a cover slip were added.

Confocal microscopy and image analysis

At least five images per section were taken using the ZEISS Axiovert 200M with fluorescent equipment (Carl Zeiss Microscopy, Jena, Germany) using the 40x dry objective. Background subtraction was performed based on a negative control. Images were deconvolved using Huygens Professional 22.4 (Scientific Volume Imaging, the Netherlands, using Classic MLE algorithm, Acuity 26.30, theoretical PSF, SNR 38.00, 94 iterations, Relative background +20). Each image was manually evaluated to exclude images containing artefacts, out of focus areas, (high) localized background and large areas with connective tissue.

GLUT4 translocation.

Deconvolved images were analysed in FIJI using the JACoP plugin to compute the Mander's colocalization coefficients between GLUT4 and the sarcolemma[18-82]. The mean of the Mander's overlap coefficient of every image was computed per time point for each participant.

Western blotting

Protein content was determined as previously described[83]. Tissue samples were emerged in RIPA lysis buffer (Sigma-Aldrich, Cat#R0278) containing protease and phosphate inhibitors (Roche, Cat#04693124001 and Cat#04906837001, respectively) with six stainless beads (2.4 mm; Omni International, Cat#19-640-3). Samples were homogenized using the Fisherbrand Bead Mill 4 homogenizer at speed 4 for 3x45 s three times, with 1 min on ice in between. After sonication, samples were centrifuged at 12000g for 10 min at 4 °C. The Pierce BCA Protein

Assay Kit (ThermoFisher Scientific, #23225, Waltham, MA, USA) was used to assess total protein concentration in collected supernatants through spectrophotometry (Epoch Biotek, Winooski, VT, USA). Approximately 10 µg of separated denatured proteins supplemented with sample buffer were loaded onto a precast polyacrylamide gel with a 4-20% gradient (Biorad, Cat#4561096) located in a Mini-PROTEAN Tetra electrophoresis cell (Biorad, Cat#1658004EDU). Gel electrophoresis was started off with 30 min at 50 V, followed by 90-120 min at 120 V and was run under frigid conditions. Subsequently, proteins were electrically transferred to a polyvinylidene fluoride membrane at 80 V for 60 min in blotting buffer using the Mini Trans-Blot cell (Biorad, Cat#1660827EDU). The membrane was washed with Tris-buffered saline, 0.1% Tween (TBS-T). To check for equal loading, membranes were incubated in No-Stain Protein Labelling Reagent (Thermo Fisher Scientific, Cat#A44717) for 10 minutes before blocking. Subsequently, the membrane was blocked with 2% blocking buffer made of ECL Prime Blocking agent (Amersham, Cat#RPN418) dissolved in TBS-T for 60 minutes at 4 °C. After addition of either GLUT4 Polyclonal Antibody (1:1000; Thermo Fisher Scientific, Cat#PA5-23052) or OxPhos Human WB Antibody Cocktail (1:1000; Thermo Fisher Scientific, Cat#45-8199), the membrane was incubated in blocking buffer overnight at 4 °C. The next day, the membrane was washed in TBS-T (3 x 5 min) and incubated with the appropriate horseradish peroxidase secondary antibody in blocking buffer (1:4000; Agilent Dako, Cat#P0448; Thermo Fisher Scientific, Cat#61-6520) for 60 min at room temperature. The membrane was washed in TBS-T again (3 x 5 min). ECL Select Western Blotting Detection Reagent (Amersham, Cat#RPN2235) was used to detect protein bands. The Sapphire Biomolecular Imager (Azure Bioxystems) recorded the chemiluminescent signal, and ImageJ software was used for performing quantification with intensities normalized to control.

Histochemistry

To identify glycogen accumulation, a Periodic acid–Schiff staining was performed as described before[84]. After 5 min of fixation in 3.7% paraformaldehyde, sections were incubated for 25 min in 1% periodic acid followed by 25 min incubation in Schiff's reagent. To stain for intramyocellular lipid accumulation, a Sudan Black B staining was performed[85]. Sections were fixed in 10% formalin for 5 min. Subsequently, sections were incubated in absolute propylene glycol for two times 5 min, after which sections were transferred to Sudan black (60 ºC) for 7 min. Sections were differentiated in 85% propylene glycol for 3 min.

Electron microscopy

Mitochondrial volume density and glycogen and lipid content were determined by electron microscopy as previously described, with minor adjustments[83]. Biopsies were fixed in 2.5% glutaraldehyde, and before embedding samples were washed, fixed in 1% osmium tetroxide and 1.5% kalium ferrocyanide for 1 h, washed, and dehydrated with ethanol 2x 70%, 80%, 90%, 2x 100% for 15 min. Samples were impregnated in epon : propylene oxide (1:1) for 1 h, then with epon for 30 min at 37 ºC. Subsequently, samples were put in a mold with epon and solidified for at least 2 days at 65 ºC. For electron microscopy, ultrathin 70-nm sections were picked up and placed on 150 mesh copper grids, and stained with uranyl acetate and lead citrate. Grids were imaged using an FEI Tecnai 120 kV transmission electron microscope (Thermo Fisher scientific, Waltman, Massachusetts, VS) with a Veleta camera. Images from the intramyofibrillar region (longitudinal to the fiber orientation only) were taken at magnifications ranging from 4500x to 30000x.

Electron microscopy images were scored for glycogen and intramyocellular lipid accumulation by four independent, blinded, raters. Five images per subject per timepoint were assessed for number and size of lipid droplets from 1 (none) to 5 (extremely high), and results averaged, first between raters, then per subject timepoint. Mitochondrial volume density was determined using ImageJ by outlining individual mitochondria, and the surface area measured. All surface areas of the mitochondria in one image were summed and expressed as a percentage of the total surface area. The average mitochondrial size was computed by dividing the total mitochondrial density by the mitochondrial number per image. All researchers were blinded to the participant characteristics and timepoint of the images during the analysis.

Metabolomics

Vastus lateralis biopsies and blood plasma were processed for metabolomics and lipidomics, as described before[86]. Muscle biopsies were freeze-dried and powdered to allow equal portioning. Water, methanol, and chloroform were added to the sample before thorough mixing and centrifugation for 10 min at 14,000 rpm. The top layer, containing the polar phase, was transferred to a new tube and dried using a vacuum concentrator at 60 °C. Dried samples were reconstituted in 100 µL methanol/water (6/4 vol/vol). Metabolites were analysed using a Waters Acquity ultra-high performance liquid chromatography system coupled to a Bruker Impact II Ultra-High Resolution Qq-Time-Of-Flight mass spectrometer. Samples were kept at 12 °C during analysis, and 5 µl of each sample was injected. Chromatographic separation was achieved using a Merck Millipore SeQuant ZIC-cHILIC column (polyetheretherketone 100 × 2.1 mm, 3 µm particle size). Column temperature was held at 30 °C. The mobile phase

consisted of (A) 1:9 acetonitrile : water and (B) 9:1 acetonitrile : water, both containing 5 mM ammonium acetate. Using a flow rate of 0.25 ml/min, the liquid chromatography gradient consisted of 100% B for 0–2 min, ramp to 0% B at 28 min, 0% B for 28–30 min, ramp to 100% B at 31 min, and 100% B for 31–35 min. Mass spectrometry data were acquired using negative and ionization in full scan mode over the range of m/z 50–1,200. Data were analysed using Bruker TASQ software version 2.1.22.3. All reported metabolites were normalized to the total amount of metabolites in each sample. Metabolite identification has been based on a combination of accurate mass, (relative) retention times, and fragmentation spectra, compared with the analysis of a library of standards.

Lipidomics

One mg of dry tissue was suspended in 300 µL water and sonicated on ice for 30 s at 8 W using a tip sonicator. Lipids were extracted using a single-phase methanol-chloroform extraction. Subsequently, the mixture was sonicated in a water bath for 5 min, followed by centrifugation at 4 ^{o}C (16.000g for 5 min). The liquid phase was transferred to a glass vial and evaporated under a stream of nitrogen at 60 ^{o}C. Subsequently, the residue was dissolved in 150 µL of chloroform/methanol (9:1, v/v), and 2 µL for normal phase and 5 µL for reverse phase separation of the solution were injected into the UPLC-HRMS system.

The UPLC system consisted of an Ultimate 3000 binary HPLC pump, a vacuum degasser, a column temperature controller, and an autosampler (Thermo Fisher Scientific, Waltham, MA, USA). For normal phase separation of lipids, 2 µL lipid extract was injected on a LiChroCART 250–4 LiChrospher Si 60 (5 µm; Merck) maintained at 25 °C. For lipid separation, a linear gradient consisting of solution A (methanol/water, 85:15, v/v) and solution B (chloroform/methanol, 97:3, v/v) was used. Solutions A and B contained 5 and 0.2 mL of 25% (v/v) aqueous ammonia per liter of eluent, respectively. The gradient (0.3 mL/min) was as follows: T = 0–1 min: 10%A; T = 1–4 min: 10%A–20%A; T = 4–12 min: 20%A–85%A; T = 12–12.1 min: 85%A–100%A; T = 12.1–14.0 min: 100%A; T = 14–14.1 min: 100%A–10%A; and T = 14.1–15 min: 10%A. For reverse-phase separation of lipids, 5 µL lipid extract was injected onto an ACQUITY UPLC HSS T3, 1.8 µm particle diameter (Waters) maintained at 60 °C. For lipid separation, a linear gradient consisting of solution A (methanol/water, 40:60, v/v) and solution B (methanol/isopropanol, 10:90, v/v) was used. Both solutions A and B contained 0.1% formic acid and 10 mM ammonia. The gradient (0.4 mL/min) was as follows: T = 0–1 min: 100%A; T = 1–16 min: 80%A; T = 16–20 min: 0%A; T = 20–20.1 min: 0%A; and T = 20.1–21.0 min: 100%A. A Q Exactive Plus Orbitrap Mass Spectrometer (Thermo

Fisher Scientific) was used in the negative and positive electrospray ionization modes. Nitrogen was used as the nebulizing gas. The spray voltage used was 2500 V, and the capillary temperature was 256 °C. S-lens RF level was 50; auxiliary gas, 11; auxiliary gas temperature, 300 °C, sheath gas, 48 au; and sweep cone gas, 2 au. Mass spectra of lipids were acquired in negative and positive scan modes by continuous scanning from m/z 150 to m/z 2000 with a resolution of 280,000 full width at half maximum (FWHM) and processed using an in-house developed metabolomics pipeline written in the R programming language (http://www.r-project.org). The identified peaks were normalized to the intensity of the internal standard for each lipid class. The concentration of each added internal was previously optimized for muscle tissue. Lipids with a relative abundance of less than 0.05 were excluded from further analyses.

Mitochondrial respiration

Mitochondrial respiration was measured in freshly isolated skeletal muscle fibres using high resolution respirometry as previously described[83,87]. Thin bundles of skeletal muscle fibres were permeabilized with 50 $\mu g \cdot mL^{-1}$ saponin for 30 min at 4 ºC in a solution consisting of (in mM) CaEGTA (2.8), EGTA (7.2), ATP (5.8), $MgCl_2$ (6.6), taurine (20), phosphocreatine (15), imidazole (20), DTT (0.5) and MES (50) (pH 7.1). Tissue was subsequently washed in respiration solution, containing EGTA (0.5), $MgCl_2$ (3), K-lactobionate (60), taurine (20), KH_2PO_4 (10), HEPES (20), sucrose (110) and 1 $g \cdot L^{-1}$ fatty acid free BSA (pH 7.1), blotted dry, weighed and transferred to a respirometer (Oxygraph-2k; Oroboros Instruments, Innsbruck, Austria) in respiration solution at 37 °C. The oxygen concentration was maintained above 300 µM throughout the experiment to avoid oxygen diffusion limitations.

Leak respiration was assessed after addition of sodium malate (0.5 mM) and sodium pyruvate (5 mM). NADH-linked respiration (via mitochondrial complex I) was measured after addition of 2.5 mM ADP, 10 µM cytochrome c, which accounted for possible outer-mitochondrial membrane damage and sodium glutamate (10 mM) to assess the additional effects of glutamine oxidation. Maximal oxidative phosphorylation capacity was measured after addition of 10 mM succinate. Maximal uncoupled respiration was measured after stepwise addition of 0.01 µM carbonylcyanide-4-(trifluoromethoxy)-phenylhydrazone (FCCP). Subsequently, succinate-linked respiration was measured after blocking complex I by 0.5 µM rotenone. Residual oxygen consumption was measured after addition of antimycin A (2.5 µM) and was subtracted from all values. Two measurements per sample were performed simultaneously and results averaged. Respiration values were normalized to wet weight and expressed in pmol $O_2 \cdot s^{-1} \cdot mg^{-1}$.

Mitochondrial supercomplexes by Blue Native Polyacrylamide Gel Electrophoresis

Mitochondrial supercomplexes were determined as previously described[87]. Mitochondrial proteins were isolated from 20-25 mg of vastus lateralis muscle tissue, and 50 µg of mitochondrial proteins were solubilized in cocktail buffer (Thermo Fisher Scientific, NativePAGE sample buffer, Cat#BN2003; 5 g digitonin per 1 g of protein, Novex life technologies, BN2006) and separated using 3 - 12% Bis-Tris gradient gel (Thermo Fisher Scientific, Cat#BN2012BX10). The BN-PAGE gel was soaked in NuPAGE transfer buffer (Life Technologies, Cat#NP0006-1), after which proteins were transferred onto a polyvinylidene fluoride membrane (Amersham Hybond, Cat#10600029, GE Healthcare) using a wet transfer blotting tank (Bio-Rad) at 100 V for 60 min. Mitochondrial supercomplexes containing subunits of mitochondrial complex I were detected using an antibody directed against NDUFA9 (Thermo Fisher Scientific, Cat#459100) and subsequent incubation with a secondary horseradish peroxidase-labelled antibody rabbit anti-mouse IgG (H+L; Thermo Fisher Scientific, Cat#61-6520). Subsequently, an antibody cocktail against subunits of all mitochondrial complexes (OxPhos Human WB antibody cocktail, Invitrogen, Cat#45-8199) was used to visualize all mitochondrial complexes. Images were taken using an enhanced chemiluminescence detection kit (Amersham, Cat#RPN2235) and scanning with ImageQuant™ LAS 500 (GE Healthcare Bio-Sciences AB). Supercomplex abundance was assessed through densitometric analysis of all bands with a molecular weight >1000 kDa. Supercomplex abundance was subsequently also expressed relative to free complexes I to IV by normalisation to total supercomplex together with complex I to IV content. No-Stain Protein Labeling Reagent (Thermo Fisher Scientific, Cat#A44717) was used to check for equal loading.

Statistical analysis

Statistical analyses were performed using GraphPad Prism 10.0.2 for macOS (GraphPad Software, Boston, Massachusetts USA, www.graphpad.com) or R studio built under R version 4.2.2 (R Core Team 2022, Vienna, Austria, www.r-project.org). Datasets were tested for normality and in case of violation non-parametric testing or log-transformation was performed. In case of normal distribution, differences between groups were assessed with a repeated-measures (RM) ANOVA, or a mixed-effects model in case of missing values, with post hoc Bonferroni's or Tukey's corrections. Due to tissue scarcity, sample size varied per experiment with specifications given in corresponding figure legends. Statistical analyses were considered significant if $p \leq 0.05$. All data are presented as mean ± SEM unless stated otherwise.

Additional Resources

Clinical trial details for AGBRESA: https://drks.de/search/en/trial/DRKS00015677, and Clément et al. Front Physiol. 2022 (reference 11 herein).

References

1. Booth, F.W., Roberts, C.K., Thyfault, J.P., Ruegsegger, G.N., Toedebusch, R.G., 2017. Role of Inactivity in Chronic Diseases: Evolutionary Insight and Pathophysiological Mechanisms. Physiol Rev 97(4):1351-1402.
2. Hyatt, H.W., Powers, S.K., 2021. Mitochondrial Dysfunction Is a Common Denominator Linking Skeletal Muscle Wasting Due to Disease, Aging, and Prolonged Inactivity. Antioxidants (Basel) 10(4):588.
3. Smith, R.L., Soeters, M.R., Wüst, R.C.I., Houtkooper, R.H., 2018. Metabolic Flexibility as an Adaptation to Energy Resources and Requirements in Health and Disease. Endocr Rev 39(4):489-517.
4. Sylow, L., Tokarz, V.L., Richter, E.A., Klip, A., 2021. The many actions of insulin in skeletal muscle, the paramount tissue determining glycemia. Cell Metab 33(4):758-780.
5. Rudwill, F., O'Gorman, D., Lefai, E., Chery, I., Zahariev, A., Normand, S., et al., 2018. Metabolic Inflexibility Is an Early Marker of Bed-Rest-Induced Glucose Intolerance Even When Fat Mass Is Stable. J Clin Endocrinol Metab 103(5):1910-1920.
6. Genders, A.J., Holloway, G.P., Bishop, D.J., 2020. Are Alterations in Skeletal Muscle Mitochondria a Cause or Consequence of Insulin Resistance? Int J Mol Sci 21(18).
7. Makrecka-Kuka, M., Liepinsh, E., Murray, A.J., Lemieux, H., Dambrova, M., Tepp, K., et al., 2020. Altered mitochondrial metabolism in the insulin-resistant heart. Acta Physiol (Oxf) 228(3):e13430.
8. Picard, M., Jung, B., Liang, F., Azuelos, I., Hussain, S., Goldberg, P., et al., 2012. Mitochondrial dysfunction and lipid accumulation in the human diaphragm during mechanical ventilation. Am J Respir Crit Care Med 186(11):1140-1149.
9. Mulavara, A.P., Peters, B.T., Miller, C.A., Kofman, I.S., Reschke, M.F., Taylor, L.C., et al., 2018. Physiological and Functional Alterations after Spaceflight and Bed Rest. Med Sci Sports Exerc 50(9):1961-1980.

10. Blottner, D., Moriggi, M., Trautmann, G., Hastermann, M., Capitanio, D., Torretta, E., et al., 2023. Space Omics and Tissue Response in Astronaut Skeletal Muscle after Short and Long Duration Missions. Int J Mol Sci 24(4).

11. Clement, G., Rittweger, J., Nitsche, A., Doering, W., Frings-Meuthen, P., Hand, O., et al., 2022. Assessing the effects of artificial gravity in an analog of long-duration spaceflight: The protocol and implementation of the AGBRESA bed rest study. Front Physiol 13:976926.

12. Hendrickse, P.W., Wust, R.C.I., Ganse, B., Giakoumaki, I., Rittweger, J., Bosutti, A., et al., 2022. Capillary rarefaction during bed rest is proportionally less than fibre atrophy and loss of oxidative capacity. J Cachexia Sarcopenia Muscle 13(6):2712-2723.

13. Hoffmann, F., Rabineau, J., Mehrkens, D., Gerlach, D.A., Moestl, S., Johannes, B.W., et al., 2021. Cardiac adaptations to 60 day head-down-tilt bed rest deconditioning. Findings from the AGBRESA study. ESC Heart Fail 8(1):729-744.

14. De Martino, E., Hides, J., Elliott, J.M., Hoggarth, M.A., Zange, J., Lindsay, K., et al., 2022. Intramuscular lipid concentration increased in localized regions of the lumbar muscles following 60 day bedrest. Spine J 22(4):616-628.

15. Wallace, T.M., Levy, J.C., Matthews, D.R., 2004. Use and abuse of HOMA modeling. Diabetes Care 27(6):1487-1495.

16. Sondergaard, E., Espinosa De Ycaza, A.E., Morgan-Bathke, M., Jensen, M.D., 2017. How to Measure Adipose Tissue Insulin Sensitivity. J Clin Endocrinol Metab 102(4):1193-1199.

17. Huang, S., Czech, M.P., 2007. The GLUT4 glucose transporter. Cell Metab 5(4):237-252.

18. Bradley, H., Shaw, C.S., Bendtsen, C., Worthington, P.L., Wilson, O.J., Strauss, J.A., et al., 2015. Visualization and quantitation of GLUT4 translocation in human skeletal muscle following glucose ingestion and exercise. Physiol Rep 3(5).

19. Lundsgaard, A.M., Fritzen, A.M., Kiens, B., 2018. Molecular Regulation of Fatty Acid Oxidation in Skeletal Muscle during Aerobic Exercise. Trends Endocrinol Metab 29(1):18-30.

20. Bandet, C.L., Tan-Chen, S., Bourron, O., Le Stunff, H., Hajduch, E., 2019. Sphingolipid Metabolism: New Insight into Ceramide-Induced Lipotoxicity in Muscle Cells. Int J Mol Sci 20(3).

21. Samuel, V.T., Petersen, K.F., Shulman, G.I., 2010. Lipid-induced insulin resistance: unravelling the mechanism. Lancet 375(9733):2267-2277.

22. Wang, T.J., Ngo, D., Psychogios, N., Dejam, A., Larson, M.G., Vasan, R.S., et al., 2013. 2-Aminoadipic acid is a biomarker for diabetes risk. J Clin Invest 123(10):4309-4317.

23. Soga, T., Baran, R., Suematsu, M., Ueno, Y., Ikeda, S., Sakurakawa, T., et al., 2006. Differential metabolomics reveals ophthalmic acid as an oxidative stress biomarker indicating hepatic glutathione consumption. J Biol Chem 281(24):16768-16776.

24. Beloborodova, N., Bairamov, I., Olenin, A., Shubina, V., Teplova, V., Fedotcheva, N., 2012. Effect of phenolic acids of microbial origin on production of reactive oxygen species in mitochondria and neutrophils. J Biomed Sci 19(1):89.

25. Tan, J.K., Zakaria, S.N.A., Gunasekaran, G., Abdul Sani, N.F., Nasaruddin, M.L., Jaafar, F., et al., 2023. Metabolomics Profiling of Age-Associated Metabolites in Malay Population. Oxid Med Cell Longev 2023:4416410.

26. Schrauwen, P., Hesselink, M.K., 2004. Oxidative capacity, lipotoxicity, and mitochondrial damage in type 2 diabetes. Diabetes 53(6):1412-1417.

27. Lapuente-Brun, E., Moreno-Loshuertos, R., Acin-Perez, R., Latorre-Pellicer, A., Colas, C., Balsa, E., et al., 2013. Supercomplex assembly determines electron flux in the mitochondrial electron transport chain. Science 340(6140):1567-1570.

28. Acin-Perez, R., Enriquez, J.A., 2014. The function of the respiratory supercomplexes: the plasticity model. Biochim Biophys Acta 1837(4):444-450.

29. Greggio, C., Jha, P., Kulkarni, S.S., Lagarrigue, S., Broskey, N.T., Boutant, M., et al., 2017. Enhanced Respiratory Chain Supercomplex Formation in Response to Exercise in Human Skeletal Muscle. Cell Metab 25(2):301-311.

30. Bergouignan, A., Momken, I., Schoeller, D.A., Normand, S., Zahariev, A., Lescure, B., et al., 2010. Regulation of energy balance during long-term physical inactivity induced by bed rest with and without exercise training. J Clin Endocrinol Metab 95(3):1045-1053.

31. Trim, W.V., Walhin, J.P., Koumanov, F., Turner, J.E., Shur, N.F., Simpson, E.J., et al., 2023. The impact of physical inactivity on glucose homeostasis when diet is adjusted to maintain energy balance in healthy, young males. Clin Nutr 42(4):532-540.

32. Tran, V., De Martino, E., Hides, J., Cable, G., Elliott, J.M., Hoggarth, M., et al., 2021. Gluteal Muscle Atrophy and Increased Intramuscular Lipid Concentration Are Not Mitigated by Daily Artificial Gravity Following 60-Day Head-Down Tilt Bed Rest. Front Physiol 12:745811.

33. Goodpaster, B.H., Bergman, B.C., Brennan, A.M., Sparks, L.M., 2023. Intermuscular adipose tissue in metabolic disease. Nat Rev Endocrinol 19(5):285-298.

34. Pagano, A.F., Brioche, T., Arc-Chagnaud, C., Demangel, R., Chopard, A., Py, G., 2018. Short-term disuse promotes fatty acid infiltration into skeletal muscle. J Cachexia Sarcopenia Muscle 9(2):335-347.

35. Daemen, S., Gemmink, A., Brouwers, B., Meex, R.C.R., Huntjens, P.R., Schaart, G., et al., 2018. Distinct lipid droplet characteristics and distribution unmask the apparent contradiction of the athlete's paradox. Mol Metab 17:71-81.

36. Goodpaster, B.H., Theriault, R., Watkins, S.C., Kelley, D.E., 2000. Intramuscular lipid content is increased in obesity and decreased by weight loss. Metabolism 49(4):467-472.

37. Koves, T.R., Ussher, J.R., Noland, R.C., Slentz, D., Mosedale, M., Ilkayeva, O., et al., 2008. Mitochondrial overload and incomplete fatty acid oxidation contribute to skeletal muscle insulin resistance. Cell Metab 7(1):45-56.

38. Summermatter, S., Baum, O., Santos, G., Hoppeler, H., Handschin, C., 2010. Peroxisome proliferator-activated receptor gamma coactivator 1alpha (PGC-1alpha) promotes skeletal muscle lipid refueling in vivo by activating de novo lipogenesis and the pentose phosphate pathway. J Biol Chem 285(43):32793-32800.

39. Bonen, A., Jain, S.S., Snook, L.A., Han, X.X., Yoshida, Y., Buddo, K.H., et al., 2015. Extremely rapid increase in fatty acid transport and intramyocellular lipid accumulation but markedly delayed insulin resistance after high fat feeding in rats. Diabetologia 58(10):2381-2391.

40. Aas, V., Kase, E.T., Solberg, R., Jensen, J., Rustan, A.C., 2004. Chronic hyperglycaemia promotes lipogenesis and triacylglycerol accumulation in human skeletal muscle cells. Diabetologia 47(8):1452-1461.

41. Watt, M.J., Hoy, A.J., 2012. Lipid metabolism in skeletal muscle: generation of adaptive and maladaptive intracellular signals for cellular function. Am J Physiol Endocrinol Metab 302(11):E1315-1328.

42. Bandyopadhyay, G.K., Yu, J.G., Ofrecio, J., Olefsky, J.M., 2006. Increased malonyl-CoA levels in muscle from obese and type 2 diabetic subjects lead to decreased fatty acid oxidation and increased lipogenesis; thiazolidinedione treatment reverses these defects. Diabetes 55(8):2277-2285.

43. Pan, D.A., Lillioja, S., Kriketos, A.D., Milner, M.R., Baur, L.A., Bogardus, C., et al., 1997. Skeletal muscle triglyceride levels are inversely related to insulin action. Diabetes 46(6):983-988.

44. Weber-Carstens, S., Deja, M., Koch, S., Spranger, J., Bubser, F., Wernecke, K.D., et al., 2010. Risk factors in critical illness myopathy during the early course of critical illness: a prospective observational study. Crit Care 14(3):R119.

45. Flores-Opazo, M., McGee, S.L., Hargreaves, M., 2020. Exercise and GLUT4. Exerc Sport Sci Rev 48(3):110-118.

46. Henriquez-Olguin, C., Knudsen, J.R., Raun, S.H., Li, Z., Dalbram, E., Treebak, J.T., et al., 2019. Cytosolic ROS production by NADPH oxidase 2 regulates muscle glucose uptake during exercise. Nat Commun 10(1):4623.

47. Holloszy, J.O., 2008. Regulation by exercise of skeletal muscle content of mitochondria and GLUT4. J Physiol Pharmacol 59 Suppl 7:5-18.

48. Holloszy, J.O., 2005. Exercise-induced increase in muscle insulin sensitivity. J Appl Physiol (1985) 99(1):338-343.

49. Hansen, P.A., Nolte, L.A., Chen, M.M., Holloszy, J.O., 1998. Increased GLUT-4 translocation mediates enhanced insulin sensitivity of muscle glucose transport after exercise. J Appl Physiol (1985) 85(4):1218-1222.

50. Derave, W., Lund, S., Holman, G.D., Wojtaszewski, J., Pedersen, O., Richter, E.A., 1999. Contraction-stimulated muscle glucose transport and GLUT-4 surface content are dependent on glycogen content. Am J Physiol 277(6):E1103-1110.

51. Philp, A., Hargreaves, M., Baar, K., 2012. More than a store: regulatory roles for glycogen in skeletal muscle adaptation to exercise. Am J Physiol Endocrinol Metab 302(11):E1343-1351.

52. Lambert, M., Claeyssen, C., Bastide, B., Cieniewski-Bernard, C., 2020. O-GlcNAcylation as a regulator of the functional and structural properties of the sarcomere in skeletal muscle: An update review. Acta Physiol (Oxf) 228(1):e13301.

53. Butkinaree, C., Park, K., Hart, G.W., 2010. O-linked beta-N-acetylglucosamine (O-GlcNAc): Extensive crosstalk with phosphorylation to regulate signaling and transcription in response to nutrients and stress. Biochim Biophys Acta 1800(2):96-106.

54. Salvadego, D., Keramidas, M.E., Brocca, L., Domenis, R., Mavelli, I., Rittweger, J., et al., 2016. Separate and combined effects of a 10-d exposure to hypoxia and inactivity on oxidative function in vivo and mitochondrial respiration ex vivo in humans. J Appl Physiol (1985) 121(1):154-163.

55. Edwards, S.J., Smeuninx, B., McKendry, J., Nishimura, Y., Luo, D., Marshall, R.N., et al., 2020. High-dose leucine supplementation does not prevent muscle atrophy or strength loss over 7 days of immobilization in healthy young males. Am J Clin Nutr 112(5):1368-1381.

56. Bosutti, A., Salanova, M., Blottner, D., Buehlmeier, J., Mulder, E., Rittweger, J., et al., 2016. Whey protein with potassium bicarbonate supplement attenuates the reduction in muscle oxidative capacity during 19 days of bed rest. J Appl Physiol (1985) 121(4):838-848.

57. Kenny, H.C., Rudwill, F., Breen, L., Salanova, M., Blottner, D., Heise, T., et al., 2017. Bed rest and resistive vibration exercise unveil novel links between skeletal muscle mitochondrial function and insulin resistance. Diabetologia 60(8):1491-1501.

58. Salvadego, D., Keramidas, M.E., Kolegard, R., Brocca, L., Lazzer, S., Mavelli, I., et al., 2018. PlanHab(*) : hypoxia does not worsen the impairment of skeletal muscle oxidative function induced by bed rest alone. J Physiol 596(15):3341-3355.

59. Buso, A., Comelli, M., Picco, R., Isola, M., Magnesa, B., Pisot, R., et al., 2019. Mitochondrial Adaptations in Elderly and Young Men Skeletal Muscle Following 2 Weeks of Bed Rest and Rehabilitation. Front Physiol 10:474.

60. Dirks, M.L., Wall, B.T., van de Valk, B., Holloway, T.M., Holloway, G.P., Chabowski, A., et al., 2016. One Week of Bed Rest Leads to Substantial Muscle Atrophy and Induces Whole-Body Insulin Resistance in the Absence of Skeletal Muscle Lipid Accumulation. Diabetes 65(10):2862-2875.

61. Standley, R.A., Distefano, G., Trevino, M.B., Chen, E., Narain, N.R., Greenwood, B., et al., 2020. Skeletal Muscle Energetics and Mitochondrial Function Are Impaired Following 10 Days of Bed Rest in Older Adults. J Gerontol A Biol Sci Med Sci 75(9):1744-1753.

62. Dirks, M.L., Miotto, P.M., Goossens, G.H., Senden, J.M., Petrick, H.L., van Kranenburg, J., et al., 2020. Short-term bed rest-induced insulin resistance cannot be explained by increased mitochondrial H(2) O(2) emission. J Physiol 598(1):123-137.

63. Larsen, S., Lundby, A.M., Dandanell, S., Oberholzer, L., Keiser, S., Andersen, A.B., et al., 2018. Four days of bed rest increases intrinsic mitochondrial respiratory capacity in young healthy males. Physiol Rep 6(18):e13793.

64. Zuccarelli, L., Baldassarre, G., Magnesa, B., Degano, C., Comelli, M., Gasparini, M., et al., 2021. Peripheral impairments of oxidative metabolism after a 10-day bed rest are upstream of mitochondrial respiration. J Physiol 599(21):4813-4829.

65. Murgia, M., Ciciliot, S., Nagaraj, N., Reggiani, C., Schiaffino, S., Franchi, M.V., et al., 2022. Signatures of muscle disuse in spaceflight and bed rest revealed by single muscle fiber proteomics. PNAS Nexus 1(3):pgac086.

66. Boardman, N.T., Trani, G., Scalabrin, M., Romanello, V., Wust, R.C.I., 2023. Intra-cellular to inter-organ mitochondrial communication in striated muscle in health and disease. Endocr Rev.

67. Favaro, G., Romanello, V., Varanita, T., Andrea Desbats, M., Morbidoni, V., Tezze, C., et al., 2019. DRP1-mediated mitochondrial shape controls calcium homeostasis and muscle mass. Nat Commun 10(1):2576.

68. Granata, C., Caruana, N.J., Botella, J., Jamnick, N.A., Huynh, K., Kuang, J., et al., 2021. High-intensity training induces non-stoichiometric changes in the mitochondrial proteome of human skeletal muscle without reorganisation of respiratory chain content. Nat Commun 12(1):7056.

69. Schrauwen, P., Schrauwen-Hinderling, V., Hoeks, J., Hesselink, M.K., 2010. Mitochondrial dysfunction and lipotoxicity. Biochim Biophys Acta 1801(3):266-271.

70. Page, A., Peeters, G., Merom, D., 2015. Adjustment for physical activity in studies of sedentary behaviour. Emerg Themes Epidemiol 12:10.

71. Raichlen, D.A., Pontzer, H., Zderic, T.W., Harris, J.A., Mabulla, A.Z.P., Hamilton, M.T., et al., 2020. Sitting, squatting, and the evolutionary biology of human inactivity. Proc Natl Acad Sci U S A 117(13):7115-7121.

72. Weijs, P.J., Looijaard, W.G., Beishuizen, A., Girbes, A.R., Oudemans-van Straaten, H.M., 2014. Early high protein intake is associated with low mortality and energy overfeeding

with high mortality in non-septic mechanically ventilated critically ill patients. Crit Care 18(6):701.

73. Zaloga, G.P., Willey, S., Tomasic, P., Chernow, B., 1987. Free fatty acids alter calcium binding: a cause for misinterpretation of serum calcium values and hypocalcemia in critical illness. J Clin Endocrinol Metab 64(5):1010-1014.

74. Casaer, M.P., Mesotten, D., Hermans, G., Wouters, P.J., Schetz, M., Meyfroidt, G., et al., 2011. Early versus late parenteral nutrition in critically ill adults. N Engl J Med 365(6):506-517.

75. Viscomi, C., Bottani, E., Civiletto, G., Cerutti, R., Moggio, M., Fagiolari, G., et al., 2011. In vivo correction of COX deficiency by activation of the AMPK/PGC-1alpha axis. Cell Metab 14(1):80-90.

76. Mirzoev, T.M., Paramonova, II, Rozhkov, S.V., Kalashnikova, E.P., Belova, S.P., Tyganov, S.A., et al., 2023. Metformin Pre-Treatment as a Means of Mitigating Disuse-Induced Rat Soleus Muscle Wasting. Curr Issues Mol Biol 45(4):3068-3086.

77. Gomez, H., Del Rio-Pertuz, G., Priyanka, P., Manrique-Caballero, C.L., Chang, C.H., Wang, S., et al., 2022. Association of Metformin Use During Hospitalization and Mortality in Critically Ill Adults With Type 2 Diabetes Mellitus and Sepsis. Crit Care Med 50(6):935-944.

78. Schneider, C.A., Rasband, W.S., Eliceiri, K.W., 2012. NIH Image to ImageJ: 25 years of image analysis. Nat Methods 9(7):671-675.

79. Schindelin, J., Arganda-Carreras, I., Frise, E., Kaynig, V., Longair, M., Pietzsch, T., et al., 2012. Fiji: an open-source platform for biological-image analysis. Nat Methods 9(7):676-682.

80. Levy, J.C., Matthews, D.R., Hermans, M.P., 1998. Correct homeostasis model assessment (HOMA) evaluation uses the computer program. Diabetes Care 21(12):2191-2192.

81. Mank, E., Naninck, E.F.G., van den Akker, C.H.P., Heijboer, A.C., 2021. Rapid quantification of insulin in human milk by immunoassay. Eur J Clin Nutr 75(7):1152-1154.

82. Dunn, K.W., Kamocka, M.M., McDonald, J.H., 2011. A practical guide to evaluating colocalization in biological microscopy. Am J Physiol Cell Physiol 300(4):C723-742.

83. Wüst, R.C.I., de Vries, H.J., Wintjes, L.T., Rodenburg, R.J., Niessen, H.W., Stienen, G.J., 2016. Mitochondrial complex I dysfunction and altered NAD(P)H kinetics in rat myocardium in cardiac right ventricular hypertrophy and failure. Cardiovasc Res 111(4):362-372.

84. Vollestad, N.K., Vaage, O., Hermansen, L., 1984. Muscle glycogen depletion patterns in type I and subgroups of type II fibres during prolonged severe exercise in man. Acta Physiol Scand 122(4):433-441.

85. Messa, G.A.M., Piasecki, M., Hurst, J., Hill, C., Tallis, J., Degens, H., 2020. The impact of a high-fat diet in mice is dependent on duration and age, and differs between muscles. J Exp Biol 223(Pt 6).

86. Schomakers, B.V., Hermans, J., Jaspers, Y.R.J., Salomons, G., Vaz, F.M., van Weeghel, M., et al., 2022. Polar metabolomics in human muscle biopsies using a liquid-liquid extraction and full-scan LC-MS. STAR Protoc 3(2):101302.

87. Nollet, E.E., Duursma, I., Rozenbaum, A., Eggelbusch, M., Wust, R.C.I., Schoonvelde, S.A.C., et al., 2023. Mitochondrial dysfunction in human hypertrophic cardiomyopathy is linked to cardiomyocyte architecture disruption and corrected by improving NADH-driven mitochondrial respiration. Eur Heart J 44(13):1170-1185.

Supplementary information

Table S1. Effect of antigravitation intervention on outcome measures. Related to STAR Methods participant recruitment, Figures 1 and 5. The continuous or intermittent anti-gravitational interventions (cAG, 30 minutes daily and iAG, 6x5 minutes daily) did not mitigate the bed rest-induced alterations in HOMA2-IR scores, or oxidative phosphorylation (OXPHOS) capacity of the skeletal muscle. All data were analyzed by repeated measures ANOVA, mixed-effects model with Tukey's post hoc test, n=24 for each parameter. HOMA2-IR: homeostatic model assessment (HOMA) for insulin resistance.

HOMA2-IR

	Control	cAG (30')	iAG (6x5')	Total	*p*
Day 0	0.64 ± 0.15	0.52 ± 0.10	0.53 ± 0.22	0.56 ± 0.07	0.52
Day 6	1.04 ± 0.32	0.76 ± 0.13	0.66 ± 0.23	0.82 ± 0.20	0.13
Day 55	0.99 ± 0.43	0.80 ± 0.13	0.65 ± 0.22	0.81 ± 0.17	0.35

OXPHOS capacity

	Control	cAG (30')	iAG (6x5')	Total	*p*
Day 0	81 ± 15	75 ± 19	69 ± 22	75 ± 6	0.47
Day 6	80 ± 21	66 ± 12	65 ± 13	70 ± 9	0.12
Day 55	58 ± 8	64 ± 16	49 ± 10	57 ± 8	0.11

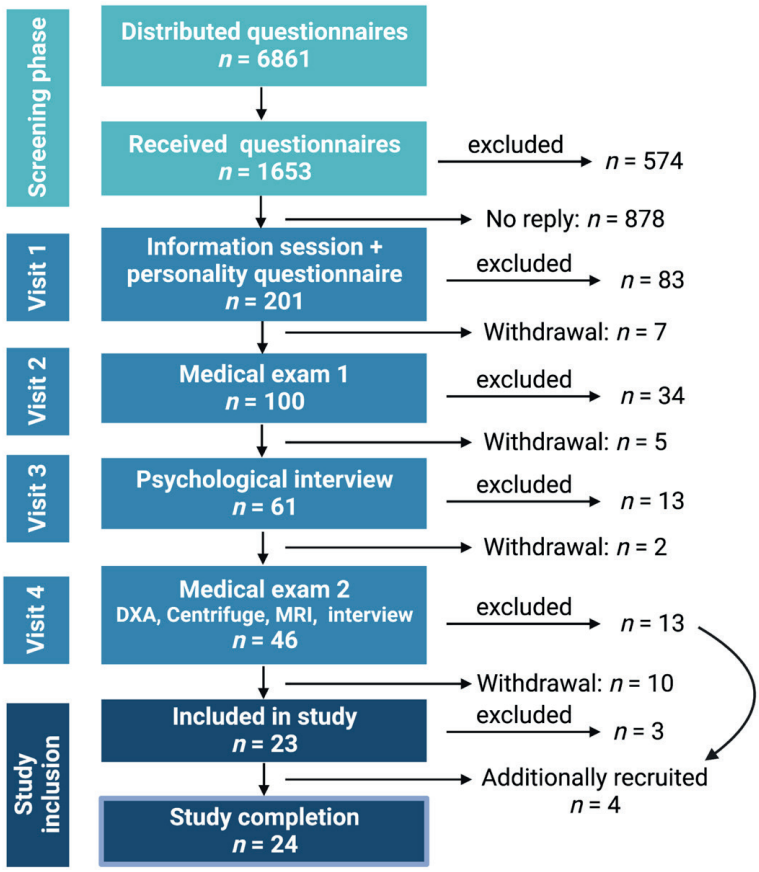


Figure S1. Participant screening process. Related to STAR Methods participant recruitment. Out of 6861 distributed questionnaires, 1653 potential participants received further information, and 201 people joined an on-site visit and assessment at the German Aerospace Centre. Three subsequent on-site visits included more rigorous assessments, and 23 healthy participants were initially included in the study. Three participants were excluded and replaced by four participants on the reserve list.

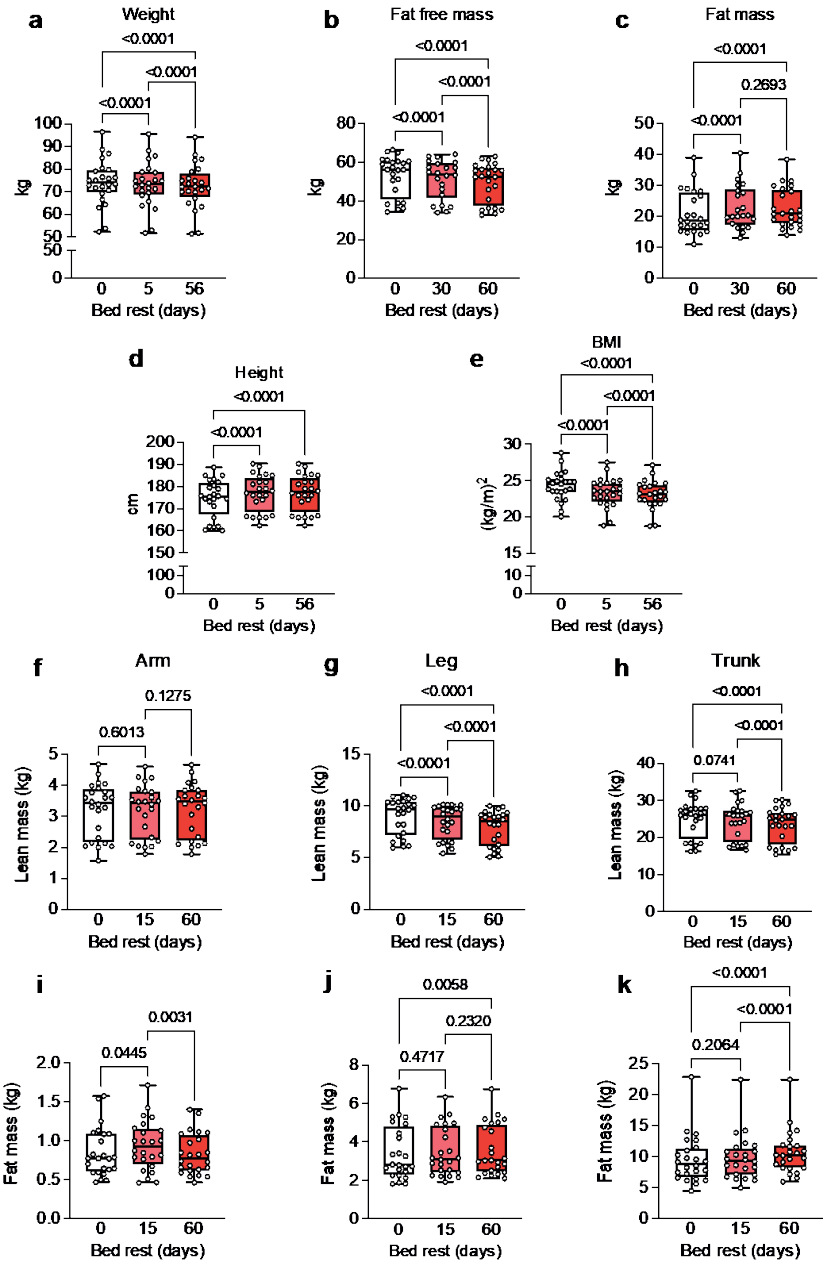


Figure S2. Bed rest decreases BMI, but increases trunk and leg body fat. Related to Figure 1. **a-d:** Participant body weight (**a**) and fat free mass (**b**) decreased throughout the bed rest. While fat mass progressively increased (**c**), and height increased (**d**), body mass index (**e**) decreased during bed rest. **f-g:** Arm lean mass remained unchanged throughout the bed rest (**f**), whereas leg (**g**) and trunk lean mass (**h**) decreased progressively throughout the bed rest. Arm fat mass (**i**) transiently increased after 15 days, but decreased to pre-

bed rest values after 60 days. Leg (**j**) and trunk fat mass (**k**) increased following 60 days of bed rest. Analysis with repeated measures ANOVA, with Tukey's post hoc test, *n*=24.

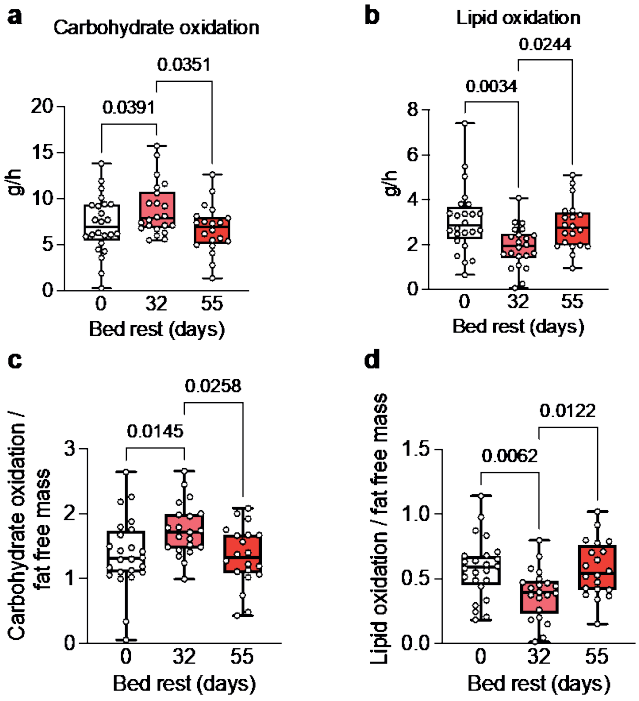


Figure S3. Bed rest alters fasted resting substrate oxidation. Related to Figure 1. a-b: Resting carbohydrate oxidation in the fasted state (**a**) increased after 32 days of bed rest, while lipid oxidation transiently decreased (**b**), and reduced to pre-bed rest values after 55 days. **c-d:** Time courses of substrate oxidation were similar after normalization for fat free mass. Analysis with repeated measures ANOVA, with Tukey's post hoc test, *n*=24.

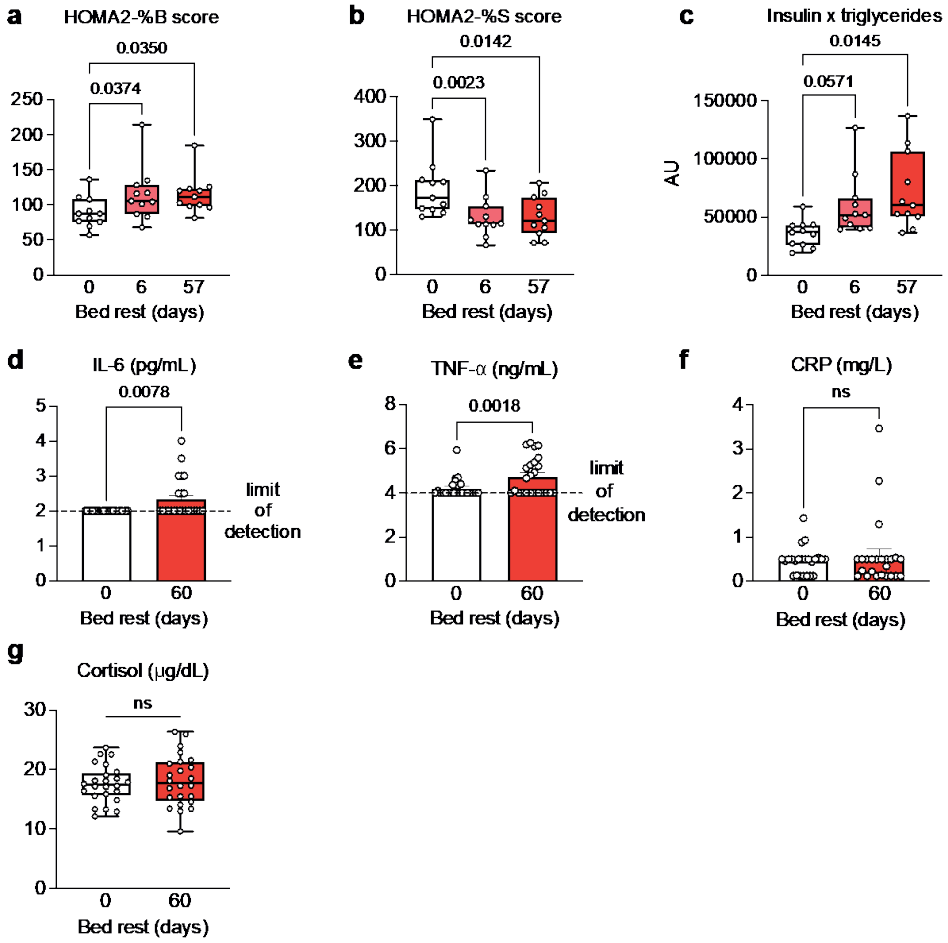


Figure S4. Bed rest acutely impairs insulin sensitivity and increases circulating pro-inflammatory cytokines after long-term bed rest while stress levels remain unchanged. Related to Figure 1. **a:** HOMA2-%B, indicative of pancreatic β-cell function, increased after short-term and long-term bed rest. **b:** HOMA2-%S reduced after short- and long-term bed rest, indicative of a reduced insulin sensitivity. **c**: The product of systemic insulin and plasma triglyceride levels as an indirect marker for adipose tissue insulin resistance (adipo-IR) increased after bed rest. **d-g:** Inflammatory markers IL-6 (**d**) and TNF-**α** (**e**) increased significantly after long-term bed rest, whilst C-reactive protein (**f**) and cortisol levels (**g**) remained unchanged. Analysis with repeated measures ANOVA, with Tukey's post hoc test, *n*=12 for panel a-c, Wilcoxon matched-pairs rank test for panel d-f, paired *t*-test for panel g, *n*=24 for stress and inflammation markers.

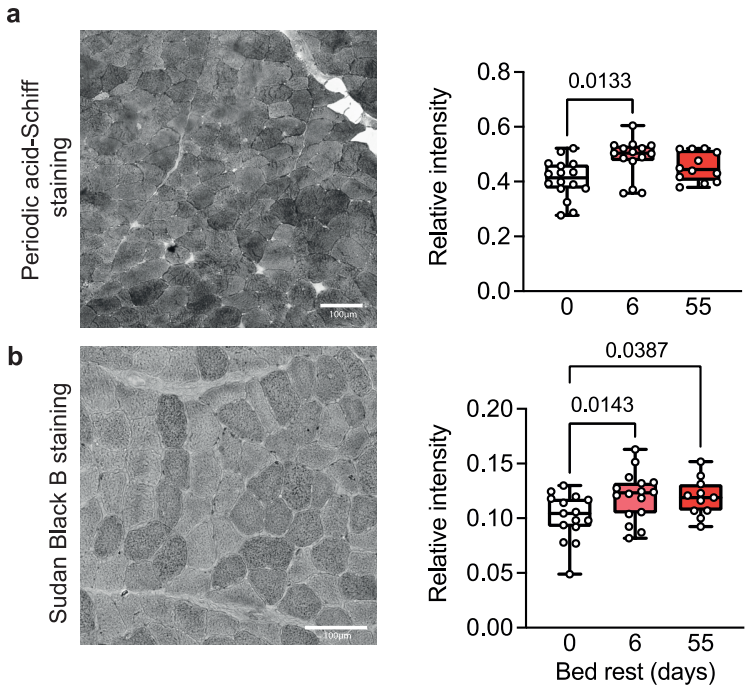


Figure S5. Bed rest-induced nutrient overload. Related to Figure 2. a: Typical example and relative optical densities of a Periodic acid-Schiff (PAS) staining, performed in muscle sections to measure glycogen concentrations according to staining intensity, showed increased glycogen accumulation after short-term bed rest. **b**: A Sudan Black B staining was performed to study intra- and extracellular lipid accumulation after short- and long-term bed rest. Intracellular lipid accumulation increased after bed rest, but no signs of extracellular lipid accumulation (intermuscular adipose tissue) were observed. PAS data were analysed by Kruskal-Wallis test, with Dunn's post-hoc test, as data were not normally distributed, *n*=12-16. Due to missing values, Sudan Black B data were analysed with a one-way ANOVA with Fisher's LSD, *n*=11-16. Scale bar=100µm.

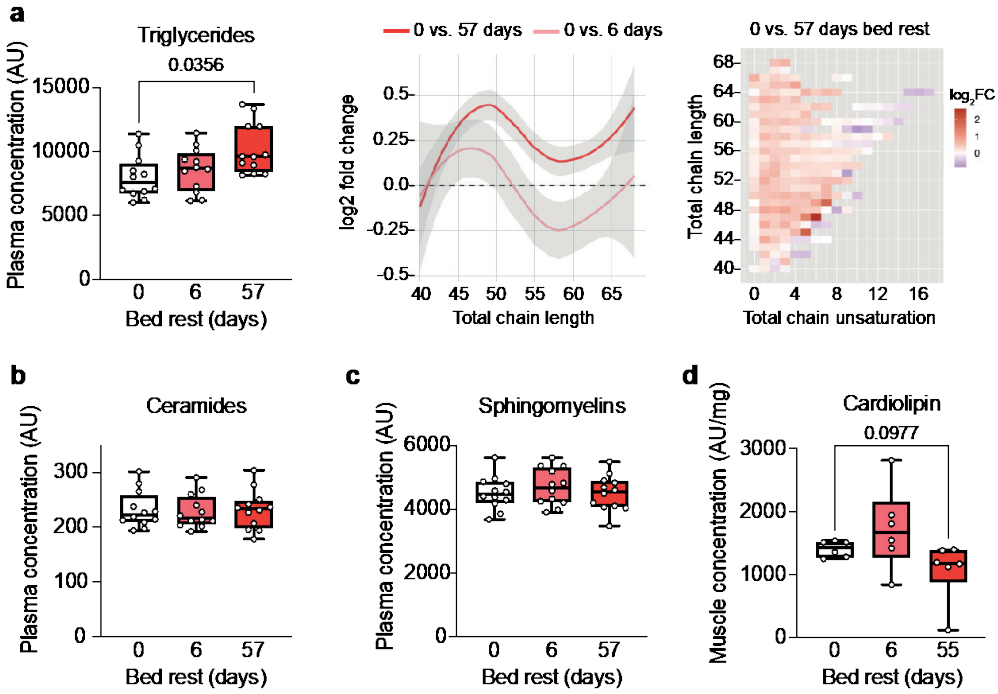


Figure S6. Blood lipidomics show few changes with short- and long-term bed rest. Related to Figure 3. Mass-spectrometry based lipidomics analysis using blood plasma collected throughout the bed rest. Out of 1402 identified lipid species, 243 were significantly altered after short- (95 downregulated) and 160 lipids changed significantly (64 downregulated) after long-term bed rest. **a:** Plasma triglyceride concentrations increased significantly after long-term bed rest, at all chain lengths, particularly at low chain unsaturations**.** Blood plasma ceramide (**b**) and sphingomyelin (**c**) concentrations did not change throughout the bed rest period. No differences were observed in other lipid classes in the blood plasma. Cardiolipin concentration in the skeletal muscle tended to be lower after long-term bed rest (**d**). Concentrations were analysed using repeated measures ANOVA, with Tukey's post hoc test, *n*=12 for plasma, *n*=6 for muscle.

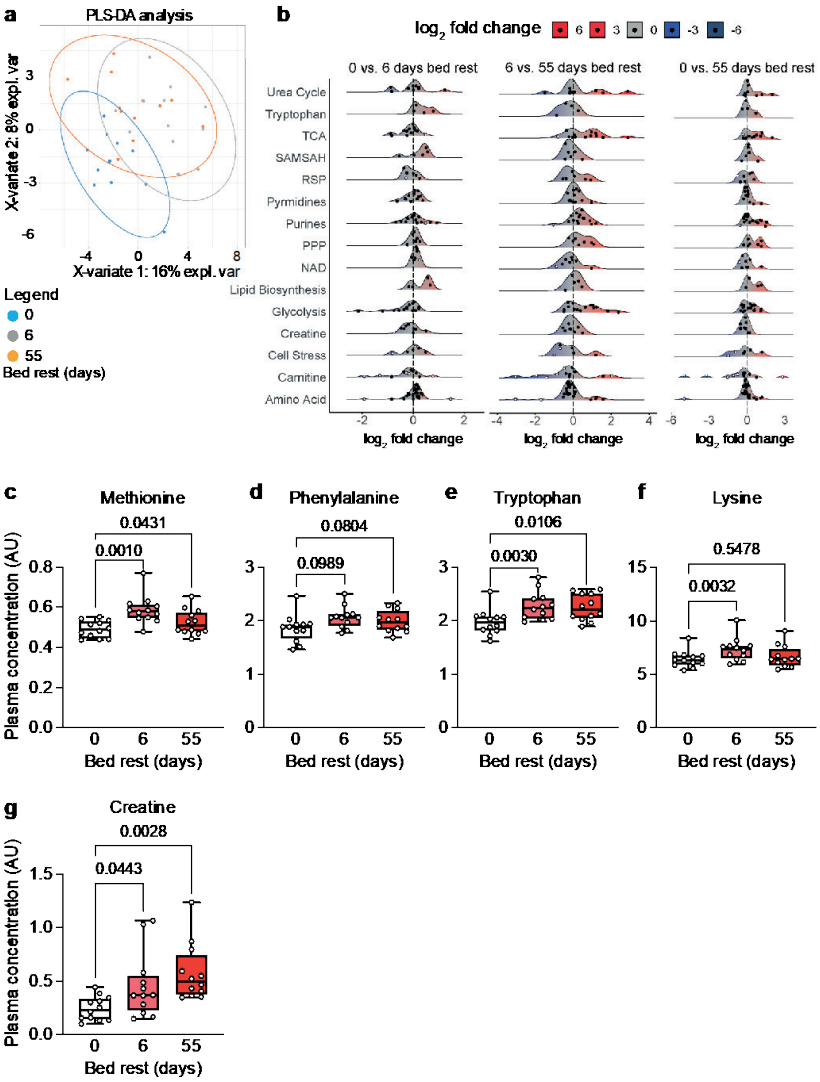


Figure S7. Blood plasma metabolomics upon bed rest. Related to Figure 4. a-b: Landscape plots of plasma metabolomics analysis, mapping the metabolic response in blood plasma upon short- and long-term bed rest. White dots represent significantly altered (p<0.05) metabolites. Metabolite concentration shifts are presented as $\log_2$ fold changes to indicate directionality of alterations. **c-g:** The differential response in the circulating branched-chain amino acids methionine (**c**), phenylalanine (**d**), tryptophan (**e**), lysine (**f**), and circulating creatine concentrations (**g**) upon short- and long-term bed rest is possibly due to increased muscle breakdown. Concentration changes of individual metabolites were analysed using repeated measures ANOVA, with Tukey's post hoc test, n=12. TCA: tricarboxylic acid cycle; SAMSAH: S-adenosylmethionine/S-adenosylhomocysteine cycle; RSP: reductive stress panel; PPP: pentose phosphate pathway; NAD: Nicotinamide adenine dinucleotide pathway.

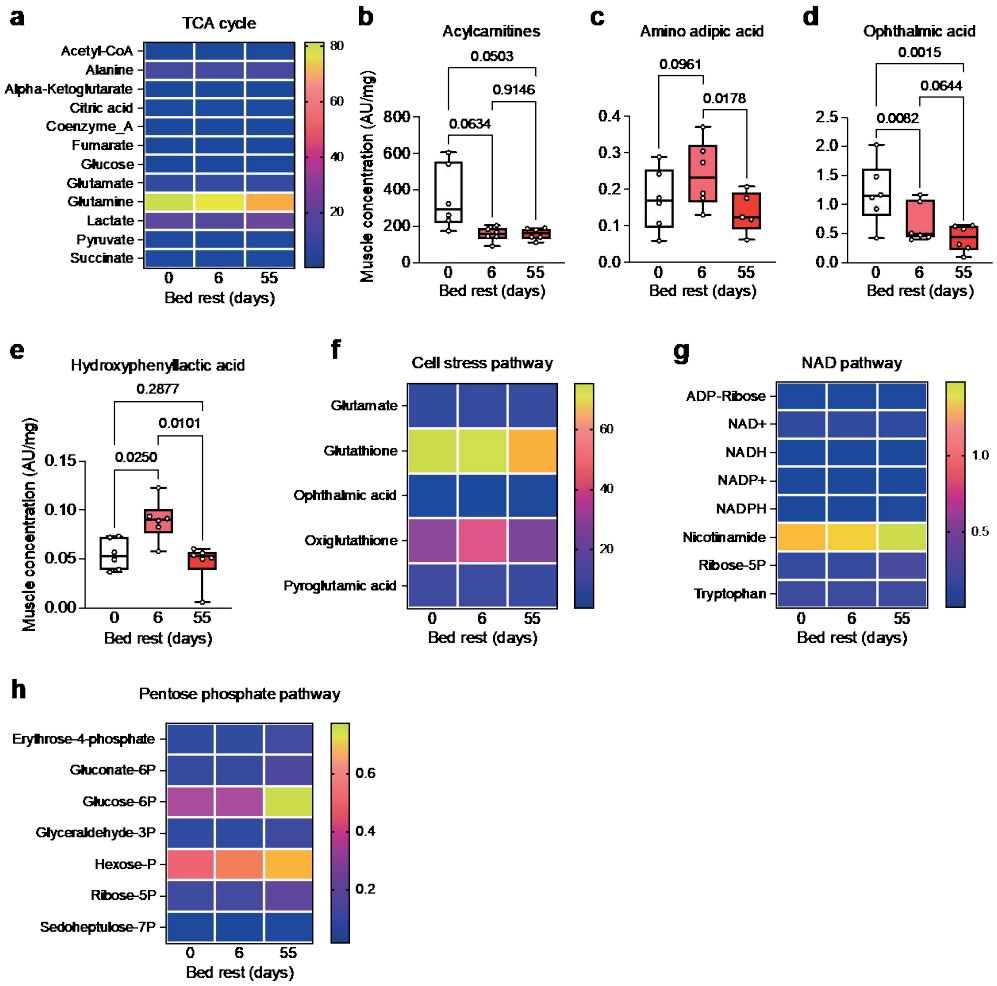


Figure S8. Muscle metabolomics confirm a bed rest-induced metabolic shift towards glucose metabolism in skeletal muscle. Related to Figure 4. a: Heat map of metabolites related to the TCA cycle show less glutamine upon long-term bed rest. **b**: Total acylcarnitines were significantly reduced after short-term bed rest and remained reduced after long-term bed rest. **c-e**: Changes in skeletal muscle, amino adipic acid (**c**), opthalmic acid (**d**) and hydroxyphenyllactic acid (**e**) over the course of the bed rest. **f-h**: Heat maps of metabolites related to cell stress (**f**), the NAD^+ pathway (**g**), and the pentose phosphate pathway (**h**) upon short- and long-term bed rest. Concentration changes of individual metabolites were analysed using repeated measures ANOVA, with Tukey's post hoc test, n=6. TCA: tricarboxylic acid cycle

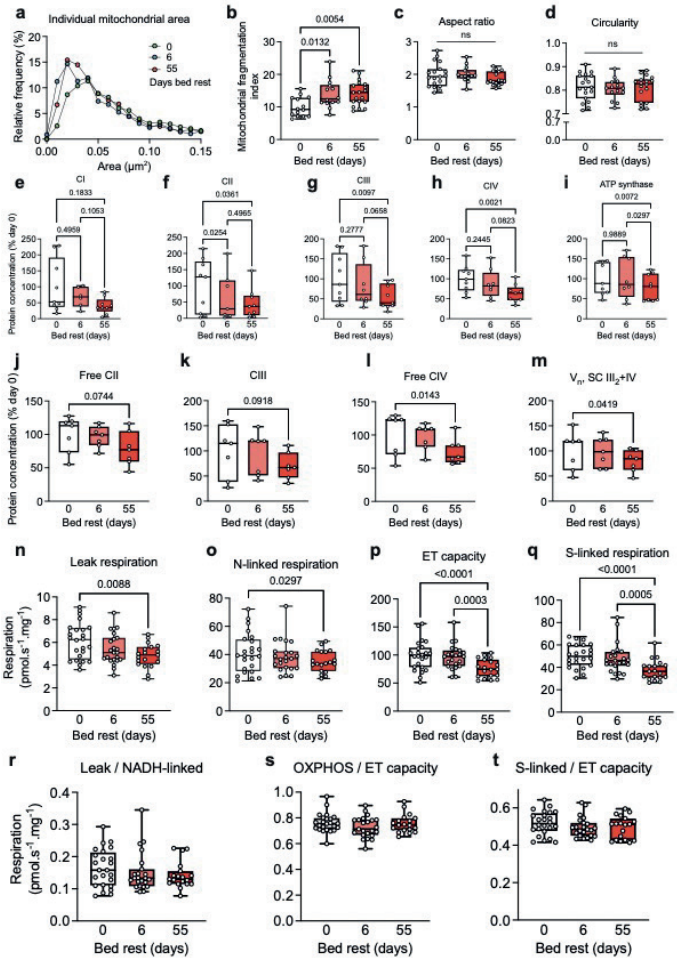


Figure S9. Alterations in mitochondrial structure and function upon bed rest. Related to Figure 5. a-b: A left-shift of the relative frequency distribution after short- and long-term bed rest (**a**) indicates a reduction in individual mitochondrial size, confirmed by an increase in the mitochondrial fragmentation index (**b**) calculated as the total mitochondrial number divided by total mitochondrial area. **c-d:** Mitochondrial aspect ratio (**c**) and circularity (**d**) did not change upon bed rest. **e-i:** Individual protein concentrations of subunits of the mitochondrial complexes were reduced after long-term, but not short-term bed rest. **j-m**: While the abundance of mitochondrial supercomplexes decreased upon bed rest (Figure 5), also the free complex II, III and IV decreased. The abundance of mitochondrial supercomplex III_2+IV decreased after long-term bed rest. **n-q**: Leak and NADH-linked respiration, electron transfer (ET) capacity, and succinate-linked respiration only decreased after long- but not short-term bed rest. **r-t:** Respiratory control ratios did not alter throughout the bed rest period. Data were analysed using repeated measures ANOVA, with Tukey's post hoc test, *n*=14-19 for mitochondrial morphology, *n*=9 for immunoblotting, *n*=7 for BN-PAGE, *n*=24 for respirometry.

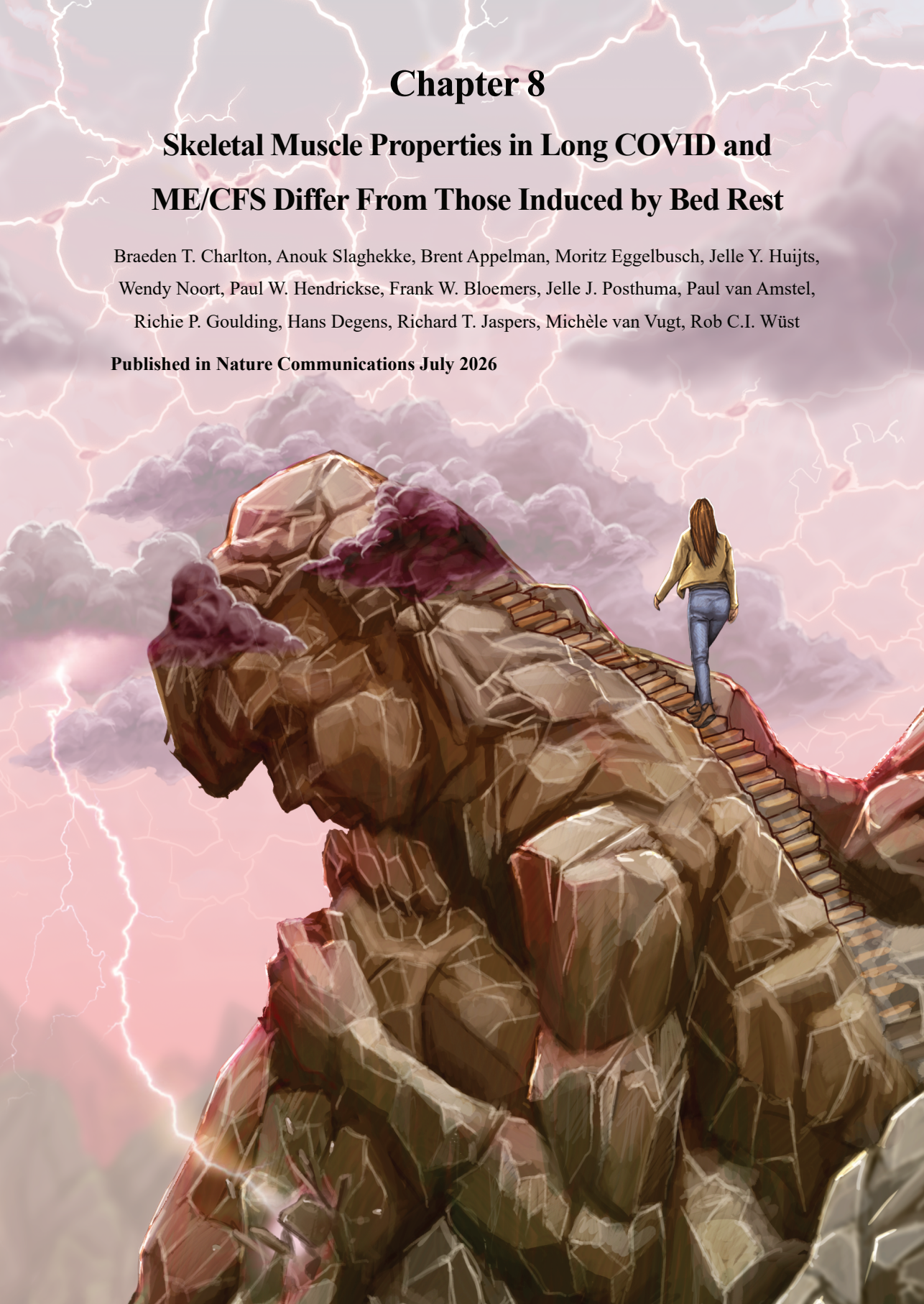


Chapter 8

Skeletal Muscle Properties in Long COVID and ME/CFS Differ From Those Induced by Bed Rest

Braeden T. Charlton, Anouk Slaghekke, Brent Appelman, Moritz Eggelbusch, Jelle Y. Huijts, Wendy Noort, Paul W. Hendrickse, Frank W. Bloemers, Jelle J. Posthuma, Paul van Amstel, Richie P. Goulding, Hans Degens, Richard T. Jaspers, Michèle van Vugt, Rob C.I. Wüst

Published in Nature Communications July 2026



Abstract

Patients with long COVID and myalgic encephalomyelitis/chronic fatigue syndrome (ME/CFS) suffer from post-exertional malaise. The accompanying physical inactivity may contribute to a lower aerobic capacity and may explain skeletal muscle adaptations in these patients. Here, we compare whole-body exercise responses and skeletal muscle adaptations after strict 60-day bed rest in healthy people with those in long COVID and ME/CFS patients, and healthy age- and sex-matched controls. Bed rest alters respiratory and cardiovascular responses to maximal exercise, which are dissimilar in patients. Bed rest causes muscle atrophy without altering fiber type. Both patient groups have more glycolytic fibers, and ME/CFS patients display type I-specific atrophy. Only after bed rest is oxidative phosphorylation capacity associated with maximal oxygen uptake. As skeletal muscle characteristics differ between patients and healthy individuals after bed rest, physical inactivity cannot solely explain the lower exercise capacity and skeletal muscle adaptations in long COVID and ME/CFS patients.

Introduction

Although most acute SARS-CoV-2 infections resolve within days to weeks, some symptoms persist or worsen in a subset of patients[1–3]. The continuation or development of symptoms after 12 weeks is termed long COVID, and patients typically experience debilitating fatigue, brain fog, postural orthostatic tachycardia, myalgia, and post-exertional malaise (PEM)[3]. PEM, experienced by ~90% of patients with long COVID[4], is the worsening of symptoms following physical or cognitive exertion. While the pathophysiology underlying long COVID remains unclear, recent evidence suggests a close resemblance to myalgic encephalomyelitis/chronic fatigue syndrome (ME/CFS)[5], another disease characterized by reduced exercise capacity, brain fog and PEM. Importantly, PEM often results in avoidance of physical activity, which may contribute to the skeletal muscle abnormalities observed in both conditions[6–12]. Due to PEM, long COVID and ME/CFS patients may not achieve intensities or durations frequently enough to induce or maintain whole body or skeletal muscle adaptations to exercise[13,14]. Depending on habitual activity levels, this may result in either maintenance of baseline muscle properties or, if activity is substantially reduced, progressive deconditioning over time[15].

Deconditioning can range from mild step reductions to strict bed rest, with more severe models leading to more rapid reductions in aerobic capacity and skeletal muscle function[16–18], including muscle atrophy, capillary rarefaction, as well as reduced mitochondrial content and mitochondrial function[16,19–21] . Cardiac output[20,22] and maximal ventilatory capacity[23,24] are also reduced after bed rest. However, whether these alterations cohere with those in patients with long COVID and ME/CFS has not been directly investigated. Patients with long COVID and ME/CFS exhibit lower aerobic exercise capacity and mitochondrial respiration [6,7,9,10], reduced capillary densities[9] , muscle fiber atrophy[7], and higher prevalences of atrophic fibers (small, triangular fibers)[6], which has often been attributed to deconditioning[15,25]. However, whether deconditioning alone accounts for these changes remains unclear.

The current study aimed to compare whole body exercise responses and skeletal muscle adaptations in patients with long COVID and ME/CFS to those observed following strict 60-day bed rest. We hypothesized that while whole-body aerobic capacity was similarly lower between patients and following bed rest, adaptations in skeletal muscle markers for oxygen supply and utilization diverged. As current literature regarding skeletal muscle alterations in long COVID patients often includes patients that have been hospitalized during acute infections, and skeletal muscle reports of patients with ME/CFS are scarce, we reasoned that non-hospitalized patients with long COVID and ME/CFS display no muscle atrophy, whilst

exhibiting lower capillary-to-fiber ratios and capillary densities. In contrast, we expected bed rest to result in severe muscle atrophy, reduced capillary-to-fiber ratios, and increased capillary density. Further, we expected muscle fiber size, capillarization and mitochondrial markers to be associated with whole-body exercise capacity in healthy participants undergoing bed rest, but that such associations are lost in patients. To test these hypotheses, we analyzed aerobic exercise responses and vastus lateralis skeletal muscle biopsies of patients with ME/CFS and long COVID, and compared these to those of age- and sex-matched healthy controls (clinical trial NCT05225688), as well as a cohort of 24 healthy individuals who completed a strict bed rest for 60 days (clinical trial DRKS00015677).

Results

Participant Characteristics

Table 1 provides the participant characteristics of the two cohorts, Figure 1A provides a graphical overview of the cohorts and study design. All healthy controls, 96.0% of patients with long COVID were vaccinated against SARS-CoV2 at the time of measurements, while ME/CFS patients were diagnosed prior to 2019, and the bed rest study was conducted before the COVID-19 pandemic. Patients with long COVID developed symptoms prior to vaccination, and met the Canadian Consensus Criteria for ME/CFS. Patients with ME/CFS were already diagnosed with ME/CFS (type of infection prior to diagnosis presented in Supplemental Figure 1) before the COVID pandemic, and were therefore ill for a significantly longer time relative to long COVID patients (Table 1). Both patient groups displayed mild symptoms (DePaul Symptom Questionnaire Post-Exertional Malaise reported in Supplemental Figure 2 and symptoms in Supplemental Figure 3), as is implied by their willingness and ability to undergo exercise testing. Patients with long COVID and ME/CFS displayed large interindividual differences in daily step count (range: 733-8609 steps/day; Table 1).

Table 1. "**Cohort characteristics."** Data presented as median (IQR), as data was non-normally distributed. Symptom duration is reported from symptom onset to day of study enrolment (February 2022 for long COVID and October 2023 for ME/CFS).

	Bed Rest		**Control**	**Long COVID**	**ME/CFS**
	Pre	**Post**			
Participants (# Females)	24 (8)	24 (8)	30 (15)	25 (13)	26 (13)
Age (years)	30 (27-38)	30 (27-37)	42 (33-54) §	43 (31-50) §	42 (32-50) §
Height (cm)	175 (172-181)	175 (170-181)	179 (174-186)	177 (171-184)	176 (171-186)
Weight (kg)	74 (70-79)	74 (69-79)	76 (64-88)	80 (69-92)	84 (75- 89)
Symptom Duration (days)	n/a	n/a	n/a	545 (455-686) †††	3793 (2510-5496)
Daily Steps (steps*day^{-1})	ND	0 (0-0)	7153 (5063-8405) †††	4718 (2794-5832) ***	3704 (2286-5052) ***

***: *vs.* control; †: *vs.* ME/CFS; §: *vs.* Bed Rest**

***: p<0.05; **: p<0.01; ***: p<0.001**

Healthy bed rest participants were on average younger than healthy controls matched to patients (p=0.02). In a sub-group analysis, we age- and sex-matched pre-bed rest participants to patient-matched healthy controls. Maximal oxygen uptake ($\dot{V}O_{2max}$, Supplemental Figure 4A) relative to weight was not different, however patient matched healthy controls had higher $\dot{V}O_{2max}$ compared to the pre-bed rest participants when expressed relative to age- and sex-predicted values (Supplemental Figure 4B). The gas exchange threshold (GET; Supplemental

Figure 4C-D) did not differ between cohorts. Fiber cross sectional area (FCSA; Supplemental Figure 4E) was also similar between groups, however, the pre-bed rest cohort exhibited lower capillary-to-fiber ratios (Supplemental Figure 4F), lower succinate dehydrogenase activity (Supplemental Figure 4G), and a tendency to have a lower oxidative phosphorylation capacity (p=0.092, Supplemental Figure 4H). As some skeletal muscle features differed between those control groups, we analyzed them separately: healthy controls were matched to patients with ME/CFS and long COVID (Table 1), whereas the long-term bed rest cohort were analyzed longitudinally.

Acute Exercise Responses

Bed rest is known to reduce maximal aerobic exercise capacity, and we expected both patient groups to exhibit lower maximal aerobic exercise capacities compared to healthy controls. Indeed, $\dot{V}O_{2max}$ (Figure 1B) and peak power output (Supplemental Figure 5A) were reduced after 60-day bed rest, and were similarly lower in patients with long COVID and ME/CFS compared to healthy controls (Figure 1B + Supplemental Figure 5A). The same trends were observed when $\dot{V}O_{2max}$ was expressed as a percentage of age- and sex-predicted values (Supplemental Figure 6).

The GET, a submaximal non-invasive marker for the lactate threshold, was reduced following bed rest (Figure 1C), and was similarly lower in both patient groups compared to healthy controls (Figure 1C). Following bed rest, GET occurred at a higher percentage of $\dot{V}O_{2max}$ (Supplemental Figure 5B), whereas in patients with ME/CFS, GET occurred at a lower percentage of $\dot{V}O_{2max}$ compared to both patients with long COVID and healthy controls (Supplemental Figure 5B), suggesting an earlier relative onset of lactate accumulation in patients.

Bed rest also altered ventilatory and cardiovascular responses to exercise. Maximal minute ventilation was reduced ($\dot{V}E_{max}$; Figure 1D), whereas ventilatory equivalents for O_2 and CO_2 ($\dot{V}E_{max}/\dot{V}CO_{2max}$ and $\dot{V}E_{max}/\dot{V}O_{2max}$), and the $\dot{V}E/\dot{V}CO_2$ slope (Figure 1E + Supplemental Figure 5C-D) increased after 60 days of strict bed rest. Cardiovascular alterations included a reduced maximal O_2-pulse (i.e. $\dot{V}O_{2max}$/maximal heart rate, equal to the product of stroke volume and arteriovenous O_2 difference; Supplemental Figure 5E); increased maximal heart rate (Supplemental Figure 4F), and increased adjusted heart rate reserve (AHRR; Supplemental Figure 5G).

While $\dot{V}E_{max}$ (Figure 1D) tended to be lower in patients compared to healthy controls (p=0.062), there were no significant differences in $\dot{V}E_{max}/\dot{V}CO_{2max}$, $\dot{V}E_{max}/\dot{V}O_{2max}$, the $\dot{V}E/\dot{V}CO_2$ slope, maximal heart rate, or AHRR (Figure 1E, Supplemental Figure 5C+D+F+G). However, both patients with long COVID and ME/CFS exhibited a lower O_2-pulse compared to healthy controls (Supplemental Figure 5E), similar to the effects of bed rest. Patients with ME/CFS had a more pronounced increase in heart rate relative to oxygen uptake (HR-$\dot{V}O_2$slope; Supplemental Figure 5H) compared to healthy controls, a pattern not seen following bed rest. These results are suggestive of either a lower stroke volume and/or an impaired peripheral oxygen extraction in patients.

Whole body exercise results suggest that altered ventilatory patterns occurred concomitantly with the reduction in $\dot{V}O_{2max}$ following bed rest, whilst ventilatory patterns in patients remain largely similar to healthy controls. Rather, patients indicate reductions in O_2 pulse and elevations in HR-$\dot{V}O_2$ slope, which are suggestive of a lower stroke volume or peripheral oxygen extraction.

Skeletal Muscle Fiber Type Alterations

As muscle unloading can induce atrophy within days[19], we assessed muscle fiber cross sectional area (FCSA), fiber-type specific FCSA, and fiber type composition using immunohistochemistry (Figure 2A). As expected, bed rest induced muscle atrophy (Figure 2B), affecting all fiber types similarly (Supplemental Figure 7A). In contrast, overall muscle FCSA of patients with long COVID and ME/CFS did not differ from healthy controls (Figure 2B). However, when assessing fiber-type specific FCSA, patients with ME/CFS exhibited significantly smaller type I fibers compared to healthy controls (Supplemental Figure 7B), while all other fiber type sizes remained similar to those of healthy controls. This suggests selective atrophy of type I fibers in patients with ME/CFS, but not after long-term bed rest.

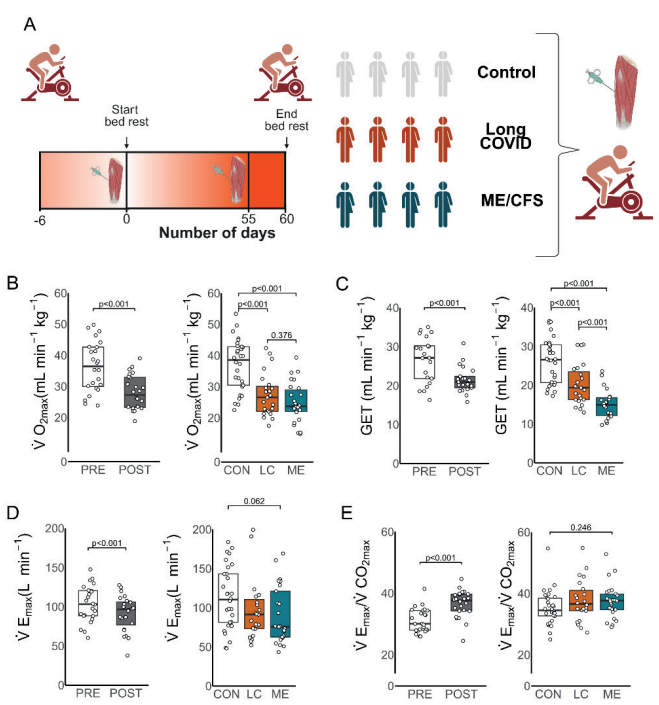


Figure 1: **Bed rest results in alterations in respiratory and cardiovascular responses to maximal exercise, which are not seen in either patients with long COVID or ME/CFS.** **A**: Study designs for the bed rest and the myalgic encephalomyelitis/chronic fatigue syndrome (ME/CFS; ME), long COVID (LC), and healthy control (CON) cohorts. Bed rest decreased $\dot{V}O_{2max}$ (**B**; p<0.001, n= 24), gas exchange threshold (GET; **C**; p<0.001, n= 21), and $\dot{V}E_{max}$ (**D**; p<0.001, n= 24), while $\dot{V}E_{max}/\dot{V}CO_{2max}$ increased (**E**; p<0.001, n=24). Patients with long COVID and ME/CFS had lower $\dot{V}O_{2max}$ (**B**; p<0.001**,** n=23 LC , p<0.001, n= 26 ME/CFS; n= 30 CON) and GET (**C**; p<0.001; n=23 LC ; p<0.001, n= 22 ME/CFS; n= 30 CON) compared to controls and $\dot{V}E$ tended to be lower (**D**; ANOVA: p=0.062; n=23 LC , n=25 ME/CFS, n=30 CON), however $\dot{V}E_{max}/\dot{V}CO_{2max}$ was not significantly different than controls (**E**; ANOVA: p=0.246, n=22 LC , n=25 ME, n=30 CON). $\dot{V}O_{2max}$ and GET were non-normally distributed following Box-Cox transformations. Comparisons between pre- and post- bed rest were assessed using two-sided paired t-tests for parametric data and two-sided Mann–Whitney *U* test for non-parametric data. Comparisons between patients with long COVID and patients with ME/CFS and healthy controls were assessed using analysis of variance, with Tukey HSD post-hoc testing for parametric data or Kruskal–Wallis *H* test, with pairwise Wilcoxon tests with Benjamini–Hochberg correction post-hoc for non-parametric data. Box plots display individual data points, median (center line) and the first and third quartiles (lower and upper bound of box). Pre-bed rest and healthy controls are displayed in white, post-bed rest is displayed in grey, patients with long COVID are displayed in orange, and patients with ME/CFS are displayed in green. Created in BioRender. Charlton, B. (2026) https://BioRender.com/gxz85by.

Following long-term bed rest, fiber type composition did not change (Figure 2C and Supplemental Figure 7C). In contrast, patients with long COVID and ME/CFS had a lower proportion of type I fibers (albeit p=0.052 for long COVID) and a greater proportion of type IIa/IIx + IIx fibers compared to healthy controls (Figure 2C), while patients with ME/CFS had an even lower proportion of type I fibers than patients with long COVID. We observed similar results when expressing fiber type distribution as numerical percentages (Supplemental Figure 7D). This indicates either a greater propensity for those with greater proportions of type IIa/IIx + IIx fibers to contract chronic illness or suggests a fiber type shift occurring in patients. As we noted a selective type I atrophy in patients, these results suggest a fiber type shift away from type I fibers towards more type II fiber types. The muscle atrophy was not fiber type-specific after long-term bed rest, and bedrest did not induce a similar fiber type shift.

Mitochondrial Respiration and Activity

Whilst we find evidence of either oxygen extraction or stroke volume being impeded in patients, we did not have the resources to measure stroke volume. Thus, we focused on parameters related oxygen extraction and utilization in the skeletal muscle. Given that physical activity has been shown to shift limitations of maximal aerobic capacity from oxygen utilization to oxygen supply[26] and the association between mitochondrial function and whole-body aerobic exercise capacity[27], we assessed mitochondrial respiration of permeabilized muscle fibers and succinate dehydrogenase (SDH) activity in sections, to provide further insight into mitochondrial alterations upon bed rest and in patients. Bed rest resulted in lower SDH activity and oxidative phosphorylation capacity (Figure 3A+B). Compared to healthy controls, only patients with ME/CFS, but not long COVID, exhibited lower SDH activity (Figure 3A). Both patients with long COVID and ME/CFS presented with lower oxidative phosphorylation capacities compared to healthy controls (Figure 3B). As mitochondria are the ultimate recipients in the oxygen cascade, we hypothesized that either SDH activity or oxidative phosphorylation correlated with $\dot{V}O_{2max}$. Both SDH activity and oxidative phosphorylation capacity were correlated with $\dot{V}O_{2max}$ in healthy controls (Figure 3C+D), and such a relation was present following bed rest. However, this association was absent in patients with long COVID and ME/CFS. While the precise limitation of $\dot{V}O_{2max}$ in patients is obscured, the lack of association of $\dot{V}O_{2max}$ with mitochondrial variables suggests that reductions in exercise capacity are not limited by mitochondrial density or respiratory capacity *per se*.

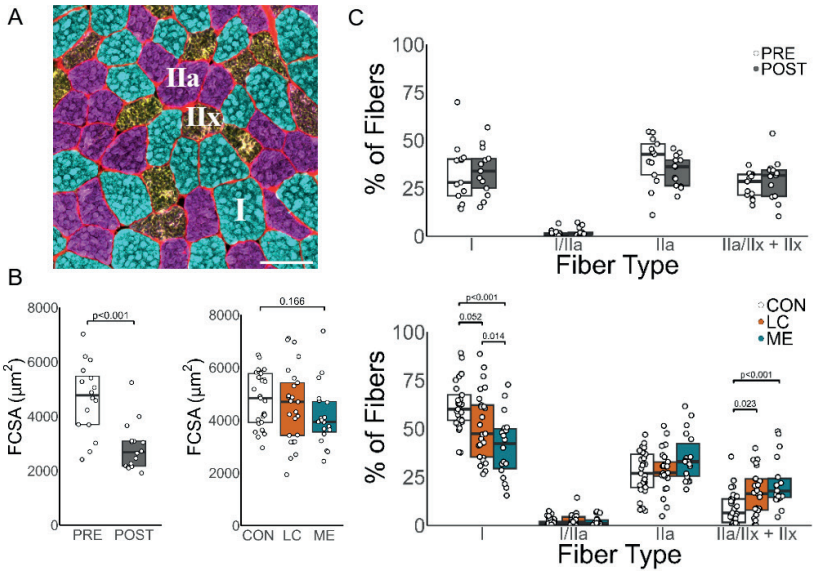


Figure 2: **Bed rest induces muscle atrophy, with no change to fiber type composition. Both patients with long COVID and ME/CFS have more glycolytic fibers than healthy, matched controls.** **A:** A typical example of muscle fiber type staining with colors adjusted to be color-blind visible. Scale bar represents 100µm. Severe fiber atrophy was observed following bed rest (**B**; $p<0.001$, n=16), whereas fiber cross-sectional area (FCSA) was not different between patients with long COVID (LC, n=25) and myalgic encephalomyelitis/chronic fatigue syndrome (ME/CFS; ME, n=19) and healthy controls (**B**; ANOVA: $p=0.174$, n=29 CON). Following bed rest, fiber type composition was not significantly altered (**C**; Linear mixed model: $p=0.877$, n=16). Fiber type composition was significantly different between patients with long COVID, patients with ME/CFS and healthy controls (**C**; Linear mixed model: $p=0.004$, n=25 long COVID, n=19 ME/CFS, n=29 healthy controls). Long COVID ($p=0.052$, n=25) and ME/CFS ($p<0.001$, n=19) patients exhibited lower proportions of type I fibers compared to healthy controls (n=29, albeit $p=0.052$ for long COVID), while both patients with long COVID ($p=0.023$, n=25) and ME/CFS ($p<0.001$, n=19) had significantly higher proportions of type IIa/IIx+IIx fibers compared to healthy controls (**C**; n=29 CON). All data was normally distributed following Box-Cox transformations, except proportions of IIa/IIx+IIx fibers. Fiber type proportions were assessed using a linear mixed random effects model using % of proportion as the dependent variable and group x fiber type as the fixed effects, with subject ID as the random effects variable, and post-hoc testing carried out per fiber type as described below. Two-sided paired t-tests were used to assess parametric data from the bed rest cohort. Non-parametric data from the bed rest cohort was assessed using two-sided Mann–Whitney *U* tests. Analysis of variance, with Tukey HSD post-hoc testing or Kruskal–Wallis *H* test, with pairwise Wilcoxon tests with Benjamini–Hochberg correction post-hoc were used to assess parametric and non-parametric data for patient cohorts. Box plots display individual data points, median (center line) and the first and third quartiles (lower and upper bound of box). Pre-bed rest and healthy controls are displayed in white, post-bed rest is displayed in grey, patients with long COVID are displayed in orange, and patients with ME/CFS are displayed in green..

As mitochondrial respiration reflects both mitochondrial content and function, we subsequently normalized mitochondrial respiration to gain insight into alterations of intrinsic mitochondrial function. After normalizing mitochondrial respiration to SDH activity, there was no effect of bed rest on oxidative phosphorylation capacity (Supplemental Figure 8A). In contrast, patients with long COVID still displayed lower oxidative phosphorylation capacity normalized to SDH activity compared to healthy controls, while patients with ME/CFS tended to exhibit lower oxidative phosphorylation capacity (p=0.063, Supplemental Figure 8A). Normalizing maximal uncoupled respiration to leak respiration (E/L coupling efficiency) is reflective of intrinsic mitochondrial biochemical coupling, wherein a less coupled system (lower values) indicates higher proton leak. Bed rest did not alter the E/L coupling efficiency, however both patients tended to display lower E/L coupling efficiency compared to healthy controls (p=0.066, Supplemental Figure 8B). The relative NADH-linked respiration (NADH-linked respiration normalized to oxidative phosphorylation capacity) increased and the relative succinate-linked respiration (succinate-linked normalized to maximal uncoupled respiration) decreased after long-term bed rest (Supplemental Figure 8C-D). No such differences were observed between patients and healthy controls.

Bed rest reduced maximal oxidative phosphorylation, consistent with lower SDH activity, and slightly altered intrinsic respiration, suggesting a shift in the contributions of complex I and II. In contrast, the lower oxidative phosphorylation capacity in both patient groups were accompanied by a lower coupling efficiency with no changes to qualitative changes in the electron flux through complex I or complex II.

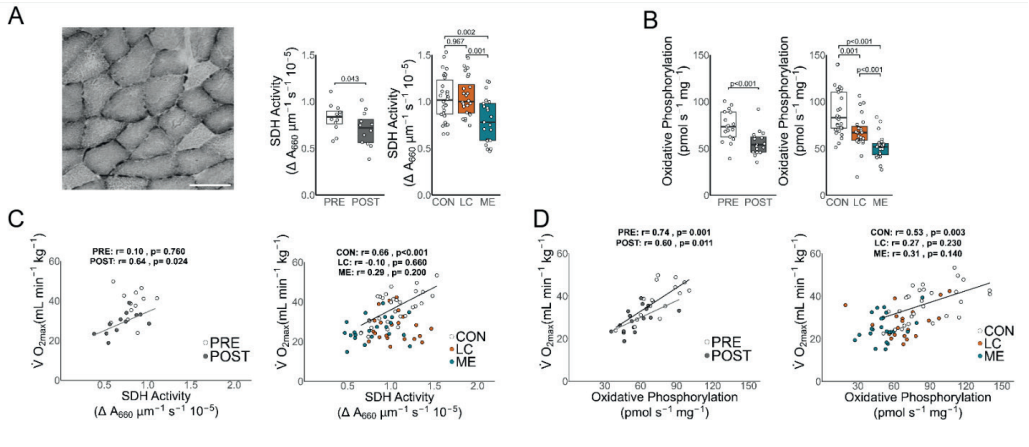


Figure 3: **Bed rest decreases both SDH activity and oxidative phosphorylation capacity, which relate to maximal oxygen uptake. Lower SDH activity and oxidative phosphorylation capacity in patients with long COVID and ME/CFS do not relate to maximal oxygen uptake.** Succinate dehydrogenase (SDH) activity (**A**) was significantly reduced following bed rest (p=0.043, n=12). SDH activity in patients with long COVID (LC, n=24) was not different to healthy controls (CON; p=0.967, n=30), but lower in myalgic encephalomyelitis/chronic fatigue syndrome (ME/CFS; ME, n=21, p=0.002; **A**). Oxidative phosphorylation capacity (**B**) was reduced following bed rest (p<0.001 , n=17) and was lower in both patients with long COVID (p=0.001, n=23) and ME/CFS (p<0.001, n=23) compared to healthy controls (n=30). SDH was associated with $\dot{V}O_{2max}$ (**C**) after bed rest (r=0.65, p=0.024, n=12) and in healthy controls (r=0.66, p<0.001, n=30). The relationship between oxidative phosphorylation capacity and $\dot{V}O_{2max}$ (**D**) was significant in pre- and post-bed rest (r=0.74, p<0.001, n=17; r=0.60, p=0.0113, n=17) and healthy controls (r=0.53, p=0.003, n=29), but not in patients with ME/CFS (r=0.31, p=0.144, n=23) or long COVID (r=0.27, p=0.231, n=21). Bars represent 100µm. Oxidative phosphorylation data in the patient cohort remained non-normally distributed following Box-Cox transformation. Two-sided paired t-tests were used to assess parametric data from the bed rest cohort. Non-parametric data from the bed rest cohort was assessed using two-sided Mann–Whitney *U* tests. Analysis of variance, with Tukey HSD post-hoc testing or Kruskal–Wallis *H* test, with pairwise Wilcoxon tests with Benjamini–Hochberg correction post-hoc were used to assess parametric and non-parametric data for patient cohorts. Linear relationships were assessed using Pearson's correlation on non-transformed data, solid lines represent significant correlations (p<0.05). Box plots display individual data points, median (center line) and the first and third quartiles (lower and upper bound of box). Pre-bed rest and healthy controls are displayed in white, post-bed rest is displayed in grey, patients with long COVID are displayed in orange, and patients with ME/CFS are displayed in green.

Skeletal Muscle Capillarization

As bed rest induced muscle fiber atrophy and patients exhibited a lower proportion of type I fibers, we hypothesized that capillary supply may be differentially affected. Following bed rest, the average capillary-to-fiber ratio was unchanged (Figure 4B), however the cross-sectional area of each capillary was significantly reduced (Supplemental Figure 9A). Due to greater muscle atrophy relative to capillary loss[19], capillary density was increased following long-term bed rest (Figure 4C). These changes were not observed in patients with long COVID or ME/CFS. Patients with ME/CFS displayed lower capillary-to-fiber ratios and capillary densities (Figure 4C) compared to healthy controls and patients with long COVID, while capillary measures in patients with long COVID were not different from healthy controls. The relationship between muscle fiber size and the capillary-to-fiber ratio is reflective of adaptive remodeling to support the tight link between these two parameters to maintain adequate diffusive oxygen supply in larger fibers[28]. As we found differential intrinsic mitochondrial alterations between patients and bed rest, we queried whether alterations of mitochondrial capacities and capillarization subsequently were reflected by an altered the capillary-fiber size relationship. In all groups, capillary-to-fiber ratios were proportional to FCSA, with a trend following long-term bed rest (p=0.062; Figure 4D). Both patient groups had significantly lower intercepts than healthy controls (both p<0.05), indicating less capillary supply for a given fiber cross-sectional area.

Due to the selective type I fiber atrophy in patients, we queried whether the capillary alterations were different by fiber type. To this end, we calculated the capillary-to-fiber ratio on a fiber type basis, comparing type I to type II fibers (Supplemental Figure 11) in a subgroup of participants. In all conditions, type I fibers had a greater capillary-to-fiber ratio than type II fibers. Bed rest reduced capillary-to-fiber ratio in both type I and type II fibers equally. ME/CFS patients had lower capillarization compared to both healthy controls and long COVID patients independent of fiber type. There was no effect of disease on fiber type specific capillarization.

Due to the reduced capillary-to-fiber ratio for a given fiber size, despite no fiber-specific alterations to capillary indices, we queried whether intramyocyte diffusive parameters may be altered. To this end, we evaluated the intracellular myoglobin content in a subset of participants. Following bed rest, myoglobin content increased unexpectedly (Supplemental Figure 10B), whereas patients and healthy controls did not differ (Supplemental Figure 10C).

Therefore, the results indicate that capillary number for a given FCSA remains largely unchanged after long-term bedrest. In both patient groups, however, capillary number for a given FCSA was lower, with patients with ME/CFS exhibiting an overall reduction in capillary-to-fiber ratios, independent of fiber type. Myoglobin content was not different between patients and healthy controls.

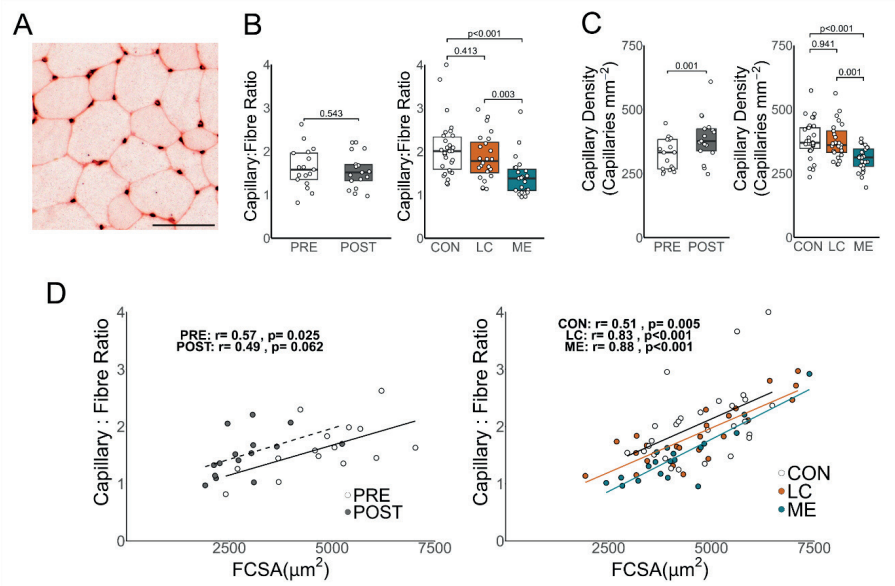


Figure 4: **Capillary-to-fiber ratio following bed rest is proportional to muscle fiber size, while both patients with long COVID and ME/CFS have reduced capillary-to-fiber ratio for a given fiber size.** A typical example of a lectin stain for capillaries is shown in **A**. Scale bar represents 100µm. Following bed rest, capillary-to-fiber ratio was not significantly different (**B**; p=0.543, n=17), while patients with myalgic encephalomyelitis/chronic fatigue syndrome (ME/CFS; ME, n=23) had a significantly lower capillary-to-fiber ratio compared to patients with long COVID (p=0.001, n=24) and healthy controls (p<0.001, n=30; **B**). Capillary density (**C**) was significantly increased following bed rest (p=0.001, n=17), while both patients with long COVID (n=25) and patients ME/CFS (n=24) had significantly lower capillary densities compared to healthy controls (**D**; p<0.001, n=30). The relationship between fiber cross-sectional area (FCSA) and capillary-to-fiber ratio significantly correlated in all conditions, except post-bed rest (albeit p=0.062 following bed rest). The relationship between FCSA and capillary-to-fiber ratio was not significantly different following bed rest (z=0.495, p=0.621), however compared to healthy controls, both patients with long COVID (z= -2.176, p=0.030) and patients with ME/CFS (z= -2.602, p=0.009) displayed significantly different relationships (**G**). Capillary density and capillary-to-fiber ratio data were normally distributed following Box-Cox transformation. Two-sided paired t-tests were used to assess parametric data from the bed rest cohort. Non-parametric data from

the bed rest cohort was assessed using two-sided Mann–Whitney *U* tests. Analysis of variance, with Tukey HSD post-hoc testing or Kruskal–Wallis *H* test, with pairwise Wilcoxon tests with Benjamini–Hochberg correction post-hoc were used to assess parametric and non-parametric data for patient cohorts. Linear relationships were assessed using Pearson's correlation on non-transformed data. Solid lines represent significant correlations, dashed lines represent correlations with $p<0.10$. Box plots display individual data points, median (center line) and the first and third quartiles (lower and upper bound of box). Pre-bed rest and healthy controls are displayed in white, post-bed rest is displayed in grey, patients with long COVID are displayed in orange, and patients with ME/CFS are displayed in green.

Comparing skeletal muscle alterations in long COVID and ME/CFS with long-term bed rest

Since both patient groups had lower daily physical activity levels than healthy controls, we reasoned that the healthy participants after bed rest could serve as an alternative control group. We therefore analyzed a subgroup of 13 patients with ME/CFS, 13 patients with long COVID and 13 age- and sex-matched healthy individuals following long-term bed rest (participant characteristics outlined in Supplemental Table 1).

$\dot{V}O_{2max}$ did not differ between groups (Supplemental Figure 12A), however patients with long COVID tended to have a higher $\dot{V}O_{2max}$ than post-bed rest individuals when expressed relative to age- and sex-predicted values (ANOVA: p=0.076, post-hoc: p=0.031 Supplemental Figure 12B). Patients with ME/CFS had significantly lower GET than those with long COVID and healthy post-bed rest individuals (Supplemental Figure 12C). GET occurred at a lower relative intensity in patients with ME/CFS than in both patients with long COVID and participants following bed rest (Supplemental Figure 12D).

Participants after bed rest had significantly smaller FCSA compared to both patient groups (Supplemental Figure 12E). Patients with long COVID displayed higher capillary-to-fiber ratios, SDH activity and oxidative phosphorylation capacity compared to participants after bed rest and patients with ME/CFS (Supplemental Figure 12F+G+H).

When assessing the relationships between capillary-to-fiber ratio and FCSA, only patients with long COVID displayed a significant relationship, while patients with ME/CFS showed a similar trend (Supplemental Figure 12I). Conversely, only participants after bed rest displayed a significant correlation between $\dot{V}O_{2max}$ and SDH activity and oxidative phosphorylation capacity (Supplemental Figure 12J-K). These results suggest that capillary supply and mitochondrial function are disrupted differently in long COVID and ME/CFS compared to bed rest-induced deconditioning.

Thus, when retrospectively comparing patients to age- and sex-matched participants after bed rest, patients with long COVID and ME/CFS still display alterations that are different than those found after bed rest. Despite similar $\dot{V}O_{2max}$, patients show no associations with skeletal muscle oxidative function compared to those observed with bed rest.

Discussion

The major finding of the present study is that acute exercise responses and skeletal muscle alterations in long COVID and ME/CFS differ from those caused by bed rest-induced deconditioning *per se*. Despite similar whole-body exercise capacity in both patient groups and participants after bed rest, the pulmonary and cardiovascular responses to acute exercise were distinct. Long-term (60 days) bed rest induced severe muscle atrophy, which was not observed in patients with long COVID or ME/CFS. Instead, both patient groups displayed a lower proportion of type I fibers, whereas only patients with ME/CFS exhibited lower capillary-to-fiber ratios and type I specific atrophy. Further, the lower oxidative phosphorylation capacity in both patient groups did not correlate with $\dot{V}O_{2max}$, in contrast to bed rest participants, suggesting that physiological impairments distinct from inactivity drive reduced exercise capacity in patients. These findings challenge the notion that deconditioning is the primary driver of reduced exercise capacity in long COVID and ME/CFS. Rather, our observations suggest intrinsic skeletal muscle abnormalities contribute to limited exercise capacity, including reduced capillary supply relative to muscle fiber size and mitochondrial impairments.

Maximal aerobic capacity was similar between patients with long COVID and ME/CFS, and those undergoing a strict 60-day bed rest. However, the physiological determinants underpinning this reduction differed. Ventilatory responses to acute exercise differed following bed rest compared to the patient groups. Bed rest resulted in reduced $\dot{V}E_{max}$, consistent with the decrease in $\dot{V}O_{2max}$, whereas the $\dot{V}E_{max}/\dot{V}CO_{2max}$ and the $\dot{V}E - \dot{V}CO_2$ slope were increased. Patients only exhibited higher $\dot{V}E - \dot{V}CO_2$ slope during submaximal exercise, and a tendency of lower $\dot{V}E_{max}$ and higher $\dot{V}E - \dot{V}CO_2$ slope for the entirety of the exercise test. While arterial PCO_2 was not measured, reductions in $\dot{V}E_{max}$ and increases in $\dot{V}E_{max}/\dot{V}CO_{2max}$ and the $\dot{V}E - \dot{V}CO_2$ slope at submaximal exercise suggests earlier indications of hyperpnea [29–31] in patients. The causes of these findings are currently unclear, however reduced blood or muscle CO_2 buffering capacity[32], increased chemoreceptor sensitivity[33], or pulmonary vascular dysfunction resulting in increased dead space ventilation[34] may contribute.

Acute cardiovascular responses to exercise also differed between cohorts. Previous studies report that deconditioning typically leads to an increase of the HR-$\dot{V}O_2$[20], reflecting a greater heart rate increase per unit change in $\dot{V}O_2$, which is often associated with reduced oxygen extraction[20,35,36]. However, in our study, bed rest participants did not present with this pattern, which may be attributed to the disproportionate increase in baseline heart rate (+30%) relative to their maximal heart rate (+5%) and reduction in $\dot{V}O_{2max}$ (-24%) following bed rest. The increase in both resting and maximal heart rate following bed rest, which has been noted previously[37–39], is not fully understood, but may be related to reductions in plasma and stroke volume[38], altered baroreflex function[39], or shifts in the balance between parasympathetic and sympathetic nervous system activity[37]observed after bed rest. In contrast, our patient groups exhibited an increased HR-$\dot{V}O_2$ slope, suggesting a greater reliance on changes in heart rate to satisfy a given oxygen demand. While this may be indicative of either decreased stroke volume or reduced peripheral oxygen extraction[20], it is consistent with results from invasive CPET studies, which have shown preload failure and marked reduction in peripheral oxygen extraction in long COVID and ME/CFS patients[40,41]. Future studies in long COVID and ME/CFS should focus on measuring markers of cardiovascular function during exercise, such as stroke volume, peripheral oxygen extraction, and baroreflex sensitivity to further elucidate the underlying mechanism.

We showed that the reduction in oxidative phosphorylation capacity following bed rest was primarily attributed to a reduction in SDH activity, often used as a proxy for mitochondrial density[42]. In contrast, the reduced oxidative phosphorylation capacity in both patient groups was still present following normalization to SDH activity, suggesting that intrinsic mitochondrial respiration may be primarily affected. Furthermore, while E/L coupling efficiency tended to be reduced in both patient groups, this was not observed following bed rest. These results suggest that skeletal muscle oxidative impairments in long COVID and ME/CFS cannot solely be attributed to deconditioning. Indeed, previous work suggests abnormal ultrastructure, particularly reduced cristae density, in patients with long COVID and ME/CFS[11], while bed rest is typically associated with more fragmented mitochondria[16]. What the cause of the intrinsic mitochondrial alterations in long COVID and ME/CFS is, is currently unclear. Future work is required to quantify skeletal muscle mitochondrial ultrastructure in long COVID and ME/CFS.

Notably, oxidative phosphorylation capacity and SDH activity correlated with whole-body maximal oxygen uptake in healthy individuals (before and after bed rest), whereas these were

absent in long COVID and ME/CFS. This suggests that factors beyond skeletal muscle mitochondrial respiration constrain exercise capacity in long COVID and ME/CFS, including impairments in endothelial function[43–47], a reduced venous return and cardiac preload[40], or a reduction in muscle diffusive capacity[48] contributing to impaired peripheral oxygen extraction[41]. Conversely, mitochondrial respiration contributes to $\dot{V}O_{2max}$ in healthy sedentary, untrained individuals[26,49], which is consistent with the associations observed between mitochondrial markers and $\dot{V}O_{2max}$ across all healthy cohorts. Thus, it is likely the constraints on $\dot{V}O_{2max}$ imposed by bed rest, long COVID and ME/CFS differ, implying that the reduced aerobic exercise capacity in long COVID and ME/CFS cannot solely be ascribed to deconditioning.

Capillary-to-fiber ratios and capillary density were lower in patients with ME/CFS, but not long COVID, compared to healthy controls, reducing the structural potential to adequately supply oxygen and nutrients, and remove metabolic byproducts during exercise. These findings are contrary to previous reports of lower capillary densities in long COVID[9,50]. While capillary-to-fiber ratio was unaltered following bed rest, capillary density increased due to significant muscle atrophy[19,51], consistent with the principle that alterations in muscle size typically occur before capillary alterations[19,52,53]. Intriguingly, the average area of individual capillaries was reduced following bed rest (Supplemental Figure 9A). This may be due to reduced diameter or capillary tortuosity[54,55] resulting in less obliquely cut capillaries, or due to the lack of shear stress experienced during head-down tilt resulting in a structural remodeling of the capillary beds[56]. That skeletal muscle microvascular-endothelial function was impaired following a 10-day bed rest[57] is consistent with this notion. Although we report unaltered structural indices of capillarization in long COVID, it is unknown whether skeletal muscle capillary perfusion (and oxygen diffusion) was altered during exercise in either long COVID or ME/CFS, as direct measurements of skeletal muscle capillary blood flow are challenging to assess in humans *in vivo*.

Capillary-to-fiber ratio is related to muscle FCSA, wherein larger muscle fibers typically have more capillary contacts to accommodate oxygen and nutrient supply, and metabolite removal[52,53]. While these relations existed in all groups, except following bed rest, this relationship was downshifted in both long COVID and ME/CFS patients compared to healthy controls. This suggests that fewer capillaries are available per unit fiber area in patients, which is distinct from the capillary alterations following strict bed rest[19]. This reduces the surface area and spatial distribution for gas exchange at high metabolic rates, and represents a structural

limitation to oxygen diffusion, irrespective of upstream regulation of blood flow at the arteriolar level. Future work on endothelial alterations in long COVID and ME/CFS might provide further mechanistic insight[58].

$\dot{V}O_{2max}$ is determined by the integrated function of convective oxygen delivery, diffusive oxygen transport, and mitochondrial oxygen utilization, as conceptualized in the Wagner diagram[59,60]. Although we measured several components of this pathway, we did not assess all sites required to localize the dominant limitation. Importantly, while mitochondrial oxidative capacity was reduced in patients, its lack of association with $\dot{V}O_{2max}$ (in contrast to healthy controls and bed rest participants) argues against a purely mitochondrial limitation. Instead, our findings are consistent with the presence of interacting limitations upstream of the mitochondria, including impaired muscle oxygen diffusive capacity or maximal convective oxygen delivery, which cannot be resolved within the current dataset. Notably, reduced whole-body oxygen extraction does not necessarily imply low intramyocyte PO_2, as a reduction in mitochondrial oxygen utilization would be expected to reduce the diffusion gradient required to support $\dot{V}O_2$ rather than increase it. Localized reductions in tissue PO_2 would therefore require sufficiently impaired diffusive conductance or microvascular perfusion heterogeneity, mechanisms that were not directly assessed here. This situation contrasts with healthy sedentary individuals, where mitochondrial capacity is the primary limitation to $\dot{V}O_{2max}$ in small muscle mass exercise (i.e. under conditions where cardiovascular limitations are minimized)[26]. Although we utilized whole-body exercise in the current study, and the mitochondrial oxidative ceiling is far less likely to be reached in this mode of exercise, our observation of the significant association between SDH-activity and oxidative phosphorylation and $\dot{V}O_{2max}$ that occurs after bed rest (Figure 3C), and across different populations[27] is at least consistent with the notion of a role for mitochondria in explaining the variation of $\dot{V}O_{2max}$ in patient populations.

Invasive CPET results indicate that at maximal exercise, arterial PO_2 in long COVID and ME/CFS is similar to that in healthy people[40,41]. Intramyocyte oxygen movement is dependent on convective oxygen delivery, oxygen diffusion through the tissue, and mitochondrial oxygen consumption[61]. The decrease in capillary-to-fiber ratio for a given fiber size reduces the potential for oxygen convective delivery. While the reduced mitochondrial oxidative capacity in both patients with long COVID and ME/CFS would suggest a higher intracellular PO_2, we were not able to measure intracellular PO_2 directly. However, as myoglobin is an integral piece in intramyocyte oxygen diffusion, we suspected that if intracellular PO_2 was indeed higher and

oxygen convective delivery was impaired, there may be a compensatory response of myoglobin in order to maintain the oxygen diffusion gradient. As myoglobin content was similar amongst the groups, it would suggest that intramyocyte diffusion capacity may be maintained. However, it is unknown whether any of hemoglobin, capillary or myocyte membrane function is altered, which also impacts oxygen diffusive capacity. Future work should aim to address whether membrane functions are altered and may contribute to impaired oxygen extraction. We confirmed that bed rest causes significant atrophy across all fiber types[62–64]. Conversely, overall FCSA in patients with long COVID ME/CFS was not different from that of healthy controls. However, we observed selective type I fiber atrophy in patients with ME/CFS, suggesting fiber-type specific vulnerability to atrophy. The underlying mechanism remains unclear, as we lack the longitudinal data to determine whether these changes result from the disease progression or pre-disease differences.

Previous studies show conflicting results regarding changes in fiber type composition following bed rest[19,65–68]. In our cohort, fiber type composition remained unchanged following bed rest, calculated as both area occupied by fiber type and as the numerical proportion of fibers of a given type relative to all fibers present. In contrast, both patients with long COVID and ME/CFS exhibited higher proportions of type IIa/IIx fibers and lower proportions of type I fibers compared to healthy controls, expressed both as relative to area occupied and total number of fibers. Since we did not obtain longitudinal muscle biopsies from patients, we cannot determine whether this is due to a fiber type transition, or whether individuals with higher proportions of type IIa/IIx fibers are predisposed to developing long COVID or ME/CFS. However, given the type I fiber-specific atrophy pattern observed in patients with ME/CFS, the lower proportion of type I fibers and higher proportions of type IIa/IIx fibers in patients, our findings suggest that a shift towards type IIa/IIx fibers may occur in ME/CFS. The type I atrophy and the higher prevalence of type IIa/IIx fibers were more pronounced in ME/CFS compared to long COVID patients, possibly because ME/CFS patients were diagnosed before the COVID pandemic, and therefore were ill for a significantly longer time. Whether the disease duration or intrinsic differences between long COVID and ME/CFS underlie these differences is therefore unknown.

Previous studies have indicated an overlap in potential pathological mechanisms in both long COVID and ME/CFS, that include (but certainly not limited to) autonomic dysfunction, microclot formation in the blood, endothelial dysfunction and mitochondrial dysfunction[69]. In our current study, we provide evidence for skeletal muscle mitochondrial impairments to be

implicated in both long COVID and ME/CFS. However, as both diseases are heterogenous, other mechanisms may be involved depending on clinical presentation. In our current cohort, we focused on long COVID patients that exhibited PEM as a key symptom. Thus, it may be that the mitochondrial dysfunction we highlight is more unique to those patients that exhibit PEM rather than other long COVID symptoms.

The current study indicates that skeletal muscle adaptations and lower aerobic exercise capacities observed in patients with long COVID and ME/CFS are different from those occurring after bed rest, however there are several limitations. A limitation of the present study is its cross-sectional design in patients with long COVID and ME/CFS, which precludes inference on temporal disease progression or causality. While longitudinal muscle biopsies would be informative, such data are currently unavailable, and ethical constraints limit experimental manipulation of activity levels in patients. Consequently, our conclusions are restricted to demonstrating that the skeletal muscle phenotype observed in patients differs from that induced by prolonged bed rest, rather than establishing the temporal origin of these abnormalities. We did not induce physical inactivity in patients with ME/CFS or long COVID. Patients are typically more sedentary because PEM worsens both their symptoms and skeletal muscle abnormalities[6]. We also cannot completely exclude the contribution of physical inactivity to the skeletal muscle alterations observed in patients with long COVID and ME/CFS, however our results do indicate that physical inactivity alone is insufficient to explain the skeletal muscle changes in patients. There was likely self-selection bias towards patients with milder symptoms, as they volunteered to travel to the laboratory for multiple occasions and undergo a maximal exercise test. Our results are therefore not directly applicable to home-bound patients [70]. Similarly, we were unable to account for training status before disease onset. We do not know if previous training status influences susceptibility of skeletal muscle alterations[71,72]. Additionally, the current research design precludes us to draw conclusions about the differences in pathophysiology of long COVID and ME/CFS. ME/CFS patients were diagnosed before 2020, and therefore ill for a significantly longer period. Therefore, we cannot distinguish between disease duration and disease pathophysiology. While we only found a lower capillarization in patients with ME/CFS, we did not assess qualitative markers for microvascular blood flow or red blood cell flux through capillaries in long COVID or ME/CFS. While we attempted to account for any sex differences, we cannot exclude any sex-specific alterations that may occur during bed rest, due to an underpowered comparison. A further limitation is the use of head-down tilt bed rest as a comparator for clinical deconditioning.

Although this model enables long-term experimental control of physical inactivity, it introduces hemodynamic alterations that differ from those experienced by ambulatory patients, particularly with respect to fluid redistribution and orthostatic loading. As such, conclusions drawn from the bed-rest comparison are most robust for skeletal muscle structural and metabolic outcomes, whereas cardiovascular interpretations are necessarily more constrained. Additionally, head-down tilt bed rest may differently affect women due to sex-specific hormones on blood pressure regulation[73].

This study demonstrates that the skeletal muscle determinants of exercise capacity in long COVID and ME/CFS differ from those induced by prolonged bed rest. While $\dot{V}O_{2max}$ and markers for aerobic exercise capacity were similarly low in patients with long COVID and ME/CFS compared to long-term bed rest, respiratory and cardiovascular responses to acute exercise were distinct. Patients with long COVID and ME/CFS displayed higher proportions of type IIa/IIx fibers, and signs of intrinsic mitochondrial dysfunction, observations that were not seen following bed rest. These findings indicate that the lower exercise capacity in patients with long COVID and ME/CFS is not solely due to physical inactivity; therefore rehabilitation strategies for patients should consider that patients with long COVID and ME/CFS are not simply deconditioned, and should be treated as unique cases with alternative rehabilitation strategies. As mitochondrial and endothelial dysfunction appear prominent in both long COVID and ME/CFS, with clear implications on oxygen extraction, future studies should aim to investigate the viability of improving patient mitochondrial and/or endothelial health to reduce patient burden.

Methods

Study Approval and Previous Clinical Trial Primary Outcomes

Two cohorts were compared: one consisting of 24 bed rest participants undergoing a strict 60-day head-down tilt bed rest (occurring before 2020), and one consisting of a cross-sectional design cohort of 25 patients with long COVID, 26 patients with ME/CFS and 30 age- and sex-matched healthy controls that had successfully recovered from an acute SARS CoV-2 infection. The comparison between the two different cohorts was done as a non-pre-specified exploratory analysis, approved by the Amsterdam UMC Medical Research Ethics Committee as an amendment. Sex was considered in both study designs. Recruitment for the bed rest study aimed to obtain a 50:50 sex divide, but since only 8 women were included, sex was used an exploratory variable. The patient cohort study aimed to age- and sex-match all patient

participants with healthy controls, thus reducing the influence of sex. As such, no sex-specific analysis was conducted in either cohort. Sex was determined by self-report by participants.

Participants undergoing bed rest were part of the AGBRESA study (registered at DRKS00015677)[19]. The protocol was approved by the ethics commissions of the Medical Association North Rhine (number 2018143) and NASA (Johnson Space Center, Houston, United States). The AGBRESA study was registered as a clinical trial with the aim to investigate the effects of continuous and intermittent centrifugation on 6° head down tilt bed rest. Written informed consent was obtained from all participants and included the reuse of data for subsequent studies. The primary outcomes from this study have been published previously[16,19,74–76].

Patients with long COVID and patients with ME/CFS were part of a case-control study in the Amsterdam University Medical Center (AUMC) and the Faculty of Behavioral and Movement Sciences (Vrije Universiteit Amsterdam). The study protocol was approved by the medical ethics committee of the Amsterdam UMC (NL78394.018.21) and registered at www.clinicaltrials.gov (NCT05225688). All participants signed a written informed consent before participation. The study was conducted in accordance with the Declaration of Helsinki. The primary outcomes of this trial were 1) skeletal muscle mitochondrial respiratory function before and 24-hours following maximal aerobic exercise and 2) investigate local and systemic inflammation following maximal aerobic exercise to understand post-exertional malaise in patients with long COVID and ME/CFS (in an amendment). Data pertaining to 21 healthy controls and 25 long COVID have been previously published[6]. Primary outcome measurements related to post-exertional malaise in patients with ME/CFS have not yet been published. Here, we present the baseline mitochondrial parameters from patients with ME/CFS.

Study populations

Bed rest

The study details have been reported previously[19]. Briefly, 24 healthy participants underwent a 60-day strict 6 degrees head-down tilt bed rest (Table 1). Participants followed standardized diets, consuming 1.6 times their resting metabolic rate before bed rest and 1.3 times their resting metabolic rate during bed rest. Fluid intake was controlled, and ingestion of caffeine and alcohol were prohibited.

Long COVID and ME/CFS cohort

Patients with long COVID were diagnosed by two experienced clinicians for long COVID symptomology and exclusion of potential differential diagnoses. All long COVID patients were diagnosed with post-exertional malaise (PEM) by the DSQ-PEM[77], had a minimum period of long COVID-related symptoms of six months, and were between 18 and 65 years old. No symptoms were present before the confirmed diagnosis of SARS-CoV-2. None of the included participants were admitted to the hospital during acute SARS-CoV-2 infection and were healthy prior to NAAT or serology-proven SARS-CoV-2 infection. Reported symptom durations (Table 1) were from symptom onset to study enrolment (February 2022 for long COVID and October 2023 for ME/CFS). Exclusion criteria were a medical history of cardiovascular/pulmonary disease, diabetes mellitus, concurrent treatment with metabolism or coagulant-altering drugs during the study period (statins, corticosteroids, SGLT2 inhibitors, GLP1 receptor agonists, platelet aggregation blockers and any anticoagulants), adiposity and body mass index >35 (related to muscle biopsy obtainment), pregnancy, active infection, severe renal dysfunction or any other prior chronic illness or >6 alcohol units per day or >14 alcohol units per week. Smoking was not an exclusion criterion. One long COVID patient was excluded due to a recent SARS-CoV-2 re-infection (<7 days).

Patients with ME/CFS all fulfilled the Canadian Consensus Criteria (CCC), exhibited PEM according to the DSQ-PEM and consulted with a ME/CFS specialist or post-COVID physician, and were between 18 and 65 years old. ME/CFS diagnosis was prior to 2020, and all patients had a confirmed previous diagnosis of SARS-CoV-2. Exclusion criteria were identical to those of the patients with long COVID.

None of the healthy controls had residual symptoms after the SARS-CoV-2 infection and none were hospitalized within 6 months of study participation. Healthy controls withdrew because of the invasive nature of the protocol ($n = 2$), symptoms related to a burn-out ($n = 1$), and a novel diagnosis of uncontrolled hypertension ($n = 1$).

Cardiopulmonary Exercise Testing

All participants underwent cardiopulmonary exercise testing (CPET) on an electronically braked cycle ergometer to assess aerobic exercise capacity. Generally, each test was preceded rest on the ergometer, followed by a baseline cycling phase before beginning the incremental exercise test.

Bed rest participants performed a step incremental test (Lode Excalibur, Lode, Groningen, The Netherlands), whereas patients with long COVID and ME/CFS performed a ramp incremental

exercise test (Lode Excalibur Sport, Lode, Groningen, The Netherlands; Monark L7TT, Monark Sports & Medical, Vansbro, Sweden). Step and ramp protocols have been reported to yield comparable $\dot{V}O_{2max}$ values [78].

Step Test Protocol (bed rest cohort)

Participants first completed 5-min of quiet rest on the cycle ergometer, followed by 3-min of baseline cycling at 50W. Power output then increased by 25 W min^{-1} until task failure. Participants were instructed to maintain 75 RPM, and task failure was defined as the point at which cadence dropped below 70 RPM despite verbal encouragement.

Ramp incremental test (Long COVID & ME/CFS cohort)

Participants completed 2-min quiet rest on the ergometer and 4-min baseline cycling at low intensity between 0 and 20 W. This was followed by a ramped, linear increase in power output (10-60W min^{-1}) until task failure. The individual baseline work rates and ramp slopes were selected based on each participant's anthropometric characteristics and physical activity levels and designed to elicit task failure within 8–12 min. Participants were instructed to maintain their cadence between 70 and 90 revolutions/min, and task failure was defined as the point at which cadence dropped below 60 revolutions/min despite verbal encouragement. Capillary lactate concentrations were determined at rest prior to the onset of the test, during baseline cycling, and immediately following task failure (Lactate Pro 2 LT-1730, ARKRAY Ltd., United Kingdom). Pulmonary gas exchange and ventilation were measured on a breath-by-breath basis (Bed rest: Innocor, Innovision, Odense, Denmark; Patients with long COVID and patients with ME/CFS: Cosmed Quark CPET; Cosmed, Rome, Italy). In all studies, $\dot{V}O_{2max}$ was defined as the highest 30 second rolling average $\dot{V}O_2$ achieved during the test. Achievement of $\dot{V}O_{2max}$ was primarily determined by the presence of a plateau in the $\dot{V}O_2$ as defined by either: 1) increase of $\dot{V}O_2$<100ml/min in the final 2-minutes of testing[79], 2) a $\dot{V}O_2$ slope in the final 2-minutes of exercise that was >50% different of the extrapolated $\dot{V}O_2$ slope prior to the gas exchange threshold[80], or 3) data points in the final 2-minutes lying outside of the 95% confidence interval of the extrapolated $\dot{V}O_2$ slope prior to the gas exchange threshold[79] . Secondary endpoint criteria were also assessed, namely achievement of 1) maximal age-predicted heart rate, 2) blood lactate >8.0 mM, and 3) respiratory exchange ratio >1.15.

The gas exchange threshold (GET) was assessed using 10-second binned averages as the point of non-linear rise in $\dot{V}CO_2$ relative to $\dot{V}O_2$ using the V-slope method[81], and verified with visual inspection. The GET was then confirmed visually by assessing $\dot{V}E$ vs $\dot{V}O_2$, $\dot{V}E/\dot{V}CO_2$ vs $\dot{V}O_2$,

and $\dot{V}E/\dot{V}O_2$ vs $\dot{V}O_2$. Respiratory compensation point (RCP) was assessed as the point of non-linear rise in $\dot{V}E$ relative to $\dot{V}O_2$ using the V-slope method, and again verified visually. Presence of the RCP was confirmed by visual inspection of the $\dot{V}E/\dot{V}CO_2$ vs $\dot{V}O_2$ and $PetCO_2$ vs $\dot{V}O_2$.

Maximal acute exercise values were taken as the highest 30-second rolling averages of the respective parameters. The $\dot{V}E/\dot{V}CO_2$ slope was calculated as the linear rise until RCP. Heart rate-$\dot{V}O_2$ slopes were calculated using the entirety of the exercise test and taken as the slope of heart rate compared to $\dot{V}O_2$. Baseline heart rate was calculated using an average over the 5-minute quiet rest, with the first 30-seconds and last 30-seconds being disregarded. Adjusted heart rate reserve was calculated as the $(HR_{max}- HR_{baseline})/(220- age-HR_{baseline})$.

Due to software issues, three patients with ME/CFS undertook ramp rates that were too high, resulting in a duration of exercise that was not sufficient to establish acute exercise responses. Evaluation of maximal exercise was still possible in these participants, thus submaximal values were excluded.

Skeletal muscle measurements

Biopsy Procedure

Muscle biopsies were obtained from the vastus lateralis at one-third of the distal length (approximately 150mg weight wet) using a rongeur (4mm diameter for the bed rest cohort) or a suction-supported 5mm Bergström needle (Pelomi, Albertslund Denmark; for the long COVID & ME/CFS patient cohort) under sterile conditions after skin disinfection and local anesthesia with 2% lidocaine[6,16]. Muscle biopsies were taken before and after 55 days of head-down tilt bed rest. One ~30 mg piece was aligned according to the muscle fiber arrangement under a light microscope and frozen in liquid nitrogen for histochemistry, and another ~15 mg piece was utilized for high-resolution respirometry experiments. Muscle biopsies from patients and healthy controls were obtained 6 days prior to the CPET, and all participants were instructed to refrain from strenuous activity at least 24 hours prior to the biopsy procedure.

All biopsies used for histochemistry were frozen in liquid nitrogen and stored in liquid nitrogen at −196°C. Frozen muscle samples were mounted using freeze-gel (Q Path, VWR, Netherlands) and cut into 10 µm thick sections in transverse orientation in a cryostat (Microm HM550, Adamas Instrumenten, Netherlands) at -20ºC, before being mounted on polylysine-coated slides, and stored at −80°C until staining. Due to issues with tissue freezing, histological

analysis was completed on samples from 17 participants pre- and post-bed rest, 24 patients with long COVID, 23 patients with ME/CFS, and 30 healthy controls.

Skeletal muscle respirometry

Mitochondrial respiration was assessed in permeabilized fibers as described previously[6]. Small bundles of freshly isolated fibers were permeabilized with 50 µg mL^{-1} saponin for 20 min at 4 °C in a solution consisting of (in mM) CaEGTA (2.8), EGTA (7.2), ATP (5.8), $MgCl_2$ (6.6), taurine (20), phosphocreatine (15), imidazole (20), DTT (0.5) and MES (50) (pH 7.1). Tissue was washed in respiration solution containing EGTA (0.5), $MgCl_2$ (3), K-lactobionate (60), taurine (20), KH_2PO_4 (10), HEPES (20), sucrose (110) and 1 g L^{-1} fatty acid-free BSA (pH 7.1), quickly blotted dry, weighed and transferred to a respirometer (Oxygraph-2k; Oroboros Instruments, Innsbruck, Austria) in respiration solution at 37 °C. Oxygen concentration was maintained above 300 µM throughout the experiment to avoid limitations in oxygen supply. Background respiration was assessed before adding substrates and was subtracted from all subsequent values. Leak respiration (L) was assessed after the addition of sodium glutamate (10 mM), sodium malate (0.5 mM), and sodium pyruvate (5 mM). NADH (Complex I)-linked respiration was assessed after the addition of 5 mM ADP, and 10 µM cytochrome c to confirm the absence of outer-mitochondrial membrane damage. Maximal oxidative phosphorylation capacity, with simultaneous convergent electron input via NADH and FADH-linked pathways, was measured after the addition of 10 mM succinate. Maximum uncoupled respiration (E) was determined via titration of carbonylcyanide-4-trifluoro-methoxyphenylhydrazone (FCCP) in 0.5 µM steps until no further increase in oxygen consumption was observed. Succinate-linked respiration was measured after blocking mitochondrial complex I with 0.5 µM rotenone. Two measurements per sample were performed simultaneously, and the results were averaged. Respiration values were normalized to wet weight and expressed in pmol $O_2 \cdot s^{-1}$ mg^{-1}. Samples that increased more than 10% from the addition of 5mM of ADP to 10 µM cytochrome c were excluded from analysis. E/L coupling efficiency was calculated as the difference between maximum uncoupled respiration and leak respiration divided by the maximum uncoupled respiration. The phosphorylation capacity through complex I (normalized NADH-linked respiration) and complex II (normalized succinate-linked respiration) were calculated as Complex I-linked respiration normalized to maximal oxidative phosphorylation capacity, and Complex II-linked respiration normalized to maximal uncoupled respiration, respectively.

Immuno-histochemistry

To visualize muscle fiber type and cross-sectional area, immunohistochemistry was carried out on 10 µm thick sections from the vastus lateralis muscle biopsies. Details about dilutions and vendors can be found in Table 2.

Table 2: List of antibody vendors.

Parameter	**Primary antibody, dilution, vendor**	**Catalog #/RRID**	**Secondary Antibody, dilution, vendor**	**Catalog #/RRID**
Muscle Fiber Type	BA-D5, 1µg/mL, DSHB 6H1, 5µg/mL, DSHB SC-71 1µg/mL, DSHB WGA 350, 1:25, Invitrogen	DSHB Cat# BA-D5, RRID:AB_2235587 DSHB Cat# 6H1, RRID:AB_1157897 DSHB Cat# SC-71, RRID:AB_2147165 W11263	Goat Anti-mouse IgG2B 555, 1:2000, Invitrogen Goat Anti-mouse IgM 488, 1:2000, Invitrogen Goat Anti-mouse IgG1 647,1:2000, Invitrogen	Thermo Fisher Scientific Cat# A-21147, RRID:AB_2535783 Thermo Fisher Scientific Cat# A-21042, RRID:AB_2535711 Thermo Fisher Scientific Cat# A-21240, RRID:AB_2535809
Capillaries	Ulex europaeus agglutinin I, 20µg/mL , Vector Laboratories	Vector Laboratories Cat# B-1065, RRID:AB_2336766	Vectastain Elite ABC Kit PK-6100, Vector Laboratories ImmPACT™ AMEC Red Peroxidase Substrate, Vector Laboratories	Vector Laboratories Cat# PK-6100, RRID:AB_2336819 Vector Laboratories Cat# SK-4285, RRID:AB_2336519

Fiber-type composition

Skeletal muscle fiber type quantification and size were assessed using immunofluorescence techniques using primary antibodies against myosin heavy chain (MHC) I (BA-D5), MHC IIa (SC-71), and MHC IIx (6H1)[6]. Firstly, sections were air-dried for 10 min and then blocked with 10% normal goat serum (NGS) for 60 min. Subsequently, slides were washed 3 times for 5 min each in 1x phosphate-buffered saline (PBS) and incubated with the primary antibodies for 60 min at room temperature. Slides were washed, and subsequently incubated with the secondary antibodies for 60 min in the dark at room temperature. Another washing step was performed and subsequently, the slides were incubated with Wheat Germ Agglutinin (WGA) for 30 minutes in the dark at room temperature. This was followed by a final washing step before the sections were mounted with coverslips using Vectashield Vibrance. Analysis was performed with ImageJ and a modified version of Sandia Matlab AnalysiS Hierarchy (SMASH) Toolbox (version 1.0) in Matlab (Version 2022a). Fiber type composition was expressed as the cross-sectional area occupied by each fiber type as a percentage of the cross-sectional area of all fibers. This allowed for quantification of fiber type specific fiber cross-sectional area.

Succinate dehydrogenase activity

Sections were stained for SDH activity as described previously[6]. Immediately after cutting, sections were air-dried for 15 min and then immersed in a pre-heated (37 °C) solution containing sodium phosphate buffer (0.1 M, pH 7.6), sodium succinate (0.2 M), sodium azide (14 mM) and tetranitro blue tetrazolium (TNBT, 0.55 mM, Sigma-Aldrich) for 20 min in the dark, and the reaction was stopped by brief HCl (0.01 M) exposure before sections were washed and mounted with glycerin-gelatin. Sections were stored at 4 °C and imaged within ten days. The averaged SDH activity was obtained by outlining 40 individual skeletal muscle fibers per participant and absorbance was assessed using ImageJ (Version 1.54f, NIH, Bethesda, USA). Values were expressed as ΔA_{660} per µm tissue thickness per second of staining time ($\Delta A_{660}\ \mu m^{-1}\ s^{-1}$).

Capillarization

Capillarization was assessed by staining for Ulex Europaeus Agglutinin 1 lectin (UEA-1)[6]. Sections were air-dried for 10 min and fixated in ice-cold acetone (−20 °C) for 15 min. Subsequently, slides were washed 3 times for 2 min in PBS and blocked with 1% bovine serum

album for 30 min. Afterwards, slides were incubated with UEA-1 for 30 min at room temperature, followed by wash steps and incubation with Vectastain Elite ABC kit for 30 min at room temperature. After washing, incubation with Red Peroxidase substrate for 10 min at room temperature was performed, washed, and sections were mounted with glycerin-gelatin (heated at 37 °C). Capillary-to-fiber ratio and capillary density by capillaries per mm^2 muscle tissue, and capillary cross sectional area were determined in ImageJ. Where available, capillary images were overlain with fiber type images to quantify fiber specific capillary-to-fiber ratios, wherein a minimum of 20 type I and 20 type II fibers were analyzed per participant. Fibers were deemed either type I positive (type I) or type I negative (type II), and capillaries were summed as capillary divided by # of fiber contacts per capillary.

Myoglobin Content

To assess intracellular myoglobin content, muscle biopsy sections were freeze-dried and fixed with paraformaldehyde (158127, Sigma-Aldrich) at 70-75°C for 60min using a vapor-fixation technique[82]. Slides were fixed with 2.5% glutaraldehyde (G5882, Sigma-Aldrich) buffer for 10min before a 60min incubation in O-tolidine-containing solution. The O-tolidine-containing solution was prepared in 62 ml 50 mM Tris-80 mM KCl buffer containing 25 mg ortho-tolidine (T8533, Sigma- Aldrich), dissolved in 2 ml 95% ethanol, and 1.43 ml 70% tertiary-butyl-hydroperoxide (458139, Sigma- Aldrich). Incubations were performed at 50 °C. Sections were washed and mounted with glycerin-gelatin. Ninety randomly selected fibers regardless of fiber type were analyzed using Fiji[83]. Values were expressed as arbitrary unit (AU).

Image acquisition

Slides were dried overnight at 4 °C before imaging. Images for fiber type and capillarization analysis were taken at ×20 magnification with VS200 Research Slide Scanner (Olympus) using Slideview 5.0. SDH images were taken with a DMRB microscope (Leica, Wetzlar) using a CCD camera, calibrated gray filters, and an individual calibration curve at 660 nm. Myoglobin images were captured with ×20/0.4 objective using a CCD camera at 436±9nm absorbance. Approximately fifteen images were taken per sample, with 5 images per slide-section. All images were manually evaluated to exclude those containing out-of-focus areas, artifacts, and large areas of connective tissue. Image processing and analysis was conducted using ImageJ (version 1.53u and later). Fiber type composition was performed with ImageJ and Sandia Matlab AnalysiS Hierarchy (SMASH) Toolbox (version 1.0) in Matlab (version 2022a).

Statistical analysis

Distributions were assessed with histograms and Shapiro–Wilk tests. Parametric quantitative variables are presented as means ± standard deviation (SD), and nonparametric quantitative variables are presented as median and interquartile ranges (IQR; 25th and 75th percentiles). Jitter plots are plotted with means represented as single bars. All individual points represent a participant.

Non-normally distributed data were transformed using Box-Cox transformation in order to obtain a normal distribution for statistical analysis. Continuous parametric data were analyzed using a 2-tailed paired *t*-test or analysis of variance, with Tukey HSD post-hoc testing, where appropriate. If data remained non-normally distributed following the Box-Cox transformation, the continuous nonparametric data were analyzed using the Mann–Whitney *U* test, Kruskal–Wallis *H* test, or pairwise Wilcoxon test with Benjamini–Hochberg correction where appropriate. Correlations were analyzed using the Pearson correlation coefficient for linear relationships. Correlation coefficients were compared using the R package *cocor*. Pertinent to bed rest data, if data was missing in either the before or after bed rest condition, the participant was removed from the analysis to maintain equal sample sizes and appropriate pairing. All data were analyzed using R studio built under R version 4.0.3 (R Core Team 2013, Vienna, Austria).

Reuse of previously published data

Some results from bed rest participants were reanalyzed from previously published data[19,75]. Biopsies were restained and analyzed for capillarization, muscle fiber type, and myoglobin content to account for differences in staining protocols and analysis procedures. A part of the results from patients with long COVID and 21 healthy controls were previously published[6].

Data Availability

The processed data generated in this study are publicly available via the GitHub repository (doi: 10.5281/zenodo.20642303)[84]. The raw data are not publicly available due to data privacy laws. For access to raw data files, please submit a request to Dr. Rob Wüst (r.wust@vu.nl) with a detailed description of which raw data is being requested and planned uses of raw data files. Requests that satisfy reuse policies will be approved within 2 months. The source data file is available in the supplemental files. Source data can also be accessed via the GitHub repository: https://github.com/bcn95/LC_ME_CFS_BED_REST.

Code Availability

R codes are available in the supplemental files and via the GitHub repository[84]. All codes and a ReadMe file can be found at https://github.com/bcn95/LC_ME_CFS_BED_REST.

Acknowledgements

We thank Ellen A. Breedveld, Esmee van den Berg, Tom Kerkhoff, Jules Verwee, Luuk Groeneveld, Augustijn M Klarenbeek, Jessie Hulscher, and Noor Bijvang for their help during the data collection of the long COVID and ME/CFS patients, and Bergita Ganse, Alessandra Bosutti, Edwin Mulder and Jörn Rittweger for their help in the AGBRESA bed rest study. The authors want to thank our patient representatives for insightful discussions.

Funding

This study was supported by the Patient-Led Research Collaborative for Long COVID, the AMC and VU Foundations, ZonMw Onderzoeksprogramma for ME/CVS and post-COVID (numbers 10091012110025 and 11080022410019), the Solve ME 2022 Ramsay Grant Program, ME Research UK, ME Stars of Tomorrow Scholarship award from the ICanCME Research Network (to B.T.C.), Amsterdam Movement Sciences and Stichting Long COVID Nederland. M.E. is currently a member of the FOR 5795 “HyperMet”, which is funded by the Deutsche Forschungsgemeinschaft (DFG, German Research Foundation, 536691227). We acknowledge the UK Space Agency (ST/S0001735/1 and ST/T00066X/1), the European Space Agency (ESA; 16-16ESA AGBR-0013, contract number 4000113871/15/NL/PG), the National Aeronautics and Space Administration (NASA; contract number 80JSC018P0078).

Author Contributions

Study design and concept: BTC, BA, RPG, HD, MvV, RCIW

Data acquisition: BTC, AS, BA, RPG, JYH, ME, WN, PWH, FWB, JJP, PvA,

Data analysis: BTC, AS, JH, RPG, ME

Writing manuscript: BTC, AS, BA, JYH, ME, WN, PWH, FWB, JJP, PvA, RPG, HD, RTJ, MvV, RCIW

Competing interests

All authors have declared no conflict of interest.

References

1. Shah, W., Hillman, T., Playford, E. D. & Hishmeh, L. Managing the long term effects of covid-19: summary of NICE, SIGN, and RCGP rapid guideline. *BMJ* n136 (2021) doi:10.1136/bmj.n136.

2. Michelen, M. *et al.* Characterising long COVID: a living systematic review. *BMJ Glob. Health* **6**, e005427 (2021).

3. Nalbandian, A. *et al.* Post-acute COVID-19 syndrome. *Nat. Med.* **27**, 601–615 (2021).

4. Thaweethai, T. *et al.* Development of a Definition of Postacute Sequelae of SARS-CoV-2 Infection. *JAMA* **329**, 1934–1946 (2023).

5. Komaroff, A. L. & Lipkin, W. I. ME/CFS and Long COVID share similar symptoms and biological abnormalities: road map to the literature. *Front. Med. (Lausanne).* **10**, (2023).

6. Appelman, B. *et al.* Muscle abnormalities worsen after post-exertional malaise in long COVID. *Nat. Commun.* **15**, 17 (2024).

7. Colosio, M. *et al.* Structural and functional impairments of skeletal muscle in patients with postacute sequelae of SARS-CoV-2 infection. *J. Appl. Physiol.* **135**, 902–917 (2023).

8. Behan, W. M. H., More, I. A. R. & Behan, P. O. Mitochondrial abnormalities in the postviral fatigue syndrome. *Acta Neuropathol.* **83**, 61–65 (1991).

9. Aschman, T. *et al.* Post-COVID exercise intolerance is associated with capillary alterations and immune dysregulations in skeletal muscles. *Acta Neuropathol. Commun.* **11**, 193 (2023).

10. Bizjak, D. A. *et al.* Functional and Morphological Differences of Muscle Mitochondria in Chronic Fatigue Syndrome and Post-COVID Syndrome. *Int. J. Mol. Sci.* **25**, 1675 (2024).

11. Hejbøl, E. K. *et al.* Myopathy as a cause of fatigue in long-term post-COVID-19 symptoms: Evidence of skeletal muscle histopathology. *Eur. J. Neurol.* **29**, 2832–2841 (2022).

12. Agergaard, J. *et al.* Myopathy as a cause of Long COVID fatigue: Evidence from quantitative and single fiber EMG and muscle histopathology. *Clinical Neurophysiology* **148**, 65–75 (2023).

13. Inglis, E. C. *et al.* Heavy-, Severe-, and Extreme-, but Not Moderate-Intensity Exercise Increase V̇O2max and Thresholds after 6 wk of Training. *Med. Sci. Sports Exerc.* **56**, 1307–1316 (2024).

14. Mølmen, K. S., Almquist, N. W. & Skattebo, Ø. Effects of Exercise Training on Mitochondrial and Capillary Growth in Human Skeletal Muscle: A Systematic Review and Meta-Regression. *Sports Medicine* **55**, 115–144 (2025).

15. Edward, J. A. *et al.* Characteristics and Treatment of Exercise Intolerance in Patients With Long COVID. *J. Cardiopulm. Rehabil. Prev.* **43**, 400–406 (2023).

16. Eggelbusch, M. *et al.* The impact of bed rest on human skeletal muscle metabolism. *Cell Rep. Med.* **5**, 101372 (2024).

17. Buso, A. *et al.* Mitochondrial Adaptations in Elderly and Young Men Skeletal Muscle Following 2 Weeks of Bed Rest and Rehabilitation. *Front. Physiol.* **10**, (2019).

18. Coyle, E. F., Martin, W. H., Bloomfield, S. A., Lowry, O. H. & Holloszy, J. O. Effects of detraining on responses to submaximal exercise. *J. Appl. Physiol.* **59**, 853–859 (1985).

19. Hendrickse, P. W. *et al.* Capillary rarefaction during bed rest is proportionally less than fibre atrophy and loss of oxidative capacity. *J. Cachexia Sarcopenia Muscle* **13**, 2712–2723 (2022).

20. Coyle, E. F. *et al.* Time course of loss of adaptations after stopping prolonged intense endurance training. *J. Appl. Physiol.* **57**, 1857–1864 (1984).

21. Chi, M. M. *et al.* Effects of detraining on enzymes of energy metabolism in individual human muscle fibers. *American Journal of Physiology-Cell Physiology* **244**, C276–C287 (1983).

22. Hoffmann, F. *et al.* Cardiac adaptations to 60 day head-down-tilt bed rest deconditioning. Findings from the AGBRESA study. *ESC Heart Fail.* **8**, 729–744 (2021).

23. Miyamura, M. & Ishida, K. Adaptive changes in hypercapnic ventilatory response during training and detraining. *Eur. J. Appl. Physiol. Occup. Physiol.* **60**, 353–359 (1990).

24. Chen, Y., Hsieh, Y., Ho, J., Lin, T. & Lin, J. Two weeks of detraining reduces cardiopulmonary function and muscular fitness in endurance athletes. *Eur. J. Sport Sci.* **22**, 399–406 (2022).

25. Naeije, R. & Caravita, S. Phenotyping long COVID. *European Respiratory Journal* **58**, 2101763 (2021).

26. Broxterman, R. M., Wagner, P. D. & Richardson, R. S. Endurance exercise training changes the limitation on muscle V̇O2max in normoxia from the capacity to utilize O_2 to the capacity to transport O_2. *J. Physiol.* **602**, 445–459 (2024).

27. van der Zwaard, S. *et al.* Maximal oxygen uptake is proportional to muscle fiber oxidative capacity, from chronic heart failure patients to professional cyclists. *J. Appl. Physiol.* **121**, 636–645 (2016).

28. Degens, H. *et al.* Diffusion and physical constraints limit oxidative capacity, capillary supply and size of muscle fibres in mice and humans. *Exp. Physiol.* **111**, 212–225 (2026).

29. Watson, M., Ionescu, M. F., Sylvester, K. & Fuld, J. Minute ventilation/carbon dioxide production in patients with dysfunctional breathing. *European Respiratory Review* **30**, 200182 (2021).

30. Clark, A. L., Volterrani, M., Swan, J. W. & Coats, A. J. The increased ventilatory response to exercise in chronic heart failure: relation to pulmonary pathology. *Heart* **77**, 138–146 (1997).

31. Padilla, D. J., McDonough, P., Kindig, C. A., Erickson, H. H. & Poole, D. C. Ventilatory dynamics and control of blood gases after maximal exercise in the Thoroughbred horse. *J. Appl. Physiol.* **96**, 2187–2193 (2004).

32. Zhang, Y. Y., Sietsema, K. E., Sullivan, C. S. & Wasserman, K. A method for estimating bicarbonate buffering of lactic acid during constant work rate exercise. *Eur. J. Appl. Physiol. Occup. Physiol.* **69**, 309–315 (1994).

33. Casey, K., Duffin, J. & McAvoy, G. V. The effect of exercise on the central-chemoreceptor threshold in man. *J. Physiol.* **383**, 9–18 (1987).

34. Santolicandro, A. *et al.* Mechanisms of hypoxemia and hypocapnia in pulmonary embolism. *Am. J. Respir. Crit. Care Med.* **152**, 336–347 (1995).

35. Porcelli, S. *et al.* Role of skeletal muscles impairment and brain oxygenation in limiting oxidative metabolism during exercise after bed rest. *J. Appl. Physiol.* **109**, 101–111 (2010).

36. Salvadego, D. *et al.* Separate and combined effects of a 10-d exposure to hypoxia and inactivity on oxidative function in vivo and mitochondrial respiration ex vivo in humans. *J. Appl. Physiol.* **121**, 154–163 (2016).

37. Kamiya, A. *et al.* Pathophysiology of orthostatic hypotension after bed rest: paradoxical sympathetic withdrawal. *American Journal of Physiology-Heart and Circulatory Physiology* **285**, H1158–H1167 (2003).

38. Spaak, J., Montmerle, S., Sundblad, P. & Linnarsson, D. Long-term bed rest-induced reductions in stroke volume during rest and exercise: cardiac dysfunction vs. volume depletion. *J. Appl. Physiol.* **98**, 648–654 (2005).

39. Convertino, V. A., Doerr, D. F., Eckberg, D. L., Fritsch, J. M. & Vernikos-Danellis, J. Head-down bed rest impairs vagal baroreflex responses and provokes orthostatic hypotension. *J. Appl. Physiol.* **68**, 1458–1464 (1990).

40. Joseph, P. *et al.* Insights From Invasive Cardiopulmonary Exercise Testing of Patients With Myalgic Encephalomyelitis/Chronic Fatigue Syndrome. *Chest* **160**, 642–651 (2021).

41. Singh, I. *et al.* Persistent Exertional Intolerance After COVID-19: Insights From Invasive Cardiopulmonary Exercise Testing. *Chest* **161**, 54–63 (2022).

42. Smith, R. S. & Ovalle, W. K. Varieties of fast and slow extrafusal muscle fibres in amphibian hind limb muscles. *J. Anat.* **116**, 1–24 (1973).

43. McCully, K. K., Smith, S., Rajaei, S., Leigh, J. S. & Natelson, B. H. Muscle metabolism with blood flow restriction in chronic fatigue syndrome. *J. Appl. Physiol.* **96**, 871–878 (2004).

44. Scherbakov, N. *et al.* Peripheral endothelial dysfunction in myalgic encephalomyelitis/chronic fatigue syndrome. *ESC Heart Fail.* **7**, 1064–1071 (2020).

45. Newton, D. J. *et al.* Large and small artery endothelial dysfunction in chronic fatigue syndrome. *Int. J. Cardiol.* **154**, 335–336 (2012).

46. Haffke, M. *et al.* Endothelial dysfunction and altered endothelial biomarkers in patients with post-COVID-19 syndrome and chronic fatigue syndrome (ME/CFS). *J. Transl. Med.* **20**, 138 (2022).

47. Sandvik, M. K. *et al.* Endothelial dysfunction in ME/CFS patients. *PLoS One* **18**, e0280942 (2023).

48. Goulding, R. P. Re-evaluating central *versus* peripheral contributions to maximal oxygen uptake: the role of muscle diffusive capacity. *J. Physiol.* **602**, 5391–5393 (2024).

49. Gifford, J. R. *et al.* Symmorphosis and skeletal muscle : *in vivo* and *in vitro* measures reveal differing constraints in the exercise-trained and untrained human. *J. Physiol.* **594**, 1741–1751 (2016).

50. Osiaevi, I. *et al.* Persistent capillary rarefication in long COVID syndrome. *Angiogenesis* **26**, 53–61 (2023).

51. Bosutti, A. *et al.* Whey protein with potassium bicarbonate supplement attenuates the reduction in muscle oxidative capacity during 19 days of bed rest. *J. Appl. Physiol.* **121**, 838–848 (2016).

52. Plyley, M. J., Olmstead, B. J. & Noble, E. G. Time course of changes in capillarization in hypertrophied rat plantaris muscle. *J. Appl. Physiol.* **84**, 902–907 (1998).

53. Bosutti, A. *et al.* Local capillary supply in muscle is not determined by local oxidative capacity. *Journal of Experimental Biology* https://doi.org/10.1242/jeb.126664 (2015) doi:10.1242/jeb.126664.

54. Vincent, L. *et al.* Effects of regular physical activity on skeletal muscle structural, energetic, and microvascular properties in carriers of sickle cell trait. *J. Appl. Physiol.* **113**, 549–556 (2012).

55. Charifi, N. *et al.* Enhancement of microvessel tortuosity in the vastus lateralis muscle of old men in response to endurance training. *J. Physiol.* **554**, 559–569 (2004).

56. Pries, A. R., Reglin, B. & Secomb, T. W. Remodeling of Blood Vessels. *Hypertension* **46**, 725–731 (2005).

57. Zuccarelli, L. *et al.* Peripheral impairments of oxidative metabolism after a 10-day bed rest are upstream of mitochondrial respiration. *J. Physiol.* **599**, 4813–4829 (2021).

58. Nunes, M. *et al.* Virus-induced endothelial senescence as a cause and driving factor for ME/CFS and long COVID: mediated by a dysfunctional immune system. *Cell Death Dis.* **17**, 16 (2026).

59. Wagner, P. D. Systemic oxygen transport and utilization. *J. Breath Res.* **2**, 024001 (2008).

60. Wagner, P. D. Determinants of maximal oxygen consumption. *J. Muscle Res. Cell Motil.* **44**, 73–88 (2023).

61. Poole, D. C., Musch, T. I. & Colburn, T. D. Oxygen flux from capillary to mitochondria: integration of contemporary discoveries. *Eur. J. Appl. Physiol.* **122**, 7–28 (2022).

62. Narici, M. V., Roi, G. S., Landoni, L., Minetti, A. E. & Cerretelli, P. Changes in force, cross-sectional area and neural activation during strength training and detraining of the human quadriceps. *Eur. J. Appl. Physiol. Occup. Physiol.* **59**, 310–319 (1989).

63. Klausen, K., Andersen, L. B. & Pelle, I. Adaptive changes in work capacity, skeletal muscle capillarization and enzyme levels during training and detraining. *Acta Physiol. Scand.* **113**, 9–16 (1981).

64. Houston, M. E., Froese, E. A., Valeriote, St. P., Green, H. J. & Ranney, D. A. Muscle performance, morphology and metabolic capacity during strength training and detraining: A one leg model. *Eur. J. Appl. Physiol. Occup. Physiol.* **51**, 25–35 (1983).

65. Trappe, S. *et al.* Human single muscle fibre function with 84 day bed-rest and resistance exercise. *J. Physiol.* **557**, 501–513 (2004).

66. Gallagher, P. *et al.* Effects of 84-days of bedrest and resistance training on single muscle fibre myosin heavy chain distribution in human vastus lateralis and soleus muscles. *Acta Physiol. Scand.* **185**, 61–69 (2005).

67. Borina, E., Pellegrino, M. A., D'Antona, G. & Bottinelli, R. Myosin and actin content of human skeletal muscle fibers following 35 days bed rest. *Scand. J. Med. Sci. Sports* **20**, 65–73 (2010).

68. Murgia, M. *et al.* Signatures of muscle disuse in spaceflight and bed rest revealed by single muscle fiber proteomics. *PNAS Nexus* **1**, (2022).

69. Haunhorst, S. *et al.* Towards an understanding of physical activity-induced post-exertional malaise: Insights into microvascular alterations and immunometabolic interactions in post-COVID condition and myalgic encephalomyelitis/chronic fatigue syndrome. *Infection* **53**, 1–13 (2025).

70. Sommerfelt, K., Schei, T. & Angelsen, A. Severe and Very Severe Myalgic Encephalopathy/Chronic Fatigue Syndrome ME/CFS in Norway: Symptom Burden and Access to Care. *J. Clin. Med.* **12**, 1487 (2023).

71. Balan, E. *et al.* No effect of the endurance training status on senescence despite reduced inflammation in skeletal muscle of older individuals. *American Journal of Physiology-Endocrinology and Metabolism* **319**, E447–E454 (2020).

72. Carrick-Ranson, G. *et al.* The effect of lifelong exercise dose on cardiovascular function during exercise. *J. Appl. Physiol.* **116**, 736–745 (2014).

73. Pavy-Le Traon, A., Heer, M., Narici, M. V., Rittweger, J. & Vernikos, J. From space to Earth: advances in human physiology from 20 years of bed rest studies (1986–2006). *Eur. J. Appl. Physiol.* **101**, 143–194 (2007).

74. Laurie, S. S. *et al.* Optic disc edema and chorioretinal folds develop during strict 6° head-down tilt bed rest with or without artificial gravity. *Physiol. Rep.* **9**, (2021).

75. Kramer, A. *et al.* Daily 30-min exposure to artificial gravity during 60 days of bed rest does not maintain aerobic exercise capacity but mitigates some deteriorations of muscle function: results from the AGBRESA RCT. *Eur. J. Appl. Physiol.* **121**, 2015–2026 (2021).

76. Clément, G. *et al.* Assessing the effects of artificial gravity in an analog of long-duration spaceflight: The protocol and implementation of the AGBRESA bed rest study. *Front. Physiol.* **13**, (2022).

77. Cotler, J., Holtzman, C., Dudun, C. & Jason, L. A. A Brief Questionnaire to Assess Post-Exertional Malaise. *Diagnostics* **8**, 66 (2018).

78. Zhang, Y. Y., Johnson, M. C., Chow, N. & Wasserman, K. Effect of exercise testing protocol on parameters of aerobic function. *Med. Sci. Sports Exerc.* **23**, 625–30 (1991).

79. Poole, D. C., Wilkerson, D. P. & Jones, A. M. Validity of criteria for establishing maximal O2 uptake during ramp exercise tests. *Eur. J. Appl. Physiol.* **102**, 403–410 (2008).

80. Midgley, A. W., Carroll, S., Marchant, D., McNaughton, L. R. & Siegler, J. Evaluation of true maximal oxygen uptake based on a novel set of standardized criteria. *Applied Physiology, Nutrition, and Metabolism* **34**, 115–123 (2009).

81. Beaver, W. L., Wasserman, K. & Whipp, B. J. A new method for detecting anaerobic threshold by gas exchange. *J. Appl. Physiol.* **60**, 2020–2027 (1986).

82. van Beek-Harmsen, B. J., Bekedam, M. A., Feenstra, H. M., Visser, F. C. & van der Laarse, W. J. Determination of myoglobin concentration and oxidative capacity in cryostat sections of human and rat skeletal muscle fibres and rat cardiomyocytes. *Histochem. Cell Biol.* **121**, 335–342 (2004).

83. Schindelin, J. *et al.* Fiji: an open-source platform for biological-image analysis. *Nat. Methods* **9**, 676–682 (2012).

84. Charlton, B. T. *et al.* Skeletal muscle properties in Long COVID and ME/CFS differ from those induced by bed rest. *GitHub* (2026). DOI: 10.5281/zenodo.20642303.

Supplemental Information

Supplemental Table 1. Sub-cohort characteristics with both cohorts now matched for age and sex. Data presented as median (IQR). Pre-bed rest participants were shorter than healthy, patient-matched controls (p=0.038). Patients with long COVID had experienced symptoms for a shorter time-period than patients with myalgic encephalomyelitis/chronic fatigue syndrome (ME/CFS, p<0.001). All data remained non-normally distributed following Box-Cox transformations. Group differences between pre-bed rest and healthy, patient-matched controls were assessed using Group differences between post-bed rest, long COVID and ME/CFS were compared using a Kruskal-Wallis test, with pairwise Wilcoxon signed-rank test post-hoc where applicable. Differences between patients with long COVID and patients with ME/CFS in symptom duration and daily steps were assessed using Wilcoxon signed-rank tests.

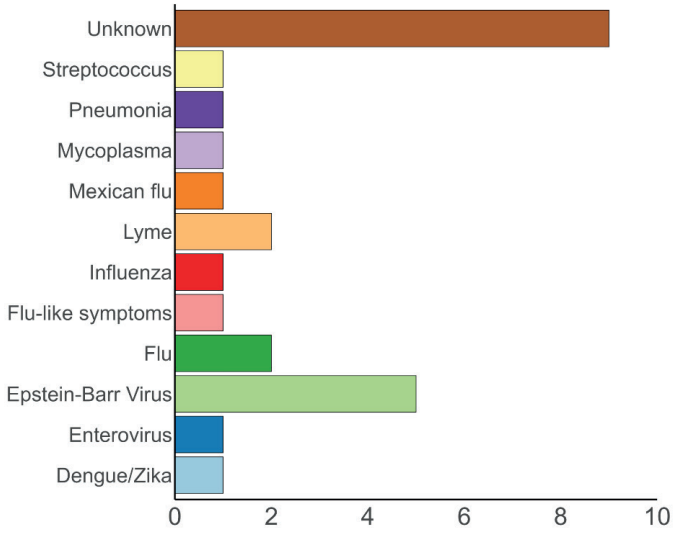
	Bed rest	**Healthy Control**	**Bed rest**	**Long COVID**	**ME/CFS**
	Pre		**Post**		
Participants (# Females)	**17 (7)**	**17 (7)**	**13 (7)**	**13 (7)**	**13 (7)**
Age (years)	**34 (29-43)**	**34 (29-42)**	**29 (27-40)**	**31 (28-42)**	**32 (28-42)**
Height (cm)	**175 (172-179) ***	**180 (176-186)**	**174 (162-175)**	**177 (168-191)**	**175 (172-186)**
Weight (kg)	**76 (69-80)**	**74 (63-86)**	**70 (66-76)**	**82 (71-90)**	**84 (75- 86)**
Symptom Duration (days)	**n/a**	**n/a**	**n/a**	**500 (408-599) †††**	**3793 (2463-4613)**
Daily Steps (steps.day^{-1})	**ND**	**7011 (4770-8316)**	**0 (0 0)**	**3970 (2794-5030)**	**3827 (2722-4901)**

***: *vs.* healthy control; †: *vs.* ME/CFS; §: *vs*. Bed rest**

***: p<0.05; **: p<0.01; ***: p<0.001**

Supplemental Table 2. Primary and secondary Endpoints for exercise testing. Data pertaining to primary and secondary endpoint criteria of cardiopulmonary exercise tests are summarized below. Across 129 tests, 40 tests did not meet any of the primary endpoint criteria, while only 7 tests failed to meet any primary or secondary endpoint criteria. Lactate values were not collected during the bed rest study.

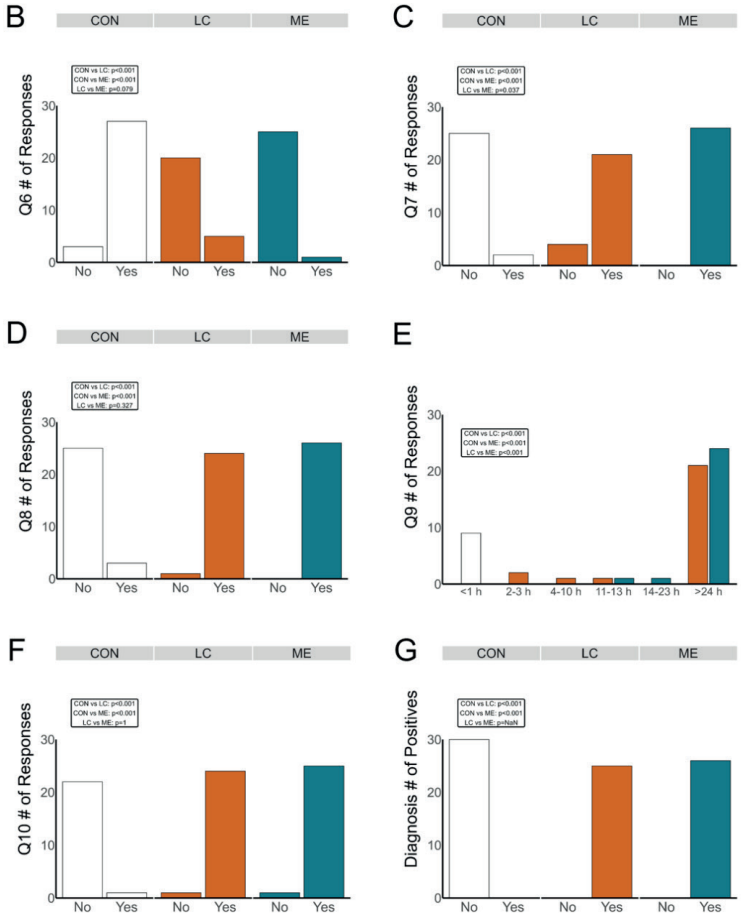
Primary Endpoints	**Before Bed rest (n=24)**	**After Bed rest (n=24)**	**CON (n=30)**	**LC (n=25)**	**ME/CFS (n=26)**
Final 2min $\dot{V}O_2$ slope <100ml/min (n)	**4**	**3**	**5**	**10**	**10**
Final 2min $\dot{V}O_2$ Slope >50% difference (n)	**1**	**9**	**7**	**13**	**7**
Points outside 95% CI in final 2min (n)	**11**	**7**	**17**	**11**	**7**
Secondary Endpoints					
Achieved Adjusted Max Heart Rate (n)	**2**	**9**	**13**	**8**	**4**
Achieved blood lactate >8mM (n)	**ND**	**ND**	**24**	**19**	**11**
Achieved RER >1.15 (n)	**19**	**18**	**20**	**16**	**8**
Number of participants that failed to meet any endpoint criteria (n)	**3**	**1**	**0**	**0**	**3**



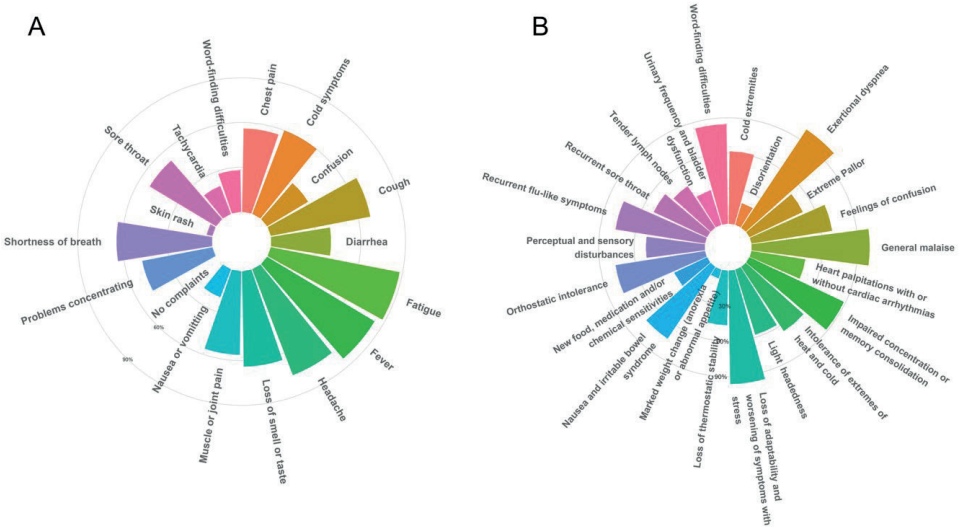
Supplemental Figure 1: Patients with ME/CFS report a range of infections prior to disease onset. Infection type prior to myalgic encephalomyelitis/chronic fatigue syndrome (ME/CFS) diagnosis, based on responses from participants and not necessarily clinically confirmed. All ME/CFS diagnoses (n=26) were made prior to 2020. Bars display the total number of responses.

A

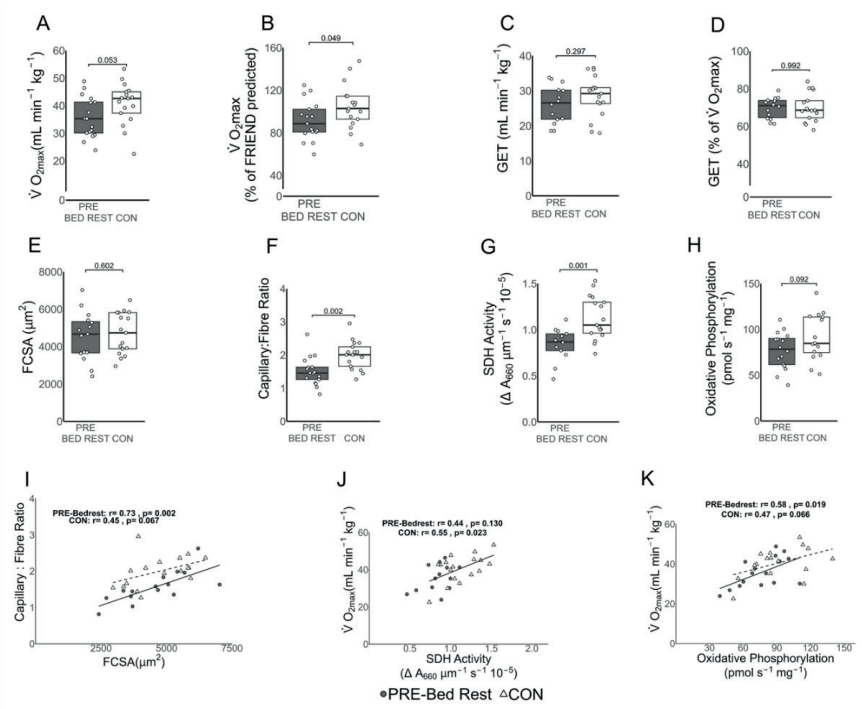
		CON	LC	ME/CFS
Frequency	DSQ-PEM1	0 (0,1)$^{***, \dagger\dagger\dagger}$	4 (1,4)**	4 (2,4)
	DSQ-PEM2	0 (0,1)$^{***, \dagger\dagger\dagger}$	3 (0,4)	3.5 (1,4)
	DSQ-PEM3	0 (0,0)$^{***, \dagger\dagger\dagger}$	3 (2,4)	3 (1,4)
	DSQ-PEM4	0 (0,0)$^{***, \dagger\dagger\dagger}$	3 (0,4)*	3 (1,4)
	DSQ-PEM5	0 (0,0)$^{***, \dagger\dagger\dagger}$	3 (1,4)	3 (2,4)
Severity	DSQ-PEM1	0 (0,1)$^{***, \dagger\dagger\dagger}$	3 (1,4)***	3 (3,4)
	DSQ-PEM2	0 (0,1)$^{***, \dagger\dagger\dagger}$	2 (0,3)**	3 (1,4)
	DSQ-PEM3	0 (0,0)$^{***, \dagger\dagger\dagger}$	3 (1,4)	3 (1,4)
	DSQ-PEM4	0 (0,0)$^{***, \dagger\dagger\dagger}$	2 (0,4)**	3 (1,4)
	DSQ-PEM5	0 (0,0)$^{***, \dagger\dagger\dagger}$	3 (1,4)*	3 (2,4)



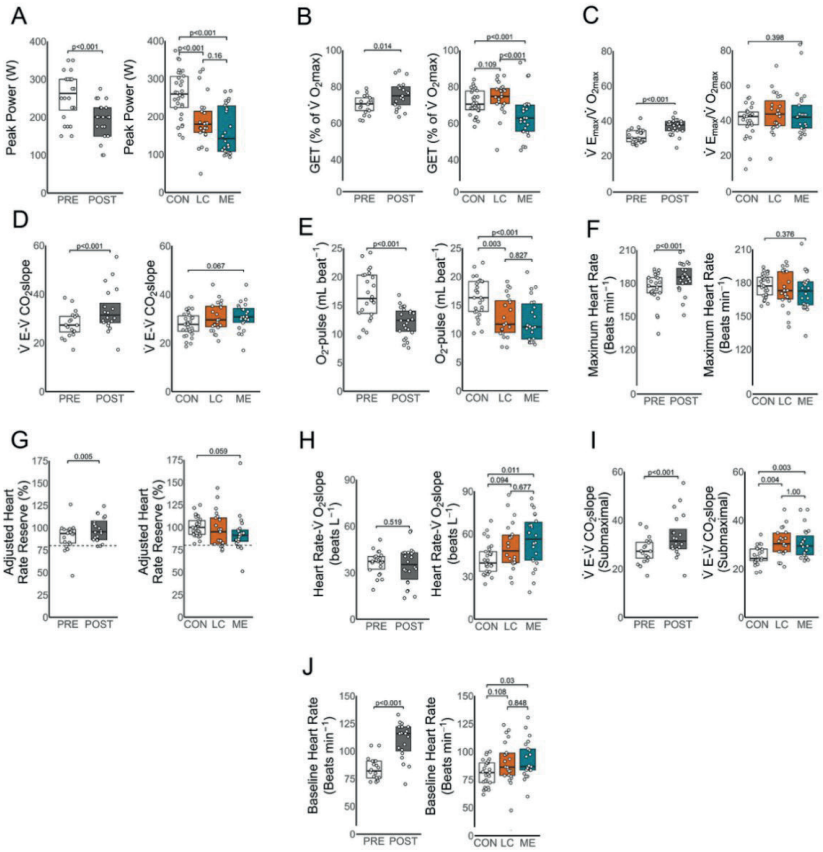
Supplemental Figure 2: The DSQ-PEM distinguishes both patients with long COVID and ME/CFS from healthy controls. DePaul Symptom Questionnaire-Post-exertional Malaise (DSQ-PEM) responses. Patients with long COVID (LC, n=25) and myalgic encephalomyelitis/chronic fatigue syndrome (ME/CFS; ME, n=26) reported significantly higher DSQ-PEM severity and frequency scores (A) compared to healthy controls (n=30). Patients with ME/CFS scored higher than patients with long COVID in DSQ-PEM F1 (p=0.024), DSQ-PEM F4 (p=0.028), DSQ-PEM S1 (p<0.001, DSQ-PEM S2 (p=0.008), DSQ-PEM S4, (p=0.009) and DSQ-PEM S5 (p=0.018). Patients with long COVID and ME/CFS responded more negatively to questions 6-8 and 10 of the DSQ-PEM (B-D,F) and indicated longer durations of feeling worse following activities (E) compared to healthy controls. All patients with long COVID and ME/CFS had a positive PEM diagnosis using the DSQ-PEM (G), while no controls were positive for PEM. Responses in A are displayed as median (minimum, maximum). Comparisons were made using a Kruskal–Wallis H test, with pairwise Wilcoxon tests with Benjamini–Hochberg correction post-hoc. *p<0.05, **p<0.01, ***p<0.001. *Compared to ME/CFS, †Compared to long COVID. Patients with long COVID are displayed in orange, and patients with ME/CFS are displayed in green.



Supplemental Figure 3. Patients with long COVID and ME/CFS report a range of symptoms. Circular bar plots of symptoms reported by patients with long COVID (A, n=25) and myalgic encephalomyelitis/chronic fatigue syndrome (n=26, B). Bars represent percentage of patients indicating positively for the given symptom.

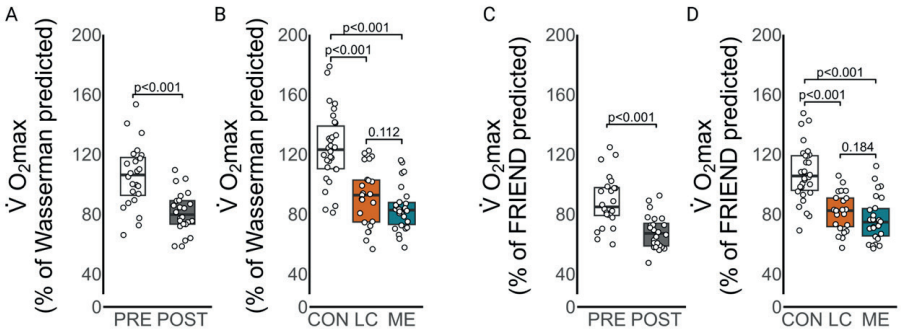


Supplemental Figure 4. Healthy bed rest participants tend to have lower oxidative capacity than patient-matched healthy controls. A sub-analysis was conducted on age- and sex-matched individuals between healthy individuals pre-bed rest (n=17) and healthy individuals matched to patients with long COVID and myalgic encephalomyelitis/chronic fatigue syndrome (CON, n=17; Supplemental Table 1). There was a tendency for $\dot{V}O_{2max}$ to be lower in bed rest participants compared to the patient-matched healthy controls (A, p=0.053) when expressed relative to body weight, and a significant difference when expressed as % of predicted $\dot{V}O_{2max}$ based on the FRIEND equation (B). However, there were no differences in in gas exchange threshold (GET) (C), the occurrence of the gas exchange threshold relative to $\dot{V}O_{2max}$ (D) or fiber cross sectional area (FCSA, E) between groups. Participants before bed rest had a lower capillary-to-fiber ratio (F), lower succinate dehydrogenase (SDH) activity (G), and oxidative phosphorylation capacity (H) than patient-matched healthy controls. Both groups had, or tended to have a significant relation between FCSA and capillary-to-fiber ratio (I). Only patient-matched healthy controls had a significant relation between $\dot{V}O_{2max}$ and SDH activity (J). Both groups had, or tended to have, a significant association between $\dot{V}O_{2max}$ and oxidative phosphorylation capacity (K). Data for $\dot{V}O_{2max}$, FCSA, and SDH activity remained non-normally distributed after Box-Cox transformations. Parametric comparisons were assessed using non-paired two-sided t-tests. Non-parametric comparisons were assessed using two-sided Wilcoxon signed rank tests. Solid lines represent significant correlations, dashed lines represent correlations with p<0.10. Box plots display individual data points, median (center line) and the first and third quartiles (lower and upper bound of box). Pre-bed rest and healthy controls are displayed in white, post-bed rest is displayed in grey, patients with long COVID are displayed in orange, and patients with ME/CFS are displayed in green.

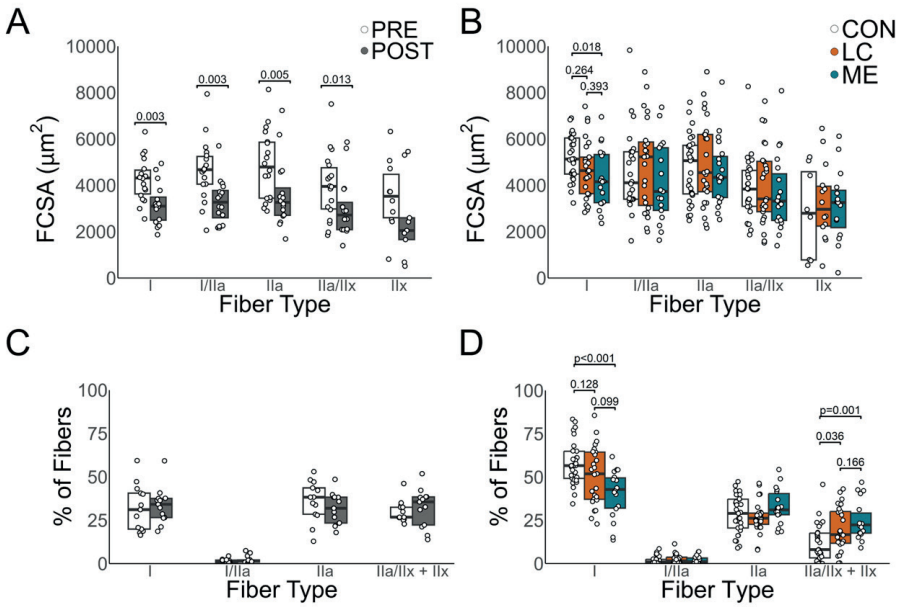


Supplementary Figure 5. Bed rest results in alterations in respiratory and cardiovascular responses to maximal exercise, which are not seen in either patients with long COVID or ME/CFS. Cardiopulmonary exercise test (CPET) data from pre- and post-bed rest, healthy controls (CON), patients with long COVID (LC) and patients with myalgic encephalomyelitis/chronic fatigue syndrome (ME/CFS; ME). Peak power was reduced following bed rest (A; n=24), and was also lower in LC and ME/CFS. Following bed rest, $\dot{V}E_{max}/\dot{V}CO_{2max}$ (B, n=24), $\dot{V}E_{max}/\dot{V}O_{2max}$ (C; n=24), and $\dot{V}E/\dot{V}CO_2$ slope (D; n=20) all increased, whereas LC and ME/CFS were not significantly different from CON. O_2-pulse was significantly lower following bed rest (E; n=24), and lower in LC (n=22) and ME/CFS (n=22) compared to CON (n=29). Maximal heart rate was increased following bed rest (n=24), while LC (n=22) and ME/CFS (n=22) had similar maximal heart rates to CON (n=22; F). Following bed rest (n=20), adjusted heart rate reserve (AHRR) was significantly higher, but ME/CFS (n=21) had the tendency have a lower AHRR compared to CON (n=29; G). The $\dot{V}O_2$-heart rate slope was not altered following bed rest (n=22), while both LC (n=22) and ME/CFS (n=22) had, or tended to have, a higher $\dot{V}O_2$-heart rate slope compared to CON (n=29; H). After bed rest (n=21), the gas exchange threshold (GET) occurred at a higher percentage of $\dot{V}O_{2max}$, whereas the GET occurred at a lower percentage of $\dot{V}O_{2max}$

in ME/CFS (n=22) compared to both CON (n=30) and LC (n=23; I). Submaximal $\dot{V}E/\dot{V}CO_2$ slope was increased following bed rest (n=20), and also increased in both LC (n=21) and ME/CFS (n=23) compared to CON (n=27; J). Baseline heart rates were elevated following bed rest (n=20; K), and tended to be higher in LC (n=22) and ME/CFS (n=21) than CON (n=29). Comparisons between pre- and post- bed rest were assessed using paired t-tests for parametric data and Mann–Whitney *U* test for non-parametric data. Comparisons between LC, ME/CFS and healthy controls were assessed using ANOVA, with Tukey HSD post-hoc testing for parametric data or Kruskal–Wallis *H* test, with pairwise Wilcoxon tests with Benjamini–Hochberg correction post-hoc for non-parametric data. Box plots display individual data **points, median (center line) and the first and third quartiles (lower and upper bound of box).**

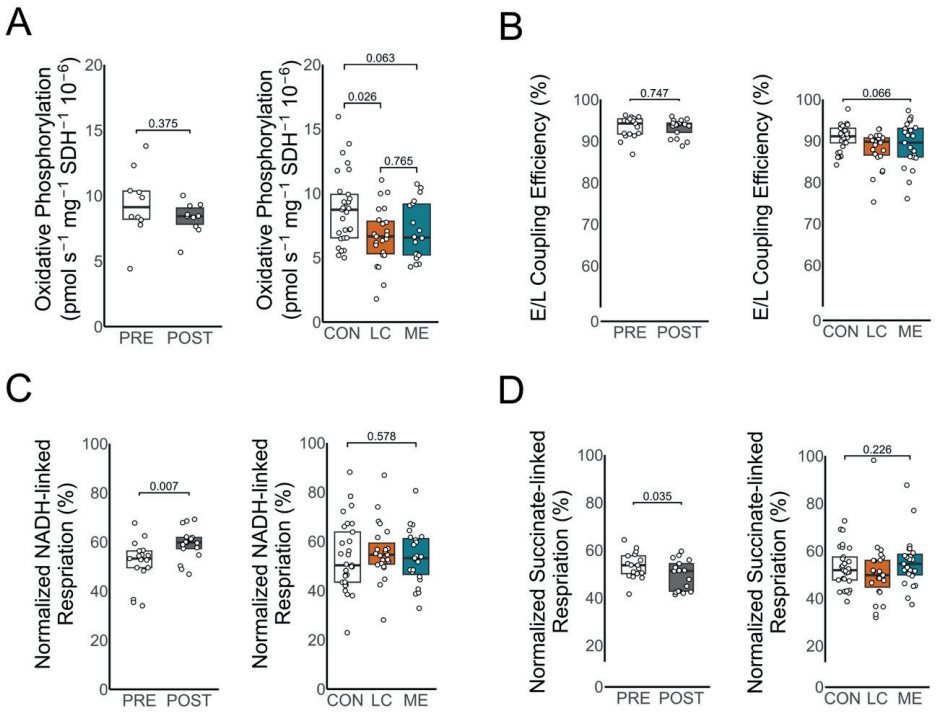


Supplemental Figure 6. Lower $\dot{V}O_{2max}$ still exists after bed rest and in both patients with long COVID and ME/CFS after correcting for predicted $\dot{V}O_{2max}$. Maximal oxygen consumption ($\dot{V}O_{2max}$) presented as a percentage of predicted $\dot{V}O_{2max}$, using the Wasserman (A,B) and the FRIEND equation (C,D). After Box-Cox transformations, only data from bed rest participants calculated with the Wasserman equation were normally distributed, all others remained non-normally distributed. Comparisons between pre- and post- bed rest (n=24) were assessed using paired t-tests for parametric data and Mann–Whitney *U* test for non-parametric data. Comparisons between patients with long COVID (LC, n=23) and patients with myalgic encephalomyelitis/chronic fatigue syndrome (ME/CFS; ME, n=26) and healthy controls (CON, n=30) were assessed using a Kruskal–Wallis *H* test, with pairwise Wilcoxon tests with Benjamini–Hochberg correction post-hoc for non-parametric data. Box plots display individual data points, median (center line) and the first and third quartiles (lower and upper bound of box). Pre-bed rest and healthy controls are displayed in white, post-bed rest is displayed in grey, patients with long COVID are displayed in orange, and patients with ME/CFS are displayed in green.



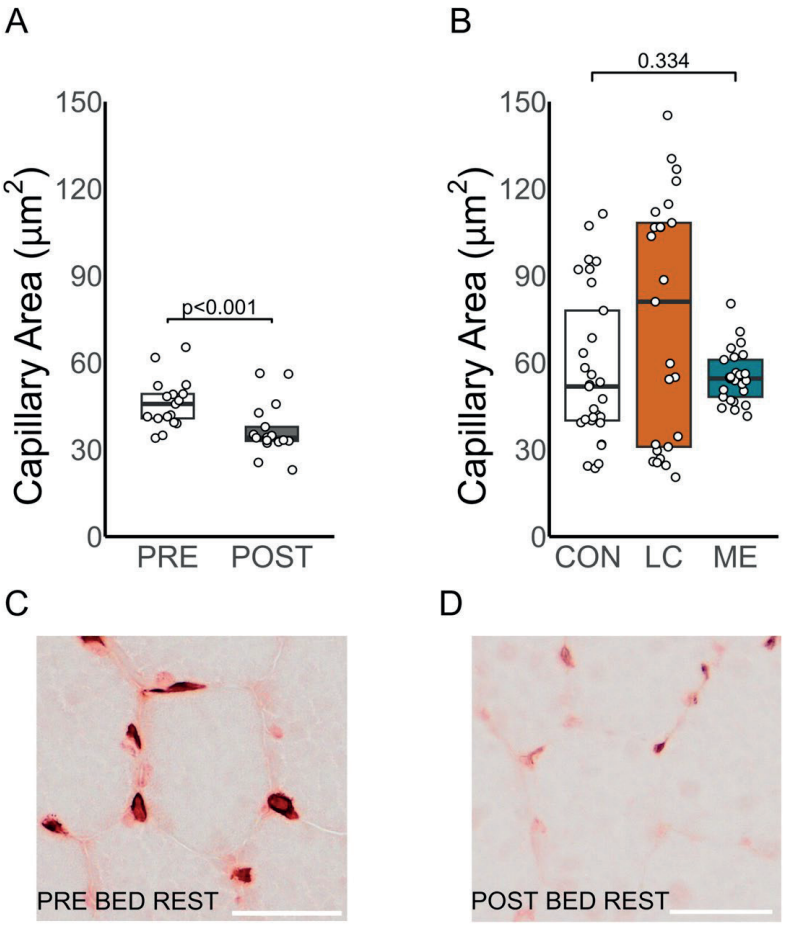
Supplementary Figure 7. Bed rest induces atrophy across all muscle fiber types, while patients with ME/CFS have a type-I specific atrophy. Average fiber cross-sectional area (FCSA) for each individual fiber type was reduced from pre- to post-bed rest (n=13; A), with the exception of the few pure type IIx fibers (p=0.329). Type I fiber FCSA was significantly lower in patients with myalgic encephalomyelitis (ME/CFS; ME; ANOVA: p=0.022, post-hoc: p=0.018, n=19; B) compared to healthy controls (CON, n=29), while long COVID patients (LC; p=0.393, n=25) were not significantly different from controls. Other fiber types were not significantly different in either patient group compared to healthy controls (ANOVA/ Kruskal-Wallis: I/IIa p=0.410, IIa p=0.847, IIa/IIx p=0.683, IIx p=0.817). Fiber type was subsequently calculated as the numerical percentage relative to total fiber number (C,D). Bed rest did not change fiber type distribution (C; Linear mixed model: p=0.629). ME/CFS patients had less type I fibers compared to controls (p<0.001) and tended to have less than long COVID patients (D; p=0.099). Both long COVID and ME/CFS patients had more type IIa/IIx hybrid fibers than controls. After Box-Cox transformations, FCSA data of type I, type I/IIa and IIa fibers were normally distributed, while FCSA data of type IIa/IIx and IIx fibers remained non-normally distributed. Data for percentage of type I in bed rest, percentage of I/II hybrids in all groups, and percentage of IIa fibers in all groups were normally distributed after Box-Cox transformations; all other data was non-normally distributed. Fiber type proportions were assessed using a linear mixed random effects model using % of proportion as the dependent variable and group*fiber type as the fixed effects, with subject ID as the random effects with post-hoc testing carried out per fiber type as described below. Comparisons between pre- and post- bed rest were assessed using paired t-tests for parametric data and Mann–Whitney U test for non-parametric data. Comparisons long COVID patients, ME/CFS patients, and controls were assessed using ANOVA, with Tukey HSD post-hoc testing for parametric data or Kruskal–Wallis H test, with pairwise Wilcoxon tests with Benjamini–Hochberg correction

post-hoc for non-parametric data. Box plots display individual data points, median (center line) and the first and third quartiles (lower and upper bound of box).

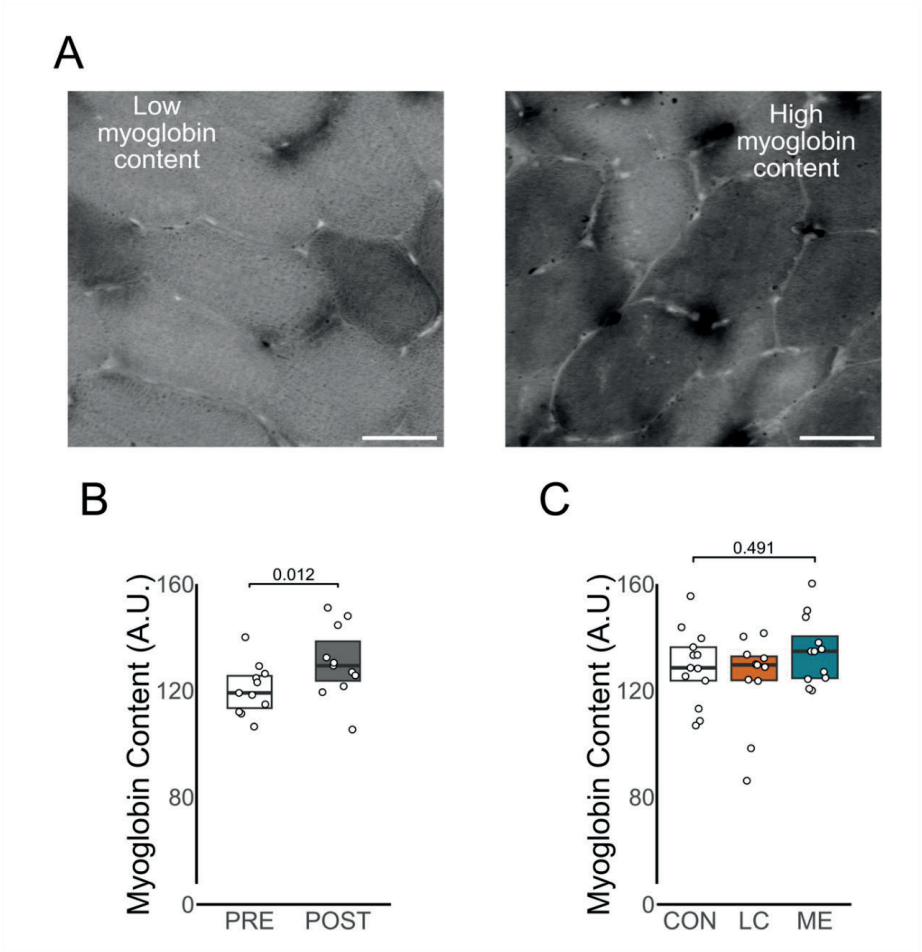


Supplementary Figure 8. Bed rest does not affect intrinsic mitochondrial respiration, while both patients with long COVID and ME/CFS have reduced intrinsic mitochondrial capacity. Oxidative phosphorylation capacity was normalized to succinate dehydrogenase (SDH) activity to provide a marker for intrinsic mitochondrial respiration. Bed rest (n=10) did not alter the normalized oxidative phosphorylation capacity, while patients with long COVID (LC, n=23) and myalgic encephalomyelitis/chronic fatigue (ME/CFS; ME, n=18) displayed lower capacities than healthy controls (CON, n=29, A). Bed rest (n=17) did not alter biochemical coupling (uncoupled/leak (E/L) coupling efficiency), while both patients with long COVID (n=23) and ME/CFS (n=23) tended to have lower biochemical coupling compared to healthy controls (Kruskal-Wallis: p=0.066, n=29, B). Bed rest (n=17) increased the normalized NADH-linked respiration (NADH-linked respiration normalized to oxidative phosphorylation capacity; C) and decreased the normalized succinate-linked respiration (rotenone-linked respiration normalized to electron transport capacity; D), whereas neither patients with long COVID (n=23) nor ME/CFS (n=23) were not different from healthy controls (n=29, NADH-linked normalized Kruskal-Wallis: p=0.578, Succinate-linked normalized Kruskal-Wallis: p=0.226). After Box-Cox transformations, all data remained non-normally distributed. Data from bed rest participants were compared using a paired Wilcoxon Signed Rank test. Data from patients with long COVID and ME/CFS and healthy controls

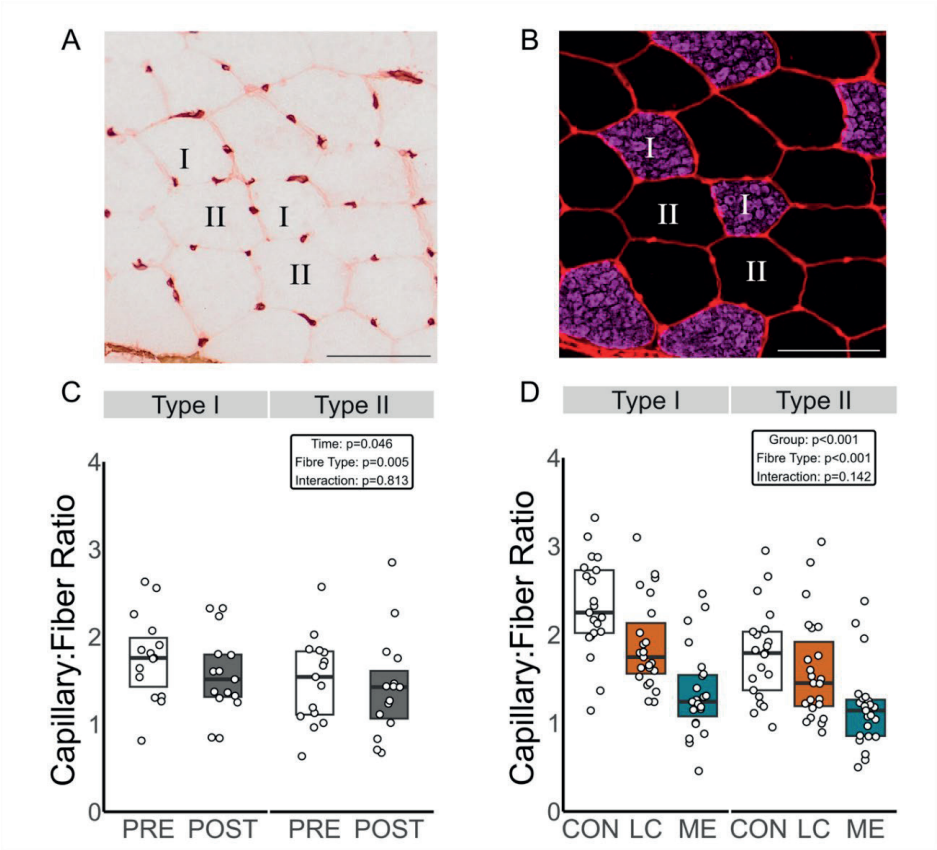
were compared using a Kruskal-Wallis *H* test, with pairwise Wilcoxon tests with Benjamini–Hochberg correction post-hoc where applicable. Box plots display individual data points, median (center line) and the first and third quartiles (lower and upper bound of box). Pre-bed rest and healthy controls are displayed in white, post-bed rest is displayed in grey, patients with long COVID are displayed in orange, and patients with ME/CFS are displayed in green.



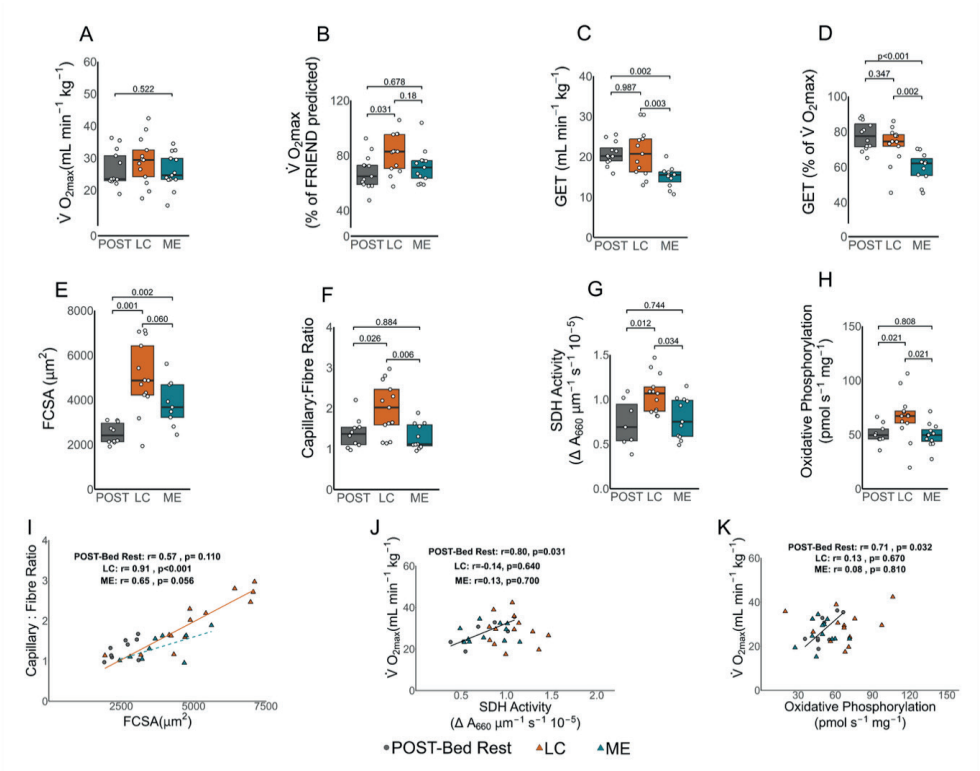
Supplementary Figure 9. Bed rest induces a reduction in capillary area, while neither patient group is different to healthy controls. Average capillary area decreased significantly following bed rest (n=17, A). Capillary area was not different between healthy controls (CON, n=29) and patients with myalgic encephalomyelitis/chronic fatigue syndrome (ME/CFS; ME, n=25, Kruskal-Wallis: p=0.334) or long COVID (LC, n=25; B). Typical examples of capillary staining in bed rest are shown in C. After Box-Cox transformations, capillary area data from bed rest participants was normally distributed, but data from patients with ME/CFS and long COVID and healthy controls remained non-normally distributed. Data from patients with ME/CFS and long COVID and healthy controls were compared using a Kruskal-Wallis H test. Box plots display individual data points, median (center line) and the first and third quartiles (lower and upper bound of box). Pre-bed rest and healthy controls are displayed in white, post-bed rest is displayed in grey, patients with long COVID are displayed in orange, and patients with ME/CFS are displayed in green. Scale bars represent 100µm.



Supplementary Figure 10. Myoglobin increases following bed rest, while neither patients with long COVID nor ME/CFS are different to healthy controls. Typical examples of low myoglobin content and high myoglobin content are displayed (A). Myoglobin content was measured in a subset of participants. Following bed rest myoglobin content was significantly elevated (B; n=11), while no differences were found between healthy controls (C; n=13), patients with long COVID (LC, n=11), and patients with myalgic encephalomyelitis/chronic fatigue syndrome (ME/CFS; ME, n=12). Scale bar represents 50 µm. After Box-Cox transformations, myoglobin data from bed rest participants was normally distributed, but data from patients with ME/CFS and long COVID and healthy controls remained non-normally distributed. Data from bed rest participants were compared using a paired t-test. Data from patients with ME and long COVID and healthy controls were compared using a Kruskal-Wallis *H* test. Box plots display individual data points, median (center line) and the first and third quartiles (lower and upper bound of box). Pre-bed rest and healthy controls are displayed in white, post-bed rest is displayed in grey, patients with long COVID are displayed in orange, and patients with ME/CFS are displayed in green.

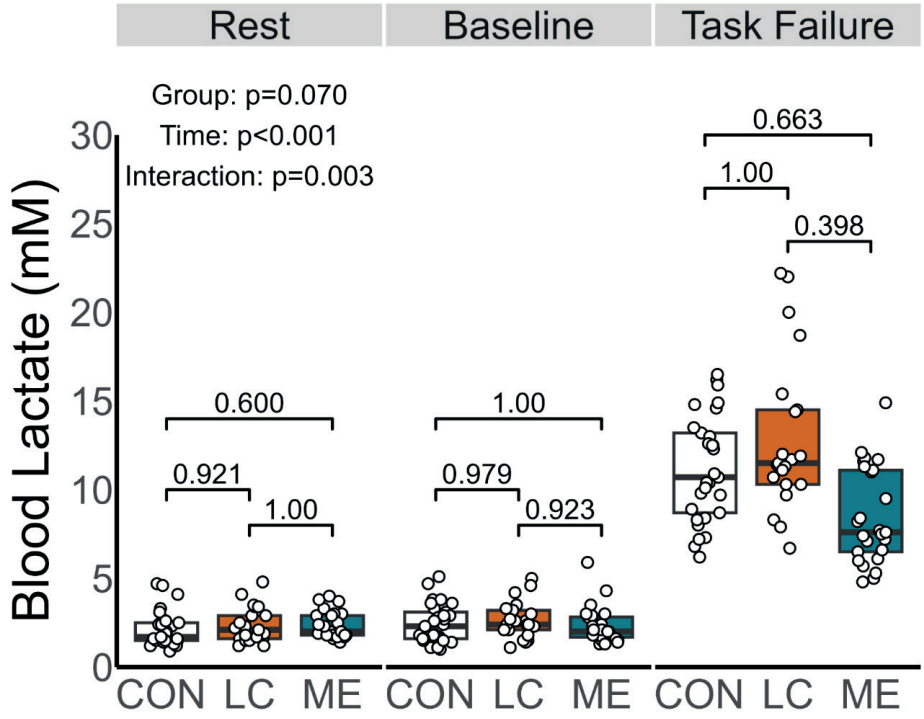


Supplemental Figure 11. Capillary-to-fiber ratio is higher in type I fibers compared to type II fibers in all groups, while bed rest and both patient groups have lower capillary-to-fiber ratios in both fiber types. Fiber type specific capillary-to-fiber ratios were analyzed by overlaying capillary staining (A) with fiber type staining (B) in a subgroup of participants, where possible. Fiber types were classified as type I positive (I) or type I negative (II). Bed rest participants (n=15) exhibited a reduction in capillary-to-fiber ratio for both fiber types ubiquitously (C). Patients with ME/CFS (ME/CFS; ME, n=23) had lower capillary-to-fiber ratios in both fiber types compared to both patients with long COVID (LC, p=0.0013, n=23) and healthy controls (CON, p<0.001, n=21; D). Patients with long COVID had the tendency (p=0.096) to have lower capillary-to-fiber ratios than healthy controls. In all groups, type I fibers displayed greater capillary-to-fiber ratios compared to type II fibers. After Box-Cox transformations, all data remained non-normally distributed. Data from bed rest participants were compared using a repeated measures 2-way aligned rank transform test. Data from patients with ME/CFS, patients with long COVID and healthy controls were compared using a 2-way aligned rank transform test, with a pairwise estimated marginal means post-hoc test for group effects. Box plots display individual data points, median (center line) and the first and third quartiles (lower and upper bound of box). Pre-bed rest and healthy controls are displayed in white, post-bed rest is displayed in grey, patients with long COVID are displayed in orange, and patients with ME/CFS are displayed in green. Scale bars represent 100 µm.



Supplemental Figure 12. Despite similar $\dot{V}O_{2max}$ between post-bed rest and both patients with long COVID and ME/CFS, skeletal muscle alterations are different following bed rest compared to both patients with long COVID and ME/CFS. A sub-analysis was conducted on age- and sex-matched individuals between post-bed rest (n=13), patients with long COVID (LC, n=13) and patients with myalgic encephalomyelitis/chronic fatigue syndrome (ME/CFS; ME, n=13). There were no differences in $\dot{V}O_{2max}$ between groups (A), however patients with long COVID tended to have higher % of predicted $\dot{V}O_{2max}$ based on the FRIEND equation (ANOVA: p=0.076; B). The gas exchange threshold was lower in patients with ME/CFS (n=11) than patients with long COVID (n=13; C). The gas exchange threshold relative to $\dot{V}O_{2max}$ was also earlier in patients with ME/CFS compared to post-bed rest and patients with long COVID (D). Skeletal muscle fiber cross-sectional area (FCSA) was lower after bed rest (n=10) compared to either ME/CFS (n=9) or long COVID (n=13), while there was a trend for patients with ME/CFS to present with smaller fibers than patients with long COVID (E; p=0.060). Capillary-to-fiber ratio was higher in long COVID (n=13) than either post-bed rest (n=10) or patients with ME/CFS (n=11; F). Similarly, succinate dehydrogenase (SDH) activity (G) and oxidative phosphorylation capacities (H) were higher in patients with long COVID (n=13, n=13) than either post-bed rest (n=7, n=13) or patients with ME/CFS (n=11, n=13). All groups had, or tended to have, a significant relation between FCSA and capillary-to-fiber ratio (I). There was a correlation between $\dot{V}O_{2max}$ and either SDH activity (J) or oxidative phosphorylation capacity (K) in participants after bed rest, but not in either patient group. Data from $\dot{V}O_{2max}$, gas exchange threshold relative to $\dot{V}O_{2max}$, FCSA, and oxidative phosphorylation remained non-normally distributed after Box-Cox transformations. Parametric comparisons were

assessed using ANOVA, with Tukey HSD post-hoc testing. Non-parametric comparisons were assessed using Kruskal–Wallis *H* test, with pairwise Wilcoxon tests with Benjamini–Hochberg correction post-hoc. Box plots display individual data points, median (center line) and the first and third quartiles (lower and upper bound of box). Pre-bed rest and healthy controls are displayed in white, post-bed rest is displayed in grey, patients with long COVID are displayed in orange, and patients with ME/CFS are displayed in green. Solid lines represent significant correlations, dashed lines represent correlations with $p<0.10$.



Supplemental Figure 13. Blood lactate increased in patients with long COVID, patients with ME/CFS, and healthy controls, with patients with ME/CFS having a smaller increase in blood lactate at task failure. Blood lactate measurements of healthy controls (CON, n=29), patients with long COVID (LC, n=21), and patients with myalgic encephalomyelitis/chronic fatigue syndrome (ME/CFS; ME, n=24) before and after maximal cardiopulmonary exercise testing. All groups showed elevations of blood lactate at task failure. No differences were found between rest and baseline in any group. Neither patient group was significantly different from healthy controls at any timepoint. After Box-Cox transformations, data at task failure was non-normally distributed. Data was compared using a repeated measures aligned rank transformation test with pairwise estimated marginal means post-hoc for interaction effects. Box plots display individual data points, median (center line) and the first and third quartiles (lower and upper bound of box). Pre-bed rest and healthy controls are displayed in white, post-bed rest is displayed in grey, patients with long COVID are displayed in orange, and patients with ME/CFS are displayed in green.

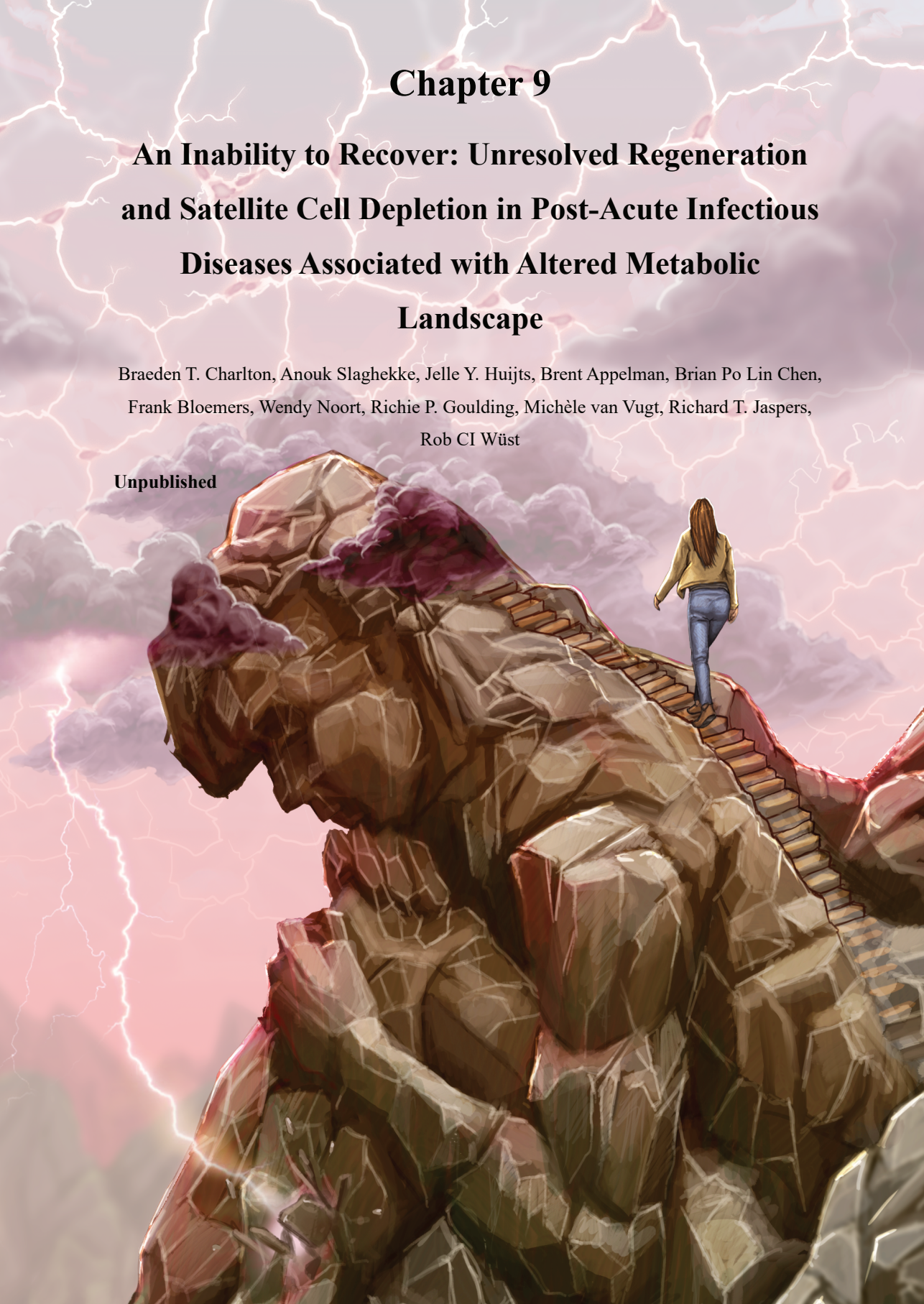


Chapter 9

An Inability to Recover: Unresolved Regeneration and Satellite Cell Depletion in Post-Acute Infectious Diseases Associated with Altered Metabolic Landscape

Braeden T. Charlton, Anouk Slaghekke, Jelle Y. Huijts, Brent Appelman, Brian Po Lin Chen, Frank Bloemers, Wendy Noort, Richie P. Goulding, Michèle van Vugt, Richard T. Jaspers, Rob CI Wüst

Unpublished



Abstract

Introduction: Myalgic encephalomyelitis/Chronic Fatigue Syndrome (ME/CFS) and long COVID patients frequently report with myalgia and post-exertional malaise (PEM), which is the worsening of symptoms upon exertion. However, it is currently unknown whether PEM results in higher amounts of muscle damage, and whether any damage or regenerative features are present in patient skeletal muscle.

Methods: Sections of vastus lateralis biopsies of 26 ME/CFS patients, 25 long COVID patients, and 30 healthy age- and sex-matched controls were stained for Pax7 to visualize satellite cells, PDGFRα to visualize fibroadipogenic progenitor (FAP) cells, and collagen IV and embryonic myosin heavy chain (eMHC) to assess damage and regeneration. Skeletal muscle metabolomics and lipidomics were performed by liquid chromatography mass spectrometry.

Results: Both patient groups had less $Pax7^+$ cells ($P<0.001$), while FAP cells were lower in ME/CFS patients ($P=0.017$). Both patient groups had more collagen IV surrounding myofibers ($P<0.001$). Expression of eMHC was not different between groups. Oxidative and antioxidant metabolites were lower in patients, while several essential amino acids were lower in patients with ME/CFS. Membrane-associated lipids were significantly lower in both patient groups ($P<0.001$), predominantly phospholipid species and cardiolipin. $Pax7^+$ satellite cell density was positively associated with membrane lipids ($r=0.39$, $P<0.001$), cardiolipin ($r=0.28$, $P=0.004$), taurine ($r=0.36$, $P=0.006$), CoA-glutathione ($r=0.36$, $P=0.010$), creatine ($r=0.34$, $P=0.013$), creatinine ($r=0.33$, $P=0.019$), FAD ($r=0.31$, $P=0.026$), and mitochondrial respiration ($r=0.21$, $P=0.034$), and negatively associated with collagen IV ($r=-0.35$, $P<0.001$). Collagen IV was negatively associated to membrane-associated lipids ($r=-0.31$, $P<0.001$).

Conclusions: ME/CFS and long COVID patients have a reduced potential regenerative capacity, marked by signs of unresolved regeneration, collagen deposition, and altered membrane-associated lipids, possibly impacting organelle function.

Introduction

Myalgic encephalomyelitis (ME/CFS) is diagnosed commonly after viral or bacterial insults in which symptoms persist or worsen. According to the Canadian Consensus Criteria (CCC) for ME/CFS, patients must exhibit post-exertional malaise (PEM), which is the worsening or development of new symptoms with either cognitive or physical exertion[1]. PEM contributes to a severe reduction in quality of life, limiting daily activity, social interaction, and ultimately impacting mental health. Up to 20% of people that experience an acute SARS CoV-2 infection will develop symptoms that persist beyond 3 months, which is subsequently termed long COVID. Of those patients with long COVID, around 85% of patients will experience PEM as one of their symptoms[2], thus also meeting the CCC criteria for ME/CFS.

In both long COVID and ME/CFS, previous reports suggest dysregulated immune responses[3,4], mitochondrial dysfunction[5–14] in multiple tissue types, and impaired endothelial function[15–20]. Specifically, patients with long COVID and ME/CFS that exhibit mitochondrial dysfunction may be exposed to more pronounced oxidative damage, potentially resulting in cell injury. It has previously been shown that patients with long COVID have high amounts of necrosis and tissue damage 24-hrs following exhaustive exercise[9]. Whether these same markers of damage are seen in patients with ME/CFS has yet to be reported. Further, in neither patients with ME/CFS nor long COVID has regenerative markers been assessed in skeletal muscle.

It is well reported that proper activation of the immune system following exercise is necessary to restore musculoskeletal homeostasis[21,22]. Acute exercise will often result in the activation of neutrophils, T-cells, and M1 macrophages within the first few hours after exercise[22]. As local tissue damage is resolved, neutrophil and T-cells are removed locally, and macrophages are polarized to M2 phenotypes, with macrophages being the dominant immune cell two to several days following muscle damage[23]. The M2 subset of macrophages is necessary for the activation of fibroadipogenic progenitor (FAP) cells[24,25], and subsequently satellite cells[26,27].

FAP cells activated via the IL4R will further release myogenic factors to promote satellite cell activation and differentiation into myonuclei[24,28,29]. Moreso, FAP cells are important regulators of ECM composition, wherein activation of FAP cells generally increases collagen composition in the extracellular matrix[30], of which the composition is integral in appropriate regeneration[31]. However, FAP cells if stimulated by TGF-β aids in transient ECM remodelling, however long-term exposure leads to the chronic deposition of ECM proteins, adipose, and hinders overall muscle regeneration[29,32].

A necessary component of muscle regeneration is the activation of satellite cells by FAP cells, exposure to mechano growth factor, interleukin-6, insulin-like growth factor-1, fibroblast growth factor, hepatocyte growth factor or tumour necrosis factor (TNF)-α[33–35], or mechanical stimuli [36,37]. Once activated, satellite cells will begin to undergo proliferation and differentiation, in which a handful of the satellite cells will incorporate into the myofibre as new myonuclei, while the rest of the satellite cell pool will return to quiescence to maintain the overall satellite cell pool[38,39]. Remodelling of the myofibre occurs throughout regeneration, often with transient expression of embryonic myosin heavy chain[40,41], increases in non-fibrillar collagens (IV, VI, etc.)[42–44], and restructuring of the extracellular matrix[30,31,45]. The remodelling that accompanies regeneration increases the flux of protein synthesis and degradation to accommodate the restructuring[46].

Mitochondrial function and signaling has been shown to influence regenerative processes in skeletal muscle[47–49] . Mitochondrial dysfunction and morphological alterations have been shown in both patients with ME/CFS and long COVID[5–9,14], as well as a shift towards glycolytic metabolism[5,9,50]. This in turn may predispose patients to more frequent oxidative damage. However, it is currently unknown whether the alterations to metabolic profiles coincide with either damage or regenerative features in patients with long COVID or ME/CFS.

The aims of this study, therefore, were to quantify and evaluate damage-associated and regenerative features of skeletal muscle in both patients with long COVID and patients with ME/CFS. Additionally, we aimed to quantify the relative proportions of skeletal muscle resident mononuclear cells typically involved in muscle repair in patients with long COVID and ME/CFS, and investigate how changes in these populations then relate to damage-associated or regenerative features of skeletal muscle, such as fibrosis, expression of embryonic myosin heavy chain, and irregular deposition of lipids. Furthermore, we aimed to investigate whether changes in metabolic or lipid profiles of patients relate to damage-associated or regenerative features. We hypothesized that resident immune cells are elevated in both patients with long COVID and ME/CFS, while satellite cells and FAP cells are lower in patients compared to controls. Upon PEM induction, we expect to see a further increase in macrophages, and an increase in satellite cell content, due to their proliferation in response to exercise. As basal levels of satellite cells and FAP cells are expected to be lower in patients, we then expect to see increased signs of damage in patient skeletal muscle, notably increase in eMHC expression, collagen deposition surrounding myofibres, and increased lipid content, consistent with damaged and fibrotic tissue. We will then conduct an exploratory analysis to

investigate how alterations in either metabolic or lipid profiles relate to damage-associated or regenerative features, and changes in resident mononuclear cell content.

Methods

The study design has been reported previously[9,14]. The study protocol was approved by the medical ethics committee of the Amsterdam University Medical Centre (AUMC (NL78394.018.21) and registered at www.clinicaltrials.gov (NCT05225688). All participants signed a written informed consent before participation. The study was conducted in accordance with the Declaration of Helsinki. Briefly, 26 patients with ME/CFS and 25 patients with long COVID were recruited from the outpatient clinic at the AUMC. Patients were subsequently age- and sex-matched with 30 healthy controls, whom had successfully recovered from an acute SARS-CoV-2 infection.

Patients

Patients with long COVID were diagnosed by two experienced clinicians for long COVID symptomology and exclusion of potential differential diagnoses. All long COVID patients were diagnosed with post-exertional malaise (PEM) by the DSQ-PEM[51], had a minimum period of long COVID-related symptoms of six months, and were between 18 and 65 years old. No symptoms were present before the confirmed diagnosis of SARS-CoV-2. None of the included participants were admitted to the hospital during acute SARS-CoV-2 infection and were healthy prior to NAAT or serology-proven SARS-CoV-2 infection. Exclusion criteria were a medical history of cardiovascular/pulmonary disease, diabetes mellitus, concurrent treatment with metabolism or coagulant-altering drugs during the study period (statins, corticosteroids, SGLT2 inhibitors, GLP1 receptor agonists, platelet aggregation blockers and any anticoagulants), adiposity and body mass index >35 (related to ability of muscle biopsy obtainment), pregnancy, active infection, severe renal dysfunction or any other prior chronic illness or >6 alcohol units per day or >14 alcohol units per week. Smoking was not an exclusion criterion. One long COVID patient was excluded due to a recent SARS-CoV-2 re-infection (<7 days).

Patients with ME/CFS all fulfilled the Canadian Consensus Criteria (CCC), exhibited PEM according to the DSQ-PEM and consulted with a ME/CFS specialist or post-COVID physician, and were between 18 and 65 years old. ME/CFS diagnosis was prior to 2020, and all patients had a confirmed previous diagnosis of SARS-CoV-2. Exclusion criteria were identical to those of the patients with long COVID.

None of the healthy controls had residual symptoms after the SARS-CoV-2 infection and none were hospitalized within 6 months of study participation. Healthy controls withdrew because of the invasive nature of the protocol ($n = 2$), symptoms related to a burn-out ($n = 1$), and a novel diagnosis of uncontrolled hypertension ($n = 1$).

Biopsy Procedure

Muscle biopsies were obtained from the vastus lateralis at one-third of the distal length (approximately 150mg weight wet) using a suction-supported 4mm Bergström needle (Pelomi, Albertslund Denmark) under sterile conditions after skin disinfection and local anesthesia with 2% lidocaine[9]. One ~30 mg piece was aligned according to the muscle fiber arrangement under a light microscope and frozen in liquid nitrogen for histochemistry, and another ~15 mg piece was utilized for metabolomic and lipidomic analyses. Muscle biopsies from patients and healthy controls were obtained 6 days prior to a cardiopulmonary exercise test and 24 hours after. All participants were instructed to refrain from strenuous activity at least 24 hours prior to the biopsy procedure.

All biopsies used for histochemistry were frozen in liquid nitrogen and stored in liquid nitrogen at −196°C. Frozen muscle samples were mounted using freeze-gel (Q Path, VWR, Netherlands) and cut into 10 µm thick sections in transverse orientation in a cryostat (Microm HM550, Adamas Instrumenten, Netherlands) at -20ºC, before being mounted on polylysine-coated slides, and stored at −80°C until staining. Due to issues with tissue freezing, histological analysis was completed on samples from 24 patients with long COVID, 23 patients with ME/CFS, and 30 healthy controls.

Immuno- and histochemical staining

To visualize mononuclear cell populations, collagen formation, and embryonic myosin heavy chain expression, immunohistochemistry was carried out on 10 µm thick sections from the vastus lateralis muscle biopsies. Details about antibody dilutions and suppliers can be found in Table 2.

$CD68^+$ Macrophages, $CD3^+$ T-cells and Collagen IV

Sections were stained for CD68 (PG-M1 IgG 3, 1:200, DAKO M0876), CD3 (SP7 (rabbit moab), 1:200, Thermo Sc. Rm-9107-S), and collagen IV (Cell Marque, 1:100) by the AUMC The Department of Pathology for visualization of macrophages, T-cells and the extracellular matrix, respectively. Sections were air-dried, and subsequently fixed in acetone for 10min, and incubated with the primary antibody for either CD68, CD3 or collagen IV for 1 hour. Detection

was performed using the BrightVision + poly-horseradish peroxidase anti-mouse/rabbit/rat IgG system (ImmunoLogic), with 3-amino-9-ethyl-carbazole as the chromogen and hematoxylin as counterstain.

Oil Red O Stain

Sections were stained for hydrophobic and neutral lipid formation (i.e. triglycerides, diacylglycerols and cholesterol esters)[52,53] by the Department of Pathology. Briefly, sections were air dried for 10min and subsequently fixed in formalin. Slides were washed for 5min under running tap water, followed by a rinse with 60% isopropanol. Sections were then stained with Oil Red O solution (0.003g/mL, company)). Sections were subsequently rinsed with 60% isopropanol and counterstained with haematoxylin to visualize nuclei. After this, they were rinsed with distilled water and coverslips mounted with glycerine.

Satellite Cells and Fibroadipogenic Progenitor Cells

Slides were airdried for 10min and subsequently fixed in paraformaldehyde for 10min. Slides were then washed 3 times with PBST (5min each) and subsequently blocked with 10% normal goat serum for 30min at room temperature. Slides were then washed 3 times with PBST (5min each) and blocked with 0.1% bovine serum albumin for 30min at room temperature. Slides were then washed 3 times with PBST (5min each) and incubated with the primary antibodies overnight at 4°C (minimum 12 hours). Following overnight incubation, slides were washed again 3 times with PBST (5min each) and subsequently incubated with the secondary antibodies for 30min at room temperature. Subsequently, slides were again washed 3 times in PBST (5min each) and then incubated with wheat germ agglutinin (WGA) 555 for 30min at room temperature. The slides were then washed 3 times in PBS (5min each), after which coverslips were applied using Vectashield mounting medium with DAPI (Stock Keeping Unit (SKU): H-1200-10).

Embryonic Myosin Heavy Chain and Type I Myosin Heavy Chain

Slides were airdried for 10min and subsequently blocked with 10% normal goat serum for 60min at room temperature. Slides were then washed 3 times with PBS (5min each) and incubated with the primary antibodies overnight at 4°C (minimum 12 hours). Following overnight incubation, slides were washed again 3 times with PBS (5min each) and subsequently incubated with the secondary antibodies for 60min at room temperature. Slides were again washed 3 times in PBS (5min each) and then incubated with WGA 555 for 30min at room

temperature. Finally, slides were washed 3 times in PBS (5min each), after which coverslips were applied using Vectashield mounting medium (SKU: H-1000-10).

Image acquisition

Slides were dried overnight at 4°C before imaging. Images for satellite cells, FAP cells, and eMHC expression were taken at ×40 magnification with a fluorescent microscope (Axiovert 200M, Zeiss) and image processing software Slidebook 5.0. Approximately 15 images were taken per sample, with each image containing 3-8 visible whole myofibres. Images for $CD68^+$, $CD3^+$, collagen IV, and Oil Red O expression were taken at x20 magnification with a brightfield microscope (Slideview VS200 Research Slide Scanner, Olympus) and SlideViewer 5.0 software, with whole biopsy sections being analyzed. All images were manually evaluated to exclude those containing out-of-focus areas, artifacts, and large areas of connective tissue.

Image analysis

Background signal was removed from all fluorescent images using a negative stain control. For $PAX7^+$ and $PDGFR\alpha^+$ cells, signal was deemed positive if the size of the remaining particle was >5um^2 in area and overlapped with DAPI signal. As we previously reported no differences in fibre cross sectional area (FCSA)[14], and there was no difference of nuclear count (Supplemental Figure 1), the number of positive areas was subsequently normalized to the number of nuclei present to yield positive cells per nuclei in addition to positive cells per myofibre. In order to quantify myofibre injury, centralized nuclei were quantified on PAX7/PDGFRα/DAPI stained images, over an average of 113 myofibres. Centralized nuclei were defined as nuclei that were >5µm from the subsarcolemma, taken as the closest point of the DAPI signal from the membrane.

After removing areas with folds and debris, $CD68^+$ and $CD3^+$ cells were calculated as the number of nuclei expressing either CD68 or CD3, normalized to the total number of nuclei present in the entire section. An average of ~5110 (+/- 2639) nuclei were measured per participant per time point.

For eMHC expression, after removal of background signal using a negative stain control, signal overlapping with the type I myosin heavy chain was subtracted for any non-specific signal. The remaining signal was then quantified per cell, with 10 type I^+ and 10 type I^- cells analyzed per participant. Collagen IV expression was calculated as the % area of collagen IV present in a given image normalized to the number of fibres present and subsequently corrected for fibre cross sectional area, yielding an approximation of collagen IV per myofibre. The correction for

fibre cross sectional area (FCSA) was to account for differences in fibre radius that may affect the surface area in contact with collagenous material. As the average myofibre FCSA did not differ between groups, we calculated then the average thickness surrounding the myofibre. As Oil Red O images were obtained using brightfield imaging, Oil Red O was quantified as the percentage of signal within a given myofibre, corrected for the background signal outside of the biopsy area. Myofibres did not include any crystalized Oil Red O particulate and 20-40 myofibres were manually circled and quantified per participant.

Metabolomics and Lipidomics

Skeletal muscle metabolomics analysis was performed as described previously[54]. The HPLC system consisted of an Acquity binary HPLC pump, a vacuum degasser, a column temperature controller, and an auto sampler (Waters, Milford, MA, USA). The column temperature was maintained at 30°C. The metabolite extract was injected onto a SeQuant 100 x 2.1mm ZIC-cHILIC column, 3µm particle diameter (Merck, Darmstadt, Germany). An Impact II QTOF (Bruker Daltoniks) mass spectrometer was used in the negative and/or positive electrospray ionization mode. In both the negative and positive ionization mode, mass spectra of the metabolites were obtained by continuous scanning from m/z 50 to m/z 1200 with a resolution of 50000 FHMW.

Lipidomics analysis was performed as described[55]. The HPLC system consisted of an Ultimate 3000 binary HPLC pump, a vacuum degasser, a column temperature controller, and an auto sampler (Thermo Scientific, Waltham, MA, USA). The column temperature was maintained at 25°C. The lipid extract was injected onto a "normal phase column" LiChrospher 2x250-mm silica-60 column, 5µm particle diameter (Merck, Darmstadt, Germany) and a "reverse phase column" Acquity UPLC HSS T3, 1.8µm particle diameter (Waters, Milford Massachusetts, USA). A Q Exactive Plus Orbitrap (Thermo Scientific) mass spectrometer was used in the negative and positive electrospray ionization mode. In both ionization modes, mass spectra of the lipid species were obtained by continuous scanning from m/z 150 to m/z 2000 with a resolving power of 280,000 based on full width at half maximum (FWHM).

As the data was collected during two different time frames, datasets were filtered so that only metabolites and lipids existing across both datasets remained. Data was then normalized using ROBUST transformations, and combined. Metabolites and lipids were analyzed as individual species and as classes/families of metabolites/lipids separately. Due to the multiple groups and timepoints, a mixed models approach was utilized to obtain group, time, and interaction effects

for each species, which was subsequently corrected using the false discovery rate method. Tukey HSD with Benjamini-Hochberg correction was used for the post-hoc analysis of any individual species or classes that indicated group or interaction effects following FDR corrections.

Statistical Analysis

Distributions were assessed using histograms and Shapiro-Wilk tests. Parametric quantitative variables are presented as means ± standard deviation (SD), and nonparametric quantitative variables are presented as median and interquartile ranges (IQR; 25th and 75th percentiles). Jitter plots are plotted with means represented as single bars. All individual points represent a single participant. Continuous parametric data were analyzed using a 2-way mixed models analysis of variance, with Tukey HSD post-hoc testing. Non-normally distributed continuous nonparametric data were analyzed using 2-way align rank transform analysis of variance with pairwise Wilcoxon test with Benjamini–Hochberg correction. Correlations were analyzed using the Pearson correlation coefficient for linear relationships. Significance was set at $P < 0.05$.)

Results

Markers of muscle damage

As we previously reported increased signs of necrosis in patients with long COVID[9], we first sought to investigate whether other signs of damage or regeneration were present in patients. We first utilized collagen IV to investigate the extracellular matrix thickness surrounding the fibres, as inflammatory states are known to increase collagen IV content[44,56]. Here, we found that the area of collagen IV present per area was higher in both patient groups compared to healthy controls, with no differences between groups (Figure 1B). As exercise and the subsequent hypertrophying of muscle is paralleled with increases collagen IV content[57–60], we corrected the collagen IV for myofibre FCSA, which yielded the same results.

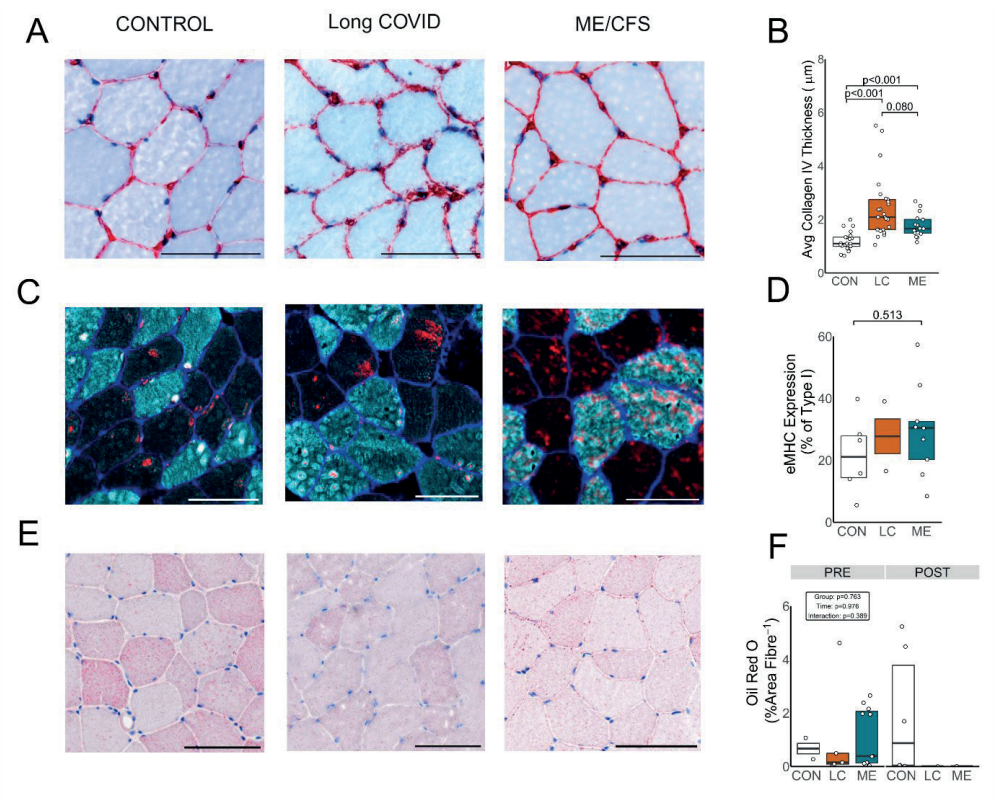


Figure 1: "Long COVID and ME/CFS patients exhibit more collagen IV than healthy controls, but eMHC and neutral lipid content are not different than controls." Biopsy sections were stained for collagen IV (**A**) to assess unresolved regeneration or damage. Both patient groups had higher proportions of collagen IV surrounding myofibres compared to healthy controls (**B**). Biopsies were stained for embryonic myosin heavy chain and type I fibres (eMHC, **C**, eMHC=red, Type I=cyan, membrane=blue) to investigate ongoing regeneration and fibre type specific occurrences. Neither group displayed markedly different eMHC expression compared to healthy controls, irrespective of fibre type (**D**). Skeletal muscle neutral lipids, were stained using Oil Red O (**E**), but the proportion of neutral lipids per myofibre was not different between groups (**F**). *P<0.05, **P<0.01, ***P<0.001, scale bar = 100 µm.

In order to visualize recurrent regeneration cycling, we immunohistochemically stained muscle sections for embryonic myosin heavy chain (eMHC), which is expressed by muscle fibres undergoing remodelling and regeneration[46,61]. As we previously reported that both patients with long COVID and ME/CFS have higher proportions of glycolytic fibres compared to healthy controls[9,14], which are more susceptible to both oxidative[62,63] and mechanical damage[64], we hypothesized that both patient groups would exhibit more eMHC compared to controls. However, the amount of eMHC-positive fibers was not different between groups (Figure 1D).

As incomplete regeneration and fibrosis often coincides with fatty infiltration[65–67], we assessed hydrophobic and neutral lipid formation (i.e. triglycerides, diacylglycerols and cholesterol esters)[52,53] using Oil Red O. Unexpectedly, lipids per myofibre did not differ between groups (Figure 1F). However, due to tissue availability only a small subset of patients and controls were assessed. Additionally, the number of centralized myonuclei that could be seen was not different between groups (Supplemental 1B).

Resident Cell Populations

Due to the higher collagen IV accumulation in patient skeletal muscle, we queried whether resident cell populations may differ. As skeletal muscle nucleation has been shown to relate to overall ability to synthesize protein[68,69], we first questioned whether skeletal muscle nucleation differed between groups. There was no difference in nuclear count per myofibre in skeletal muscle from patients (Supplemental 1A), and that in all groups nuclear count was related to FCSA (Supplemental 1C). We then aimed to determine the relative proportions of resident mononuclear cells, focusing on $CD68^+$ macrophages, $CD3^+$ T-cells, $PAX7^+$ satellite cells, and $PDGFR\alpha^+$ FAP cells. The proportion of nuclei expressing CD68, was markedly lower in ME/CFS compared to both healthy controls and long COVID patients (Figure 2E). The proportion of $CD68^+$ nuclei increased one day after a maximal exercise test in all groups. Prior to exercise, there was no difference in $CD3^+$ nuclei between groups (Figure 2F). However, following exercise, only healthy controls and patients with long COVID had increases in $CD3^+$ nuclei (Figure 2F).

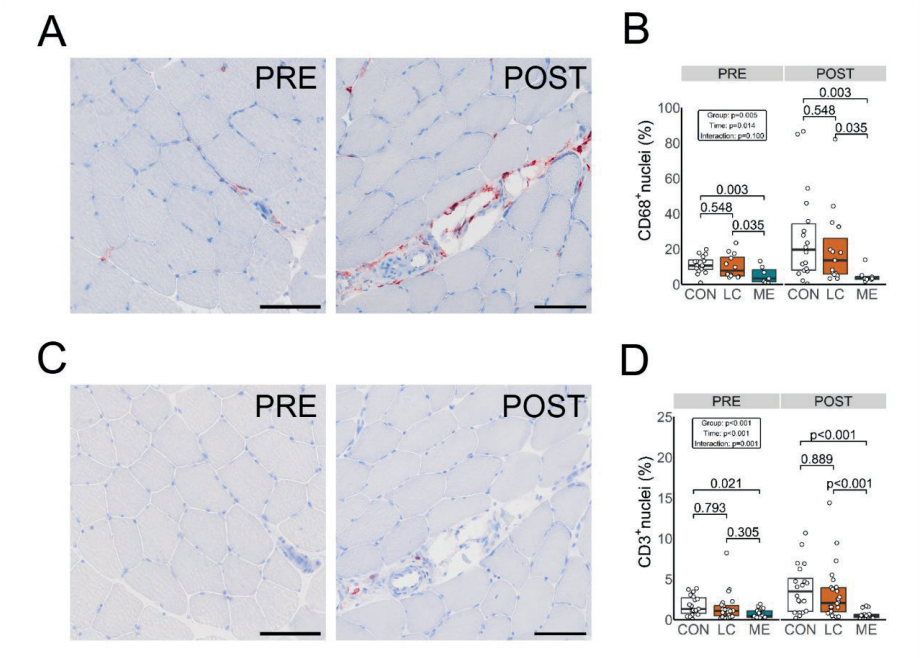


Figure 2: "ME/CFS patients have less CD68$^+$ macrophages and CD3$^+$ T-cells compared to both healthy controls and long COVID patients, and do not exhibit a typical increase in resident immune cells in response to exercise." Biopsies taken 1 week before and 24 hours following an exhaustive exercise test were stained for CD68 (**A**) and CD3 (**C**) to assess the amounts of resident macrophages and T-cells respectively. Long COVID patients exhibited similar amounts of CD68$^+$ nuclei compared to healthy controls, which subsequently increased following exercise, whilst ME/CFS patients had lower proportions of CD68$^+$ nuclei compared to both long COVID and healthy controls (**B**). Both ME/CFS and long COVID patients exhibited less CD3$^+$ nuclei compared to healthy controls (**D**). Scale bar= 100µm.

Subsequently, we queried whether satellite cell and FAP cell populations differed, as both are necessary for complete muscle regeneration. The proportion of PAX7$^+$ nuclei was markedly lower in both patients with ME/CFS and long COVID (Figure 3C), in which PEM induction did not change the relative proportions of PAX7$^+$ nuclei. FAP cell numbers (PDGFRα$^+$) were lower in ME/CFS patients compared to healthy controls (Figure 3D), while patients with long COVID had a tendency to have less FAP cells compared to controls. Neither PAX7$^+$ nor FAP cell number was altered following PEM induction.

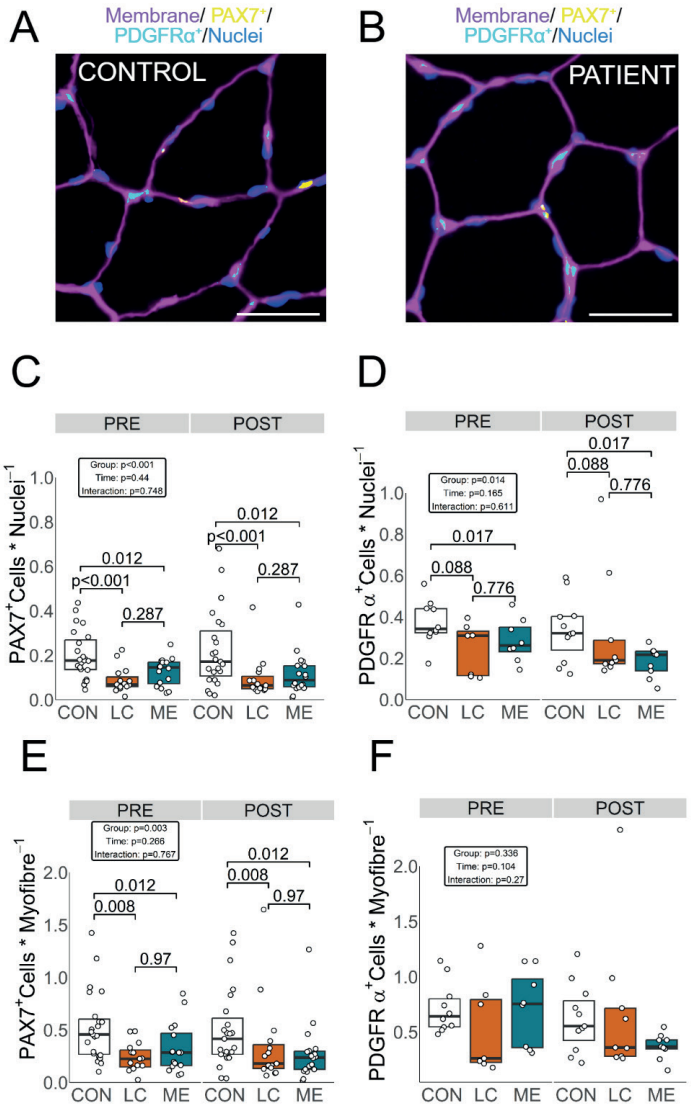


Figure 3: "Both long COVID and ME/CFS patients have less satellite cells and fibroadipogenic progenitor cells compared to healthy controls." Biopsy sections from healthy controls (**A**) and patients (**B**) were stained for PAX7 (satellite cells, yellow), PDGFRα (fibroadipogenic progenitor cells, cyan), DAPI (nuclei, blue), and WGA (membranes, magenta). Both patient groups had decreased proportions of $PAX7^+$ nuclei compared to healthy controls (**C**). Patients with ME/CFS had less $PDGFR\alpha^+$ nuclei compared to healthy controls, while patients with long COVID had a tendency to have less $PDGFR\alpha^+$ nuclei than healthy controls. between groups (**D**). When assessing $PAX7^+$ and $PDGFR\alpha^+$ nuclei for a given myofibre, both long COVID and ME/CFS

still had lower PAX7^{+} nuclei per myofibre (**E**), where as PDGFRα^{+} nuclei per myofibre was not different between groups (**F**). Scale bar= 50µm.

Altered Metabolic Landscape in long COVID and ME/CFS

As we previously reported mitochondrial dysfunction in both patients with long COVID and ME/CFS[9,14], we sought to investigate whether patient skeletal muscle observed alterations in the metabolic landscape that may relate to either collagen IV accumulation or reductions in resident mononuclear cells. In both patient groups, most metabolites were reduced compared to those in healthy controls (Figure 4A), with those related to the tricarboxylic acid (TCA) cycle, pyrimidine metabolism, and cell stress panel being the most commonly affected metabolite groups (Figure 4B).

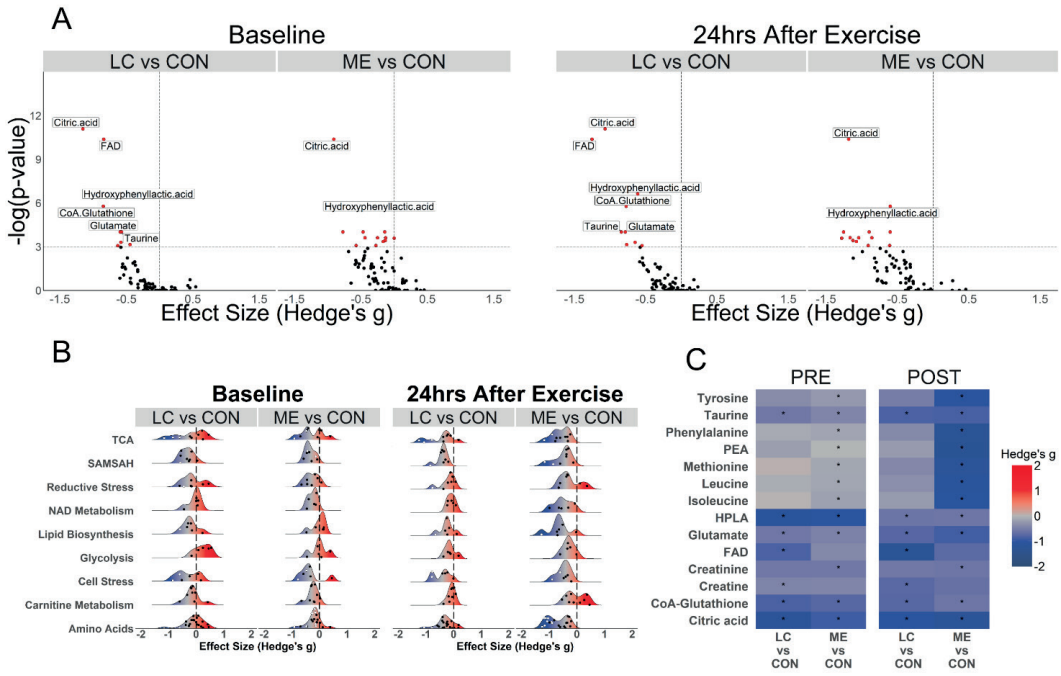


Figure 4: "Patients with long COVID and ME/CFS have lower amounts of oxidative and antioxidant metabolites, indicative of a shift towards glycolysis, while patients with ME/CFS have lower amounts of essential amino acids." Volcano plots (**A**) illustrate that most metabolites were lower in both ME/CFS and long COVID patients compared to healthy controls, while 14 metabolites (denoted in red) were found to be significantly different after post-hoc corrections. Significantly lower metabolites were involved in TCA cycling, SAMSAH metabolism, cell stress metabolism, amino acid metabolism and one-carbon

metabolism (**B**). All metabolites with a P<0.05 group difference (**C**), were lower in both patient groups. 5 metabolites were commonly reduced in both patient groups, while glutamate was only decreased significantly in long COVID patients. Red dots in A and white dots in B denote significantly altered metabolites at the group effect level, *P<0.05, **P<0.01, ***P<0.001

After post-hoc corrections, 14 metabolites were significantly altered in either patient group compared to healthy controls (Figure 4C). Metabolites that were lower in both patient groups compared to controls included citric acid, FAD^{2+}, glutamate, creatine, which are implicated in the TCA cycle or ATP production, and hydroxyphenyllactic acid, taurine[70], and CoA-Glutathione[71], which have been implicated in cell redox status. Whilst glutamate was the only common amino acid low in both patient groups, patients with ME/CFS also exhibited lower levels of the essential and large amino acids phenylalanine, tyrosine, methionine, isoleucine, and leucine, most prominently following exercise (Figure 4C).

We expected that patients would exhibit increased lipotoxic species, while lipids related to mitochondrial function and content would be reduced in patients. However, all lipid families were either not different or were lower in both long COVID and ME/CFS patient skeletal muscle (Figure 5A). Lipid families that were significantly lower were cardiolipins, sphingomyelins, PE, and PC, all of which are typically implicated in lipid membrane integrity (Figure 5B). No lipid species were significantly altered following 24 hours following exhaustive exercise (Supplemental Figure 2).

Metabolic contributions to muscle regenerative capacity

To elucidate whether indices of regeneration were related to metabolic function in patients and healthy controls, we compared metabolomic and lipidomic data with resident mononuclear cell populations and collagen IV deposition surrounding the myofibre at rest (Figure 6 A-C). $CD3^+$ T-cells were negatively associated with 2-aminobutyric acid, methylmalonylcarnitine, and glucose, while $CD63^+$ macrophages were positively associated with hippuric acid. Collagen IV deposition was positively associated with succinate, fructose 1,6 bisphosphate, and asparagine, and negatively associated with hydroxyphenyllactic acid and citric acid. FAP cell prevalence was negatively associated with glutathione and citrulline, whilst satellite cells were only negatively associated with carnitine 4.0. Moreso, satellite cell numbers were positively associated with multiple metabolites involved in oxidative metabolism or antioxidant metabolism. Collagen IV was negatively associated with membrane associated lipids, whilst $CD3^+$ T-cells, FAP cells and satellite cells were positively associated with membrane lipids (Figure 6B).

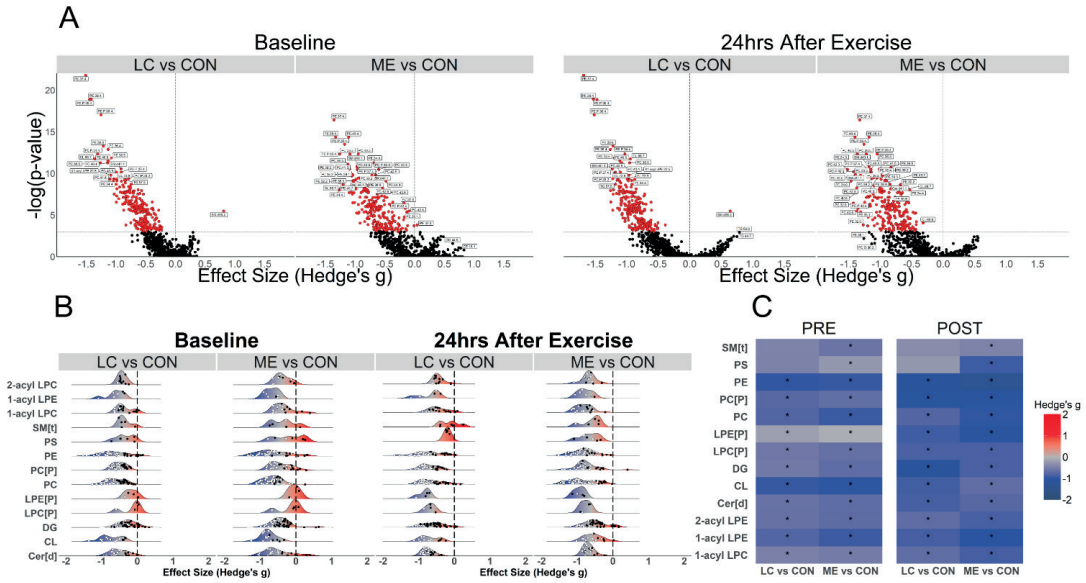


Figure 5: "Patients with long COVID and ME/CFS have lower amounts of membrane-associated lipid species, particularly related to the endoplasmic reticulum and mitochondria." Volcano plots (**A**) indicate effect sizes of individual lipid species, where the majority of species are lower (negative Hedge's g values) in long COVID and ME/CFS compared to healthy controls. Many of the significantly reduced lipid species are implicated in lipid membrane integrity (**B**), primarily those in the phosphatidylserine (PS), phosphatidylethanolamine (PE and PE[P]), phosphatidylcholine (PC), and cardiolipin (CL) classes. These classes are predominantly implicated in the cell membrane, endoplasmic reticulum, and the mitochondrial membrane.

As previous studies have indicated that myofibre integrity is important in satellite cell and FAP cell response[27,72,73], we queried whether there was an association between collagen IV and regenerative cell populations. Collagen IV was negatively associated with satellite cell count (Figure 6C). Conversely, satellite cell prevalence was positively associated with both $CD3^+$ cell prevalence and oxidative phosphorylation capacity (Figure 6C).

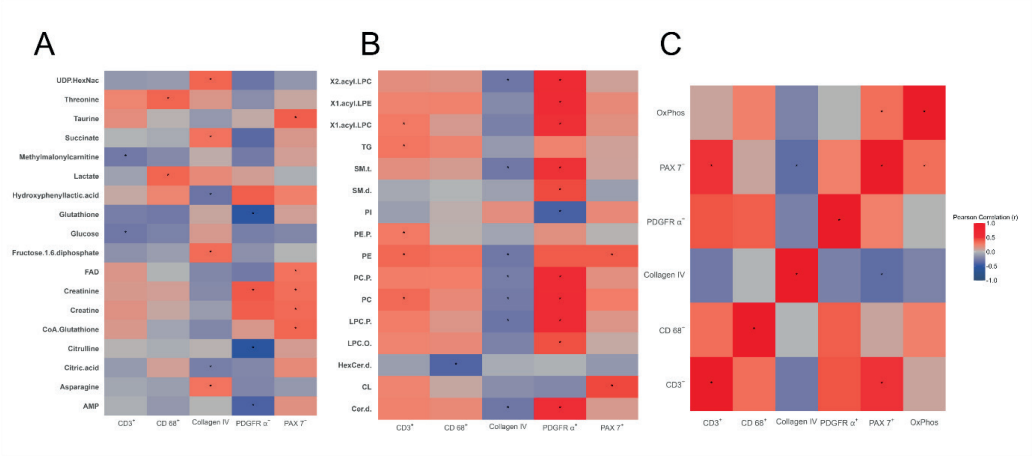


Figure 6: "Regenerative features and mononuclear cell populations were related with oxidative and antioxidant metabolites, and membrane-associated species." Correlation plots between regenerative features and metabolites (**A**), lipid classes (**B**) and other regenerative markers (**C**). Collagen IV surrounding the myofibre was negatively associated with membrane-associated lipids, while PDGFRα^+ cell count was positively associated with membrane-associated lipids. Satellite (PAX7$^+$) cells were predominantly associated with antioxidant metabolites, CD3$^+$ cells and oxidative phosphorylation capacity, while being negatively associated to collagen IV surrounding myofibres. *P<0.05

Discussion

In the current study, we sought to investigate to whether evidence of damage and repair was evident in PAIS skeletal muscle, and how differences in mononuclear cell populations may relate to altered regenerative features. Further, in an exploratory analysis, we sought to investigate whether changes to the skeletal muscle metabolic or lipid profiles related to regenerative features or alterations to mononuclear cell populations. Collagen IV was higher in both patients with long COVID and ME/CFS, coinciding with reductions in mononuclear cell populations. Patients with long COVID and ME/CFS exhibited less satellite cells and less FAP cells, while patients with ME/CFS had less CD3$^+$ and CD68$^+$ cells compared to healthy controls.

Lower potential for muscle tissue regeneration

The lower proportions of satellite cells in both patient groups indicates a lower propensity for regeneration at the myonuclear level. As satellite cells are required for muscle damage response and resolution of regeneration, the lower abundance of satellite cells would suggest that the

ability to respond to either mechanical or oxidative damage is reduced. Satellite cell number has been previously shown to decrease with aging, particularly in type II fibres[74,75], which has also been associated with more oxidative damage[76,77].

Moreso, the reduction of satellite cell proportions coincided with lower FAP cell counts in patients in ME/CFS and a tendency for lower FAP cell counts in patients with long COVID. FAP cells are necessary for proper satellite cell activation, and typically reside in greater proportions to satellite cells in skeletal muscle[29,78,79]. FAP cell numbers decrease with aging[26], which reduces the ability for satellite cells to integrate into myonuclei, and hence tissue regeneration is impaired. Further, intact FAP cell signalling is necessary for non-differentiated satellite cells to replenish the satellite cell pool and return to quiescence. Thus, the combination of lower number of satellite cells and FAP cells suggests a depletion of the satellite pool either by recurring damage or by improper restoration of the satellite cell pool via FAP cell signalling.

We further found evidence that $CD68^+$ cells were reduced in ME/CFS patients compared to healthy controls. The overall decrease in macrophages is in line with reports of immune exhaustion in ME/CFS patients. Previous studies investigating the peripheral blood mononuclear cells of ME/CFS and long COVID patients have shown that PBMCs have reduced metabolic activities or show reduced cytotoxic activity[11,80–83]. Additionally, the alternative macrophage activation pathways appear to be similarly impaired in long COVID and ME/CFS patients[84]. However, in the current study, we were unable to investigate the mononuclear cell function in skeletal muscle, and thus future studies should aim to address this.

Unresolved Regeneration and Impact on Myofibre Structure

In the current study, we observed a clear distinction between both patient groups and healthy controls in the amount of collagen IV surrounding muscle fibres. While abnormal collagen accumulation is typically indicative of fibrosis, and thus unresolved damage repair, which may relate to chronic inflammation[85], we found no differences between groups with respect to eMHC expression or myofibre lipid accumulation. Fibrosis, the result of abnormal collagen accumulation typically consisting of collagen I and III, is mediated by TGF-β and TNF-α[86–88]. However, how collagen IV is regulated in these scenarios is less completely understood, where in TGF-β signalling can reduce *COLIV* gene expression[89], and Wnt signalling promotes *COLIV* gene expression[90]. Additionally, exercise mediated collagen IV accumulation has been associated with Akt pathway signalling[91,92]. Thus, the results suggest that the collagen IV is not indicative of fibrosis *per se*, but possibly another mechanism that may be adjacently related.

Despite this, we found that collagen IV was negatively associated to satellite cell number. Previous studies have shown that stiffening of the ECM composition and fibrosis impair the ability for muscle to regenerate[93–95]. Therefore, the collagen IV accumulation observed in patient skeletal muscle likely confers a negative influence on regenerative processes.

Subsequently, we found that eMHC expression was not significantly different between groups, suggesting that ongoing regeneration or remodelling was not different between groups. However, as we previously noted a type I specific atrophy in both patient groups[9,14], it may be that remodelling is occurring in both patients and healthy controls, however the end product of such remodelling may not be similar between groups. More detailed evaluations of cell signalling related to the remodelling processes are warranted to draw apt conclusions.

Despite no obvious differences in ongoing damage and repair, we found that collectively the amount of collagen IV surrounding the myofibre was inversely related to lipids that contribute predominantly to cell membrane structure[96]. Specifically, phosphoethanolamines and phosphatidylcholines, which collectively account for ~80% of all cell membranes[97,98], were negatively correlated with collagen IV. As both these lipid classes were also found to be significantly lower in patients (Figure 3B), the data suggests a disruption of cellular membrane structure integrity and a potential compensation by increasing components of the extracellular matrix to maintain skeletal myofibre structure. Duchenne's muscular dystrophy, in which the lack of dystrophin results in unstable membrane formation, is also known to have collagen accumulation [99–101] as well as reduced satellite cell functionality[73]. While we did not query the presence of dystrophin here or membrane integrity directly, it is plausible that membrane disorganization relates to increased collagen deposition.

Above we noted that both satellite cell and FAP cell numbers are lower in both patients with long COVID and with ME/CFS, whilst ME/CFS patients additionally have lower $CD68^+$ and $CD3^+$ nuclei. It is well reported that proper skeletal muscle regeneration requires the coordination of multiple cell types[23,27] and appropriate transition from pro- to anti-inflammatory state[102,103] via signalling such as IL6, TGF-β1, WNT and WISP1, and IGF-1. Macrophage depletion has been shown to reduce TGF-β1 signalling resulting in increases in fibrosis[104], while recent evidence suggests that IGF-1 secreted by FAP cells is necessary for regeneration and ECM remodelling regulation[105]. Thus, future studies should aim to investigate whether specific signalling pathways related to regeneration are affected in patients.

Metabolic Contributions to Mononuclear Resident Cell Populations and Unresolved Regeneration

Previous reports show that mitochondrial oxidative phosphorylation capacity and metabolites relating to oxidative metabolism are lower in long COVID and ME/CFS patients[5,9,106]. Here, we observed that metabolites involved in both oxidative metabolism and anti-oxidant function were lower in both patients with long COVID and ME/CFS. A striking pattern observed in both long COVID and ME/CFS was the reduction of metabolites implicated in oxidative phosphorylation. Citric acid, FAD (P=0.056 in ME/CFS) and glutamate are implicated in the TCA cycle, which occurs in the mitochondrial matrix; while creatine (P=0.070 in ME/CFS) is essential for rapid cytosolic ATP generation and shuttling ADP and ATP between the cytosol and mitochondria[107,108]. Thus, reduction in these metabolites indicates a reduced capacity to generate reducing equivalents and reduced ability to shuttle ATP to the cytosol for biochemical use. As we previously report higher proportions of type IIa/IIx fibres and impaired mitochondrial respiratory capacity in both patient groups[9,14], these findings support a glycolytic shift in long COVID and ME/CFS.

Of the reduced metabolites taurine, FAD, creatine, creatinine, and CoA-glutathione were positively associated with satellite cell prevalence. This suggests that a balance between oxidative capacity and ability to reduce oxidative stress is necessary to maintain the satellite cell pool[109–111]. Generally, oxidative fibres contain more satellite cells than glycolytic fibres[75,112], however this is not always consistent in human studies[113]. In the contrary, it is well known that increases in oxidative stress of satellite cells reduces satellite cell efficacy, and over time depletes the viable satellite cell pool[114–117]. However, how satellite cell pools are altered in response to skeletal muscle fibre oxidative stress (rather than satellite cell oxidative stress) is more nuanced, and less studies have investigated this interaction.

Several amino acids were lower in skeletal muscle in both patient groups, but most specifically in patients with ME/CFS, and more prominently following exercise (Figure 2C). Notably, glutamate was lower in both patient groups, while tyrosine tended to be lower in long COVID patients (P=0.053), but was significantly lower in ME/CFS patients compared to healthy controls. ME/CFS patients also exhibited lower phenylalanine, methionine, isoleucine and leucine, all of which are essential amino acids. As amino acids are essential in protein synthesis, the reduced pool of available amino acids suggests a lower ability to synthesize proteins. Specifically, leucine is known to be one of two amino acids distinctly implicated in mTOR activation[118,119], and thus the lower levels of leucine in ME/CFS patients may indicate anabolic

resistance[120]. Additionally, all amino acids that were altered in either patient group are large amino acids and typically hydrophobic, which all use the same transporter: LAT1[121–123]. This then may indicate, particularly in ME/CFS patients, impairments in skeletal muscle uptake of large amino acids, impairing protein synthesis following damage or in response to cell stressors. LAT1 inhibition has been shown to result in insulin resistance and reduced mTOR activation[118,124]. Future work should investigate whether skeletal muscle gene expression or enzyme activity of LAT1 is altered in patients with long COVID and ME/CFS.

Reductions of satellite cell prevalence and increases in oxidative stress often coincide with remodelling of the extracellular matrix[109,111,125], notably resulting in increased collagen deposition and fibrosis surrounding muscle fibres, resulting in stiffening of the ECM[111,125,126]. Indeed, we observed that satellite cell prevalence was positively associated with membrane-associated lipids, while being negatively associated with collagen IV surrounding the myofibre (Figure 5), suggesting that satellite cell pools are interrelated with membrane composition. Further, collagen IV was found to be negatively associated with membrane-associated lipids, suggesting that alterations to membrane integrity may then relate to compensatory regulation of collagen IV, similarly to what has been reported in Duchenne's muscular dystrophy[127]. In the current study, we did not assess membrane integrity directly, and additionally we lack the time-resolution to distinguish whether impaired membrane integrity, collagen deposition, oxidative stress, or depletion of the satellite cell pool occurs first. Despite this, previous studies indicate that aerobic exercise training increases membrane fluidity[128], and thus it may be that the altered balance between oxidative capacity and oxidative stress seen in patients disrupts the myofibre membrane, resulting in an increase need for collagen IV deposition.

Multiple membrane lipid classes were reduced in patients compared to controls, similarly to other studies[129]. Notably, three significantly reduced classes also account for ~90% of the inner mitochondrial membrane lipids: phosphatidylcholines, phosphatidylethanolamines, and cardiolipins[97]. (Normalized) oxidative phosphorylation capacity both correlated with multiple membrane lipid species, particularly cardiolipins and phosphatidylethanolamines (Supplemental Figure 3), suggesting that mitochondrial integrity in particular may be affected in patients. Our observation that mitochondrial membrane lipids are altered in patients may help to resolve these differences, as the anchoring and activity of different mitochondrial subunits in the mitochondrial membrane are dependent on the lipid composition[130]. It is currently unknown if the altered lipid profiles underlie changes in skeletal muscle

mitochondrial density in patients with post-acute infectious diseases, as conflicting reports of about mitochondrial density or enzyme activity have been reported[5,14,131].

Limitations

One limitation of the current study is the lack of repeated biopsies to better understand the time course and causality of skeletal muscle alterations in patients with post-acute infectious diseases, as the second biopsy was taken 24 hours after the maximal exercise test, which is too short to observe structural changes. We did observe time-related changes in resident cell populations, metabolites, and lipid species after one maximal exercise session that help to understand how acute responses to exercise are different in patients compared to healthy controls.

We indicated that several alterations within the skeletal muscle microenvironment were associated with each other, namely the increased collagen IV coinciding with reduced membrane-associated lipids and reduced satellite cells. Due to the lack of longitudinal biopsies beyond a 24-hr time period, we cannot resolve what may be the instigating event. It may be that collagen IV accumulation precedes alterations in lipid-associated membrane composition and reductions in mononuclear cell populations, or vice-versa. Future studies should aim to investigate these temporal relationships from disease onset to better understand the physiological responses.

Although we indicated that there was no alteration in the number of nuclei per myofibre, we reported that mononuclear cell populations were reduced in patients, suggesting that a greater proportion of nuclei located between myofibres then may be associated to the myofibre itself. However, we lack the ability to resolve whether nuclei are myofibre specific. This may be aided in part with spatial transcriptomics.

While we reported that resident mononuclear cells were lower in patients, we lack the ability to comment on the functionality of these cells. This is of particular interest in the relation between satellite cells and FAP cells, in which a reduced ability for FAP cells to instigate satellite cell quiescence may precede the reduction of satellite cells. Further, we did not investigate whether satellite cells were activated, quiescent or senescent in this current study. Thus, future work should aim to assess the satellite cell-FAP cell interaction in patients and what state patient satellite cells exist in.

With regards to macrophages and T-cells, we employed a generic marker for both immune cell types. As different subsets of immune cells can promote or absolve inflammatory environments

differently, it would be of interest to further separate which subtypes of immune cell populations may be affected. This would require detailed spatially resolved proteomics or transcriptomics to study in more detail.

A second limitation is the spatial resolution of metabolites and lipid species within the skeletal muscle. We attribute most metabolites changes to the skeletal muscle, but we cannot resolve whether membrane-specific lipid species are integrated into cell membranes, endoplasmic reticular membrane, mitochondrial membrane, or other organelles. Any association between lipid species or classes with skeletal muscle structure can therefore be confounded by other intracellular factors, such as other organelles. Spatially-resolved metabolomics would then provide additional insights in future studies.

Conclusions

Here, we report that long COVID and ME/CFS patients exhibit increased myofibre fibrosis that coincides with lower content of satellite cells and FAP cells in skeletal muscle, which subsequently occurs alongside lower membrane-associated lipids and lower metabolites related to oxidative and anti-oxidant function. The lower satellite cell content in patients was related to increases in collagen IV surrounding the myofibre, however not indicative of fibrosis *per se*, decreases in membrane lipid species, and changes in oxidative and antioxidant metabolites. Thus, increased presence of unresolved regeneration in both long COVID and ME/CFS patients is likely a repercussion of lower satellite cell content, of which alterations to membrane structure and metabolic landscape may also influence skeletal muscle damage response. Thus, both patients with long COVID and ME/CFS whom experience PEM likely possess a reduced ability to recover following exercise (particularly damaging exercise), which may in part explain the occurrence of PEM.

References

1. Carruthers, B. M. *et al.* Myalgic Encephalomyelitis/Chronic Fatigue Syndrome. *J. Chronic Fatigue Syndr.* **11**, 7–115 (2003).
2. Thaweethai, T. *et al.* Development of a Definition of Postacute Sequelae of SARS-CoV-2 Infection. *JAMA* **329**, 1934–1946 (2023).
3. Cliff, J. M. *et al.* Cellular Immune Function in Myalgic Encephalomyelitis / Chronic Fatigue Syndrome (ME / CFS). *Front. Immunol.* **10**, 1–15 (2019).

4. Klein, J. *et al.* Distinguishing features of long COVID identified through immune profiling. *Nature* **623**, 139–148 (2023).

5. Colosio, M. *et al.* Structural and functional impairments of skeletal muscle in patients with postacute sequelae of SARS-CoV-2 infection. *J. Appl. Physiol.* **135**, 902–917 (2023).

6. Agergaard, J. *et al.* Myopathy as a cause of Long COVID fatigue: Evidence from quantitative and single fiber EMG and muscle histopathology. *Clinical Neurophysiology* **148**, 65–75 (2023).

7. Hejbøl, E. K. *et al.* Myopathy as a cause of fatigue in long-term post-COVID-19 symptoms: Evidence of skeletal muscle histopathology. *Eur. J. Neurol.* **29**, 2832–2841 (2022).

8. Agergaard, J. *et al.* Myopathic changes in patients with long-term fatigue after COVID-19. *Clinical Neurophysiology* **132**, 1974–1981 (2021).

9. Appelman, B. *et al.* Muscle abnormalities worsen after post-exertional malaise in long COVID. *Nat. Commun.* **15**, 17 (2024).

10. Missailidis, D. *et al.* An Isolated Complex V Inefficiency and Dysregulated Mitochondrial Function in Immortalized Lymphocytes from ME/CFS Patients. *International Journal of Molecular Sciences 2020, Vol. 21, Page 1074* **21**, 1074 (2020).

11. Macnaughtan, J. *et al.* Mitochondrial function is impaired in long COVID patients. *Ann. Med.* **57**, 2528167 (2025).

12. Szögi, T. *et al.* Novel biomarkers of mitochondrial dysfunction in Long COVID patients. *Geroscience* **47**, 2245–2261 (2024).

13. Wang, P. *et al.* WASF3 disrupts mitochondrial respiration and may mediate exercise intolerance in myalgic encephalomyelitis/chronic fatigue syndrome. *Proceedings of the National Academy of Sciences* **120**, (2023).

14. Nunes, M. *et al.* Virus-induced endothelial senescence as a cause and driving factor for ME/CFS and long COVID: mediated by a dysfunctional immune system. *Cell Death Dis.* **17**, 16 (2026).

15. Turner, S. *et al.* Increased Levels of Inflammatory and Endothelial Biomarkers in Blood of Long COVID Patients Point to Thrombotic Endotheliali tis. *Semin. Thromb. Hemost.* https://doi.org/10.1055/s-0043-1769014 (2023) doi:10.1055/s-0043-1769014.

16. Sandvik, M. K. *et al.* Endothelial dysfunction in ME/CFS patients. *PLoS One* **18**, e0280942 (2023).

17. Haffke, M. *et al.* Endothelial dysfunction and altered endothelial biomarkers in patients with post-COVID-19 syndrome and chronic fatigue syndrome (ME/CFS). *J. Transl. Med.* **20**, 138 (2022).

18. Scherbakov, N. *et al.* Peripheral endothelial dysfunction in myalgic encephalomyelitis/chronic fatigue syndrome. *ESC Heart Fail.* **7**, 1064–1071 (2020).

19. Aschman, T. *et al.* Post-COVID exercise intolerance is associated with capillary alterations and immune dysregulations in skeletal muscles. *Acta Neuropathol. Commun.* **11**, 193 (2023).

20. Tidball, J. G. & Villalta, S. A. Regulatory interactions between muscle and the immune system during muscle regeneration. *American Journal of Physiology-Regulatory, Integrative and Comparative Physiology* **298**, R1173–R1187 (2010).

21. Peake, J. M., Neubauer, O., Della Gatta, P. A. & Nosaka, K. Muscle damage and inflammation during recovery from exercise. *J. Appl. Physiol.* **122**, 559–570 (2017).

22. Oprescu, S. N., Yue, F., Qiu, J., Brito, L. F. & Kuang, S. Temporal Dynamics and Heterogeneity of Cell Populations during Skeletal Muscle Regeneration. *iScience* **23**, 100993 (2020).

23. Heredia, J. E. *et al.* Type 2 Innate Signals Stimulate Fibro/Adipogenic Progenitors to Facilitate Muscle Regeneration. *Cell* **153**, 376–388 (2013).

24. Nawaz, A. *et al.* Depletion of CD206+ M2-like macrophages induces fibro-adipogenic progenitors activation and muscle regeneration. *Nat. Commun.* **13**, 7058 (2022).

25. Lukjanenko, L. *et al.* Aging Disrupts Muscle Stem Cell Function by Impairing Matricellular WISP1 Secretion from Fibro-Adipogenic Progenitors. *Cell Stem Cell* **24**, 433-446.e7 (2019).

26. Brorson, J. *et al.* Complementing muscle regeneration—fibro-adipogenic progenitor and macrophage-mediated repair of elderly human skeletal muscle. *Nat. Commun.* **16**, 5233 (2025).

27. Schmidt, M., Schüler, S. C., Hüttner, S. S., von Eyss, B. & von Maltzahn, J. Adult stem cells at work: regenerating skeletal muscle. *Cellular and Molecular Life Sciences* **76**, 2559–2570 (2019).

28. Joe, A. W. B. *et al.* Muscle injury activates resident fibro/adipogenic progenitors that facilitate myogenesis. *Nat. Cell Biol.* **12**, 153–163 (2010).

29. Chapman, M. A., Mukund, K., Subramaniam, S., Brenner, D. & Lieber, R. L. Three distinct cell populations express extracellular matrix proteins and increase in number during skeletal muscle fibrosis. *American Journal of Physiology-Cell Physiology* **312**, C131–C143 (2017).

30. Calve, S., Odelberg, S. J. & Simon, H.-G. A transitional extracellular matrix instructs cell behavior during muscle regeneration. *Dev. Biol.* **344**, 259–271 (2010).

31. Bensalah, M. *et al.* A negative feedback loop between fibroadipogenic progenitors and muscle fibres involving endothelin promotes human muscle fibrosis. *J. Cachexia Sarcopenia Muscle* **13**, 1771–1784 (2022).

32. Schiaffino, S. & Mammucari, C. Regulation of skeletal muscle growth by the IGF1-Akt/PKB pathway: insights from genetic models. *Skelet. Muscle* **1**, 4 (2011).

33. Almada, A. E. & Wagers, A. J. Molecular circuitry of stem cell fate in skeletal muscle regeneration, ageing and disease. *Nat. Rev. Mol. Cell Biol.* **17**, 267–279 (2016).

34. Serrano, A. L., Baeza-Raja, B., Perdiguero, E., Jardí, M. & Muñoz-Cánoves, P. Interleukin-6 Is an Essential Regulator of Satellite Cell-Mediated Skeletal Muscle Hypertrophy. *Cell Metab.* **7**, 33–44 (2008).

35. Peng, Y. *et al.* Mechano-signaling via Piezo1 prevents activation and p53-mediated senescence of muscle stem cells. *Redox Biol.* **52**, 102309 (2022).

36. Wang, W. *et al.* GsMTx4-blocked PIEZO1 channel promotes myogenic differentiation and alleviates myofiber damage in Duchenne muscular dystrophy. *Skelet. Muscle* **15**, 13 (2025).

37. Le Grand, F., Jones, A. E., Seale, V., Scimè, A. & Rudnicki, M. A. Wnt7a Activates the Planar Cell Polarity Pathway to Drive the Symmetric Expansion of Satellite Stem Cells. *Cell Stem Cell* **4**, 535–547 (2009).

38. Kuang, S., Gillespie, M. A. & Rudnicki, M. A. Niche Regulation of Muscle Satellite Cell Self-Renewal and Differentiation. *Cell Stem Cell* **2**, 22–31 (2008).

39. Whalen, R. G., Harris, J. B., Butler-Browne, G. S. & Sesodia, S. Expression of myosin isoforms during notexin-induced regeneration of rat soleus muscles. *Dev. Biol.* **141**, 24–40 (1990).

40. Ciciliot, S. & Schiaffino, S. Regeneration of Mammalian Skeletal Muscle: Basic Mechanisms and Clinical Implications. *Curr. Pharm. Des.* **16**, 906–914 (2010).

41. Csapo, R., Gumpenberger, M. & Wessner, B. Skeletal Muscle Extracellular Matrix – What Do We Know About Its Composition, Regulation, and Physiological Roles? A Narrative Review. *Front. Physiol.* **11**, (2020).

42. Gillies, A. R. & Lieber, R. L. Structure and function of the skeletal muscle extracellular matrix. *Muscle Nerve* **44**, 318–331 (2011).

43. Wohlgemuth, R. P., Brashear, S. E. & Smith, L. R. Alignment, cross linking, and beyond: a collagen architect's guide to the skeletal muscle extracellular matrix. *American Journal of Physiology-Cell Physiology* **325**, C1017–C1030 (2023).

44. Urciuolo, A. *et al.* Collagen VI regulates satellite cell self-renewal and muscle regeneration. *Nat. Commun.* **4**, 1964 (2013).

45. Bizieff, A. *et al.* Changes in protein fluxes in skeletal muscle during sequential stages of muscle regeneration after acute injury in male mice. *Sci. Rep.* **14**, 13172 (2024).

46. Nichenko, A. S. *et al.* Mitochondrial maintenance via autophagy contributes to functional skeletal muscle regeneration and remodeling. *American Journal of Physiology-Cell Physiology* **311**, C190–C200 (2016).

47. Tezze, C. *et al.* Age-Associated Loss of OPA1 in Muscle Impacts Muscle Mass, Metabolic Homeostasis, Systemic Inflammation, and Epithelial Senescence. *Cell Metab.* **25**, 1374-1389.e6 (2017).

48. Liu, X. *et al.* Mitochondrial glycerol 3-phosphate dehydrogenase promotes skeletal muscle regeneration. *EMBO Mol. Med.* **10**, (2018).

49. de Boer, E. *et al.* Decreased Fatty Acid Oxidation and Altered Lactate Production during Exercise in Patients with Post-acute COVID-19 Syndrome. *Am. J. Respir. Crit. Care Med.* **205**, 126–129 (2022).

50. Cotler, J., Holtzman, C., Dudun, C. & Jason, L. A. A Brief Questionnaire to Assess Post-Exertional Malaise. *Diagnostics* **8**, 66 (2018).

51. Mehlem, A., Hagberg, C. E., Muhl, L., Eriksson, U. & Falkevall, A. Imaging of neutral lipids by oil red O for analyzing the metabolic status in health and disease. *Nat. Protoc.* **8**, 1149–1154 (2013).

52. Fowler, S. D. & Greenspan, P. Application of Nile red, a fluorescent hydrophobic probe, for the detection of neutral lipid deposits in tissue sections: comparison with oil red O. *Journal of Histochemistry & Cytochemistry* **33**, 833–836 (1985).

53. van Weeghel, M. *et al.* Profiling of intracellular metabolites produced from galactose and its potential for galactosemia research. *Orphanet J. Rare Dis.* **13**, 146 (2018).

54. Herzog, K. *et al.* Lipidomic analysis of fibroblasts from Zellweger spectrum disorder patients identifies disease-specific phospholipid ratios. *J. Lipid Res.* **57**, 1447–1454 (2016).

55. Foidart, M., Foidart, J.-M. & Engel, W. K. Collagen Localization in Normal and Fibrotic Human Skeletal Muscle. *Arch. Neurol.* **38**, 152–157 (1981).

56. Mendias, C. L., Schwartz, A. J., Grekin, J. A., Gumucio, J. P. & Sugg, K. B. Changes in muscle fiber contractility and extracellular matrix production during skeletal muscle hypertrophy. *J. Appl. Physiol.* **122**, 571–579 (2017).

57. Koskinen, S. O. *et al.* Short-term effects of forced eccentric contractions on collagen synthesis and degradation in rat skeletal muscle. *Pflügers Archiv* **444**, 59–72 (2002).

58. Mackey, A. L., Donnelly, A. E., Turpeenniemi-Hujanen, T. & Roper, H. P. Skeletal muscle collagen content in humans after high-force eccentric contractions. *J. Appl. Physiol.* **97**, 197–203 (2004).

59. Kanazawa, Y., Nagano, M., Koinuma, S., Sugiyo, S. & Shigeyoshi, Y. Effects of Endurance Exercise on Basement Membrane in the Soleus Muscle of Aged Rats. *Acta Histochem. Cytochem.* **54**, 21–00057 (2021).

60. Agarwal, M. *et al.* Myosin heavy chain-embryonic regulates skeletal muscle differentiation during mammalian development. *Development* **147**, (2020).

61. Anderson, E. J. & Neufer, P. D. Type II skeletal myofibers possess unique properties that potentiate mitochondrial H_2O_2 generation. *American Journal of Physiology-Cell Physiology* **290**, C844–C851 (2006).

62. Yu, Z. *et al.* Fiber Type-Specific Nitric Oxide Protects Oxidative Myofibers against Cachectic Stimuli. *PLoS One* **3**, e2086 (2008).

63. Choi, S. J. *et al.* Eccentric contraction-induced injury to type I, IIa, and IIa/IIx muscle fibers of elderly adults. *Age (Omaha).* **34**, 215–226 (2012).

64. Norris, A. M. *et al.* Studying intramuscular fat deposition and muscle regeneration: insights from a comparative analysis of mouse strains, injury models, and sex differences. *Skelet. Muscle* **14**, 12 (2024).

65. Mann, C. J. *et al.* Aberrant repair and fibrosis development in skeletal muscle. *Skelet. Muscle* **1**, 21 (2011).

66. Natarajan, A., Lemos, D. R. & Rossi, F. M. V. Fibro/adipogenic progenitors: A double-edged sword in skeletal muscle regeneration. *Cell Cycle* **9**, 2045–2046 (2010).

67. Ato, S. & Ogasawara, R. The relationship between myonuclear number and protein synthesis in individual rat skeletal muscle fibres. *Journal of Experimental Biology* **224**, (2021).

68. Schiaffino, S., Dyar, K. A., Ciciliot, S., Blaauw, B. & Sandri, M. Mechanisms regulating skeletal muscle growth and atrophy. *FEBS J.* **280**, 4294–4314 (2013).

69. Spriet, L. L. & Whitfield, J. Taurine and skeletal muscle function. *Curr. Opin. Clin. Nutr. Metab. Care* **18**, 96–101 (2015).

70. Ondarza, R. N., Escamilla, E., Gutiérrez, J. & de la Chica, G. CoAS-Sglutathione and GSSG reductases from rat liver. *Biochimica et Biophysica Acta (BBA) - Enzymology* **341**, 162–171 (1974).

71. Malecova, B. *et al.* Dynamics of cellular states of fibro-adipogenic progenitors during myogenesis and muscular dystrophy. *Nat. Commun.* **9**, 3670 (2018).

72. Granet, J. A. *et al.* Muscle stem cells in Duchenne muscular dystrophy exhibit molecular impairments and altered cell fate trajectories impacting regenerative capacity. *Cell Death Dis.* **16**, 437 (2025).

73. Runyan, C. E. *et al.* Impaired phagocytic function in CX3CR1 $^{+}$ tissue-resident skeletal muscle macrophages prevents muscle recovery after influenza A virus-induced pneumonia in old mice. *Aging Cell* **19**, (2020).

74. Parker, E. & Hamrick, M. W. Role of fibro-adipogenic progenitor cells in muscle atrophy and musculoskeletal diseases. *Curr. Opin. Pharmacol.* **58**, 1–7 (2021).

75. Peppercorn, K., Edgar, C. D., Kleffmann, T. & Tate, W. P. A pilot study on the immune cell proteome of long COVID patients shows changes to physiological pathways similar to those in myalgic encephalomyelitis/chronic fatigue syndrome. *Sci. Rep.* **13**, 22068 (2023).

76. Sweetman, E. *et al.* A SWATH-MS analysis of Myalgic Encephalomyelitis/Chronic Fatigue Syndrome peripheral blood mononuclear cell proteomes reveals mitochondrial dysfunction. *J. Transl. Med.* **18**, 365 (2020).

77. Shahbaz, S. *et al.* Single-cell analysis reveals immune remodeling of monocytes, NK cells, T cell exhaustion, and Galectin-9–associated depletion of gamma delta and mucosal-associated invariant T cells in Long COVID with ME/CFS. *Front. Immunol.* **17**, (2026).

78. Fluge, Ø. *et al.* Metabolic profiling indicates impaired pyruvate dehydrogenase function in myalgic encephalopathy/chronic fatigue syndrome. *JCI Insight* **1**, (2016).

79. Eaton-Fitch, N. *et al.* Immune exhaustion in ME/CFS and long COVID. *JCI Insight* **9**, (2024).

80. Grounds, M. D. Age-associated Changes in the Response of Skeletal Muscle Cells to Exercise and Regeneration [a]. *Ann. N. Y. Acad. Sci.* **854**, 78–91 (1998).

81. Smith, L. R. & Barton, E. R. Regulation of fibrosis in muscular dystrophy. *Matrix Biology* **68–69**, 602–615 (2018).

82. Lemos, D. R. *et al.* Nilotinib reduces muscle fibrosis in chronic muscle injury by promoting TNF-mediated apoptosis of fibro/adipogenic progenitors. *Nat. Med.* **21**, 786–794 (2015).

83. Wynn, T. A. & Vannella, K. M. Macrophages in Tissue Repair, Regeneration, and Fibrosis. *Immunity* **44**, 450–462 (2016).

84. Jayadev, R. *et al.* A basement membrane discovery pipeline uncovers network complexity, regulators, and human disease associations. *Sci. Adv.* **8**, (2022).

85. Pietilä, I. *et al.* Wnt5a Deficiency Leads to Anomalies in Ureteric Tree Development, Tubular Epithelial Cell Organization and Basement Membrane Integrity Pointing to a Role in Kidney Collecting Duct Patterning. *PLoS One* **11**, e0147171 (2016).

86. Li, X. *et al.* Akt/PKB regulates laminin and collagen IV isotypes of the basement membrane. *Proceedings of the National Academy of Sciences* **98**, 14416–14421 (2001).

87. Chen, L., Bai, J. & Li, Y. miR-29 mediates exercise-induced skeletal muscle angiogenesis by targeting VEGFA, COL4A1 and COL4A2 via the PI3K/Akt signaling pathway. *Mol. Med. Rep.* **22**, 661–670 (2020).

88. Petrocelli, J. J. *et al.* Metformin and leucine increase satellite cells and collagen remodeling during disuse and recovery in aged muscle. *The FASEB Journal* **35**, (2021).

89. Csapo, R., Gumpenberger, M. & Wessner, B. Skeletal Muscle Extracellular Matrix – What Do We Know About Its Composition, Regulation, and Physiological Roles? A Narrative Review. *Front. Physiol.* **11**, (2020).

90. Snow, MikelH. The effects of aging on satellite cells in skeletal muscles of mice and rats. *Cell Tissue Res.* **185**, (1977).

91. van Meer, G., Voelker, D. R. & Feigenson, G. W. Membrane lipids: where they are and how they behave. *Nat. Rev. Mol. Cell Biol.* **9**, 112–124 (2008).

92. Horvath, S. E. & Daum, G. Lipids of mitochondria. *Progress in Lipid Research* vol. 52 590–614 Preprint at https://doi.org/10.1016/j.plipres.2013.07.002 (2013).

93. van der Veen, J. N. *et al.* The critical role of phosphatidylcholine and phosphatidylethanolamine metabolism in health and disease. *Biochimica et Biophysica Acta (BBA) - Biomembranes* **1859**, 1558–1572 (2017).

94. Li, Y. *et al.* Skeletal muscle stem cells modulate niche function in Duchenne muscular dystrophy mouse through YY1-CCL5 axis. *Nat. Commun.* **16**, 1324 (2025).

95. Dulos, J. *et al.* ADAMTS-5 inhibition reduces muscle inflammation and fibrosis and improves function in mouse models of Duchenne muscular dystrophy. *Sci. Transl. Med.* **17**, (2025).

96. Russell, A. J. *et al.* Modulating fast skeletal muscle contraction protects skeletal muscle in animal models of Duchenne muscular dystrophy. *Journal of Clinical Investigation* **133**, (2023).

97. Yang, W. & Hu, P. Skeletal muscle regeneration is modulated by inflammation. *J. Orthop. Translat.* **13**, 25–32 (2018).

98. Bentzinger, C. F., Wang, Y. X., Dumont, N. A. & Rudnicki, M. A. Cellular dynamics in the muscle satellite cell niche. *The EMBO Reports* **14**, 1062–1072 (2013).

99. Xiao, W., Liu, Y. & Chen, P. Macrophage Depletion Impairs Skeletal Muscle Regeneration: the Roles of Pro-fibrotic Factors, Inflammation, and Oxidative Stress. *Inflammation* **39**, 2016–2028 (2016).

100. Luo, Y. E. *et al.* Resident mesenchymal progenitor cells require autocrine IGF-I in homeostatic and regenerating skeletal muscle. *Stem Cell Reports* **21**, 102973 (2026).

101. Tasoula, A. *et al.* Multi-omics analysis of long COVID (post-COVID-19 condition) reveals persistent mitochondrial dysfunction, suppressed oxidative phosphorylation, and immune dysregulation. *Front. Immunol.* **17**, (2026).

102. Perry, C. G. R. *et al.* Mitochondrial creatine kinase activity and phosphate shuttling are acutely regulated by exercise in human skeletal muscle. *Journal of Physiology* **590**, 5475–5486 (2012).

103. Su, Y. Three-dimensional network of creatine metabolism: From intracellular energy shuttle to systemic metabolic regulatory switch. *Mol. Metab.* **100**, 102228 (2025).

104. Fulle, S. *et al.* Age-dependent imbalance of the antioxidative system in human satellite cells. *Exp. Gerontol.* **40**, 189–197 (2005).

105. Wang, Y. *et al.* Cell biomechanics on muscle atrophy: from intricate mechanisms to therapeutic frontiers. *Ann. Med.* **57**, (2025).

106. Beccafico, S. *et al.* Age-Dependent Effects on Functional Aspects in Human Satellite Cells. *Ann. N. Y. Acad. Sci.* **1100**, 345–352 (2007).

107. Verdijk, L. B. *et al.* Skeletal Muscle Hypertrophy Following Resistance Training Is Accompanied by a Fiber Type-Specific Increase in Satellite Cell Content in Elderly Men. *J. Gerontol. A Biol. Sci. Med. Sci.* **64A**, 332–339 (2009).

108. Mackey, A. L. *et al.* Differential satellite cell density of type <scp>I</scp> and <scp>II</scp> fibres with lifelong endurance running in old men. *Acta Physiologica* **210**, 612–627 (2014).

109. Kadi, F., Charifi, N. & Henriksson, J. The number of satellite cells in slow and fast fibres from human vastus lateralis muscle. *Histochem. Cell Biol.* **126**, 83–87 (2006).

110. Le Moal, E. *et al.* Redox Control of Skeletal Muscle Regeneration. *Antioxid. Redox Signal.* **27**, 276–310 (2017).

111. Barbieri, E. & Sestili, P. Reactive Oxygen Species in Skeletal Muscle Signaling. *J. Signal Transduct.* **2012**, 1–17 (2012).

112. Yao, Y. *et al.* The role of oxidative stress-mediated fibro-adipogenic progenitor senescence in skeletal muscle regeneration and repair. *Stem Cell Res. Ther.* **16**, 104 (2025).

113. Hong, X. *et al.* Mitochondrial dynamics maintain muscle stem cell regenerative competence throughout adult life by regulating metabolism and mitophagy. *Cell Stem Cell* **29**, 1298-1314.e10 (2022).

114. Milkereit, R. *et al.* LAPTM4b recruits the LAT1-4F2hc Leu transporter to lysosomes and promotes mTORC1 activation. *Nat. Commun.* **6**, 7250 (2015).

115. Atherton, P. J., Smith, K., Etheridge, T., Rankin, D. & Rennie, M. J. Distinct anabolic signalling responses to amino acids in C2C12 skeletal muscle cells. *Amino Acids* **38**, 1533–1539 (2010).

116. Devries, M. C. *et al.* Leucine, Not Total Protein, Content of a Supplement Is the Primary Determinant of Muscle Protein Anabolic Responses in Healthy Older Women. *J. Nutr.* **148**, 1088–1095 (2018).

117. Scalise, M., Galluccio, M., Console, L., Pochini, L. & Indiveri, C. The Human SLC7A5 (LAT1): The Intriguing Histidine/Large Neutral Amino Acid Transporter and Its Relevance to Human Health. *Front. Chem.* **6**, (2018).

118. Zhang, J. *et al.* Review of the Correlation of LAT1 With Diseases: Mechanism and Treatment. *Front. Chem.* **8**, (2020).

119. Scalise, M., Galluccio, M., Console, L., Pochini, L. & Indiveri, C. The Human SLC7A5 (LAT1): The Intriguing Histidine/Large Neutral Amino Acid Transporter and Its Relevance to Human Health. *Front. Chem.* **6**, (2018).

120. Takegaki, J., Saneyasu, T. & Honda, K. Treatment with L-type amino acid transporter 1 inhibitor JPH203 enhances protein synthesis in C2C12 myotubes. *Sci. Rep.* **15**, 40805 (2025).

121. Murphy, M. M., Lawson, J. A., Mathew, S. J., Hutcheson, D. A. & Kardon, G. Satellite cells, connective tissue fibroblasts and their interactions are crucial for muscle regeneration. *Development* **138**, 3625–3637 (2011).

122. Fry, C. S., Kirby, T. J., Kosmac, K., McCarthy, J. J. & Peterson, C. A. Myogenic Progenitor Cells Control Extracellular Matrix Production by Fibroblasts during Skeletal Muscle Hypertrophy. *Cell Stem Cell* **20**, 56–69 (2017).

123. Jama, A. *et al.* Lipin1 plays complementary roles in myofibre stability and regeneration in dystrophic muscles. *J. Physiol.* **601**, 961–978 (2023).

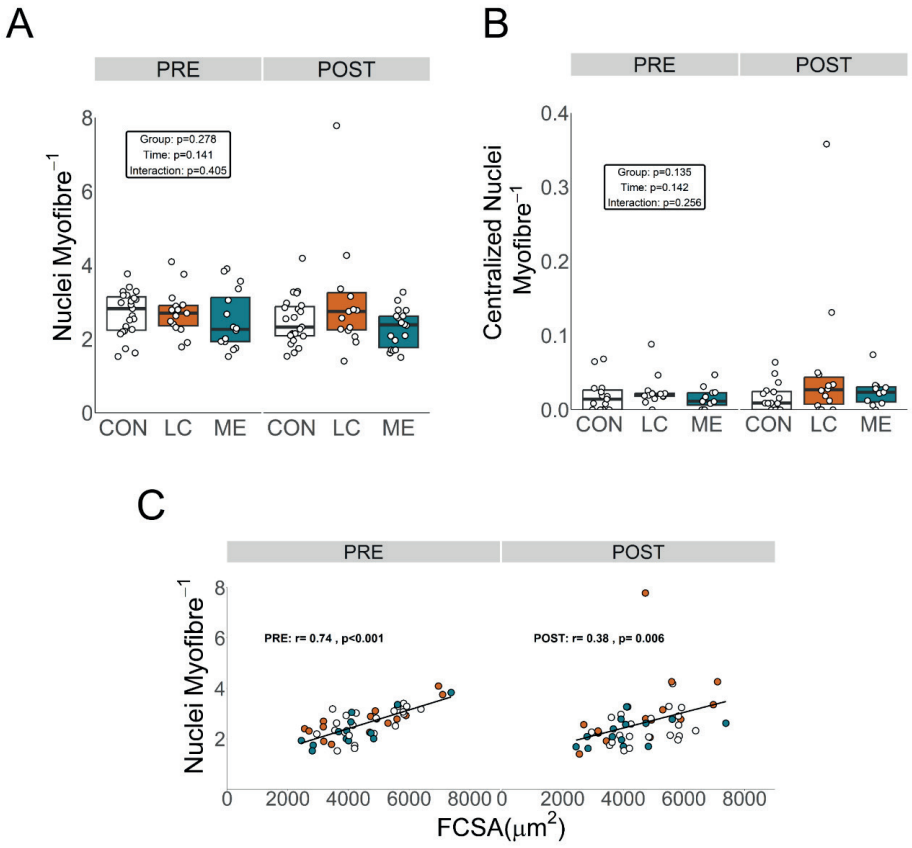
124. Piedrafita, E., Bascuas, P. J., Bataller-Cervero, A. V. & Berzosa, C. Aerobic Running Training Attenuates Lipid and Protein Oxidation and Modulates Membrane Dynamics in Metabolically Active Tissues. *Frontiers in Bioscience-Landmark* **31**, (2026).

125. Tryfonos, A. *et al.* Muscle Abnormalities in Nonhospitalised Patients With Post–COVID-19 Condition. *J. Cachexia Sarcopenia Muscle* **16**, (2025).

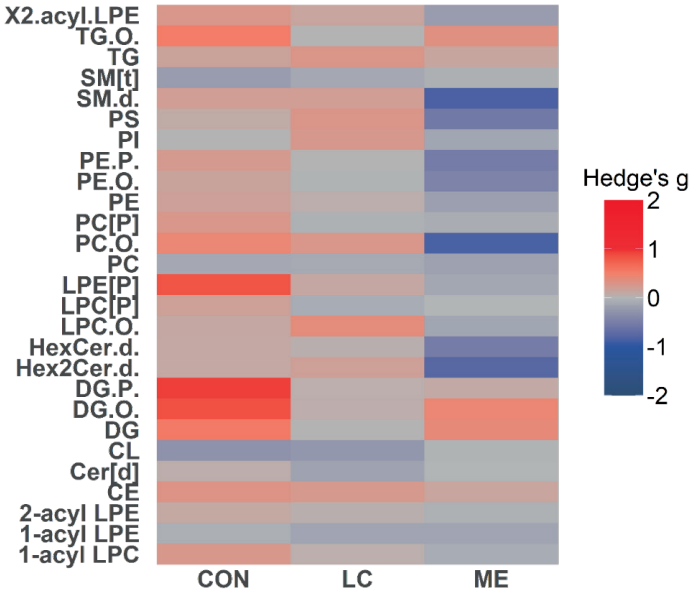
126. Baker, C. D., Basu Ball, W., Pryce, E. N. & Gohil, V. M. Specific requirements of nonbilayer phospholipids in mitochondrial respiratory chain function and formation. *Mol. Biol. Cell* **27**, 2161–2171 (2016).

127. Charlton, B. T. *et al.* Skeletal muscle adaptations and post-exertional malaise in long COVID. *Trends in Endocrinology & Metabolism* **36**, 614–622 (2025).

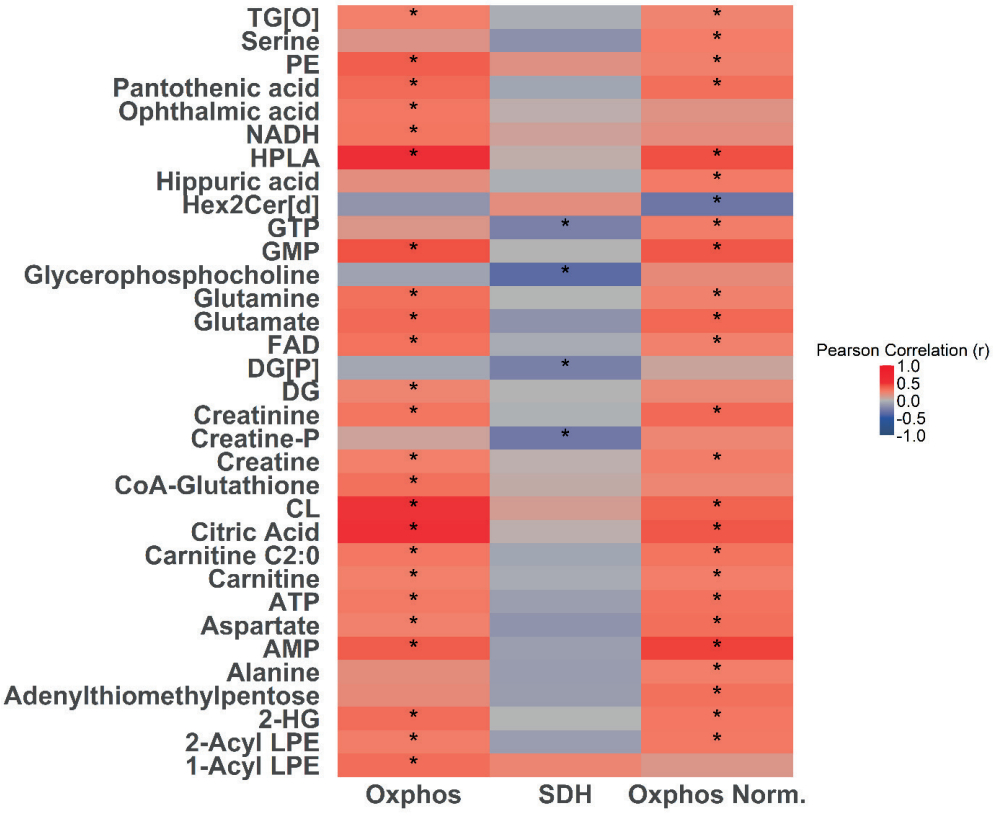
Supplemental Figures



Supplemental Figure 1: Number of nuclei per myofibre (**A**) was not different between groups either before or 24 hours after exercise. The number of observed centralized nuclei per myofibre was not different between groups, nor before or 24 hours after exercise (**B**). Nuclear content was related to fibre cross sectional area (FCSA, **C**).



Supplemental Figure 2: Prior to multiple testing corrections, diacylglycerols (DG, DG[O], and DG[P]) were significantly increased following exercise (unadjusted p=0.034, p=0.012, p=0.042 respectively). Following Benjamini-Hochberg corrections, no classes were significantly altered 24 hours after maximal cardiopulmonary exercise testing. *P<0.05.



Supplemental Figure 3: Associations of metabolites and lipid classes with oxidative phosphorylation capacity, succinate dehydrogenase activity (as a proxy for mitochondrial content), and normalized oxidative phosphorylation capacity. *P<0.05.



Chapter 10

General Discussion



Worldwide, chronic illnesses account for a large proportion of disease burden, including diabetes, HIV/AIDS, and SARS-CoV2[1]. Many of these diseases have a known pathophysiology and health effects can be mitigated through a triage of treatments, including physical activity[2]. However, little is known about the pathophysiological mechanisms underlying both long COVID and ME/CFS, two chronic diseases which many patients are defined by post-exertional malaise (PEM)[3]. PEM-episodes result in worsening of patient symptoms or development of new symptoms, which occurs over days and can last for months[4–7]. Ultimately, this results in patients avoiding activities that trigger PEM, most commonly physical activity[8,9]. While little is known about the physiological repercussions of PEM, it is certain that long-term physical inactivity also results in severe health decrements[10,11]. Thus, this thesis aimed to resolve several unknowns in the field of long COVID and ME/CFS, namely:

1. Do patients with long COVID that experience PEM exhibit skeletal muscle alterations that may contribute to symptoms, such as myalgia and PEM (chapter 2)?
2. Can whole-body aerobic capacities and skeletal muscle alterations in patients with long COVID and ME/CFS be attributed to physical inactivity alone (chapters 6 and 8)?
3. Do long COVID and ME/CFS share similar skeletal muscle adaptations (chapters 8 and 9)?
4. How are resident mononuclear cell populations affected in long COVID and ME/CFS? Particularly, are distinct populations of resident mononuclear cells preferentially affected that may partially explain patient symptoms, such as myalgia and PEM (chapter 9)?
5. With the onset of post-exertional malaise, how does the metabolic landscape of skeletal muscle change (chapters 2 and 9)?
6. Is the ability for patients to respond to exercise affected by differences in either a) resident mononuclear cells or b) alterations to metabolic landscapes following exercise (chapter 9)?

In chapter 2, whether long COVID patients display any whole-body or skeletal muscle characteristics that are distinct from healthy individuals, and whether that may in part explain symptoms was investigated. Here, it was resolved that there are skeletal muscle alterations distinct in long COVID patients from those of healthy individuals that likely contribute to multiple symptoms, including severe fatigue, myalgia, and PEM. Specifically, long COVID

patients exhibit lower mitochondrial function, higher proportions of glycolytic fibres, lower oxidative metabolites, and more frequently show signs of necrosis and damage.

As long COVID is a relatively novel disease, and little is known about PEM pathophysiology, chapter 3 thus sought to summarize the likely contributing factors to skeletal muscle alterations in long COVID and PEM pathophysiology. In this chapter, skeletal muscle adaptations in patients and PEM pathophysiology were highlighted by possible mitochondrial dysfunction, endothelial dysfunction, autoimmunity, localized hypoxia, electrophysiological alterations, central nervous system impairments, and deconditioning.

Whilst chapter 2 refutes the concept that long COVID is a psychological disorder, skepticism arose as to whether alterations observed in long COVID patients were simply due to deconditioning[12,13]. Thus, chapters 3b, 4b, 6, 7 and 8 aimed to address skeletal muscle and cardiac adaptations that occur due to deconditioning, long COVID, and due to ME/CFS. In chapter 8, it was highlighted that although whole-body aerobic exercise is similarly reduced in deconditioning, long COVID and ME/CFS, the underlying physiological changes occur uniquely. Bed rest (or deconditioning) is primarily associated by a reduction in muscle mass, mitochondrial content, decreases in carnitine metabolites, and increases in lipotoxic species. Patients with long COVID and ME/CFS had mitochondrial dysfunction (rather than just mitochondrial loss), higher proportions of glycolytic fibres. Patients with ME/CFS were distinct in some aspects compared to patients with long COVID, primarily with less capillarization, and lower succinate dehydrogenase (SDH) activity. However, the skeletal muscle characteristics of the two diseases largely resemble each other.

Due to the alterations seen in long COVID and ME/CFS largely resembling one another, and due to the presence of PEM in patients, I further queried how exercise may 1) damage the muscle and therefore contribute to myalgia, and 2) how regeneration may be affected in patients and therefore how this may contribute to PEM onset. In chapter 9, I therefore assessed resident mononuclear cell populations that are involved in muscle damage response and regeneration, markers of ongoing and unresolved regeneration, and how the metabolic landscapes of patients may result in altered regenerative processes. Here, I observed that not only did patients with long COVID and ME/CFS present with more indications of fibrosis compared to healthy individuals, satellite cell populations were reduced, likely further contributing to an ability to respond to damage. While both healthy controls and long COVID patients showed the typical increase in resident immune cell populations following exercise, patients with ME/CFS further exhibited reduced macrophage and T-cell populations, suggesting immune system

exhaustion[14–16]. Collagen IV deposition, an indicator of fibrosis, was found to be negatively associated with lipids associated with membrane integrity, whilst satellite cell prevalence was positively associated with metabolites related to antioxidant function, oxidative phosphorylation capacity, and negatively associated with collagen IV.

Skeletal Muscle Alterations in Long COVID and ME/CFS: What's the difference?

One of the major aims of the thesis was to investigate whether long COVID and ME/CFS share a similar underlying pathophysiology. In chapters 2 and 8, I highlight that whole-body exercise in both long COVID and ME/CFS patients was reduced predominantly as a result of either reduced cardiac stroke volume or impaired peripheral oxygen extraction and utilization (as indicated by the relative decreases in maximal oxygen pulse and increased HR-VO_2 relationships). We found little evidence for respiratory limitations in maximal aerobic capacity compared to controls. Within these measures, I did not have the ability to measure stroke volume, and thus the cardiac contribution to reduced aerobic capacity in patients is largely unknown, despite indications that cardiac morphology and function in both long COVID and ME/CFS patients is comparable to healthy persons[17–22]. However, I further investigated whether peripheral adaptations may contribute to lower aerobic capacities, under the premise that if little adaptations were seen, then it would be likely that cardiac alterations contribute largely to the decreased aerobic capacities. While this would not exclude the involvement of the cardiac system to reduced aerobic capacity, it would provide indications whether cardiac impairments would solely explain reduced aerobic capacity.

When assessing peripheral skeletal muscle alterations, it was apparent that long COVID and ME/CFS exhibited similar adaptations, namely increased proportions of fast-twitch, glycolytic fibres, reduced oxidative phosphorylation capacity (even when normalized to a proxy for mitochondrial content), increased fibrosis surrounding the myofibre, decreased satellite cell populations, reduced oxidative and antioxidant metabolites, and reductions to lipid species associated with cell membrane integrity. The key differences that distinguished long COVID patients from ME/CFS was the lower capillary fibre ratios found in ME/CFS patients, decreased SDH activity (a proxy for mitochondrial content), and lower resident immune cell populations, possibly indicative of immune exhaustion[14,15]. In many of these measures, it appeared to be near step-wise effects moving from healthy controls to long COVID patients to

ME/CFS patients. The exception being collagen IV deposition around myofibres, in which long COVID patients had more compared to ME/CFS patients.

When evaluating metabolite signatures, more differences begin to emerge between the two diseases. Particularly, compared to controls, ME/CFS patients had lower amino acid pools, of which 5 are essential amino acids, and all utilize the same LAT1 transporter for large amino acids. Long COVID patients, however, only displayed lower glutamate levels compared to healthy controls. Despite this, they only differed from ME/CFS patients in levels of isoleucine and tryptophan, in which ME/CFS patients had lower of both, particularly following exercise. While protein synthesis rates were not measured in this thesis, the lower pool of available amino acids would implicate reduced integration of amino acids into proteins in both patient groups.

A large confounder between distinguishing long COVID patients from ME/CFS is duration of disease. In general, long COVID patients, at the time of testing, had been ill for a shorter duration of time than the most recently diagnoses ME/CFS patient. With the many parameters that indicate near step-wise patterns between healthy controls, long COVID, and ME/CFS patients, it is tempting to suggest that long COVID is perhaps just an early stage of ME/CFS. Unfortunately, this would require follow up of patients years after long COVID diagnosis to evaluate the temporal progression of the disease. Likewise, for all ME/CFS patients, I lack earlier obtained biopsies to understand the trajectory of their disease. Thus, it may well be that the repercussions of both diseases are largely similar, but perhaps the event of onset defines certain unique alterations that occur. In order to investigate this, large scale studies are certainly required, in which the mechanism of onset is clearly defined and represented within the cohorts.

As the repercussions of PEM are experienced by patients systemically, it is possible that circulating factors may contribute to PEM onset in both long COVID and ME/CFS, such as the contents of extracellular vesicles[23], which may be released during exercise bouts. A simple experiment to elucidate whether PEM occurs via similar mechanisms in both long COVID and ME/CFS would be to expose C2C12 myoblasts and myotubes to patient sera and healthy control sera obtained both before and after exercise. C2C12 cells exposed to patient sera collected following exercise should therefore exhibit similar morphological, protein expression, and gene expression alterations in both long COVID and ME/CFS. Further, C2C12 cells exposed to sera can be stimulated electrically to recapitulate the effects of exercise. Therefore, whether patient sera at baseline contains PEM-contributing factors can also be investigated.

PEM pathophysiology

Two major goals of this thesis were to investigate 1) whether the PEM experienced by long COVID and ME/CFS patients had a similar underlying physiological basis, and 2) whether there were distinct patterns that may indicate PEM occurrence. While in multiple instances, long COVID patients and ME/CFS patients showed similar physiological alterations compared to healthy controls, there was an overall lack of distinguishing features relating to PEM onset. In chapter 2, skeletal muscle SDH activity and metabolite concentrations of asparagine and DHAP declined in long COVID patients 24hrs after exercise, and the number of long COVID patients positive for $CD3^+$ cell infiltration increased less than healthy controls following exercise. In chapter 9, however, after accounting for total nuclear content, there was no impaired increase of $CD3^+$ cell numbers following exercise in long COVID patients. This disparity may be in part due to variability amongst pathology grading[24–26].

When considering the metabolite quantities, however, two metabolites indicated differential effects in long COVID patients and ME/CFS compared to controls: UDP-HexNac and phosphorylethanolamine. Following exercise, UDP-HexNac increased in healthy controls, but in neither patient group. UDP-HexNac has been implicated as a sugar donor in O-GlcNac protein modifications, which is thought to reduce proteoasomal breakdown[27–29], and typically increases following stress[30,31]. Thus, lower levels of UDP-HexNac may rather indicate a lower ability to protect against unwanted protein degradation following stress events in long COVID and ME/CFS patients.

Phosphorylethanolamine on the other hand similarly increased following exercise in both healthy controls and long COVID patients, but failed to increase in ME/CFS patients. Phosphorylethanolamine is implicated in osmolarity regulation[32,33] and the synthesis in phospholipids[32,34], and therefore may be central to the eventual disruption of phospholipids observed in patients. This appeared to be a distinguishing feature between ME/CFS and long COVID patients, where ME/CFS patient phospholipids decreased following exercise, where healthy controls and long COVID patients remained relatively unchanged. Therefore, future studies that investigate skeletal muscle biopsies before and after PEM in patients, should also aim to quantify these metabolites and associated enzymes to understand whether the inability for UDP-HexNAC and phosphorylethanolamine to increase following exercise are contributing factors in PEM pathophysiology.

While most mitochondrial measures changed in all groups similarly, notably a decrease in overall tissue respiration following exercise, long COVID patients were the only group to exhibit a decrease in SDH activity 24 hours after exhaustive exercise. While long COVID patients had SDH activities similar to those of healthy controls prior to exhaustive exercise, these were reduced to levels similar to those of ME/CFS patients following exercise. The reason for this is unclear, however, this may be indicative of widespread mitophagy and hindered mitochondrial remodelling. As other reports have indicated morphological abnormalities in long COVID patients consistent with altered mitochondrial fusion/fission regulation[35], it may be that the decrease in SDH activity is therefore related to an increase in mitophagy following exercise, due to a likely increase in oxidative stress. It is curious that this is not recapitulated in the ME/CFS cohort, however this may be due to the already low amount of mitochondria that may be existing in these patients[36]. Future studies should aim to understand this phenomenon further. While overall there were many similarities observed between long COVID and ME/CFS patients in terms of metabolic function, skeletal muscle architecture, and whole-body aerobic capacity, there was no single defining feature that appeared to implicate PEM. As PEM is a systemic symptom, affecting multiple organs, it may be that the skeletal muscle itself does not account for PEM symptomology, but rather skeletal muscle alterations may result in altered myokine/cytokine signalling, which may lend itself to developing systemic features. However, it is very clear that more research in this regard is warranted.

Putative Pathophysiological Mechanisms of Skeletal Muscle Alterations in Long COVID and ME/CFS

Localized hypoxia: Impaired oxygen extraction and utilization

In chapter 8, I found that ME/CFS patients exhibited reduced capillarization compared to both long COVID patients and healthy controls, with no difference in the capillary sizes. As capillarization is typically reflective of the area needing to be perfused[37–42] (i.e. larger fibre cross sectional areas require higher capillarization), I initially expected FCSA to be subsequently reduced in ME/CFS patients. However, FCSA in both ME/CFS and long COVID patients were comparable to those of healthy controls. Indeed, when I plotted capillarization (capillary-to-fibre ratio) against FCSA, all groups showed the expected linear relation. Both ME/CFS and long COVID patients had reduced intercepts, suggesting that for any given FCSA, less capillaries were supplying that area. Even though I did not measure capillary function, this

would suggest that in the instance that capillary function is similar between groups, less oxygen is supplied for a given fibre size, which may limit skeletal muscle oxidative capacity. Other studies similarly reported alterations to capillarization that would suggest that oxygen flow may be impeded[43].

The flux of any gas across a membrane can be described by Fick's law of diffusion, wherein the flux is proportional to the concentration gradient of the gas multiplied by the permeability and solubility of the gas, and inversely proportional to the distance it must diffuse across. No evidence exists to suggest that oxygen solubility differs between different disease states, and thus we are left with the oxygen gradient and oxygen diffusion distance as the primary determinants of oxygen diffusion in patients. Evidence suggests that arterial blood oxygenation is not altered in either long COVID or ME/CFS patients[44–47], however it is unknown whether intracellular oxygen pressures (PO_2) are altered.

Recent evidence further suggests that not only is the number of capillaries affected, but capillary basement membrane are thickened in patients with long COVID and ME/CFS (Slaghekke et al. in prep). The thickening of capillary basement membrane in combination with the increased myofibre collagen IV deposition I reported in chapter 9, increases the diffusion distance of oxygen. Further, chapter 9 also provides evidence for altered membrane structure, due to the lower amount of membrane-associated lipid species in patients. It is suggested that cholesterol is the main determinant for oxygen permeability across membranes[48], and while I did not find evidence of altered cholesterols in patients, there was evidence of reduced phosphatidylcholines and phosphatidylethanolamines in patients. Both phosphatidylcholines and phosphatidylethanolamines, but specifically phosphatidylcholines interact with cholesterol to surround neutral lipids in order to form lipid droplets[49], which are thought to enhance oxygen solubility[50,51].

As oxygen is the final electron recipient of the electron transport chain, mitochondrial respiratory capacity determines myocyte intracellular PO_2. The current evidence suggests that tissue respiration is reduced in both long COVID and ME/CFS, which is either due to reduced mitochondrial density or dysfunctional mitochondria[52,53]. Thus, less mitochondria or poorer functioning mitochondria would likely result in increased intracellular PO_2. Data from invasive cardiopulmonary exercise tests indicate that arterial PO_2 in patients is largely similar to that in healthy individuals, with an increase in venous PO_2, suggesting that oxygen extraction at the muscle is impeded. The combination of reduced phospholipid species, increased diffusion

distance, and potential increase in intracellular PO_2 due to reduced mitochondrial oxidative capacity would certainly lend to a reduced oxygen flux at the myocyte.

The current thesis provides evidence that oxygen extraction is impeded, in part by increased collagen surrounding the muscle fibre and decreased tissue respiratory capacity in both patient groups. The repercussions of this may be seen in reduced maximal oxygen extraction and higher HR-$\dot{V}O_2$ slope during exercise, however we cannot distinguish whether this is entirely driven by alterations in the skeletal muscle or due to reduced cardiac contractility. Patients with ME/CFS may be further hindered by the decrease in capillarization. However, future work should aim to investigate how intracellular PO_2 is altered in both patient groups, and whether this is due primarily to the increased diffusion distances or due to reduced tissue respiratory capacity. This can be done using magnetic resonance spectroscopy[54], of which ^{31}P spectra can be analyzed to evaluate mitochondrial oxidative capacity, while ^{1}H spectra may be utilized to evaluate intracellular PO_2. However, a limitation in these methods is that to obtain the coexistence of mitochondrial oxidative response and changes in PO_2, interleaving of spectra is necessary[55].

Alternatively, positron electron tomography scans using tracers specific to hypoxia and glucose. In using hypoxia tracers, such as ^{18}F-FAZA[56,57], tissue specific hypoxia can be elucidated, whilst glucose tracers, such as [^{18}F]2-Fluoro-2-deoxy-D-glucose[58], would allow for quantification of tissue specific energy demand. In both MRI and PET scans, using additional doppler ultrasound methods to study blood flow, would help indicate whether any oxygen or glucose restrictions are then upstream of capillaries or downstream.

Mitochondrial dysfunction in long COVID and ME/CFS

Recent evidence has been accumulating that mitochondrial dysfunction is one of the predominant features of both long COVID and ME/CFS. Recent work has shown altered mitochondrial morphology[59–61] , while some studies have indicated reduced mitochondrial enzyme activity[52], and overall reduced tissue oxidative phosphorylation activity[52,61]. However, it is worth defining mitochondrial dysfunction, and how this may appear in the context of long COVID and ME/CFS.

Mitochondria, once thought to simply be the “power house of the cell”, are now known to be multifunctional organelles that are involved in various cell signalling pathways including damage response and metabolic adaptation[62]. Further, it is now understood that mitochondria are not necessarily individual entities, but rather part of a reticular network throughout

myofibres. This reticulum can be divided into several distinct areas: the paravascular, perinuclear, subsarcolemmal, and the intermyofibrillar mitochondrial regions[63–65]. Each region therefore has its own distinct role, aside from ATP production. Those residing in the intermyofibrillar space predominantly generate ATP for contractile function, while perinuclear are thought to predominantly generate ATP to support nuclear functions. The subsarcolemmal and perivascular mitochondria largely account for the initial drop in oxygen pressure moving from the capillary to the myocyte. It is not fully known whether these distinct populations have distinct roles in other mitochondrial-related responses[66]. The major contributor to intracellular oxygen pressures, however, is the mitochondria, as they are the ultimate recipients of oxygen at cytochrome c oxidase (or complex IV). As electrons are shuttled from complexes I and II (NADH:ubiquinone oxidoreductase and succinate dehydrogenase) towards complex IV, which uses oxygen as the final electron acceptor, results in transfer of hydrogen ions to the intermembrane space. This creates a hydrogen ion gradient, which can then be used by ATPsynthase (complex V) to generate ATP. Therefore, by stimulating or inhibiting various complexes, the relative contribution of each complex to whole tissue respiration can be assessed, yielding a qualitative assessment of the mitochondria. Thus, for the purposes of this thesis, mitochondrial dysfunction will refer to the reduced respiratory capacity of mitochondria or intact cells that cannot be explained by mitochondrial loss alone.

In the current work, the resolution of the mitochondria by the assessment of SDH activity is limited, and therefore can only regard mitochondria as one entity, rather than their distinct subpopulations. However, the differences in normalized tissue respiration can be assessed to allow a view on qualitative and quantitative changes in mitochondria. This is best highlighted in chapter 8, in which whole tissue respiration measures were similarly low in long COVID and ME/CFS patients compared to individuals after 55 days of bed rest. We found that following bed rest, normalized S-linked and N-linked respiration differed, with a shift towards a greater reliance in N-linked respiration. This shift can be accounted for by the relative decrease in complex II proteins compared to complex I (chapter 6). However, as all other complexes were lower following 55 days of bed rest, in combination with a reduced mitochondrial density, the findings suggest that during bed rest, mitochondrial number is preferentially affected rather than mitochondrial function. Further, neither E/L coupling nor E/P coupling (presented below) differed before or after bed rest, which implies the coupling from complexes I and II through complex IV and V are relatively maintained. Indeed,

supercomplex formation composition did not change, and only the abundance of supercomplexes decreased as a result of decreased mitochondrial density.

Comparatively, both long COVID and ME/CFS patients did not differ from healthy controls in their normalized N-linked and S-linked respiration rates, suggesting that electron flow through complex I and II is likely not affected. Rather, the E/L coupling efficiency tended to differ between these groups (P=0.06), with long COVID patients having lower E/L coupling efficiency than controls and ME/CFS patients not being different to controls. This is driven by the lower uncoupled respiration (i.e. electrons are allowed to freely flow through the transport chain without restriction from complex V) in long COVID patients compared to their leak. ME/CFS patients rather have reduced leak respiration and uncoupled respiration, resulting in no difference in the E/L coupling efficiency compared to healthy controls. It may be posited that the decline in respiration in ME/CFS patients then reflects more a decline in mitochondrial density, this is partially refuted by the occurrence of a decreased normalized oxidative phosphorylation capacity. Thus, while they may exhibit more mitochondrial loss than long COVID patients, there is still a degree of reduced mitochondrial functionality. Neither group indicates differences in the E/P coupling, which assesses the restriction of complex V on the electron transport chain. Together, the mitochondrial measures suggest that deficits in long COVID and ME/CFS patients lie downstream of complex I and II, but upstream of complex V. However, the current work lacks the resolution to determine whether complex III or complex IV are affected.

As different mitochondrial populations provide different functions within skeletal muscle, it is worth considering what impact this may then yield for oxygen extraction and utilization. Subsarcolemmal mitochondria and paravascular mitochondria typically display an uncoupling between complex IV and ATPsynthase, which is thought to generate the proton motive force across the reticulum, but consequently results in higher oxygen utilization rates and contributing to the initial large drop in intracellular PO_2, and may contribute to the oxygen gradient[62,63,65,67] . Therefore, if the subsarcolemmal or paravascular mitochondria are preferentially affected in either disease, this may reduce the capacity to generate the initial drop in PO_2 to efficiently extract oxygen. Further, it was noted that increased collagen deposition surrounding the myofibre likely increases the diffusion distance of oxygen. In order to maintain the same flux of oxygen across the myofibre membrane would require a lower PO_2, and thus either more mitochondria or more uncoupled mitochondria to drop intracellular PO_2. In chapter 8, there was a tendency for long COVID patients to have a more uncoupled respiration, due to

the lower E/L coupling, suggesting that this may be a compensatory response in attempt to drive PO_2 down. We did not observe the same phenomenon in ME/CFS patients, however, which may indicate either a difference in mitochondrial adaptation between the two diseases or possibly an end-point at which the mitochondria can only become uncoupled before becoming completely non-functioning.

In chapter 9, both long COVID and ME/CFS patients had lower abundances of membrane-associated lipids, of which phosphatidylethanolamines and cardiolipins account for nearly 90% of mitochondrial membrane lipids. Previous research has highlighted that mitochondrial membrane composition is integral in properly embedding proteins and respiratory chain complexes, but also the formation of cristae[68,69]. While the reduction in cardiolipins may signal an overall reduction in mitochondrial density, which other studies have observed in long COVID populations[52] , in the current cohort there was less evidence of mitochondrial loss and a greater propensity for mitochondrial dysfunction, as noted by a tendency for reduced E/L coupling and after normalizing oxidative phosphorylation capacity to SDH activity.

In a preliminary analysis, complex IV (COX IV) and ATP synthase (ATPB) were stained in sections of biopsies from patients with long COVID and ME/CFS and healthy controls. Regions were separated into the subsarcolemmal and intermyofibrillar regions and assessed for the relative distribution of COX IV and ATPB (Figure 1A). While healthy controls had lower intermyofibrillar ATPB:COX IV signal, indicating an uneven distribution of the complexes as expected, this was not seen in either patient group. Particularly, ATPB appeared to be higher in patients with long COVID and lower in patients with ME/CFS compared to healthy controls (Figure 1C). COX IV distribution appeared similar between groups, only indicating regional differences between the subsarcolemmal and intermyofibrillar regions (Figure 1D). As complex IV is the major site of oxygen utilization, it would be expected that there should be a relation between COX IV and permeabilized tissue respiration. However, only healthy controls had an association between oxidative phosphorylation capacity and COX IV (Figure 1E). In no groups were SDH activity and oxidative phosphorylation capacity associated. While this is an exploratory analysis, it suggests differential regulation of mitochondrial complex prevalence or functionality that separates not just controls from patients, but may indicate patient-specific alterations. Due to the limitations of immunohistochemical stains, it is imperative that future research investigates further whether the particular subpopulations of mitochondria are unequally affected and whether specific complexes are impaired or perhaps not present.

Evaluation with western blots and Blue Native PAGE or with targeted proteomics would aid in understanding mitochondrial permutations further.

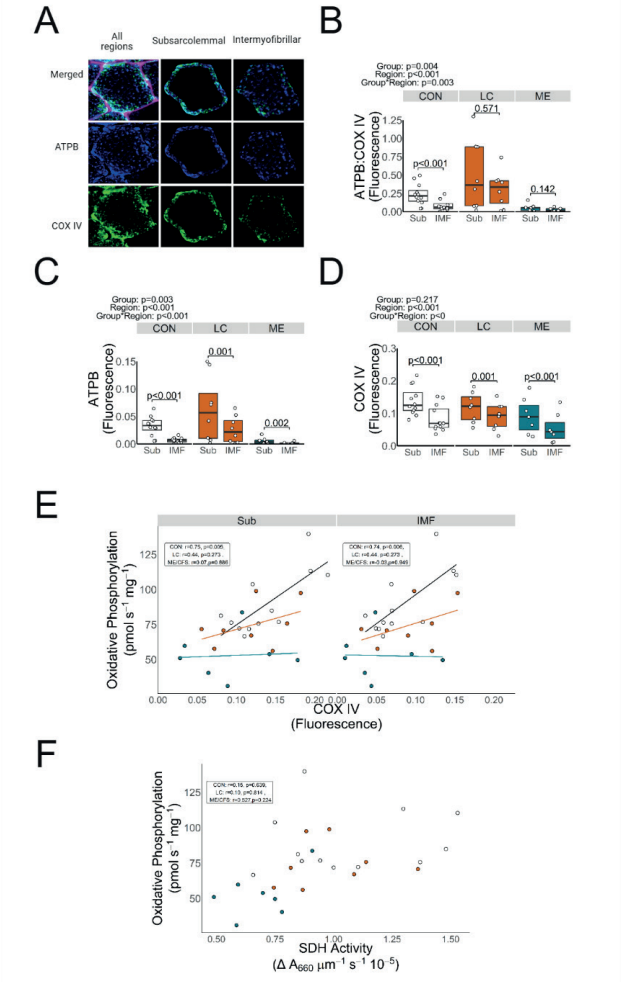


Figure 1: Typical examples of immunohistochemical stain for COX IV (green), ATPB (blue) and membrane (cyan) with separate subsarcolemmal and intermyofibrillar regions (**A**). ATPB:COX IV was lower in the intermyofibrillar region of healthy controls, whereas neither long COVID nor ME/CFS patients had regional differences (**B**), while long COVID patients had higher ATPB:COX IV compared to patients with ME/CFS in both regions (Sub: p=0.028, IMF: p=0.010). Patients with ME/CFS tended to have less subsarcolemmal ATPB:COX IV than healthy controls (p=0.052). All groups had higher subsarcolemmal ATPB compared to intermyofibrillar ATPB, while long COVID patients had higher ATPB than ME/CFS patients (Sub: p=0.012, IMF: p=0.009), while

healthy controls were not different from either group in either region (**C**). All groups had higher subsarcolemmal COX IV than intermyofibrillar COX IV, however long COVID patients had a smaller difference between subsarcolemmal and intermyofibrillar regions (CON -39.6%, LC=-23.1%, ME/CFS= -41.2%), while there were no group differences in any region (**D**). Both subsarcolemmal and intermyofibrillar COX IV was positively associated with oxidative phosphorylation capacity in healthy controls, however this was not seen in either patient group (**E**). Oxidative phosphorylation capacity was not associated with SDH activity in any groups (**F**).

Notably, while other studies have not necessarily quantified mitochondrial morphology in patients with long COVID and ME/CFS[59–61], deranged mitochondria have been highlighted in both populations. Particularly, some studies note that cristae (the mitochondrial folds) appear to be less pronounced in patients. Recent evidence suggests that the supercomplex I-III2-IV2[70,71] is implicated in cristae formation, which cardiolipin content is known to increase supercomplex formation[72–74]. While the formation of supercomplexes in patients was not assessed, based on the evidence suggesting reduced cristae formation and the reduction in either complex III or IV, it can be speculated that patients are likely to have altered proportions of supercomplexes. Future studies should aim to investigate the relative proportions of the various complexes and supercomplexes. In doing so, this would help to understand whether interventions that bypass complex I and II (i.e. supplementing with glycerol-3-phosphate), interventions that reduce reactive oxygen species (ROS) (i.e. Solicrominol), or interventions that target either complex III, IV or V would be useful for patients.

Early studies in SARS-CoV-2 showed that the virus could interact with a protein located on the outer mitochondrial membrane: translocase of the outer mitochondrial membrane (TOMM)[75,76], which is necessary to import various subunits involved in respiratory complexes[77,78]. Recent evidence has further shown that the binding of SARS-CoV-2 to TOMM20 in cell culture results in a depolarization of the mitochondrial membrane and increase in ROS production[79]. Other viruses have also been shown to interact with mitochondrial protein structures[80]. Currently, however, there is not any evidence of persistent viral accumulation in patient mitochondria. Thus, future work should aim to address whether the functional and morphological mitochondrial changes are repercussions of viral interactions with the mitochondria or a repercussion of an alternative mechanism, such as interaction with other organelles or chronic inflammation. In chapter 2, viral remnants of SARS CoV-2, specifically the nucleocapsid protein, were found in long COVID patients. While there was no difference between healthy controls and long COVID patients, it may be that the localization of the virus may be different between patients and healthy controls. In order to resolve this, muscle sections from animals infected with SARS CoV-2 (both acutely and after several

weeks/months) can be stained for the nucleocapsid and spike proteins of the virus alongside mitochondrial markers, such as TOMM20 or TOMM40. This enables us to visualize the time course of which the virus is cleared from skeletal muscle, and whether viral remnants colocalize with mitochondria.

While there is a growing body of evidence indicating reduced mitochondrial function in long COVID and ME/CFS[35,52,53,59–61,81–84], it is important to understand the effects within particular tissue compartments. Therefore, it may be that mitochondrial dysfunction is widespread throughout different tissues, however whether the tissue level repercussions remain the same are unclear. Indeed, cells like PBMCs may not reflect alterations in other tissue compartments[85], and as such specific tissue populations need to be studied further. Particularly, endothelial tissue would be of interest, as blood flow regulation would be impeded if there is mitochondrial dysfunction in endothelial cells or other vascular cell types.

Autoimmunity in Long COVID and ME/CFS

One of the most promising theories of the development of long COVID and ME/CFS is that of autoimmunity[86–92]. While there exists a wide range of reported autoantibodies in both long COVID and ME/CFS patients, the most commonly observed are autoantibodies against adrenergic receptors[87,89,90], muscarinic receptors[87,89,90], endothelin receptor A[90], and angiotensin II receptor type I[90]. As both long COVID and ME/CFS patients report a wealth of systemic symptoms, it is no surprise that many of the proteins potentially targeted by autoantibodies are rather ubiquitously expressed. All of the aforementioned receptors are implicated in blood flow regulation, and thus dysregulation of these receptors may reduce local oxygen and nutrient availability, particularly in response to stress[93–99]. However, it is not known whether this is a feature of all patients or just subsets that experience particular symptoms such as postural orthostatic intolerance[100–102]. Further, β2-adrenergic stimulation is known to increase lactate formation, irrespective of oxygen availability[103]. Thus, if autoantibodies against β2 adrenergic receptors were present in patients, it may be expected to decrease glycolysis rather than increase. As this is an acute response, however, it is uncertain how repeated insults to this pathway may alter metabolism.

Electrophysiological alterations

Currently, some evidence exists to suggest that patients with long COVID and ME/CFS may exhibit ion disbalances, resulting in alterations to electrophysiological function. Specifically, patients with ME/CFS appear to exhibit higher intramuscular sodium content[104]. The increase

in intracellular sodium, if not counterbalanced by an equal extrusion of other ionic species, would increase the osmolality, resulting in increased water absorption at the tissue. It is hypothesized that this results in hypovolemia[105,106], which may contribute to reduced cardiac filling, reduced blood flow, and poor tissue perfusion. Further, the potential swelling within the muscle tissue would increase the lattice space, wherein miniscule increases in the space may have large repercussions on force generation[107], namely reducing specific force.

In the current thesis, as there is evidence of impaired oxidative ATP production, which subsequently reduces the capacity to ensure functioning of several key ATPase enzymes, one of which being the Na-K ATPase. As the role of the Na-K ATPase is sodium extrusion and potassium import, reduction in Na-K ATPase function would result in sequestering of sodium intracellularly, due to the inherently large electrochemical gradient. Additionally, there are two forms of the Na-K ATPase, one which is constitutively active that mainly regulates the electrochemical gradients at rest, and an alternative isoform that is stimulated in response to insulin[108]. The higher activity of this isoform helps to restore the membrane potential during high EC coupling repetition[108], and thus it may be that this particular isoform is affected in long COVID and ME/CFS patients, lending to the PEM episodes.

Dysfunction of either isoform of Na-K ATPase may have subsequent downstream effects on other channels and exchangers, namely the sodium-hydrogen exchanger (NHE) and sodium-calcium exchanger (NCX). Increases in intracellular sodium would slow the activities of both these exchangers, as they are largely dependent on the sodium electrochemical gradient. This subsequently may result in increased intracellular hydrogen and calcium. Increases in hydrogen ion, reducing the pH, alters the functionality of many proteins and enzymes, whilst alterations in Ca^{2+} concentrations interfere with Ca^{2+} signalling. Increased Ca^{2+} concentrations, likely leading to reduced Ca^{2+} cycling, would also result in decreased force generation[109].

In the face of reduced inefficient ATP production, sarcoplasmic reticular calcium ATPase (SERCA) activity may also be reduced. SERCA acts to remove Ca^{2+} from the cytosol and sequester it in the sarcoplasmic reticulum following muscular contractions. Thus, reduction in SERCA activity would result in increased intracellular Ca^{2+}. Overtime, this reduces the amount of Ca^{2+} released with each excitation-contraction coupling event, in which the flux of Ca^{2+} rather than the absolute concentration is necessary for several signalling pathways[110]. Further, if the ability of the NCX to extrude Ca^{2+} is reduced, as described above, the removal of Ca^{2+} from the cytosol then falls upon the mitochondria via voltage dependent anion channels (VDAC). While this typically results in transient signalling to promote ATP production,

overtime Ca^{2+} sequestration in mitochondria can result in depression of the respiratory chain function[111]. This may result in higher free radical formation, resulting in more mitochondrial Ca^{2+} sequestration[112] and lower sarcoplasmic reticular Ca2+ release[113], further impairing contractile function.

Less considered channels that may also be impacted in alterations due to ATP availability also include the inward rectifying K_{ATP} channels[114], and thus function to hyperpolarize the membrane. These channels open in response to lower ATP or higher ADP levels, and are imperative in a wide variety of tissues, including the pancreas (being involved in insulin secretion) and cardiomyocytes (being involved with reducing ischemic injury). A reduction in ATP, therefore, may lead to an increase in K_{ATP} channel opening, which can result in a hyperpolarized membrane[115] resulting in "electrically fatigued"[116,117] cells or reduced contractility[118]. Some evidence suggests that patients with long COVID have reduced qEMG signal durations[119], which may indicate a hyperpolarized state.

Skeletal muscle metabolome and lipidome alterations

Following both short and long-term bed rest and in patients with long COVID and ME/CFS, metabolites related to glycolysis were higher compared to their respective controls. However, while bed rest also led to reductions in various carnitines, indicating a reduction in fatty acid oxidation, this was largely absent in both long COVID and ME/CFS. Rather patients with long COVID and ME/CFS had lower levels of antioxidant metabolites, suggesting that while the increased reliance in glycolysis may be similar to that of inactivity, the underlying physiology creating this shift may differ. As individuals undergoing bed rest were otherwise healthy individuals, the reduction in energy utilization resulted in overabundance of energetic substrates. This subsequently coincided with insulin resistance and increase lipid droplets. This is also noted in the lipidomic analysis, in which there are increases in skeletal muscle triglycerides with increasing bed rest. While lipid droplet formation in EM images of long COVID and ME/CFS patients was not assessed, oil red o staining indicated no differences in neutral lipid content compared to health controls, and lipidomic data suggested reductions in diacylglycerols, while triglycerides were largely the same.

In chapters 2 and 8, hydroxyphenyllactic acid was significantly lower in both long COVID and ME/CFS patients compared to their matched healthy controls. In chapter 6, there was an increase in hydroxyphenyllactic acid from pre-bed rest to short term bed rest, and a subsequent decline from short- to long-term bed rest. Literature regarding hydroxyphenyllactic acid in

skeletal muscle is very minimal[120–122]. Hydroxyphenyllactic acid has been observed to increase in the blood in septic patients[123], it has yet to be studied directly in the muscle, although there are indications that skeletal muscle may release hydroxyphenyllactic acid[124]. In all cohorts, it was detected in both blood and muscle, however only long COVID and ME/CFS patients appeared to show significantly lower proportions in skeletal muscle. Hydroxyphenyllactic acid is part of the phenol class of metabolites, normally known for metabolites arising from plants or the gut microbiome. Phenols have been suggested to reduce oxidative stress and promote oxidative metabolism[125]. Thus, it may be an indicator of increased oxidative stress and glycolytic reliance.

In chapter 6, it was highlighted that one of the defining characteristics of physical inactivity is loss of muscle mass, defined by reductions in muscle volume, FCSA, and the coincidence of increased plasma amino acids, thought to be a consequence of the increased protein catabolism occurring during bed rest. The pool of amino acids appeared to be largely unchanged following bed rest within the skeletal muscle, indicating sufficient supply of amino acids given the metabolic requirements. In chapters 2 and 8, there was no difference in muscle FCSA between long COVID patients and ME/CFS patients, suggesting a preservation of muscle mass. Subsequently in chapter 9, several essential amino acids were lower, predominantly in ME/CFS patients, and that all amino acids affected in either patient group are large, and require LAT1 for muscle uptake[126]. Interestingly, no circulating amino acids were altered in either patient group, suggesting that large amino acids may not be taken up at the muscle. However, whether this is due to dysfunction of the LAT1 channel or due to increased degradation of those particular amino acids requires further studies.

As one of the predominant theories with the development of long COVID and ME/CFS is that of autoimmunity, I performed an exploratory analysis on skeletal muscle metabolome and lipidome alterations in a known autoimmune disease to compare to what was found in patients with long COVID and patients with ME/CFS. While multiple sclerosis (MS) is defined by the demyelination of neurons, which has not been reported to occur in either long COVID or ME/CFS populations, MS patients do frequently present with severe fatigue and on occasion have been reported to experience PEM[127], and MS is frequently reported after Eppstein-Barr virus infection[128]. Similarly, some reports implicate dysfunction or loss of adrenergic or muscarinic receptors in MS patients[129–132]. Thus, if autoimmunity is a common mechanism to PEM, metabolic profiles may present with commonalities. In this exploratory analysis, I analyzed skeletal muscle metabolomic and lipidomic data collected from 13 patients with MS

and 6 healthy controls, in which whole-body exercise and skeletal muscle oxidative function have been previously analyzed[133]. Despite patients with MS having lower skeletal muscle oxidative capacity compared to controls[133], no metabolites were significantly different following post-hoc corrections (Figure 2). Using skeletal muscle lipidomics, patients with MS had lower skeletal muscle diglycerides compared to healthy controls (Figure 4), with other lipid classes being minimally affected.

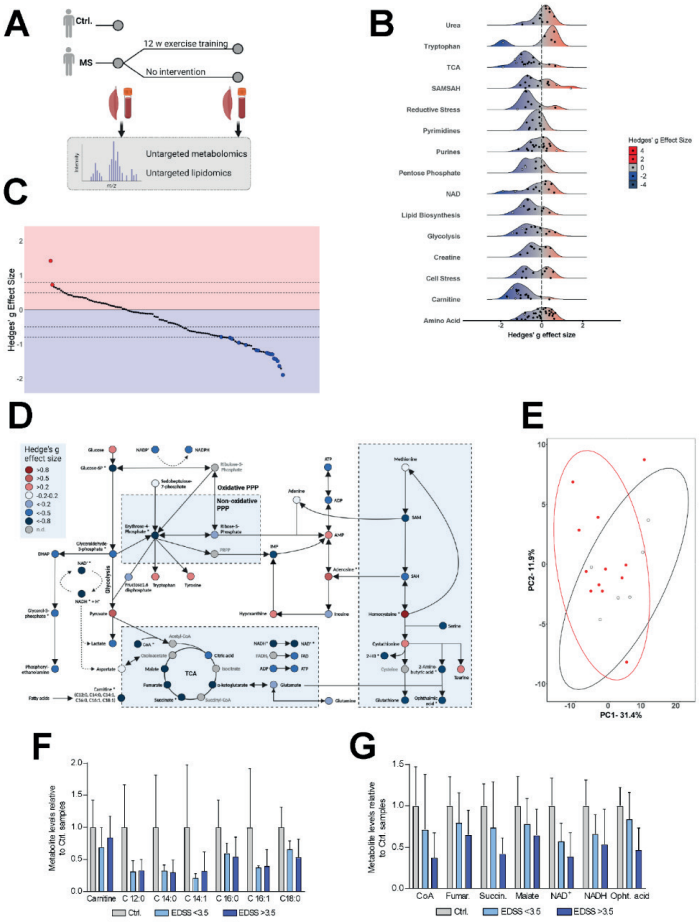


Figure 2: Graphical representation of the study design is presented in panel **A**. Homocysteine (p=0.002, BH adjusted=0.204) and adenosine (p=0.04, BH adjusted=0.329) tended to be higher in patients with MS, while succinate (p=0.002, BH adjusted=0.204), NAD^+ (p=0.008, BH adjusted=0.220), ophthalmic acid (p=0.010, BH adjusted=0.260), coenzyme A (p=0.017, BH adjusted=0.260), carnitine 14:1 (p=0.026, BH adjusted=0.260), carnitine C16:0 (p=0.017, BH adjusted=0.260), carnitine 16:1 (p=0.047, BH adjusted=0.348), carnitine C18:1 (p=0.023, BH adjusted=0.260), erythrose-4-phosphate (p=0.024, BH adjusted=0.260), NADH (p=0.024, BH adjusted=0.260), glucose-6-phosphate (p=0.024, BH adjusted=0.260), glycerol-3-phosphate (p=0.026, BH

adjusted=0.260), 2-hydroxybutyric acid (p=0.027, BH adjusted=0.260), glyceraldehyde-3-phosphate (p=0.029, BH adjusted=p=0.260), homocitrate (p=0.043, BH adjusted=0.329) tended to be lower in patients with MS (**B, C, D**). Principal components 1 and 2 explained 31.4% and 11.9% of group variance respectively (**E**). Metabolites involved in carnitine metabolism tended to be lower irrespective of expanded disability status scale (EDSS) score (**F**), while coenzyme-A, fumarate, succinate, malate, NAD^+, NADH, and ophthalmic acid tended to show stepwise decreases (**G**). After BH adjustments, no metabolites were significantly different. Metabolites that were significantly different prior to BH adjustments are indicated in white (**B**), red or blue (**C**), or denoted * (**D**).

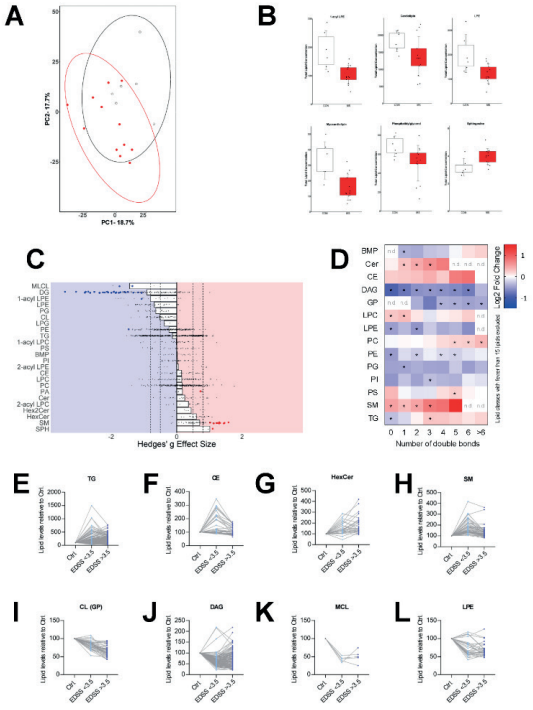


Figure 2: Principal components 1 and 2 explained 18.7% and 17.7% of the variance in lipidomic profile between patients with MS and healthy controls (A). Diacylglycerols and lipid classes related to membrane formation tended to be lower in patients with MS, while sphingomyelins tended to be increased (**B, C, D**). There was not relation between extended disability status scale (EDSS) score and lipid profiles (**E-L**). After BH adjustments, no lipid species were significantly different. Lipids and lipid classes that were significantly different prior to BH adjustments are indicated in red or blue (**C**), or denoted * (**D**).

Whilst MS patients, long COVID patients, and ME/CFS patients all exhibited lower oxidative capacity both at the whole-body and skeletal muscle level compared to healthy controls, the metabolomes and lipidomes of the patient groups were dissimilar. Long COVID and ME/CFS patients exhibited lower antioxidant metabolites, and ME/CFS patients had lower proportions of essential amino acids, whilst patients with MS do not have a significantly different metabolome compared to healthy individuals. MS patients only had lower skeletal muscle

diglycerides compared to healthy controls, whereas long COVID and ME/CFS had lower membrane-associated species. Therefore, although MS may share a similar onset to long COVID and ME/CFS (i.e. following viral infection), the skeletal muscle metabolome and lipidome alterations incurred by MS patients do not resemble those seen with either long COVID or ME/CFS. It may be that the demyelination in MS confers specific alterations to oxidative capacity without impacting metabolite and lipid species. As noted previously, autoimmunity in long COVID and ME/CFS is reported to be specific to G-coupled protein receptors rather than the myelin, as seen in MS. Thus, it may be that different autoimmune antibodies may confer specific alterations to the metabolome and lipidome. Future studies should investigate the effects of different autoantibodies by using animal models, wherein animals are exposed to autoantibodies against G-protein coupled receptors, myelin, and no autoantibodies. By doing so, the effects of the autoantibodies themselves can be studied in isolation rather than with possible other cofounders, such as severity of the primary infection (in the case of long COVID and ME/CFS).

Therapeutic Prospects

In recent years, many therapies have been proposed for both long COVID and ME/CFS, ranging from behavioural interventions to graded exercise therapy to pharmaceuticals. Within the current thesis, there is a multitude of data to support or refute the application of various therapies for patients exhibiting PEM.

Behavioural Therapy

Since ME/CFS was recognized as a disease (or more accurately historically, a disorder), the underlying basis was thought to be predominantly psyochological[134–136] . Psychologists of the 1950's and 1960's referred to ME/CFS in terms that were more reflective of hysteria rather than a disease. Thus, it was proposed that cognitive behavioural therapy may improve the well-being of ME/CFS patients[137–139]. While with many diseases that remove a person from social contact, reduces physical engagement, and hinders normal daily functioning, there will be psychological consequences, such as depression or other mood disorders[140,141], however these rates do not tend to be different to what is found in the general public[142]. Within the current thesis, there is a wealth of evidence to suggest that ME/CFS (and now long COVID) are not simply psychological disorders, and that there is a physiological underpinning to both diseases. Thus, while CBT may aid in improving mental wellbeing of some patients, it largely will not

confer benefits to diseases that directly impact the metabolic functioning of tissues, as displayed here in skeletal muscle.

Graded Exercise Therapy

Physical rehabilitation and graded exercise therapy is a staple in many different illnesses, and is particularly useful following hospitalization[2,143,144]. Like many exercise programs, the premise lies in progressive overload, where overtime patients gradually increase load or duration as they become adapted to the current load or duration[145]. The assumption made in these programs is that responses and adaptations to exercise remain intact. However, patients that experience PEM, by all accounts, likely do not exhibit similar responses to exercise as would be expected. Despite a lack of factors that were distinct during PEM-induction, chapters 2,8 and 9 illustrate that local skeletal muscle factors are detrimentally altered in long COVID and ME/CFS patients that likely affect appropriate exercise response. The lower number of resident mononuclear cells that would typically participate in exercise responses, and subsequently adaptation, increases in fibrosis, and altered metabolism, particularly oxidative metabolism and essential amino acid pools, suggests that the ability for patient skeletal muscle to respond appropriately to exercise is likely also altered. While there is not enough evidence to suggest in what way exercise responses are altered, the results from chapter 9 would suggest that long COVID and ME/CFS patients may exhibit a blunted training response. In order to assess whether appropriate training responses may exist, it would be of interest to investigate epigenetic alterations known to be related to training responses[146], and whether these are altered in the skeletal muscle of patients.

Targeting the Mitochondria: Pharmaceutical and Dietary Interventions

Progressively more evidence is accumulating that mitochondrial dysfunction is implicated in long COVID and ME/CFS[35,52,53,59–61,79,81–84,147]. This then makes treatment targeting the mitochondria with pharmaceuticals enticing. Due to the many known mitochondrial myopathies and mitochondrial-borne diseases[148–150], there is already a number of available potential pharmaceutical treatments, yet even within this sphere definitive effectiveness of certain therapeutics is lacking. While the current thesis lacked the full resolution to pinpoint which aspects of the mitochondria are dysfunctional, the evidence provided suggests several candidates for targets. The most evident targets would aim to decrease oxidative damage typically associated with mitochondrial dysfunction. Within the metabolomics analyses, it is clear that metabolites involved in reducing oxidative stress are reduced in patients with both

long COVID and ME/CFS. Thus, irrespective of which complexes may be specifically affected, a viable approach may be increasing the capacity by which patient tissue can reduce oxidative stress. We also provide evidence that it is likely either complex III, complex IV, or both may be affected in patients. While more studies are required to validate this, therapies that may aid these dysfunctions would include exogenous mitochondrial transplants[150], ketogenic diets, or supplementation with CoQ10 or L-creatine. Taking into account the lower levels of creatine and essential amino acids found in patients, ketogenic diets with creatine supplementation may be viable dietary interventions[151–154]. Currently, a clinical trial is scheduled in the Netherlands, investigating the use of sonlicromanol in long COVID patients experiencing PEM (Clinical Trials NCT07298005). As the mechanism of action of sonlicromanol is sequestering reactive oxygen species and modulating redox metabolism[155], treatment should reduce oxidative damage due to mitochondrial dysfunction.

Future Research

From the current work, it is evident that there are skeletal muscle alterations that contribute to reduction in whole-body exercise capacity, and likely a blunted exercise response in patients with long COVID and ME/CFS. However, it remains to be fully understood whether these alterations indicate simply similarities in disease presentation or that both diseases are identical, and that simply exist along a spectrum of disease progression.

As noted in previous chapters, patients with ME/CFS have been ill for longer durations than their long COVID counterparts, despite being of similar ages and sex distribution. Thus, longitudinally obtained biopsies from both cohorts would allow resolution of this issue. If the diseases are the same, it would be expected over time that the patients with long COVID would progressively exhibit reduced capillarization, further reductions in whole-body aerobic capacity, oxidative phosphorylation capacity, reductions in SDH enzyme activity, depletion of resident immune cells, and reduced quantities of several essential amino acids. As no studies have investigated skeletal muscle longitudinally in ME/CFS, it is difficult to speculate whether the changes observed were part of the disease progression over years, or whether the alterations occurred more acutely and remained unchanged over the duration of their disease. As many of the alterations reflect on the ability to generate sufficient ATP for cellular processes, it may be that over time there exists a plateau effect, wherein the adaptations occur simply to maintain energy production for the most essential cell processes.

While a sole mechanism of PEM in patients could not be identified, several areas that may contribute to PEM occurrence were noted. Specifically, the reduction in satellite cell prevalence lends itself to a lower propensity to functionally recover from damage, while the null changes in phosphorylethanolamine and UDP-HexNac following exercise may indicate altered signalling in response to exercise. Further, it appears that the lower amounts of resident immune cells likely implicates immune cell exhaustion in PEM occurrence and likely also reduces patient response to exercise. However, it is clear that more work investigated the nuances of how cell signalling may be altered in relation to these pathways occur in patients, and whether these are distinct between long COVID and ME/CFS.

Conclusion

Within this thesis, I provide evidence of altered skeletal muscle physiology in both long COVID and ME/CFS, contributing to lower whole-body exercise capacity, and thus a lower ability to perform daily tasks. These changes are highlighted by mitochondrial dysfunction, shifts towards glycolytic metabolism as evidenced both by muscle fibre contractile proteins and skeletal muscle metabolomes, and less membrane-associated lipids, which coincides with muscle fibrosis. Further, I provide evidence for physiological repercussions and contributors of PEM, indicated by muscle fibrosis, lower satellite cell and FAP cell numbers, and reduced resident immune cells in ME/CFS. As skeletal muscle is a potent regulator of whole-body metabolism and influences multiple organ systems, including immune response, future studies should aim to investigate how skeletal muscle alterations in long COVID and ME/CFS impose alterations to other organ systems and may in part contribute to systemic symptoms. Future clinical trials should investigate the feasibility of interventions aimed to addressing mitochondrial dysfunction in patients.

References

1. GBD 2023 Causes of Death Collaborators. Global burden of 292 causes of death in 204 countries and territories and 660 subnational locations, 1990-2023: a systematic analysis for the Global Burden of Disease Study 2023. *Lancet* **406**, 1811–1872 (2025).

2. Pedersen, B. K. & Saltin, B. Exercise as medicine – evidence for prescribing exercise as therapy in 26 different chronic diseases. *Scand. J. Med. Sci. Sports* **25**, 1–72 (2015).

3. Thaweethai, T. *et al.* Development of a Definition of Postacute Sequelae of SARS-CoV-2 Infection. *JAMA* **329**, 1934–1946 (2023).

4. Carruthers, B. M. *et al.* Myalgic encephalomyelitis: International Consensus Criteria. *J. Intern. Med.* **270**, 327–338 (2011).

5. Carruthers, B. M. *et al.* Myalgic Encephalomyelitis/Chronic Fatigue Syndrome. *J. Chronic Fatigue Syndr.* **11**, 7–115 (2003).

6. Holtzman, C. S., Bhatia, S., Cotler, J. & Jason, L. A. Assessment of Post-Exertional Malaise (PEM) in Patients with Myalgic Encephalomyelitis (ME) and Chronic Fatigue Syndrome (CFS): A Patient-Driven Survey. *Diagnostics* **9**, 26 (2019).

7. Hartle, M., Bateman, L. & Vernon, S. D. Dissecting the nature of post-exertional malaise. *Fatigue* **9**, 33–44 (2021).

8. Ottiger, M., Poppele, I., Sperling, N., Schlesinger, T. & Müller, K. Work ability and return-to-work of patients with post-COVID-19: a systematic review and meta-analysis. *BMC Public Health* **24**, 1811 (2024).

9. Goudsmit, E. M., Nijs, J., Jason, L. A. & Wallman, K. E. Pacing as a strategy to improve energy management in myalgic encephalomyelitis/chronic fatigue syndrome: a consensus document. *Disabil. Rehabil.* **34**, 1140–1147 (2012).

10. Bergouignan, A., Rudwill, F., Simon, C. & Blanc, S. Physical inactivity as the culprit of metabolic inflexibility: evidence from bed-rest studies. *J. Appl. Physiol.* **111**, 1201–1210 (2011).

11. Le Roux, E. *et al.* Physiology of physical inactivity, sedentary behaviours and non-exercise activity: insights from the space bedrest model Physical activity (MET.h/wk) Changes in physical activity to target. *J. Physiol.* **600**, 1037–1051 (2022).

12. Saris, C. G. J. *et al.* Should we be careful with exercise in post-exertional malaise after long COVID? *Nat. Commun.* **16**, 1724 (2025).

13. Ranque, B. *et al.* Muscle abnormalities in Long COVID. *Nat. Commun.* **16**, 1490 (2025).

14. Eaton-Fitch, N. *et al.* Immune exhaustion in ME/CFS and long COVID. *JCI Insight* **9**, (2024).

15. Shahbaz, S. *et al.* Single-cell analysis reveals immune remodeling of monocytes, NK cells, T cell exhaustion, and Galectin-9–associated depletion of gamma delta and mucosal-associated invariant T cells in Long COVID with ME/CFS. *Front. Immunol.* **17**, (2026).

16. Aid, M. *et al.* Long COVID involves activation of proinflammatory and immune exhaustion pathways. *Nat. Immunol.* **27**, 61–71 (2026).

17. Iversen, P. O., Lueder, T. G. von, Kardel, K. R. & Lien, K. Cardiac Dimensions and Function are Not Altered among Females with the Myalgic Encephalomyelitis/Chronic Fatigue Syndrome. *Healthcare* **8**, 406 (2020).

18. van Campen, C. (Linda) M. C., Rowe, P. C. & Visser, F. C. Cerebral blood flow remains reduced after tilt testing in myalgic encephalomyelitis/chronic fatigue syndrome patients. *Clin. Neurophysiol. Pract.* **6**, 245–255 (2021).

19. Nelson, M. J., Bahl, J. S., Buckley, J. D., Thomson, R. L. & Davison, K. Evidence of altered cardiac autonomic regulation in myalgic encephalomyelitis/chronic fatigue syndrome. *Medicine* **98**, e17600 (2019).

20. Satterfield, B. A., Bhatt, D. L. & Gersh, B. J. Cardiac involvement in the long-term implications of COVID-19. *Nat. Rev. Cardiol.* **19**, 332–341 (2022).

21. Roca-Fernandez, A. *et al.* Cardiac abnormalities in Long COVID 1-year post-SARS-CoV-2 infection. *Open Heart* **10**, e002241 (2023).

22. Cozma, A. *et al.* Cardiac Dysfunction and Subclinical Atherosclerosis in Post-COVID-19 Patients. *Card. Fail. Rev.* **11**, (2025).

23. Whitham, M. *et al.* Extracellular Vesicles Provide a Means for Tissue Crosstalk during Exercise. *Cell Metab.* **27**, 237-251.e4 (2018).

24. Griffin, J., Hartmann, A. & Comperat, E. Variation in cystectomy pathology reporting practice—results from an international survey of 212 pathologists. *Virchows Archiv* **485**, 879–888 (2024).

25. van Dooijeweert, C. *et al.* Significant inter- and intra-laboratory variation in grading of ductal carcinoma in situ of the breast: a nationwide study of 4901 patients in the Netherlands. *Breast Cancer Res. Treat.* **174**, 479–488 (2019).

26. Davison, B. A. *et al.* Suboptimal reliability of liver biopsy evaluation has implications for randomized clinical trials. *J. Hepatol.* **73**, 1322–1332 (2020).

27. Zhang, F. *et al.* O-GlcNAc Modification Is an Endogenous Inhibitor of the Proteasome. *Cell* **115**, 715–725 (2003).

28. Cieniewski-Bernard, C., Mounier, Y., Michalski, J.-C. & Bastide, B. *O* -GlcNAc level variations are associated with the development of skeletal muscle atrophy. *J. Appl. Physiol.* **100**, 1499–1505 (2006).

29. Zhang, R. *et al.* Muscle-specific lack of Gfpt1 triggers ER stress to alleviate misfolded protein accumulation. *Dis. Model. Mech.* **17**, (2024).

30. Lawler, J. Hindlimb unloading increases oxidative stress and disrupts antioxidant capacity in skeletal muscle. *Free Radic. Biol. Med.* **35**, 9–16 (2003).

31. Zachara, N. E. *et al.* Dynamic O-GlcNAc Modification of Nucleocytoplasmic Proteins in Response to Stress. *Journal of Biological Chemistry* **279**, 30133–30142 (2004).

32. Turner, O., Phoenix, J. & Wray, S. Developmental and gestational changes of phosphoethanolamine and taurine in rat brain, striated and smooth muscle. *Exp. Physiol.* **79**, 681–689 (1994).

33. Lehmann, A. Effects of Microdialysis-Perfusion with Anisoosmotic Media on Extracellular Amino Acids in the Rat Hippocampus and Skeletal Muscle. *J. Neurochem.* **53**, 525–535 (1989).

34. Horvath, S. E. & Daum, G. Lipids of mitochondria. *Progress in Lipid Research* vol. 52 590–614 Preprint at https://doi.org/10.1016/j.plipres.2013.07.002 (2013).

35. Szögi, T. *et al.* Novel biomarkers of mitochondrial dysfunction in Long COVID patients. *Geroscience* **47**, 2245–2261 (2024).

36. Shankar, V. *et al.* Oxidative stress is a shared characteristic of ME/CFS and Long COVID. *Proceedings of the National Academy of Sciences* **122**, (2025).

37. Plyley, M. J., Olmstead, B. J. & Noble, E. G. Time course of changes in capillarization in hypertrophied rat plantaris muscle. *J. Appl. Physiol.* **84**, 902–907 (1998).

38. Snijders, T. *et al.* Muscle fibre capillarization is a critical factor in muscle fibre hypertrophy during resistance exercise training in older men. *J. Cachexia Sarcopenia Muscle* **8**, 267–276 (2017).

39. Murias, J. M. *et al.* Adaptations in Capillarization and Citrate Synthase Activity in Response to Endurance Training in Older and Young Men. *J. Gerontol. A Biol. Sci. Med. Sci.* **66A**, 957–964 (2011).

40. Hendrickse, P. W. *et al.* Capillary rarefaction during bed rest is proportionally less than fibre atrophy and loss of oxidative capacity. *J. Cachexia Sarcopenia Muscle* **13**, 2712–2723 (2022).

41. Degens, H. *et al.* Diffusion and physical constraints limit oxidative capacity, capillary supply and size of muscle fibres in mice and humans. *Exp. Physiol.* **111**, 212–225 (2026).

42. Egginton, S. Physiological factors influencing capillary growth. *Acta Physiologica* **202**, 225–239 (2011).

43. Aschman, T. *et al.* Post-COVID exercise intolerance is associated with capillary alterations and immune dysregulations in skeletal muscles. *Acta Neuropathol. Commun.* **11**, 193 (2023).

44. Joseph, P. *et al.* Insights From Invasive Cardiopulmonary Exercise Testing of Patients With Myalgic Encephalomyelitis/Chronic Fatigue Syndrome. *Chest* **160**, 642–651 (2021).

45. Melamed, K. H. *et al.* Unexplained exertional intolerance associated with impaired systemic oxygen extraction. *Eur. J. Appl. Physiol.* **119**, 2375–2389 (2019).

46. Singh, I. *et al.* Persistent Exertional Intolerance After COVID-19: Insights From Invasive Cardiopulmonary Exercise Testing. *Chest* **161**, 54–63 (2022).

47. Joseph, P. *et al.* Exercise Pathophysiology in Myalgic Encephalomyelitis/Chronic Fatigue Syndrome and Postacute Sequelae of SARS-CoV-2. *Chest* **164**, 717–726 (2023).

48. Dotson, R. J., Smith, C. R., Bueche, K., Angles, G. & Pias, S. C. Influence of Cholesterol on the Oxygen Permeability of Membranes: Insight from Atomistic Simulations. *Biophys. J.* **112**, 2336–2347 (2017).

49. Colosio, M. *et al.* Structural and functional impairments of skeletal muscle in patients with postacute sequelae of SARS-CoV-2 infection. *J. Appl. Physiol.* **135**, 902–917 (2023).

50. Hansen, K. S. *et al.* Genetic Landscape and Mitochondrial Metabolic Dysregulation in Patients Suffering From Severe Long COVID. *J. Med. Virol.* **97**, (2025).

51. Hooijmans, M. T., Jeneson, J. A. L., Jørstad, H. T. & Bakermans, A. J. Exercise <scp>MR</scp> of Skeletal Muscles, the Heart, and the Brain. *Journal of Magnetic Resonance Imaging* **61**, 535–560 (2025).

52. Poli, S. *et al.* Interleaved trinuclear MRS for single-session investigation of carbohydrate and lipid metabolism in human liver at 7T. *NMR Biomed.* **37**, (2024).

53. Verwer, E. E. *et al.* Parametric Methods for Quantification of ^{18} F-FAZA Kinetics in Non–Small Cell Lung Cancer Patients. *Journal of Nuclear Medicine* **55**, 1772–1777 (2014).

54. Tran, L.-B.-A. *et al.* Potential role of hypoxia imaging using 18F-FAZA PET to guide hypoxia-driven interventions (carbogen breathing or dose escalation) in radiation therapy. *Radiotherapy and Oncology* **113**, 204–209 (2014).

55. Suttie, S. A., Park, K. G. M. & Smith, T. A. D. [18F]2-Fluoro-2-deoxy-D-glucose incorporation by AGS gastric adenocarcinoma cells in vitro during response to epirubicin, cisplatin and 5-fluorouracil. *Br. J. Cancer* **97**, 902–909 (2007).

56. Hejbøl, E. K. *et al.* Myopathy as a cause of fatigue in long-term post-COVID-19 symptoms: Evidence of skeletal muscle histopathology. *Eur. J. Neurol.* **29**, 2832–2841 (2022).

57. Behan, W. M. H., More, I. A. R. & Behan, P. O. Mitochondrial abnormalities in the postviral fatigue syndrome. *Acta Neuropathol.* **83**, 61–65 (1991).

58. Bizjak, D. A. *et al.* Functional and Morphological Differences of Muscle Mitochondria in Chronic Fatigue Syndrome and Post-COVID Syndrome. *Int. J. Mol. Sci.* **25**, 1675 (2024).

59. Monzel, A. S., Enríquez, J. A. & Picard, M. Multifaceted mitochondria: moving mitochondrial science beyond function and dysfunction. *Nat. Metab.* **5**, 546–562 (2023).

60. Glancy, B. *et al.* Mitochondrial reticulum for cellular energy distribution in muscle. *Nature* **523**, 617–620 (2015).

61. Willingham, T. B., Ajayi, P. T. & Glancy, B. Subcellular Specialization of Mitochondrial Form and Function in Skeletal Muscle Cells. *Front. Cell Dev. Biol.* **9**, (2021).

62. Parry, H. A. *et al.* Impact of capillary and sarcolemmal proximity on mitochondrial structure and energetic function in skeletal muscle. *J. Physiol.* **602**, 1967–1986 (2024).

63. Adhihetty, P. J., Ljubicic, V., Menzies, K. J. & Hood, D. A. Differential susceptibility of subsarcolemmal and intermyofibrillar mitochondria to apoptotic stimuli. *American Journal of Physiology-Cell Physiology* **289**, C994–C1001 (2005).

64. Ferreira, R. *et al.* Subsarcolemmal and intermyofibrillar mitochondria proteome differences disclose functional specializations in skeletal muscle. *Proteomics* **10**, 3142–3154 (2010).

65. Mårtensson, C. U., Doan, K. N. & Becker, T. Effects of lipids on mitochondrial functions. *Biochimica et Biophysica Acta (BBA) - Molecular and Cell Biology of Lipids* **1862**, 102–113 (2017).

66. Shinzawa-Itoh, K. *et al.* Structures and physiological roles of 13 integral lipids of bovine heart cytochrome c oxidase. *EMBO J.* **26**, 1713–1725 (2007).

67. Mühleip, A. *et al.* Structural basis of mitochondrial membrane bending by the I–II–III2–IV2 supercomplex. *Nature* **615**, 934–938 (2023).

68. Cogliati, S. *et al.* Mitochondrial Cristae Shape Determines Respiratory Chain Supercomplexes Assembly and Respiratory Efficiency. *Cell* **155**, 160–171 (2013).

69. Böttinger, L. *et al.* Phosphatidylethanolamine and Cardiolipin Differentially Affect the Stability of Mitochondrial Respiratory Chain Supercomplexes. *J. Mol. Biol.* **423**, 677–686 (2012).

70. Pfeiffer, K. *et al.* Cardiolipin Stabilizes Respiratory Chain Supercomplexes. *Journal of Biological Chemistry* **278**, 52873–52880 (2003).

71. Zhang, M., Mileykovskaya, E. & Dowhan, W. Gluing the Respiratory Chain Together. *Journal of Biological Chemistry* **277**, 43553–43556 (2002).

72. Gao, X. *et al.* Crystal structure of SARS-CoV-2 Orf9b in complex with human TOM70 suggests unusual virus-host interactions. *Nat. Commun.* **12**, 1–9 (2021).

73. Brandherm, L. *et al.* Phosphorylation of SARS-CoV-2 Orf9b Regulates Its Targeting to Two Binding Sites in TOM70 and Recruitment of Hsp90. *Int. J. Mol. Sci.* **22**, 9233 (2021).

74. Wu, Y. & Sha, B. Crystal structure of yeast mitochondrial outer membrane translocon member Tom70p. *Nat. Struct. Mol. Biol.* **13**, 589–593 (2006).

75. Young, J. C., Hoogenraad, N. J. & Hartl, F. U. Molecular Chaperones Hsp90 and Hsp70 Deliver Preproteins to the Mitochondrial Import Receptor Tom70. *Cell* **112**, 41–50 (2003).

76. Shang, C. *et al.* SARS-CoV-2 Causes Mitochondrial Dysfunction and Mitophagy Impairment. *Front. Microbiol.* **12**, (2022).

77. Song, S., Gong, S., Singh, P., Lyu, J. & Bai, Y. The interaction between mitochondria and oncoviruses. *Biochimica et Biophysica Acta (BBA) - Molecular Basis of Disease* **1864**, 481–487 (2018).

78. Macnaughtan, J. *et al.* Mitochondrial function is impaired in long COVID patients. *Ann. Med.* **57**, 2528167 (2025).

79. Missailidis, D. *et al.* An Isolated Complex V Inefficiency and Dysregulated Mitochondrial Function in Immortalized Lymphocytes from ME/CFS Patients. *International Journal of Molecular Sciences 2020, Vol. 21, Page 1074* **21**, 1074 (2020).

80. Myhill, S., Booth, N. E. & Mclaren-howard, J. Chronic fatigue syndrome and mitochondrial dysfunction. *Int. J. Clin. Exp. Pathol.* **2**, 1–16 (2009).

81. Finnigan, L. E. M. *et al.* ^{1}H and ^{31}P MR Spectroscopy to Assess Muscle Mitochondrial Dysfunction in Long COVID. *Radiology* **313**, (2024).

82. Hedges, C. P. *et al.* Peripheral blood mononuclear cells do not reflect skeletal muscle mitochondrial function or adaptation to high-intensity interval training in healthy young men. *J. Appl. Physiol.* **126**, 454–461 (2019).

83. Wohlrab, F. *et al.* Autoantibody targeting therapies in post COVID syndrome and myalgic encephalomyelitis/chronic fatigue syndrome. *Expert Opin. Biol. Ther.* **25**, 467–471 (2025).

84. Bynke, A. *et al.* Autoantibodies to beta-adrenergic and muscarinic cholinergic receptors in Myalgic Encephalomyelitis (ME) patients – A validation study in plasma and cerebrospinal fluid from two Swedish cohorts. *Brain Behav. Immun. Health* **7**, (2020).

85. Sotzny, F. *et al.* Myalgic Encephalomyelitis/Chronic Fatigue Syndrome – Evidence for an autoimmune disease. *Autoimmunity Reviews* vol. 17 601–609 Preprint at https://doi.org/10.1016/j.autrev.2018.01.009 (2018).

86. Loebel, M. *et al.* Antibodies to β adrenergic and muscarinic cholinergic receptors in patients with Chronic Fatigue Syndrome. *Brain Behav. Immun.* **52**, 32–39 (2016).

87. Sotzny, F. *et al.* Dysregulated autoantibodies targeting vaso- and immunoregulatory receptors in Post COVID Syndrome correlate with symptom severity. *Front. Immunol.* **13**, (2022).

88. Wilhelm, F., Cadamuro, J. & Mink, S. Autoantibodies in long COVID: a systematic review. *Lancet Infect. Dis.* **26**, e220–e230 (2026).

89. Wallukat, G. *et al.* Functional autoantibodies against G-protein coupled receptors in patients with persistent Long-COVID-19 symptoms. *J. Transl. Autoimmun.* **4**, 100100 (2021).

90. Hagström-Toft, E., Enoksson, S., Moberg, E., Bolinder, J. & Arner, P. β-Adrenergic regulation of lipolysis and blood flow in human skeletal muscle in vivo. *American Journal of Physiology-Endocrinology and Metabolism* **275**, E909–E916 (1998).

91. Pearen, M. A., Ryall, J. G., Lynch, G. S. & Muscat, G. E. Expression profiling of skeletal muscle following acute and chronic β2-adrenergic stimulation: implications for hypertrophy, metabolism and circadian rhythm. *BMC Genomics* **10**, 448 (2009).

92. Azevedo Voltarelli, V. *et al.* β2-Adrenergic Signaling Modulates Mitochondrial Function and Morphology in Skeletal Muscle in Response to Aerobic Exercise. *Cells* **10**, 146 (2021).

93. Ackland, G. L. *et al.* Physiological Significance of Endothelial M3 Muscarinic Receptors During Exercise. *Circ. Res.* **137**, 702–704 (2025).

94. Wolf, S. T., Berry, C. W. & Dillon, G. A. A role for endothelin-A receptors in altered blood flow and pressor responses during exercise in hypertensive adults. *J. Physiol.* **598**, 441–442 (2020).

95. Craig, J. C. *et al.* The role of endothelin A receptors in peripheral vascular control at rest and during exercise in patients with hypertension. *J. Physiol.* **598**, 71–84 (2020).

96. Sparks, M. A. *et al.* Vascular Type 1A Angiotensin II Receptors Control BP by Regulating Renal Blood Flow and Urinary Sodium Excretion. *Journal of the American Society of Nephrology* **26**, 2953–2962 (2015).

97. Garner, R. & Baraniuk, J. N. Orthostatic intolerance in chronic fatigue syndrome. *J. Transl. Med.* 1–10 (2019) doi:10.1186/s12967-019-1935-y.

98. van Campen, C. (Linda) M. C., Rowe, P. C. & Visser, F. C. Two Different Hemodynamic Responses in ME/CFS Patients with Postural Orthostatic Tachycardia Syndrome During Head-Up Tilt Testing. *J. Clin. Med.* **13**, 7726 (2024).

99. Han, E. *et al.* Circulating Autoantibodies Against Vasoactive Biomarkers Related to Orthostatic Intolerance in Long COVID Patients Compared to No-Long-COVID Populations: A Case-Control Study. *Biomolecules* **15**, 300 (2025).

100. Levy, B., Desebbe, O., Montemont, C. & Gibot, S. Increased Aerobic Glycolysis Through β2 Stimulation Is A Common Mechanism Involved In Lactate Formation During Shock States. *Shock* **30**, 417–421 (2008).

101. Petter, E. *et al.* Muscle sodium content in patients with Myalgic Encephalomyelitis/Chronic Fatigue Syndrome. *J. Transl. Med.* **20**, 580 (2022).

102. Wirth, K. J. & Scheibenbogen, C. Pathophysiology of skeletal muscle disturbances in Myalgic Encephalomyelitis/Chronic Fatigue Syndrome (ME/CFS). *Journal of Translational Medicine* vol. 19 Preprint at https://doi.org/10.1186/s12967-021-02833-2 (2021).

103. Scheibenbogen, C. & Wirth, K. J. Key Pathophysiological Role of Skeletal Muscle Disturbance in Post COVID and Myalgic Encephalomyelitis/Chronic Fatigue Syndrome (ME/CFS): Accumulated Evidence. *J. Cachexia Sarcopenia Muscle* **16**, (2025).

104. Tune, T. C. & Sponberg, S. Nanometer scale difference in myofilament lattice structure of muscle alters muscle function in a spatially explicit model. *PLoS Comput. Biol.* **21**, e1012862 (2025).

105. Pirkmajer, S. & Chibalin, A. V. Na,K-ATPase regulation in skeletal muscle. *American Journal of Physiology-Endocrinology and Metabolism* **311**, E1–E31 (2016).

106. Tupling, A. R., Asahi, M. & MacLennan, D. H. Sarcolipin Overexpression in Rat Slow Twitch Muscle Inhibits Sarcoplasmic Reticulum Ca2+ Uptake and Impairs Contractile Function. *Journal of Biological Chemistry* **277**, 44740–44746 (2002).

107. Berridge, M. J., Lipp, P. & Bootman, M. D. The versatility and universality of calcium signaling. *Nature Reivews* **1**, 11–21 (2000).

108. Garbincius, J. F. & Elrod, J. W. Mitochondrial calcium exchange in physiology and disease. *Physiol. Rev.* **102**, 893–992 (2022).

109. Chen, Q., Camara, A. K. S., Stowe, D. F., Hoppel, C. L. & Lesnefsky, E. J. Modulation of electron transport protects cardiac mitochondria and decreases myocardial injury during ischemia and reperfusion. *American Journal of Physiology-Cell Physiology* **292**, C137–C147 (2007).

110. Goodman, J. B. *et al.* Redox-Resistant SERCA [Sarco(endo)plasmic Reticulum Calcium ATPase] Attenuates Oxidant-Stimulated Mitochondrial Calcium and Apoptosis in Cardiac Myocytes and Pressure Overload–Induced Myocardial Failure in Mice. *Circulation* **142**, 2459–2469 (2020).

111. Tinker, A., Aziz, Q., Li, Y. & Specterman, M. ATP-Sensitive Potassium Channels and Their Physiological and Pathophysiological Roles. in *Comprehensive Physiology* 1463–1511 (Wiley, 2018). doi:10.1002/cphy.c170048.

112. van Mil, H. G. J., Kerkhof, C. J. M. & van Heukelom, J. S. Modulation of the isoprenaline-induced membrane hyperpolarization of mouse skeletal muscle cells. *Br. J. Pharmacol.* **116**, 2881–2888 (1995).

113. Scala, R. *et al.* Pathophysiological Consequences of KATP Channel Overactivity and Pharmacological Response to Glibenclamide in Skeletal Muscle of a Murine Model of Cantù Syndrome. *Front. Pharmacol.* **11**, (2020).

114. Cifelli, C. *et al.* K_{ATP} channel deficiency in mouse flexor digitorum brevis causes fibre damage and impairs Ca^{2+} release and force development during fatigue *in vitro*. *J. Physiol.* **582**, 843–857 (2007).

115. Gramolini, A. & Renaud, J. M. Blocking ATP-sensitive K+ channel during metabolic inhibition impairs muscle contractility. *American Journal of Physiology-Cell Physiology* **272**, C1936–C1946 (1997).

116. Agergaard, J. *et al.* Myopathy as a cause of Long COVID fatigue: Evidence from quantitative and single fiber EMG and muscle histopathology. *Clinical Neurophysiology* **148**, 65–75 (2023).

117. Ranganath, L. R. *et al.* Temporal adaptations in the phenylalanine/tyrosine pathway and related factors during nitisinone-induced tyrosinaemia in alkaptonuria. *Mol. Genet. Metab.* https://doi.org/10.1016/j.ymgme.2022.05.006 (2022) doi:10.1016/j.ymgme.2022.05.006.

118. Alban, C., Fatale, E., Joulani, A., Ilin, P. & Saada, A. The Relationship between Mitochondrial Respiratory Chain Activities in Muscle and Metabolites in Plasma and Urine: A Retrospective Study. *J. Clin. Med.* **6**, 31 (2017).

119. Beloborodova, N. *et al.* Effect of phenolic acids of microbial origin on production of reactive oxygen species in mitochondria and neutrophils. *J. Biomed. Sci.* **19**, 89 (2012).

120. Beloborodova, N. V., Sarshor, Y. N., Bedova, A. Yu., Chernevskaya, E. A. & Pautova, A. K. Involvement of Aromatic Metabolites in the Pathogenesis of Septic Shock. *Shock* **50**, 273–279 (2018).

121. Mercer, K. E. *et al.* Net release and uptake of xenometabolites across intestinal, hepatic, muscle, and renal tissue beds in healthy conscious pigs. *American Journal of Physiology-Gastrointestinal and Liver Physiology* **319**, G133–G141 (2020).

122. Wang, Y. *et al.* Gallic Acid Ameliorates Skeletal Muscle Metabolic Inflexibility by Regulating Lactate Metabolism and Promoting Mitochondrial Function. *Mol. Nutr. Food Res.* **69**, (2025).

123. Scalise, M., Galluccio, M., Console, L., Pochini, L. & Indiveri, C. The Human SLC7A5 (LAT1): The Intriguing Histidine/Large Neutral Amino Acid Transporter and Its Relevance to Human Health. *Front. Chem.* **6**, (2018).

124. Jason, L. A. *et al.* Differentiating Multiple Sclerosis from Myalgic Encephalomyelitis and Chronic Fatigue Syndrome. *Insights Biomed.* **02**, (2017).

125. Bjornevik, K. *et al.* Longitudinal analysis reveals high prevalence of Epstein-Barr virus associated with multiple sclerosis. *Science (1979).* **375**, 296–301 (2022).

126. Zamecnik, C. R. *et al.* An autoantibody signature predictive for multiple sclerosis. *Nat. Med.* **30**, 1300–1308 (2024).

127. Höftberger, R., Lassmann, H., Berger, T. & Reindl, M. Pathogenic autoantibodies in multiple sclerosis — from a simple idea to a complex concept. *Nat. Rev. Neurol.* **18**, 681–688 (2022).

128. De Keyser, J., Zeinstra, E. & Wilczak, N. Astrocytic β2-adrenergic receptors and multiple sclerosis. *Neurobiol. Dis.* **15**, 331–339 (2004).

129. White, A. T., Light, A. R., Hughen, R. W., VanHaitsma, T. A. & Light, K. C. Differences in Metabolite-Detecting, Adrenergic, and Immune Gene Expression After Moderate

Exercise in Patients With Chronic Fatigue Syndrome, Patients With Multiple Sclerosis, and Healthy Controls. *Psychosom. Med.* **74**, 46–54 (2012).

130. Spaas, J. *et al.* Altered muscle oxidative phenotype impairs exercise tolerance but does not improve after exercise training in multiple sclerosis. *J. Cachexia Sarcopenia Muscle* **13**, 2537–2550 (2022).

131. McEvedy, C. P. & Beard, A. W. Royal Free Epidemic of 1955: A Reconsideration. *BMJ* **1**, 7–11 (1970).

132. McEvedy, C. P. & Beard, A. W. Concept of Benign Myalgic Encephalomyelitis. *BMJ* **1**, 11–15 (1970).

133. May, P. Personality And Medical Perception In Benign Myalgic Encephalomyelitis. *The Lancet* **316**, 1122–1124 (1980).

134. Whiting, P. *et al.* Interventions for the Treatment and Management of Chronic Fatigue Syndrome. *JAMA* **286**, 1360 (2001).

135. Knoop, H., Prins, J. B., Stulemeijer, M., van der Meer, J. W. M. & Bleijenberg, G. The effect of cognitive behaviour therapy for chronic fatigue syndrome on self-reported cognitive impairments and neuropsychological test performance. *J. Neurol. Neurosurg. Psychiatry* **78**, 434–436 (2006).

136. Prins, J. B. *et al.* Cognitive behaviour therapy for chronic fatigue syndrome: a multicentre randomised controlled trial. *The Lancet* **357**, 841–847 (2001).

137. Arnaud, A. M. *et al.* Impact of Treating Depression on Associated Comorbidities. *Prim. Care Companion CNS Disord.* **25**, (2023).

138. Kang, H.-J. *et al.* Comorbidity of Depression with Physical Disorders: Research and Clinical Implications. *Chonnam Med. J.* **51**, 8 (2015).

139. Hickie, I., Lloyd, A., Wakefield, D. & Parker, G. The Psychiatric Status of Patients with the Chronic Fatigue Syndrome. *British Journal of Psychiatry* **156**, 534–540 (1990).

140. Warburton, D. E. R. & Bredin, S. S. D. Health benefits of physical activity. *Curr. Opin. Cardiol.* **32**, 541–556 (2017).

141. Thornton, J. S. *et al.* Physical activity prescription: a critical opportunity to address a modifiable risk factor for the prevention and management of chronic disease: a position

statement by the Canadian Academy of Sport and Exercise Medicine. *Clinical Journal of Sport Medicine* **26**, 259–265 (2016).

142. Plotkin, D. *et al.* Progressive overload without progressing load? The effects of load or repetition progression on muscular adaptations. *PeerJ* **10**, e14142 (2022).

143. Timmons, J. A. *et al.* Using molecular classification to predict gains in maximal aerobic capacity following endurance exercise training in humans. *J. Appl. Physiol.* **108**, 1487–1496 (2010).

144. Plioplys, A. V. & Plioplys, S. Electron-Microscopic Investigation of Muscle Mitochondria in Chronic Fatigue Syndrome. *Neuropsychobiology* **32**, 175–181 (1995).

145. Ng, Y. S. *et al.* Mitochondrial disease in adults: recent advances and future promise. *Lancet Neurol.* **20**, 573–584 (2021).

146. Hirano, M., Emmanuele, V. & Quinzii, C. M. Emerging therapies for mitochondrial diseases. *Essays Biochem.* **62**, 467–481 (2018).

147. Parikh, S. *et al.* A modern approach to the treatment of mitochondrial disease. *Curr. Treat. Options Neurol.* **11**, 414–430 (2009).

148. Li, J. *et al.* A ketogenic amino acid rich diet benefits mitochondrial homeostasis by altering the AKT/4EBP1 and autophagy signaling pathways in the gastrocnemius and soleus. *Biochimica et Biophysica Acta (BBA) - General Subjects* **1862**, 1547–1555 (2018).

149. Guevara-Cruz, M. *et al.* Intermittent fasting, calorie restriction, and a ketogenic diet improve mitochondrial function by reducing lipopolysaccharide signaling in monocytes during obesity: A randomized clinical trial. *Clinical Nutrition* **43**, 1914–1928 (2024).

150. Wallace, M. A. *et al.* The ketogenic diet preserves skeletal muscle with aging in mice. *Aging Cell* **20**, (2021).

151. You, Y. *et al.* Ketogenic diet ameliorates MASLD via balancing mitochondrial dynamics and improving mitochondrial dysfunction. *Nutr. Diabetes* **15**, 37 (2025).

152. Jiang, X. *et al.* Mechanism of action and potential applications of selective inhibition of microsomal prostaglandin E synthase-1-mediated PGE2 biosynthesis by sonlicromanol's metabolite KH176m. *Sci. Rep.* **11**, 880 (2021).



Academic Summary



In chapter 1, I summarize the current understanding of long COVID and ME/CFS. This includes what is known about their pathological onset and how muscle may be impacted in patients. As both long COVID and ME/CFS patients exhibit post-exertional malaise, I also recount regular physiological mechanisms involved in exercise and damage response, and how these may be affected in either condition.

How skeletal muscle is impacted in long COVID patients was relatively unknown. Thus, chapter 2 investigated resting and 24-hour post-exercise muscle biopsies from patients to elucidate whether long COVID impacted skeletal muscle architecture or metabolism, and whether this may in part explain the reduced exercise capacity of patients. In a cohort of patients and age- and sex-matched controls, cardiopulmonary exercise test (CPET) data indicated that the reduced capacity was likely not due to altered ventilation, but rather peripheral oxygen extraction and utilization impairments. In permeabilized fibres, I found that tissue respiration was lower in long COVID patients, while immunohistochemical staining revealed no changes in SDH activity (a proxy for mitochondrial density), suggesting reduced mitochondrial function. Further, patients had higher fraction of glycolytic fibres, whilst muscle fibre size was largely similar to that of healthy controls, suggesting a shift towards a preference for glycolytic metabolism. Metabolomics revealed multiple metabolites related to the tricarboxylic acid (TCA) cycle were lower in patients, further supporting this notion. A major finding in this study was that 24-hours following exhaustive exercise, patients with long COVID had a reduction in SDH activity, had an increase in skeletal muscle microclots, and were scored more pathological for infiltrating immune cells, small atrophic fibres, and necrosis. This study highlights that patients with long COVID exhibit physiologically changes that in part explain their reduced exercise capacity, but likely also explains the onset of PEM.

In chapters 3a and 4a, academic letters in response to chapter 2 challenged the findings, suggesting that the long COVID patients involved in this study were simply physically inactive. Thus, chapters 3b and 4b aimed to refute these points, as skeletal muscle characteristics of long COVID patients were not identical to characteristics seen with detraining or physical inactivity. Even after matching for aerobic capacity rather than just age and sex, many of the differences observed in long COVID were still evident. However, no study had done a direct comparison between long COVID patients and healthy people whom were physically inactive, and thus there remained a large gap in the literature.

PEM is one of the most mysterious symptoms of long COVID, which challenges us to rethink whether the long-held adage that “exercise is medicine” holds true. As patients have a

worsening of their symptoms upon exertion, it would suggest that a stress response is negatively altered in these patients. In chapter 5, I review the current literature surrounding skeletal muscle alterations in long COVID, and prominent hypotheses and proposed pathological mechanisms for post-exertional malaise in long COVID. Here, I found that multiple studies find indications for reduced mitochondrial respiratory capacity or altered mitochondrial morphology, suggesting that patients likely exhibit some form of mitochondrial dysfunction. Further, while some studies find atrophy, reduced capillarization, and fibre type shifts, the evidence is rather inconsistent, and more studies need to be conducted to validate findings in other populations. Highlights of the possible pathophysiological mechanisms of PEM included altered electrophysiology, central nervous system fatigue/damage, microclots either obstructing vasculature or imposing cytotoxicity to their environment, mitochondrial dysfunction, autoimmunity, and physical inactivity.

In chapter 6, I address the notion that cardiac changes in long COVID are due to physical inactivity. Although bed rest is known to reduce cardiac output by inducing cardiac atrophy, which subsequently affects cardiac contractile function. Typically, physical inactivity is not associated with inflammation-mediated scarring nor pre-load failure. Conversely, patients with long COVID are reported to show indications of myocarditis, whilst invasive CPET measures find evidence of pre-load failure, such that the cardiac filling is reduced rather than the cardiac contractility. Yet, it remains that no single study compared effects of cardiac morphological or functional changes between long COVID and physical inactivity.

Chapter 7 aimed to investigate skeletal muscle metabolic responses in both short-term (6 days) and long-term (60 days) bed rest in healthy individuals. Previous studies had suggested severe muscle wasting within days of commencing bed rest. In chapter 7, muscle atrophy is evident within 6 days of physical inactivity, which also coincided with loss of mitochondria, reduced oxidative phosphorylation capacity, increases in lipid droplet formation and lipotoxic species in the skeletal muscle, and an increase in insulin resistance. Long-term bed rest worsened many of these parameters further, however the largest changes were observed after 6 days.

Chapter 8 aimed to finally determine to what extent skeletal muscle alterations seen in patients with long COVID could be explained by physical inactivity. Moreover, as ME/CFS and long COVID also share similar symptoms, including PEM, this chapter also investigated whether long COVID and ME/CFS also shared similar pathophysiological features. Data from patients with long COVID in chapter 2, a new cohort of patients with ME/CFS, and age- and sex-matched healthy controls for every patient where then compared against the longitudinal cohort

from chapter 6. This chapter highlighted that bed rest altered the respiratory and cardiovascular responses to (sub)maximal exercise, while patients only exhibited respiratory alterations at submaximal exercise. When evaluating skeletal muscle, bed rest caused muscle atrophy and reduced oxidative phosphorylation, which the reduced oxidative phosphorylation related to reductions in maximal oxygen uptake. Contrastingly, overall muscle fibre size was not smaller in long COVID and ME/CFS patients, however patients with ME/CFS displayed type I-specific atrophy. Patients had larger proportions of glycolytic fibres, and reduced oxidative phosphorylation capacity, which was not associated with maximal oxygen uptake. Both patients with long COVID and ME/CFS had lower capillary-to-fibre ratios for a given muscle fibre size, suggesting a reduced oxygen supply for a given cross sectional area. Patients with ME/CFS had an additional overall reduction in capillary-to-fibre ratio. chapter 8 therefore concludes that while whole-body aerobic capacity is similar following bed rest compared to patients, the skeletal muscle phenotypical characteristics differed. This suggests that physical inactivity alone did not explain the lower exercise capacity and skeletal muscle adaptations in long COVID and ME/CFS.

As PEM physiology still remained unknown, and with long COVID and ME/CFS showing similar skeletal muscle characteristics, chapter 9 sought to investigate factors that may contribute to PEM pathology and exercise response in patients. As the ability to adapt to exercise is dependent on the local muscle damage incurred, the inflammatory and immune response, and mononuclear cells present around the myofibre, chapter 9 aimed to quantify these parameters. Both long COVID and ME/CFS patients had more collagen IV surrounding each muscle fibre, suggestive of fibrosis and incurring more damage. However, other damage markers did not appear different from healthy controls. Satellite cells and fibroadipogenic progenitor cells, both of which are necessary for proper myofibre growth and repair, were lower in both long COVID and ME/CFS. ME/CFS patients also had lower quantities of macrophages and T-cells prior to exercise, and showed no increase following exercise, which may indicate a lower immune response, and therefore activation of the regeneration cascade. The fibrosis and alterations in mononuclear cell populations coincided with lower amounts of oxidative and antioxidative metabolites, and lower amounts of membrane-associated lipid species. In metabolomic and lipidomic data, ME/CFS was only distinguished from long COVID in having several essential amino acids lower than healthy controls, but not than long COVID patients. The fibrosis seen in patients is then likely due to impaired membrane integrity, either as a result of or causing a reduction in satellite cell and fibroadipogenic progenitor cell densities. While

the exact mechanistic cause of PEM remained unclear in this chapter, several physiological alterations coincide that likely explain aspects of PEM in patients, and suggest that exercise response in long COVID and ME/CFS is altered compared to healthy individuals.

Chapter 10 discusses the findings of the thesis, in particular looking at the outcomes with respect to hypotheses surrounding long COVID and ME/CFS pathophysiology. The major finding in this thesis is that long COVID patients experiencing PEM and patients with ME/CFS (whom must have PEM as a symptom) showed similar skeletal muscle characteristics, suggesting that both diseases likely have similar physiology and may be classed together. This thesis also provides substantial evidence refuting the notion that physical inactivity alone explains either disease. Patients with ME/CFS, due to duration of disease, may begin to encounter additive effects of physical inactivity, but this is not the dominant explanation of their symptoms.



General Summary



The SARS-CoV-2 viral outbreak in 2020 resulted in a record number of global hospitalizations and deaths. Although most people recover from an initial COVID infection within 3 months, around 10% of people have symptoms that do not improve after 3 months, which is called long COVID. While not common, other viruses and bacterial infections can also result in long-term symptoms, which is known as myalgic encephalomyelitis/chronic fatigue syndrome (ME/CFS). One of the most common symptoms patients with either long COVID or ME/CFS experience is post-exertional malaise, which is the worsening of their symptoms or development of new symptoms after physical, mental or emotional stress. This can lead to patients leading less physically active lifestyles.

Physical activity is known to be beneficial for overall health and wellbeing, mostly by increasing exercise capacity, which is a significant predictor in long-term health. Physical inactivity, on the other hand, decreases exercise capacity and generally results in worse health outcomes. It is thought that symptoms experienced by patients with long COVID and ME/CFS are due to inactivity. However, people who are less physically active don't usually experience post-exertional malaise, which implies that there are disease-specific changes that happen in patients, but may also include changes that are seen in physical inactivity.

Many of the benefits that come from exercise come from a persons ability to adapt to an exercise session. Usually, exercise will create a short energy deficit, which then may result in small amounts of muscle damage. This then triggers a short-lived immune response, led first by neutrophils and macrophages, which clear damaged cells. This creates a small amount of local and whole-body inflammation. As the damaged cells are cleared, macrophages begin to create an anti-inflammatory environment. At the same time, they activate fibroadipogenic progenitor cells (FAP cells), which in turn activate satellite cells. Activated satellite cells will then become new nuclei around the damaged areas of the muscle cell. FAP cells can then either remain FAP cells or turn into either adipocytes (fat cells) or fibroblasts, which then communicate together to repair the outer muscle areas. Ultimately, this creates a stronger, more resilient muscle. Those who are physically inactive still have this normal response to exercise. However, patients with long COVID and ME/CFS, because of post-exertional malaise (PEM), it has be questioned whether they experience a normal exercise response.

The goal of this thesis then to 1) understand whether skeletal muscle changes in long COVID patients experiencing PEM may contribute to their symptoms, 2) whether muscle changes in long COVID and ME/CFS can be explained by physical inactivity alone, 3) whether long COVID and ME/CFS have the same changes, 4) how changes to the muscle environment and other cell types may relate to long COVID and ME/CFS symptoms, 5) how changes in metabolism with exercise may relate to PEM, and 6) whether the exercise responses in patients may be affected due to either changes in metabolism or changes in important cell populations.

In chapter 2, I use both maximal exercise testing and muscle biopsies from the upper leg of patients to show that long COVID patient exercise ability is limited by factors in the muscle, namely the mitochondria and metabolites related to oxidative function. As well, I show that

long COVID patients have more fast-twitch fibres, which are known to have lower endurance capabilities. I additionally show that 24-hours after exercise, long COVID patients were more likely to have necrosis (tissue damage), high increases in local immune cells, and a reduction in the number of mitochondria, all of which may relate to patients experiencing PEM.

In chapters 3a and 4a, the results of chapter 2 were challenged in letters to the editor, suggesting that the changes seen in patients were just due to physical inactivity. In chapters 3b and 4b, I tried to address why changes in long COVID patients were not the same as physical inactivity. However, no research at that point had studied this comparison, and so there was a large need in the field to study these similarities and differences.

Post-exertional malaise still remains an unknown phenomenon, and goes against the age old adage of "exercise is medicine". In chapter 5, I highlight the current understanding of how skeletal muscle in patients differs from healthy people. As well, I touch upon the current hypotheses that may explain how post-exertional malaise may occur in patients.

In chapter 6, I address the thought that cardiac alterations in long COVID are also due to physical inactivity. Here, I review the evidence showing that physical inactivity often results in reduced ability to produce forceful contractions with no signs of myocarditis (inflammation of the heart). Instead, long COVID patients typically have signs of myocarditis and pre-load failure, where blood returning to the heart does not fill the heart completely. However, no study had yet directly compared physical inactivity and long COVID.

Chapter 7 investigated the effects of short-term (6 days) and long-term (60 days) of bed rest on muscle of healthy people. Muscle wasting in healthy people occurred by 6 days of bed rest, while long-term bed rest resulted in loss of mitochondria, higher fat content within the muscle, and insulin resistance. This highlighted the time course of many negative changes in skeletal muscle, showing that the largest changes occurred after only 6 days of bed rest.

In chapter 8, I finally compare the effects of physical inactivity (chapter 7), long COVID (chapter 2) and ME/CFS on muscle, and how this relates to exercise capabilities. Here I highlight that physical inactivity causes general muscle atrophy and mitochondrial loss, while both long COVID and ME/CFS have atrophy of slow-twitch fibres specifically, poorer functioning mitochondria, and lower number of capillaries supplying the muscle.

The occurrence of PEM in both long COVID and ME/CFS still appeared mysterious. The goal of chapter 9 was to investigate muscle-related factors that may explain PEM. Here, I

found that both long COVID and ME/CFS have more collagen surrounding their fibres, which suggested impaired growth and repair. Both long COVID and ME/CFS had less satellite cells and FAP cells both before and after exercise compared to healthy people, while ME/CFS patients had few to no resident immune cells to participate in regeneration. These differences happened alongside lower oxidative metabolites and lipids that are important for maintaining membrane structure. Overall, these differences in the muscle environment in long COVID and ME/CFS may help to explain PEM.

Chapter 10 summarizes the work in this thesis, highlighting that long COVID and ME/CFS patients have muscle changes that impact their ability to perform exercise and their ability to recover from exercise, and that these changes are different from what is seen in physical inactivity. As ME/CFS patients have been sick for longer, they also show additional effects of physical inactivity, but by itself physical inactivity cannot explain the symptoms experienced by ME/CFS patients.



Appendices



Acknowledgements

As with all PhD trajectories, the process has been a rollercoaster, but sharing it with so many individuals along the way has made the ride that much sweeter. Through the many faces along this path, I have not only learned how to be a better scientist, but have learned how to live, laugh, and love from all of you.

First and foremost, a huge thank you to all the patients and participants in each study. None of the work would have been possible without them, and specifically for patients this was no small commitment.

To **Rob**, who has had to deal with my hard headed attitude on a daily basis for the past 5 years. What began as a small project during my Research Master's internship grew into more than I think either one of us imagined. You provided me with many opportunities to develop into a more critical and creative thinker, both in the lab and outside the lab. While sometimes we clashed, I look back on those moments and appreciate how they helped form not just new ideas, but found new ways of communicating these ideas. I'll forever be grateful for your leap of faith, and these formative five years.

To **Richard**, whom never ceased to amaze me with your excitement for exercise and muscle science. Ever since Training, Aging, and Disuse, your enthusiasm to talk about muscle physiology was infectious. I could always count on learning something in impromptu conversations in the hallway and by the coffee machine. I always left these conversations having so many new and different ways of thinking of the data and ideas in front of me.

To **Michèle**, to whom this patient oriented research could not have been done without. You always made sure that we kept a patient oriented focus. Without your drive for patient care, these projects may not have existed in the first place, and for that we are truly grateful.

To the defense committee, **Coen Ottenheijm**, **Fabien Le Grand**, **Sanne Nijhof**, **Mark Faghy**, and **Melissa Hooijmans**: thank you all for the time you gave to critically assess my thesis, and taking the time to attend the PhD defense.

To **Moritz** and **Richie**, whom shared many highs and lows throughout this process. I have been so fortunate to have met you both, learn from you, and watch you both progress in your careers as well. **Richie**, I'll never forget the first time we met, you jumping back aghast at the single leg laying in front of us while learning biopsy procedures from Frank. Whether it was you random research tangents over beers or while your sleep talking, supposedly dreaming of the ABC's of hypoxia, I love how excited you always are about research. Watching you go from post-doc research to an independent assistant professor has been a treat to be a part of, and you've really inspired me moving forward as a young researcher. **Mortiz**, teaching us all how to live, laugh and love. From the surf to the snow, and taking your passion for health and wellbeing to both your hobby and your work. I appreciate how you were my guardian angel in multiple ways throughout the years, whether that was isolating PBMCs or otherwise. You are one of the most supportive and passionate people I've had the pleasure of knowing. Those

that get to have you in their lives are lucky, and you constantly bring a smile to our faces. Ich wünsche dir immer nur das Beste, Bruder.

To **Jelle**, **Anouk**, **Koen**, **Brian** and **Brent**, whom not only were instrumental in many aspects of the projects, but also were there for many wild thought provoking discussions. I'm glad to have had such great colleagues, and more importantly friends, to share these projects with. Not only running with some bizarre or outlandish ideas, but supporting each other during the hard times. I am so excited to see where your pursuits take you next, and I will be happily following along with you all from afar. Keep those crazy ideas coming.

To the many PhD, MSc and Bachelor's students that have passed through the lab. Each of you brought your own shine to the lab, and our workspace would never have been the same without it. Wherever you are and wherever you go, I hope you all keep that unique spark and continue to make the world around you so special.

To the little family, **David**, **Kirsten**, **Brendan**, and **Megan** (and now **Cameron**): whether you guys read the whole book or just this section, I couldn't have made it this far with out you guys. Miss you guys lots, and I will forever look forward to every hike, bike or brewery we end up on or at. Lots of love to you all.

To my fiancée, **Juliette**: Tu es mon principal soutien et mon roc. Il n'y a pas assez de place ici pour exprimer tout ce que tu représentes pour moi. Tu supports mes idioties, mes changements d' humeur et mes ronchonnements. Tu rends ma vie plus belle, plus joyeuse et plus magnifique; tu fais de moi une meilleure personne. Tu m'as appris à apprécier les petits bonheurs de la vie. Je n'imagine pas avoir pu traverser ces quatre dernières années sans toi. Je t'aime. Je suis ravi de poursuivre cette vie à tes côtés et j'ai hâte de vivre tout ce qui nous attend.

And of course to my family, **Stephanie**, **Gerard**, and **Calli**. I don't think I really knew what I got myself into in the Autumn of 2020 moving halfway across the world, during a pandemic, to a city that I hardly knew. You supported me in this adventure, as you did with every concussion I've ever had, every sport I tried to play, and with every turtle I may have cried over releasing. Calli, I may have beat you to the title, but you'll forever be the better Dr. Charlton. I think having years of you comparing your grades to mine made me subconsciously try to raise the bar just a little higher. I'm glad we can both jump pretty high, and I know you're going to make a great physician. Mum and Dad, I'm sorry for all the times I worried you, was a little brat of a child, and didn't pick up the phone right away. I always wish I was a little closer to home, but I am so happy you both are supportive of the path I've chosen to take. I couldn't have asked for better parents and I love you both so much.

List of Publications

Publications as part of this thesis

1. **Charlton BT**, Slaghekke A, Appelman B, Eggelbusch M, Huijts JY, Noort W, Hendrickse PW, Bloemers FW, Posthuma JJ, van Amstel P, Goulding RP. (2026) Skeletal muscle properties in long COVID and ME/CFS differ from those induced by bed rest. *Nat Comm*. 17(9125)**.**

2. **Charlton, B. T.**, Janssen, K., Systrom, D. M., Putrino, D., & Wüst, R. C. (2026). Post-exertional malaise and the myth of cardiac deconditioning: rethinking the pathophysiology of long covid. *British journal of sports medicine*, *60*(8), 600-601.

3. **Charlton, B. T.**, Goulding, R. P., Jaspers, R. T., Appelman, B., van Vugt, M., & Wüst, R. C. (2025). Skeletal muscle adaptations and post-exertional malaise in long COVID. *Trends in endocrinology & metabolism*, *36*(7), 614-622.

4. Appelman, B.*, **Charlton, B. T.***, Goulding, R. P., Kerkhoff, T. J., Breedveld, E. A., Noort, W., ... & Wüst, R. C. I. (2025). Reply: Muscle abnormalities in Long COVID. *Nature Communications*, *16*(1), 1491. *Shared first author.

5. Appelman, B.*, **Charlton, B. T.***, Goulding, R. P., Kerkhoff, T. J., Breedveld, E. A., Noort, W., ... & Wüst, R. C. (2025). Reply to: Should we be careful with exercise in post-exertional malaise after Long COVID?. *Nature Communications*, *16*(1), 1725. *Shared first author.

6. Appelman, B.*, **Charlton, B. T.***, Goulding, R. P., Kerkhoff, T. J., Breedveld, E. A., Noort, W., ... & Wüst, R. C. (2024). Muscle abnormalities worsen after post-exertional malaise in long COVID. *Nature communications*, *15*(1), 17. *Shared first author.

7. Eggelbusch, M., **Charlton, B. T.**, Bosutti, A., Ganse, B., Giakoumaki, I., Grootemaat, A. E., ... & Wüst, R. C. (2024). The impact of bed rest on human skeletal muscle metabolism. *Cell Reports Medicine*, *5*(1).

Other Publications

1. Chen, H. J., Appelman, B., Willemen, H. L., Bos, A., Prado, J., Mak, W. A.,…, **Charlton, B.T.**, ... & den Dunnen, J. (2026). Transfer of IgG from Long COVID patients induces symptomology in mice. *Cell Reports Medicine*, *7*(4).
2. Goulding, R. P., **Charlton, B. T.**, Breedveld, E. A., van Der Laan, M., Strating, A. R., Noort, W., ... & Wüst, R. C. (2025). Skeletal muscle mitochondrial fragmentation predicts age-associated decline in physical capacity. *Aging Cell*, *24*(2), e14386.

3. Goulding, R. P., **Charlton, B. T.**, Breedveld, E. A., Huijts, J. Y., van der Laan, M., Strating, A. R., ... & Wüst, R. C. (2025). Skeletal muscle mitochondrial health in type 1 diabetes: the role of exercise capacity and lifestyle factors. *Diabetologia*, 68(8), 1823-1835.
4. Kerkhoff, T. J., **Charlton, B. T.**, Appelman, B., van Vugt, M., & Wüst, R. C. (2022). Post COVID-19 condition: critical need for a clear definition and detailed pathophysiology. *Journal of Cachexia, Sarcopenia and Muscle*, *13*(6), 2754.

5. **Charlton, B. T.**, Forsyth, S., & Clarke, D. C. (2022). Low energy availability and relative energy deficiency in sport: what coaches should know. *International Journal of Sports Science & Coaching*, *17*(2), 445-460.

Conference Presentations

"Skeletal muscle properties in long COVID and ME/CFS differ from those induced by bed rest", ISLC-PAIS Conference 2026, Amsterdam, NL. 2026 (**Oral**)

"An Inability to Recover: Impaired regenerative markers in long COVID & ME/CFS patients", Dutch Translational Metabolism Conference 2026, Wageningen, NL. 2026. (**Poster)**

"An Inability to Recover: Impaired regenerative markers in long COVID & ME/CFS patients", Dutch Translational Metabolism Conference 2026, Wageningen, NL. 2026. (**Poster)**

"An Inability to Recover: Impaired regenerative markers in long COVID & ME/CFS patients", International Biochemistry of Exercise Conference 2026, Roanoke, US. 2026. (**Poster)**

"An Inability to Recover: Impaired regenerative markers in long COVID & ME/CFS patients", International Union of Physiological Sciences 2025, Frankfurt am Main, DE. 2025. (**Oral**)

"The Inability to Recover: Reduced Regenerative Capacity in PEM Patients", European Muscle Conference 2025, Amsterdam, NL. 2025. (**Poster**)

"Physical inactivity does not explain reduced exercise capacity in long COVID and ME", ICanCME Canadian Conference on Myalgic Encephalomyelitis: Nothing About Us Without Us, Online Webinar. 2025. (**Poster**)

"Skeletal Muscle Abnormalities in Long COVID: The argument against deconditioning", Patient Led Research Meeting 2025, Online Webinar. 2025. (**Oral**)

"Physical inactivity does not explain reduced exercise capacity in long COVID and ME/CFS" 3rd International Meeting of the Charité Fatigue Center, Berlin, DE. 2025. (**Poster**)

"Muscle abnormalities worsen after post-exertional malaise in long COVID" Amsterdam Movement Sciences Annual Meeting 2025, Amsterdam, NL. 2025. (**Oral**)

"The Inability to Recover: Reduced Satellite Cells in PEM Patients" Amsterdam Movement Sciences Annual Meeting 2025, Amsterdam, NL. 2025. (**Poster, Best Poster Award**)

"Cellular interactions of skeletal muscle adaptions influencing reductions in maximal aerobic capacity" Human Physiology Workshop 2024, Cologne, DE. 2024. (**Oral**)

"Physical inactivity does not explain post-exertional malaise in long COVID and ME/CFS", International Biochemistry of Exercise Conference 2024, Limerick, IR. 2024. (**Poster**)

"Skeletal muscle structure and function contribute to exercise intolerance in Long COVID Patients", Maastricht Infectieziekten Symposium 2024, Maastricht, NL. 2024. (**Oral**)

"Physical inactivity does not explain lower exercise capacity and skeletal muscle adaptations in long COVID and ME/CFS" Human Physiology Workshop 2023, Cologne, DE. 2023. (**Oral, Best Presentation Award**)

"Skeletal muscle structure and function contribute to exercise intolerance in Long COVID Patients.", Long COVID and Post-Sequalae of SARS COV2: Pathogenesis and Treatment Keystone Symposium, Santa Fe, New Mexico. 2023. (**Oral and Poster**)

"Skeletal Muscle Abnormalities Contribute to Post-Exertional Malaise in Long COVID.", Dutch Translational Metabolism Conference 2023, Wageningen, NL. 2023. (**Oral**)



About the Author



Braeden Charlton was born in Regina, Saskatchewan, Canada on 29th May, 1995. From a young age, Braeden participated in a variety of sports, but it was swimming that captured most of his attention throughout high school and truly grew his passion for science in sport.

After graduating from Lord Byng Secondary School in 2013, Braeden would begin his Bachelor of Science in Biomedical Physiology at Simon Fraser University, whilst competing for the university's cross country and track teams. During his athletic career, Braeden would go on to attend the NCAA Division 2 championships in cross country twice, and was a 3x All-Conference finisher (2x in cross country, 1x steeplechase). While at university, Braeden also worked as a lifeguard, coached junior track and field athletes with the Vancouver Thunderbirds track club (where he would establish the Thunderbirds East program), and worked as a special education assistant, also volunteering with the Burnaby Special Olympics track and field program.
During his final year of studies, Braeden conducted a literature review on relative energy deficiency in sports (RED-S) and low energy availability (LEA). This would lead Braeden to take on an optional year to conduct an Honour's thesis, where he designed an educational program for coaches surrounding the topics of LEA and RED-S. This project was supervised by Dr. David Clarke (Simon Fraser University) and Dr. Sara Forsyth (Footbridge Centre for Integrated Orthopaedic Care), and resulted in an educational tool that was subsequently used by both BC Athletics and Athletics Canada in their coaching education programs.

Braeden took a small break from education starting in 2019. During this time, Braeden would continue coaching with the Vancouver Thunderbirds East program, working as a special education assistant, and began a part-time endeavour as a sales-associate in a specialty running store. Braeden found great joy in educating his athletes, students, and footwear customers, and further pursuing his running career.
In the Spring of 2020, with the COVID-19 pandemic at its initial height, Braeden began searching for opportunities to pursue a Master's degree. In the hopes of scratching both the itch for academics and for travel, Braeden would pursue a Research Master's degree in Human Movement Sciences at the Vrije Universiteit Amsterdam beginning in the Autumn of 2020. During this time, Braeden would attend lectures led by both Dr. Rob Wüst and Prof. Dr. Richard Jaspers, whom would become his supervisors during his PhD.

It was Dr. Wüst that proposed a project that would change the trajectory of Braeden's career, conducting an exploratory experiment on fatigue and post-exertional malaise in patients with long COVID, during which time Braeden also receive the Amsterdam Movement Sciences Research Master Talent Grant. The success of the internship project then launched Braeden into his PhD for the following 4 years, where Braeden would attend the Long COVID Keystone Symposium after obtaining the Keystone Symposia Travel Scholarship, received the Amsterdam Movement Sciences Musculoskeletal Health PhD Talent award in 2024, the ICanCME Stars of Tomorrow PhD Award in 2024 and 2025, and was awarded several best presentation and best poster awards at multiple conferences. During his PhD trajectory, Braeden also helped organizing the Dutch Translational Metabolism Conference (2024-2026). Perhaps most importantly, it was during this time he would meet his fiancée Juliette, whom he can't imagine hiking without.

Braeden will continue his academic path as a post-doctoral researcher at Universiteit Gent, under the tutelage of Prof. Dr. Wim Derave. In his new research, Braeden will aim to investigate fibre type specific metabolic and transcriptional changes at different exercise intensities, aiming to elucidate how muscle specific metabolic perturbations and thresholds relate to training adaptations.